

For Reference

NOT TO BE TAKEN FROM THIS ROOM

For Reference

NOT TO BE TAKEN FROM THIS ROOM

Ex LIBRIS
UNIVERSITATIS
ALBERTAENSIS



UNIVERSITY OF ALBERTA
LIBRARY

Regulations Regarding Theses and Dissertations

Typescript copies of theses and dissertations for Master's and Doctor's degrees deposited in the University of Alberta Library, as the official Copy of the Faculty of Graduate Studies, may be consulted in the Reference Reading Room only.

A second copy is on deposit in the Department under whose supervision the work was done. Some Departments are willing to loan their copy to libraries, through the inter-library loan service of the University of Alberta Library.

These theses and dissertations are to be used only with due regard to the rights of the author. Written permission of the author and of the Department must be obtained through the University of Alberta Library when extended passages are copied. When permission has been granted, acknowledgement must appear in the published work.

This thesis or dissertation has been used in accordance with the above regulations by the persons listed below. The borrowing library is obligated to secure the signature of each user.



Digitized by the Internet Archive
in 2019 with funding from
University of Alberta Libraries

<https://archive.org/details/Manuel1966>

Thesis
H66
#170

THE UNIVERSITY OF ALBERTA

THE BEHAVIOR OF RESTRAINED REINFORCED
CONCRETE COLUMNS UNDER SUSTAINED LOAD

by

ROBERT FRANCIS MANUEL, B.Sc.(Alberta), M.Sc.(Queen's)

A THESIS

SUBMITTED TO THE FACULTY OF GRADUATE STUDIES
IN PARTIAL FULFILMENT OF THE REQUIREMENTS FOR THE DEGREE OF
DOCTOR OF PHILOSOPHY

DEPARTMENT OF CIVIL ENGINEERING

EDMONTON, ALBERTA

JANUARY, 1966

UNIVERSITY OF ALBERTA
FACULTY OF GRADUATE STUDIES

The undersigned certify that they have read, and recommend to the Faculty of Graduate Studies for acceptance, a thesis entitled "THE BEHAVIOR OF RESTRAINED REINFORCED CONCRETE COLUMNS UNDER SUSTAINED LOAD" submitted by ROBERT FRANCIS MANUEL in partial fulfilment of the requirements for the degree of Doctor of Philosophy.

ABSTRACT

The primary objective of this investigation was the derivation of a method of analysis which can be used on a computer to determine the behavior of columns in reinforced concrete frameworks under sustained load.

The method of analysis applies discreteness to the cross-sections, the member lengths, and the duration of sustained load, and utilizes numerical integration and trial and error procedures to obtain equilibrium configurations of the frameworks under load. The properties of concrete and reinforcing steel used in the analysis were based on the investigations available in engineering literature. The concrete was represented as a visco-elasto-plastic material which also exhibits shrinkage, and the steel was considered to be an idealized elasto-plastic material with no time dependent dimensional instability. The rate of creep method was used to estimate the creep of the concrete under variable stress.

The applicability of the analysis was partially verified by comparison with experimental data reported by various investigators. A reasonably good correlation was obtained between the analytical results and the experimental results of Washa and Fluck, Martín and Olivieri, Furlong, Furlong and Ferguson, and Green.

Although the analysis has a wide range of potential uses, the application described in this thesis was limited to only two series of beam-column frames. The columns were laterally restrained and were bent in either symmetrical single curvature or double curvature with one end

of the column fixed. The major variables in the frames analysed were the column slenderness ratio and the level of sustained axial load in the column. The columns were loaded with a sustained moment and a sustained axial load which was preset at a fixed proportion of the short-time failure strength. If failure did not occur during a hypothetical 25 year period of sustained load, the columns were then quick loaded to failure. The factors held constant in the investigation included the properties of the restraining beam, the properties of the column cross-section, and the fixed end moments in the beams. The distributed moment to the column produced a small effective column end eccentricity. Results have been presented regarding load-moment behavior, deformation characteristics, stresses, and failure loads. A comparison of the failure loads with those predicted by various codes shows that the codes do not give a sufficient account of the effect of sustained load.

ACKNOWLEDGEMENTS

The author would like to express his grateful appreciation to the following for their contributions to this thesis.

Associate Professor J.G. MacGregor for his assistance and constructive criticism during the course of the research.

The Canada Council for the Special Scholarship in Engineering which enabled the author to be financially secure throughout his post graduate work.

The National Research Council of Canada for the financial assistance in the publication of the thesis and also for making available the computing facilities at the University of Alberta.

The staff of the computing centre at the University of Alberta for their contributions to the computer application in this thesis.

Technical Services for the reproduction of the graphs.

Miss Helen Wozniuk for the typing of the manuscript.

TABLE OF CONTENTS

		Page
	Title Page	i
	Approval Sheet	ii
	Abstract	iii
	Acknowledgements	v
	Table of Contents	vi
	List of Tables	xii
	List of Figures	xiii
	List of Symbols	xvi
CHAPTER I	INTRODUCTION	1
	1.1 Introduction	1
	1.2 The Present Investigation	3
CHAPTER II	REVIEW OF PREVIOUS WORK	6
	2.1 Introduction	6
	2.2 Metal Columns Under Sustained Load	7
	2.3 Short-Time Loading of Concrete Columns	7
	2.4 Experimental Investigations of Reinforced Concrete Columns Under Sustained Load	8
	2.5 Analytical Investigations of the Effect of Sustained Load on the Behavior of Reinforced Concrete Columns	9
	2.6 Conclusion	13
CHAPTER III	MATERIAL PROPERTIES	14
	3.1 Introduction	14
	3.2 Steel Reinforcement	14
	3.3 Concrete	15
	3.3.1 Concrete Composition and Curing	16
	3.3.2 Prediction of Total Concrete Strain for any Loading History	16
	3.3.3 Failure of Concrete	17
	3.3.4 Concrete Strength in Compression	18
	3.3.5 Effect of Eccentric Loading	19

TABLE OF CONTENTS (Continued)

	Page
3.3 (Continued)	
3.3.6 Instantaneous Response of Concrete	21
3.3.7 Concrete Shrinkage	24
3.3.8 Concrete Creep	24
3.4 Conclusion	31
CHAPTER IV METHOD OF ANALYSIS	33
4.1 Introduction	33
4.2 Assumptions of the Analysis	34
4.2.1 Assumptions of Fibre Analysis	34
4.2.2 Assumptions of Cross-Section Analysis	35
4.2.3 Assumptions of Member Analysis	35
4.2.4 Assumptions of Frame Analysis	36
4.3 Sign Convention	36
4.4 Analysis of a Fibre	36
4.4.1 Establishment of Stress-Strain Compatibility	37
4.4.2 Initial Assumption of Fibre Stress	37
4.4.3 Calculation of Strain from Stress	38
4.4.4 Permissible Variation in Fibre Strain	39
4.4.5 Incrementing of Fibre Stress	40
4.4.6 Fibre Failure	41
4.5 Analysis of a Cross-Section	41
4.5.1 Establishment of Load and Moment Compatibility	41
4.5.2 Calculation of Internal Load and Moment	42
4.5.3 Initial Assumption of Strain Distribution	44
4.5.4 Incrementing of the Strain Distribution	45
4.5.5 Permissible Variations in Load and Moment	46
4.5.6 Failure of a Cross-Section	46
4.6 Analysis of a Member	46
4.6.1 Analysis of the Beam	47
4.6.2 Analysis of the Column Bent in Symmetrical Single Curvature	49
4.6.3 Analysis of the Fixed Ended Column	50
4.6.4 Permissible Variation in Deflection, ΔY , and the Moment Increment ΔM	53
4.6.5 Initial Assumptions of Column Deflected Shape and Moment at the Fixed End of the Column	54
4.7 Analysis of a Framework	54

TABLE OF CONTENTS (Continued)

	Page
4.7 (Continued)	
4.7.1 Establishment of Equilibrium and Compatibility at a Joint	55
4.7.2 The Permissible Variation in Rotation	56
4.7.3 The Moment Increment $\Delta M_2(K)$	56
4.7.4 Initial Assumption of Beam End Moment	56
4.7.5 Frame Failure	56
4.8 Conclusion	57
CHAPTER V ERRORS OF THE ANALYSIS	59
5.1 Introduction	59
5.2 Errors Resulting from Discreteness in the Analysis	59
5.2.1 Comparison of the Effect of Discreteness	60
5.2.2 Conclusions Regarding Discreteness	64
5.3 Errors Resulting from Permissible Variations in the Trial and Error Procedures	65
5.4 Conclusion	65
CHAPTER VI APPLICATION OF THE ANALYSIS TO EXISTING TESTS	66
6.1 Introduction	66
6.2 Beam Tests Under Sustained Load - Washa and Fluck	67
6.2.1 Comparison of the Results of Washa and Fluck's Beam Tests with the Results of the Analysis	69
6.3 Short-Time Tests of Slender Hinged Columns - Martín and Olivieri	75
6.3.1 Comparison of the Results of Martín and Olivieri's Column Tests with the Results of the Analysis	75
6.4 Short-Time Tests of Columns in Frames - Furlong	79
6.4.1 Comparison of the Results of Furlong's Frame Tests with the Results of the Analysis	81
6.5 Sustained Load Test of Columns in a Framework - Furlong and Ferguson	84
6.5.1 Comparison of the Results of Furlong and Ferguson's Sustained Load Frame Test with the Results of the Analysis	84
6.6 Sustained Load Tests of Hinged Columns - Green	87
6.6.1 Comparison of the Results of Green's Sustained Load Column Tests with the Results of the Analysis	92

TABLE OF CONTENTS (Continued)

	Page
6.7 Conclusion	92
CHAPTER VII DESCRIPTION OF THE INVESTIGATION OF LONG COLUMNS IN FRAMEWORKS	94
7.1 Introduction	94
7.2 Description of the Frameworks	94
7.3 Scope of the Investigation	97
7.4 Data for the Analysis	98
7.4.1 Dimensions and Loads	98
7.4.2 Material Properties	102
7.4.3 Incrementing Data	103
7.4.4 Permissible Variations	104
7.5 General Comments	105
CHAPTER VIII RESULTS OF THE INVESTIGATION OF LONG COLUMNS IN FRAMEWORKS	106
8.1 Introduction	106
8.2 Analysis Using First Order Theory	107
8.3 Load-Moment Behavior	108
8.3.1 Load-Moment Behavior of the Columns Bent in Single Curvature	108
8.3.2 Load-Moment Behavior of the Double Curvature Columns	122
8.4 Maximum Column Deflections	136
8.4.1 Maximum Deflections of the Columns Bent in Single Curvature	136
8.4.2 Maximum Deflections of the Columns Bent in Double Curvature	139
8.5 Maximum Concrete Stresses	139
8.5.1 Maximum Concrete Stresses in the Single Curvature Columns	139
8.5.2 Maximum Concrete Stresses in the Double Curvature Columns	143
8.6 Maximum and Minimum Steel Stresses	146
8.6.1 Maximum and Minimum Steel Stresses in the Single Curvature Columns	146
8.6.2 Maximum and Minimum Steel Stresses in the Double Curvature Columns	149
8.7 Joint Rotations	152
8.7.1 Joint Rotations in the Single Curvature Columns	152
8.7.2 Joint Rotations in the Double Curvature Columns	155
8.8 Failure Loads	157
8.8.1 Failure of the Single Curvature Columns	157

TABLE OF CONTENTS (Continued)

	Page
8.8 (Continued)	
8.8.2 Failure of the Double Curvature Columns	162
CHAPTER IX DISCUSSION OF THE ANALYSIS AND ITS APPLICATION TO LONG COLUMNS IN FRAMEWORKS	164
9.1 Introduction	164
9.2 Resume of the Present Investigation	164
9.2.1 Effect of Sustained Load	165
9.2.2 Effect of the Restraints	166
9.2.3 Effect of Slenderness Ratio	167
9.3 Applicability of Long Column Design Formulae to Columns Subjected to Sustained Load	168
9.3.1 Comparison for the Single Curvature Columns	168
9.3.2 Comparison for the Double Curvature Columns	175
9.3.3 Moment Magnification Design Procedure	176
9.3.4 Discussion of the Design Procedures	177
9.4 Limitations of the Method of Analysis	177
9.4.1 Verification of the Method of Analysis	178
9.4.2 Evaluation of Concrete Properties	178
9.4.3 Relationship Between Deformations and Applied Loads	179
9.4.4 Computer Limitations	179
9.4.5 Calculation of Creep Strains Under Variable Stress	179
9.4.6 Errors of the Trial and Error Procedures	180
9.5 Discussion of Other Methods of Analysis	180
9.5.1 Analysis Based on First Order Theory	181
9.5.2 Analysis of Isolated Columns	181
9.5.3 Analysis of Isolated Columns Having Linearly Elastic End Restraints	181
9.5.4 Analysis of Frames Using Moment-Curvature Relationships	182
9.5.5 Reduced Modulus Approach	184
CHAPTER X SUMMARY, CONCLUSIONS, AND RECOMMENDATIONS	184
10.1 Summary	184
10.2 Recommendations for Further Research	185
10.3 Conclusions and Recommendations	185

TABLE OF CONTENTS (Continued)

	Page
LIST OF REFERENCES	188
APPENDIX A Flow Diagrams for Computer Application of the Analysis	
A.1 Nomenclature Used in Computer Application	A1
A.1.1 Subscripting Variables	A1
A.1.2 Input Variables Common to All Loading Stages	A1
A.1.3 Variables Dependent on the Loading Stage	A3
A.1.4 Calculated Variables	A3
A.2 Flow Diagram for Fibre Analysis	A7
A.3 Flow Diagrams for Cross-Section Analysis	A11
A.3.1 Beam Cross-Section	A11
A.3.2 Column Cross-Section	A16
A.4 Flow Diagrams for Member Analysis	A18
A.4.1 Beam	A18
A.4.2 Column Bent in Single Curvature	A21
A.4.3 Fixed Ended Column Bent in Double Curvature	A25
A.5 Flow Diagrams for Frame Analysis	A30
A.5.1 Framework Containing the Columns Bent in Symmetrical Single Curvature	A30
A.5.2 Framework Containing the Columns Fixed at one End and Bent in Double Curvature	A34
APPENDIX B Comparison of Results of a Beam and a Column Considering Various Degrees of Discreteness	

LIST OF TABLES

		Page
TABLE 3.1	Coefficients of the Mathematical Creep Equations	30
TABLE 6.1	Details of the Beams Tested by Washa and Fluck Under Sustained Loads	68
TABLE 6.2	Details of the Hinged Ended Columns Tested by Martín and Olivieri Under Short-Time Load	76
TABLE 6.3	Details of Furlong's Tests on Rectangular Frames with Columns Bent in Single Curvature	80
TABLE 6.4	Details of Green's Hinged End Columns Tested Under Sustained Load	88
TABLE 7.1	Beam Dimensions and Load	99
TABLE 7.2	Constant Column Dimensions	99
TABLE 7.3	Variable Data for the Columns Bent in Symmetrical Single Curvature	100
TABLE 7.4	Variable Data for the Columns Bent in Double Curvature	101
TABLE 7.5	Concrete Properties Independent of Sustained Load	102
TABLE 7.6	Sustained Load Properties of Concrete	102
TABLE 7.7	Incrementing Data	103
TABLE 7.8	Permissible Variation Data	104
TABLE 8.1	First Order Analysis of the Frames Containing the Columns Bent in Single Curvature	107
TABLE 8.2	First Order Analysis of the Frames Containing the Columns Bent in Double Curvature	108
TABLE B.1	Comparison of Beam Results for Various Degrees of Discreteness	B1
TABLE B.2	Comparison of Column Results for Various Degrees of Discreteness	B2

LIST OF FIGURES

	Page
FIGURE 3.1 Assumed Stress-Strain Behavior of Reinforcing Steel	15
FIGURE 3.2 Effect of Eccentricity on Concrete Strength	21
FIGURE 3.3 Instantaneous Stress-Strain Response for Concrete	22
FIGURE 3.4 Shrinkage-Time Curves	25
FIGURE 3.5 Concrete Strain vs Stress-Strength for Tests by Rüsç (1960)	27
FIGURE 3.6 Modified and Mathematical Creep Curves	29
FIGURE 4.1 Division of a Cross-Section into Fibres	37
FIGURE 4.2 Cross-Section Under Load and Moment	42
FIGURE 4.3 Division of a Member	48
FIGURE 4.4 Conjugate Beam for Beam Analysis	49
FIGURE 4.5 Conjugate Beam for the Fixed Ended Column	51
FIGURE 5.1 Effect of Analysis Discreteness on Beam Results	62
FIGURE 5.2 Effect of Analysis Discreteness on Column Results	63
FIGURE 6.1 Analysis Applied to the Washa and Fluck Beam Tests: Part I - Midspan Deflections	70
FIGURE 6.2 Analysis Applied to the Washa and Fluck Beam Tests: Part II - Strains at the Compressive Steel Level	72
FIGURE 6.3 Analysis Applied to Column Tests of Martín and Olivieri	77
FIGURE 6.4 Analysis Applied to Furlong Test Frame No. 2R	82
FIGURE 6.5 Analysis Applied to Furlong Test Frame No. 3R	82
FIGURE 6.6 Analysis Applied to Furlong Test Frame No. 4	83

LIST OF FIGURES (Continued)

		Page
FIGURE 6.7	Analysis Applied to Furlong Test Frame No. 6	83
FIGURE 6.8	Analysis Applied to the Test Frame of Furlong and Ferguson	86
FIGURE 6.9	Analysis Applied to the Column Tests of Green	89
FIGURE 7.1	Frameworks of the Analysis	95
FIGURE 7.2	Member Cross-Sections	96
FIGURE 8.1	Load-Moment Behavior of Columns S-10	109
FIGURE 8.2	Load-Moment Behavior of Columns S-16	109
FIGURE 8.3	Load-Moment Behavior of Columns S-22	110
FIGURE 8.4	Load-Moment Behavior of Columns S-28	110
FIGURE 8.5	Load-Moment Behavior of Columns S-34	111
FIGURE 8.6	Load-Moment Behavior of Columns S-40	111
FIGURE 8.7	Variation in Maximum Moment with Slenderness Ratio for the Columns Bent in Single Curvature	112
FIGURE 8.8	Variation in Column End Moment with Slenderness Ratio for the Columns Bent in Single Curvature	113
FIGURE 8.9	Variation in Single Curvature Column Moments with Time	114
FIGURE 8.10	Load-Moment Behavior of Columns D-10	123
FIGURE 8.11	Load-Moment Behavior of Columns D-16	123
FIGURE 8.12	Load-Moment Behavior of Columns D-22	124
FIGURE 8.13	Load-Moment Behavior of Columns D-28	124
FIGURE 8.14	Load-Moment Behavior of Columns D-34	125
FIGURE 8.15	Load-Moment Behavior of Columns D-40	125
FIGURE 8.16	Variation in Joint Moment and Maximum Moment with Slenderness Ratio for the Columns Bent in Double Curvature	126

LIST OF FIGURES (Continued)

		Page
FIGURE 8.17	Variation in Double Curvature Column Moments with Time	127
FIGURE 8.18	Effect of Sustained Load on the Ratio of Fixed End Moment to Joint Moment for the Columns Bent in Double Curvature	128
FIGURE 8.19	Effect of Sustained Load on the Maximum Deflection of the Columns Bent in Single Curvature	137
FIGURE 8.20	Effect of Sustained Load on the Maximum Deflection of the Columns Bent in Double Curvature	138
FIGURE 8.21	Effect of Sustained Load on the Maximum Concrete Stress in the Columns Bent in Single Curvature	140
FIGURE 8.22	Effect of Sustained Load on the Maximum Concrete Stress in the Columns Bent in Double Curvature	144
FIGURE 8.23	Effect of Sustained Load on the Maximum and Minimum Steel Stresses in the Columns Bent in Single Curvature	147
FIGURE 8.24	Effect of Sustained Load on the Maximum and Minimum Steel Stresses in the Columns Bent in Double Curvature	150
FIGURE 8.25	Effect of Sustained Load on the Joint Rotation of the Columns Bent in Single Curvature	153
FIGURE 8.26	Effect of Sustained Load on the Joint Rotation of the Columns Bent in Double Curvature	156
FIGURE 8.27	Failure Loads for the Frames Containing the Columns Bent in Single Curvature	158
FIGURE 8.28	Failure Loads for the Frames Containing the Columns Bent in Double Curvature	159
FIGURE 9.1	Comparison of Actual Failure Loads with Predicted Failure Loads After 25 Years Under Sustained Load for the Single Curvature Columns	169
FIGURE 9.2	Comparison of Actual Failure Loads with Predicted Failure Loads After 25 Years Under Sustained Load for the Double Curvature Columns	171

LIST OF SYMBOLS

Subscripts

- K = subscript defining the loading stage. A loading stage can be either the application of an increment of quick load or the sustaining of a load over a time increment
- J,I = subscripts referring to the position of a cross-section in a beam or column
- L = subscript referring to the position of a fibre in a cross-section

Steel Properties

- ϵ_s = steel strain
- E_s = modulus of elasticity of steel
- f_s = steel stress
- f_y = yield stress of steel

Concrete Properties

- ϵ_T = total concrete strain
- ϵ_{IN} = instantaneous component of total concrete strain
- ϵ_{SH} = shrinkage component of total concrete strain
- ϵ_{CR} = creep component of total concrete strain
- ϵ_c = concrete strain in general
- ϵ_o = instantaneous component of total strain at the first reaching of maximum stress under virgin loading
- ϵ_u = instantaneous component of total strain at failure of the concrete
- E_c = tangent modulus of elasticity of concrete at zero stress

LIST OF SYMBOLS (Continued)

f_c	= concrete stress in general
f'_{ca}	= strength of concrete in a short-time cylinder test after a days of initial curing
f_t	= strength of concrete in tension
F_1, F_2, F_3	= coefficients used in the cubic equation to determine creep
k_3	= ratio of strength of structural concrete to the short-time cylinder strength at the age of loading of the structural specimen
k_t	= ratio of the tensile strength of concrete in flexure to the short-time cylinder strength at the age of loading of the flexure specimen
t	= duration of loading in general

Dimensions and Loads

A_s	= area of reinforcing steel used in the tensile zone of a member
A'_s	= area of reinforcing steel used in the compressive zone of a member
b	= width of a member in general
b_c	= width of a column
b_B	= width of a beam
BM	= bending moment in general
d	= distance from the compression face of a member to the centroid of tension steel
d'	= distance from the compression face of a member to the centroid of compression steel
DL	= uniform dead load
e	= eccentricity of axial load in general

LIST OF SYMBOLS (Continued)

e_1	= the smaller of the two column end eccentricities
e_2	= the larger of the two column end eccentricities
L_B	= length of a beam
L_C	= length of a column
L_C/t_C	= slenderness ratio of a column
P	= axial load on a column
PULT	= ultimate axial load of a column under short-time loading
t	= depth of a member in general
t_C	= depth of a column
t_B	= depth of a beam

Analysis Variables

DELS	= variable used in the computation of stress increments
DELE	= variable used in the computation of both strain increments and allowable variations in strain
$\Delta\epsilon$	= strain increment or permissible variation in strain
ΔM_1	= moment increment applied to the fixed end of a fixed ended column bent in double curvature
ΔM_2	= moment increment applied to members at a joint to attain rotation compatibility at the joint
ΔM_B	= permissible variation in beam moment
ΔM_C	= permissible variation in column moment
ΔP_B	= permissible variation in beam axial load
ΔP_C	= permissible variation in column axial load
$\Delta\sigma$	= stress increment

LIST OF SYMBOLS (Continued)

$\Delta\theta$	= permissible variation between member end rotations at a joint
ΔY	= permissible variation in deflection
ϵ_4	= strain at the compression face of a cross-section
ϵ_1	= strain at the tension face of a cross-section
ϵ_s	= strain in the tension steel at a cross-section
ϵ'_s	= strain in the compression steel at a cross-section
ϵ_{\max}	= variable used in the determination of strain increments, permissible variations in strain, and stress increments
f_s	= stress in the tension steel at a cross-section
f'_s	= stress in the compression steel of a cross-section
M	= number of fibres in a cross-section
N	= number of panels in a member
\emptyset	= curvature at a cross-section
R	= equivalent concentrated load on the concrete cross-section
RB	= equivalent concentrated angle change on a beam
RC	= equivalent concentrated angle change on a column
θ	= rotation in general
X	= distance along a member from a datum point
XB	= length of a beam panel
XC	= length of a column panel
y	= distance from the plastic centroid of a cross-section to a fibre
\bar{y}	= distance from the compression face to the plastic centroid of a cross-section

LIST OF SYMBOLS (Continued)

- Y = deflection of a member
- ZZ = variable used in the computation of stress increments, strain increments, and allowable variations in strain

Column Designation

The column designation used consists of a letter describing the type of bending, followed by a number which is the slenderness ratio, followed by a decimal and the percentage of the short-time failure load sustained by the column. For example:

- S-10.30 = column bent in single curvature with a geometrical slenderness ratio of ten, and subjected to a sustained axial load of 0.30 PULT
- D-20.ST = column bent in double curvature with a geometrical slenderness ratio of 20, and subjected to short-time loading to failure

CHAPTER I

INTRODUCTION

1.1 Introduction

The problem investigated in this thesis is the effect of sustained load on the behavior of reinforced concrete columns in frameworks.

During a period of sustained load, concrete experiences time dependent deformations in the form of creep and shrinkage. Although the mechanisms by which these deformations are produced are not clearly understood, their existence can have a significant effect on the behavior of a structure because it is the deformations of a structure which determine the manner in which the structure resists the applied loads.

A large part of the change in the resistance of a structure to load with time can be attributed to column behavior. The secondary moments in columns are increased with time as deflections are increased, and as a result, the stiffness of the column is decreased with time. The result of these stiffness changes is frequently a transfer of moment from the columns to the beam. If the columns are short, the maximum column moments may decrease with time due to redistribution of moments. If the columns are slender, the maximum column moments will increase with time due to the increase in the deflections under sustained load, but the increase in maximum moment will be partly offset by the redistribution. Thus a short column in a frame may be strengthened by the effects of sustained load while a slender column might be weakened.

Previous investigations into the effect of sustained load on column behavior have been primarily concerned with hinged end columns. Noteable exceptions include several sustained load tests of closed, rectangular, reinforced concrete frames conducted in recent years at the University of Texas (4,14)*, and also the analytical investigations of Broms and Viest (6) and Pfrang (32) who have added linearly elastic restraints to their sustained load column models. In the case of hinged end columns, results have been obtained by subjecting the column to a sustained axial load acting through an end eccentricity, an initial deflected shape, or both, and then measuring or calculating the resultant deformations. These results may show the behavior of a column as a separate element, but they do not give a clear picture of how a column will behave in a framework because changes in column stiffness with load and time are not reflected as changes in the loads applied to a hinged column.

The analytical investigations of elastically restrained columns under sustained load may give a clearer picture of frame action. However, the applicability of the results is not known because actual column restraints are not always linearly elastic, and because the correlation between an elastic restraint and an actual beam under sustained load has not been established.

The sustained load tests of closed rectangular frames, such as those conducted at the University of Texas, give perhaps the clearest picture of the effect of frame action on the behavior of columns under sustained load. Unfortunately, the time element involved in experimental investigation limits the extent of the investigation and results must be extrapolated

*Numbers in parentheses refer to references listed at the end of the thesis.

to predict behavior under longer durations of loading.

The use of an analysis to determine the behavior of restrained reinforced concrete columns under sustained load removes the problem of the time element present in experimental investigation. The analysis, however, should be supported by experimental test results. This approach has been adopted in this thesis.

The remainder of this chapter gives a preview of the thesis contents along with the extent of the investigation.

1.2 The Present Investigation

The investigation in the thesis can be divided into essentially four parts; the review of the work of previous investigators, the development and verification of the method of analysis, the application of the method of analysis to an investigation of long columns in frameworks, and the discussion, conclusions, and recommendations of the research.

The work of previous investigators is discussed in CHAPTER II. The review deals primarily with the effect of sustained load on the behavior of reinforced concrete columns, but the related topics of creep in metal columns and short-time loading of reinforced concrete columns are also mentioned. The purpose of the review was to establish the extent of the experimental investigations and the assumptions of the analytical investigations. The results and conclusions are mentioned, but in general, these are only qualitative because of the limited extent of the investigations. The limitations of previous investigations are included at the end of CHAPTER II.

The method of analysis used in this thesis is developed in

CHAPTERS III, IV, V, and VI. The properties of concrete and reinforcing steel assumed in the analysis are discussed in CHAPTER III. They were based on the investigations available in engineering literature and are empirical in form. Concrete was assumed to be a visco-elasto-plastic material which also exhibits shrinkage. Because of the variable nature of concrete of different compositions under different curing and loading conditions, an attempt was made to define the properties for the set of conditions assumed for the investigation of columns in frames. In checking experimental data obtained for conditions other than those assumed, the appropriate concrete properties can be used in the analysis. Concrete creep data was included as creep vs stress to strength ratio curves, each of which applied to a different duration of loading. The rate of creep method was used to transform this constant stress creep data to a variable stress problem. Reinforcing steel was assumed to be an idealized elasto-plastic material.

The method of analysis is outlined in CHAPTER IV and is general in its derivation. Each structural member considered was divided into a number of cross-sections which in turn were subdivided into a number of fibres. The stress-strain-time behavior of each fibre was then analysed considering time as a discrete variable. The fibres were connected by the assumption of plane strain at any cross-section. The internal load and moment at a cross-section were determined by numerical integration and were made compatible with the external load and moment using a trial and error procedure. Member deformations were also computed using numerical integration procedures. The compatibility between deformations and moments at a joint in a structure was then established by another trial and error

procedure.

CHAPTER V discusses the sources of errors which are present in the proposed method of analysis. The sources considered were discreteness in the analysis and the permissible variations of closure in the trial and error procedures. Conclusions were drawn as to the extent of discreteness which can be used in the analysis without appreciable error.

The development of the method of analysis is completed in CHAPTER VI where the results of the analysis are compared to the results of experimental investigations of beams, columns, and frames. In most cases, a good correlation was obtained with the experimental test results.

In CHAPTERS VII and VIII, the analysis derived in CHAPTERS III to VI is used to investigate a number of laterally restrained beam-column frameworks. The columns were bent in either symmetrical single curvature or were fixed at one end to produce double curvature. The major variables of the investigation were column slenderness ratio and level of sustained load. The columns were quick loaded to failure if failure did not occur during a hypothetical duration of sustained load of 25 years. Constants of the investigation were the column cross-section properties, the beam properties, and the fixed end moment of the beam. A complete description of the investigation is included in CHAPTER VII and the results of the investigation are presented in CHAPTER VIII with regard to load-moment behavior, deformations, stresses, and failure loads.

The discussion, conclusions, and recommendations of the research are presented in CHAPTERS IX and X.

CHAPTER II

REVIEW OF PREVIOUS WORK

2.1 Introduction

The behavior of reinforced concrete columns under sustained load has attracted considerable interest in recent years. Analytical investigations include those by Dischinger (8,9), Prentis and Ross (36), Krieg (22), Ostlund (30), Broms and Viest (6), Naerlović - Veljković (25), Warner and Thurlimann (46), Holley and Mauch (18), Pfrang (32), Distefano (10), and Green (16). Because of the time involved, experimental investigations have not been as numerous. The principal tests of columns under sustained load include those by the ACI Column Committee (2), Viest, Elstner, and Hognestad (45), Gaede (15), Breen and Ferguson (4), Furlong and Ferguson (14), and Green (16).

Related topics have also attracted considerable investigation. These topics include the behavior of metal columns at high temperatures under sustained load, and the behavior of reinforced concrete columns under short-time loads.

The work of the previous investigators is briefly reviewed in the remainder of this chapter. The discussion of these investigations pertains generally to the scope of the experimental investigations and the assumptions of the mathematical models. A discussion of the individual results is not emphasized because the results are qualitative and in general all point to an increase in long column effect under sustained load.

A discussion of the limitations of the previous investigations is included at the end of this chapter.

2.2 Metal Columns Under Sustained Load

Some metals experience very large creep strains at elevated temperatures. This is in contrast to the smaller creep strains experienced by concrete at ordinary temperatures. Because of this major difference in the behavior of the two materials, and because the columns in this thesis are composed of both concrete and steel, an analytical investigation of the effect of sustained load on the behavior of reinforced concrete columns must proceed along different lines from those normally proposed for metal column investigations.

An excellent discussion of the creep buckling of idealized visco-elastic columns and an extensive list of references are presented by Hoff (17).

2.3 Short-Time Loading of Concrete Columns

Extensive analytical and experimental investigations have been made of the behavior of reinforced concrete columns under short-time load.

The analytical investigations have essentially used the general theory of von Karman (21) with the addition of a varying number of simplifying assumptions. The more recent analytical investigations include those of Broms and Viest (6), Pfrang and Siess (33,34), Breen (3), and Chang (7). Pfrang and Siess (33) present a good review of analytical column investigations prior to 1961.

The short-time strength of reinforced concrete columns has been extensively studied experimentally. Two of the major investigations have been those of the ACI Column Committee⁽²⁾ on axially loaded columns and

Hognestad (19) on eccentrically loaded columns. A complete list of reports published by the ACI Column Committee as a result of their investigation is included in the ACI Bibliography No. 5 (2) on Reinforced Concrete Columns. More recent experimental investigations at the University of Texas (3,4,13,14) consider the column as an element of a closed rectangular frame.

2.4 Experimental Investigations of Reinforced Concrete Columns Under Sustained Load

The ACI Column Committee (2) included sustained load tests as part of their extensive column investigation of 1930-34. Because the columns tested were short, axially loaded columns, observed changes in column strength were primarily due to changes in concrete strength rather than creep or shrinkage of the concrete.

Another extensive sustained load investigation was conducted in 1956 by Viest, Elstner, and Hognestad (45). Again the columns were short columns and the effect of the dimensional instability of the concrete was small. These columns were eccentrically loaded.

Gaede (15), in 1958, tested 16 pin ended columns of varying length under a sustained eccentric load. He compared the experimental results with theoretical results based on the work of Krieg (22). Gaede reported a good correlation between test results and theory and also reported a definite decrease in the buckling strength of the columns as a result of the creep of concrete.

In 1964, Breen and Ferguson (4) reported an extension of Breen's original short-time tests (3) on closed rectangular frames to include one test under a sustained load of 90 days duration. This frame was quick

loaded to failure following the duration of sustained load. They reported that the increase in the concrete strength during the period of sustained load more than offset the detrimental effects of the increased column deflection due to creep. Furlong and Ferguson ⁽¹⁴⁾ conducted a similar test as an extension of the work of Furlong ⁽¹³⁾ but found a reduction in overall strength due to the sustained load.

Green ⁽¹⁶⁾, in a recent investigation at the University of Texas, has reported sustained load tests of ten columns. These columns, which were unrestrained and of constant cross-section and length, were subjected to a sustained eccentric load for an approximate duration of loading of nine months. The major variables of the investigation were intensity of sustained load, and magnitude of end eccentricity. Green reported that the time dependent deformations did not approach limiting values at the end of the relatively short loading periods considered.

2.5 Analytical Investigations of the Effect of Sustained Load on the Behavior of Reinforced Concrete Columns

In 1937 and 1939, Dischinger ^(8,9) published a series of papers on a theoretical study of pin ended reinforced concrete columns under sustained load. The major simplifying assumptions were linear relationships between stress and creep strain and stress and instantaneous strain.

Prentis and Ross ⁽³⁶⁾, in 1948, studied the effect of creep on slender reinforced concrete columns with hinged ends. They assumed that concrete exhibited linear elastic behavior and considered the effect of creep by using an effective or reduced modulus of elasticity.

Krieg ⁽²²⁾, in 1954, investigated the buckling load of pin-ended columns having a slight initial curvature. His analysis assumed a non-

linear elastic stress-strain relationship and a linear relationship between instantaneous and creep deformations. This analysis was based on the general theory of von Karman. Krieg did not consider the redistribution of stress from concrete to steel with time which occurs when the concrete deforms relative to the steel.

In 1957, Ostlund (30) used a linearly elastic stress-strain relationship for short-time loading of concrete and introduced the exponential creep-time relationship of McHenry (24) to predict creep strains. Using the work of McHenry, the creep under varying stress is estimated through superposition of creep-time curves obtained under constant stress. From results for pin-ended columns, Ostlund concluded that the reduction in buckling strength of a concrete column due to creep is determined solely by that part of the creep which is independent of the age at first loading. In addition, he recommended the use of a reduced modulus of elasticity in a short-time analysis to predict the influence of creep.

Broms and Viest (6) included several sustained load investigations in their papers on short-time stability of long columns. The theory used for short-time loading was that of von Karman with the additional assumption of a cosine wave deflected shape. To determine the behavior of a column under sustained load, Broms and Viest modified the Hognestad (19) stress-strain curve used for short-time loads to account for creep. The modification consisted of multiplying the strain abscissae by two. Broms and Viest used this reduced modulus approach to analyse both pin ended and restrained columns. The assumed restraints were linearly elastic and did not creep.

Naerlović - Veljković (25), in 1960, used as his model a pin

ended, initially bent, axially loaded, prestressed concrete column. Concrete was assumed to be non-linearly elastic but linearly viscous. The deflected shape was approximated by a sine wave. Instability apparently occurred when the concrete crushed or the steel yielded.

Warner and Thurlimann ⁽⁴⁶⁾, in 1962, recommended several innovations in the mathematical model. These included:

1. a short-time stress-strain curve for concrete represented by three straight lines
2. the concrete strength was assumed to decrease exponentially with time to a value reflecting the long time sustained load effect on concrete strength
3. a non-linear stress-creep strain relationship for high concrete stresses.

They calculated the critical eccentricity of a pin ended column with an idealized cross-section consisting of two flanges and a web of zero thickness. The critical eccentricity for a given axial load is defined as the eccentricity below which an infinite life time results. In the calculation of this eccentricity, their analysis reduces to one which considers only the linear elastic and linear viscous portions of their proposed concrete behavior functions.

In 1963, Holley and Mauch ⁽¹⁸⁾ investigated the creep buckling of unrestrained, initially crooked, pinned, rectangular columns with symmetrical reinforcement. Their method of evaluation of concrete strain was perhaps the most realistic of recent analytical investigations. By considering the cross-section as composed of a finite number of fibres, they were able to allow for a varying stress-time condition in any fibre. The

creep in any fibre under a varying stress-time condition was evaluated using both the rate of creep and the superposition methods of estimating creep under variable stress. The instantaneous component of strain was evaluated considering the inelastic behavior of concrete. When applying this method of analysis to the investigation of column behavior, Holley and Mauch simplified the calculations by assuming that the deflected shape of the column could be represented by a portion of a sine wave. Using this assumption, only one point along the column length need be analysed.

In 1964, Pfrang ⁽³²⁾ extended his short-time investigations of restrained and unrestrained long columns to include time effects. Using an effective modulus approach, Pfrang noted that in some cases, the capacity of the restrained columns was increased by viscous effects. This occurred if the restraint moment decreased at a faster rate with time than the deflection moment increased. Pfrang investigated various values of the effective modulus but did not attempt to correlate the values to specific durations of loading. The restraints considered were linearly elastic.

Distefano has been concerned with a completely mathematical formulation of the creep buckling problem. In his latest paper ⁽¹⁰⁾, in 1965, he has extended the application of Volterra's theory of hereditary phenomena to include into his analysis the non-linearity of creep with applied stress. The complexity of the mathematics makes his method difficult to apply to non-homogeneous materials. In applications to reinforced concrete sections, Distefano has considered an idealized I section. For practical use, he recommends the use of a reduced modulus approach.

Green ⁽¹⁶⁾ has formulated a method of analysis which shows a good correlation with the experimental results of his investigation and also

with the investigations of Viest, Elstner, and Hognestad (45), and Gaede (15). The method of analysis is essentially a reduced modulus approach, but Green has defined the reduced modulus in terms of observed creep behavior. Using the derived stress-strain-time diagrams, the response of a column section was represented in terms of unique moment-curvature-load-time diagrams. An iteration process was used to predict column behavior using these diagrams.

2.6 Conclusion

Previous investigations have not adequately determined the behavior of reinforced concrete long columns in frameworks under sustained load. While experimental investigations give the best indication of behavior, only the investigations at the University of Texas (4,14) have included the column as an element in a framework. However, a duration of loading of only 90 days was considered in these investigations.

Because of the time element involved, many of the investigations have been analytical. The majority of these investigations are limited in their applicability by the varying number of simplifying assumptions which have been made, particularly with regards to concrete properties and the method of column restraint. A method of analysis which is not limited in application should consider the effects of variations in stress with time, inelastic behavior of concrete, non-linear response of the restraint, and creep and shrinkage in the restraint, as all of these factors will influence column behavior.

CHAPTER III

MATERIAL PROPERTIES

3.1 Introduction

This thesis deals with columns made up of two materials; concrete and steel. The properties of both materials have been derived empirically from the investigations available in engineering literature, and are outlined in this chapter.

The properties of concrete have been derived with respect to a fixed set of composition, curing, and loading conditions. These conditions, which are stated in SECTION 3.3.1, were assumed to apply to the investigation of columns in frameworks in CHAPTERS VII and VIII. For other than this fixed set of conditions, the properties may have to be altered.

The properties defined in this chapter were used in this thesis, but they can be changed for future applications of the analysis. In other words, they need not limit the applicability of the analysis.

3.2 Steel Reinforcement

Steel has been assumed to be an ideal elasto-plastic material. Strain hardening, rupture, and buckling of the reinforcement were not considered because of the small strains experienced when in combination with concrete. Creep or relaxation of steel under sustained stress was also neglected. The assumed stress-strain law for reinforcing steel is shown in FIGURE 3.1.

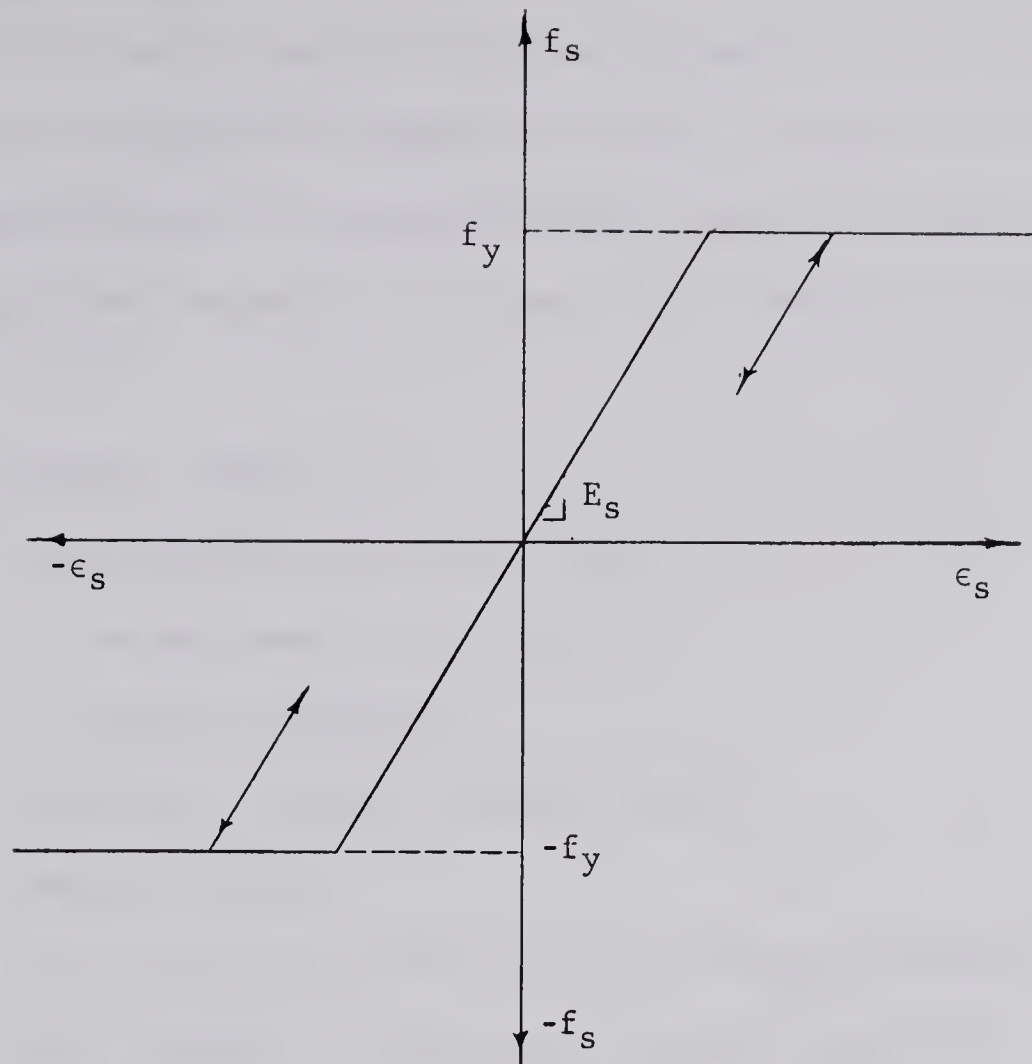


FIGURE 3.1

ASSUMED STRESS-STRAIN BEHAVIOR
FOR REINFORCING STEEL

3.3 Concrete

Concrete was assumed to be a visco-elasto-plastic material that also exhibited shrinkage. The idealized stress-strain behavior presented in this section was derived from descriptions of concrete behavior in the engineering literature. The balance of this chapter contains a discussion of the assumptions and idealizations made in deriving mathematical expressions for the concrete behavior under short-time and sustained loads.

3.3.1 Concrete Composition and Curing

It is well known that concrete properties vary with the composition of concrete and the type of curing. In order to be consistent in the presentation of a concrete behavior theory, the composition and the curing of the concrete were assumed to be constant at the following values.

1. Concrete composition:

- (a) aggregate/cement (wt) = 6.0
- (b) water/cement (wt) = 0.60
- (c) granite aggregate
- (d) Type I (normal) Portland Cement

2. Concrete curing:

- (a) seven days at 100% relative humidity and 70°F
- (b) remainder at 50% relative humidity and 70°F

3. Age of concrete at first application of load = 28 days.

The laboratory investigations of existing engineering literature used in this section have been chosen to comply approximately with the above specifications. Where this was not possible, the results of other literature have been modified using the work of various investigators to apply to these conditions.

3.3.2 Prediction of Total Concrete Strain for any Loading History

Concrete experiences three modes of deformation when subjected to normal structural conditions. These are:

- (a) instantaneous deformation including both recoverable (elastic) and irrecoverable (plastic) strains

(b) creep deformation

(c) shrinkage deformation

By assuming that each of these component strains can be assessed independently, the total strain of concrete for any loading history can be computed from

$$\epsilon_T = \epsilon_{IN} + \epsilon_{CR} + \epsilon_{SH}$$

A relationship of this form has been used previously by Bresler and Selna⁽⁵⁾.

An independent prediction of each component implies that creep and shrinkage are not related phenomena. Since this is not strictly correct⁽²⁸⁾, the creep prediction curves used in this thesis were obtained in the presence of shrinkage in order to minimize the error which could result from this assumption.

3.3.3 Failure of Concrete

Concrete was assumed to fail in compression when the instantaneous component of total strain exceeds a maximum permissible strain, ϵ_u , and to fail in tension when the tensile stress exceeds the tensile strength.

The maximum fibre strain in a concrete cross-section at failure under eccentric short-time load has been shown by Rüsçh⁽⁴⁰⁾ to depend on concrete strength, rate of loading, position of the neutral axis, and the shape of the cross-section. He shows that concrete fails when the load capacity of the section reaches a maximum rather than when the strain reaches a maximum. This helps to explain the wide divergence of values obtained for the parameter, ϵ_u , by various investigators who have not considered one or more of the variables. However, for simplicity in defining the stress-strain curve, a limiting compression strain has been used.

The value of this strain used in this thesis is the well-documented value of 0.0038 obtained by Hognestad (19) in short-time tests of eccentrically loaded, rectangular, reinforced concrete columns.

The tensile strength of concrete was computed using a value of the modulus of rupture listed by Neville (27) and credited to the European Concrete Committee.

$$f_t = 9.5 \sqrt{f'_{ca}} = k_t f'_{ca}$$

where k_t is a constant for any given compressive strength.

3.3.4 Concrete Strength in Compression

Concrete strength is defined as the maximum compressive stress which can be resisted by the concrete in a structure. It is usually taken as some fraction of the compressive strength of six inch by twelve inch cylinders from the same mix. The fraction reflects the inability to obtain the same grade of concrete in a structure as is obtained in the companion cylinders.

In this thesis, the compressive strength of the concrete in a structure was taken equal to $k_3 f'_{ca}$ where f'_{ca} is the standard cylinder strength at the time of first loading. The modification factor, k_3 , was assumed to be constant with time, or in other words, the concrete strength in the structure was assumed to be constant with time.

Rüsch (40) has studied the effect of sustained load on concrete strength, and has shown that two factors have a major effect on the strength-time relationship. Sustained high load tends to cause a reduction in strength, while continued exposure to the atmosphere promotes additional

curing accompanied by strength gain. Which factor has the dominating influence on the strength depends on the age of the concrete at first loading and on the curing conditions. For Rüsch's tests, the curing conditions under load were a relative humidity of 65 per cent and a temperature of 20°C. He shows that with these conditions, a specimen subjected to a high load at an age of ten days experiences an overall strength increase with time, and a specimen subjected to a high load at an age of 56 days experiences an overall strength decrease with time. The effect of intermediate load levels, rather than high load levels, was not investigated.

The influence of normal construction loading and curing conditions on the strength of structural concrete is unknown, but it is not inconceivable, that under the curing conditions assumed in SECTION 3.3.1, very little change in strength will be experienced with time. For this reason, the value of k_3 , and thus concrete strength, have been assumed to be independent of time in this thesis.

Although the relationship between structural concrete strength and cylinder strength is dependent on many factors, particularly in columns, the value of k_3 has been set at 0.85 for the column investigation in CHAPTERS VII and VIII. This value was proposed by Hognestad (19) and further confirmed by Hognestad, Hanson, and McHenry (20).

3.3.5 Effect of Eccentric Loading

Eccentric loading affects both the strength and the failure strain of concrete.

Sturman, Shah, and Winter (42), from tests on micro-cracking of concrete prisms, reported that the presence of a strain gradient in-

creased concrete strength by about 20 per cent over that obtained from the concentric loading of prisms of similar concrete.

Rüsch ⁽⁴⁰⁾ has also studied the effect of eccentric loading on the strength of concrete prisms. He has considered both short-time and sustained loads. According to his tests, the concrete strength under eccentric loading was virtually independent of the duration of the sustained load. With regard to the effect of eccentric loading on concrete strength, Rüsch has plotted the solid curve shown in FIGURE 3.2. By using the non-dimensional form of the average cross-section stress as the ordinate parameter, the effect of eccentricity on concrete strength was not directly visible. In order to determine the nature of this effect, the analytical curve in FIGURE 3.2 was derived using the same parameters, but considering a concrete strength which was independent of eccentricity. This curve is based on the stress-strain curve presented in FIGURE 3.3.

Comparison of the two curves in FIGURE 3.2 indicates that Rüsch found very little change in concrete strength due to eccentric loading.

Using the work of Rüsch, the assumption was made in this thesis that concrete strength is unaltered by eccentric loading.

According to the tests by Sturman, et al, and Rüsch, eccentric loading tends to increase the ultimate concrete strain ϵ_u . The choice of ϵ_u made in SECTION 3.3.3 was based on tests which considered eccentric loading.

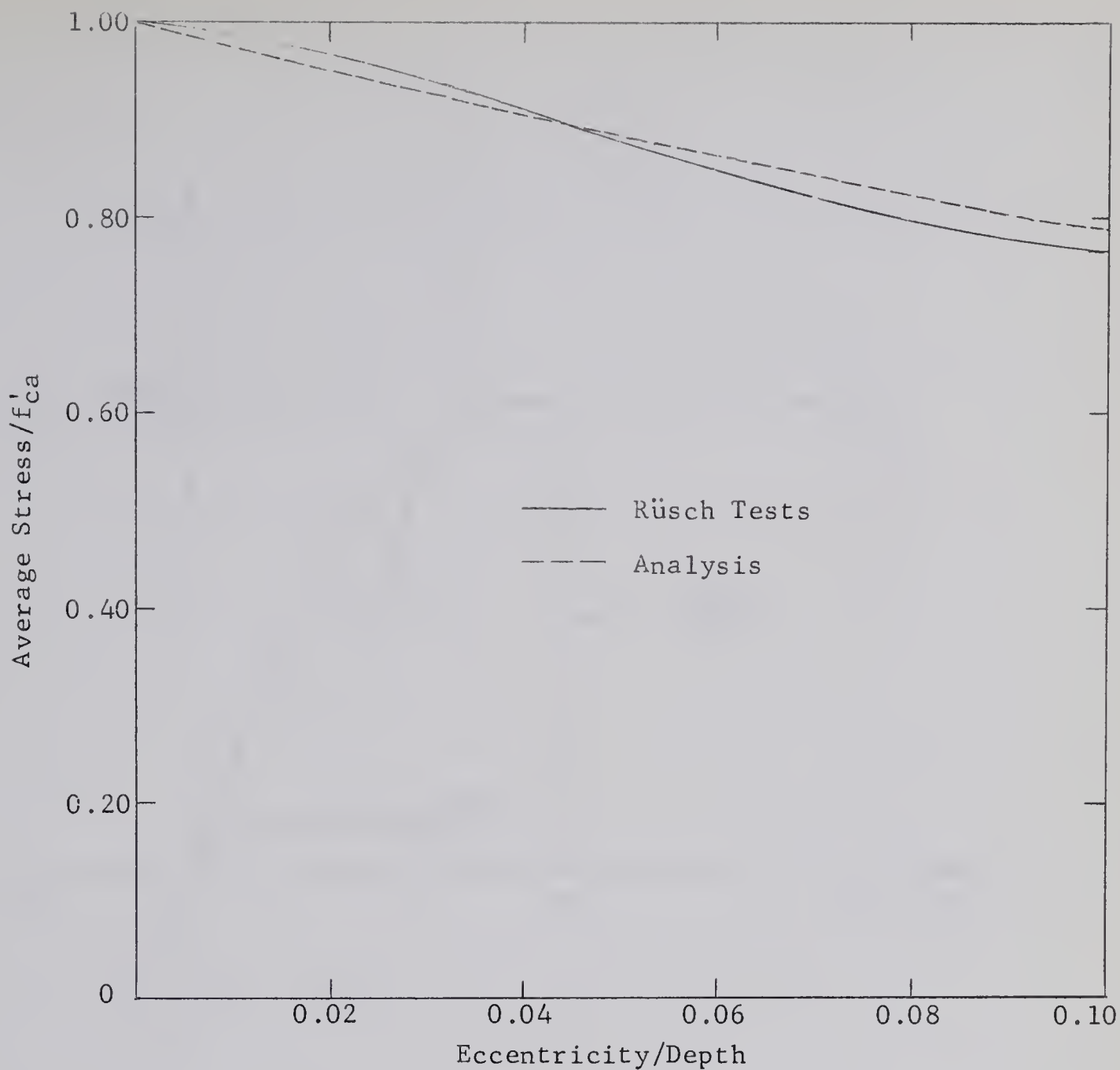


FIGURE 3.2

EFFECT OF ECCENTRICITY ON CONCRETE STRENGTH

3.3.6 Instantaneous Response of Concrete

The instantaneous strain included both recoverable (elastic) and irrecoverable (plastic) strains. The shape of the assumed stress-strain curve and the limits discussed in the preceeding sections are shown in FIGURE 3.3.

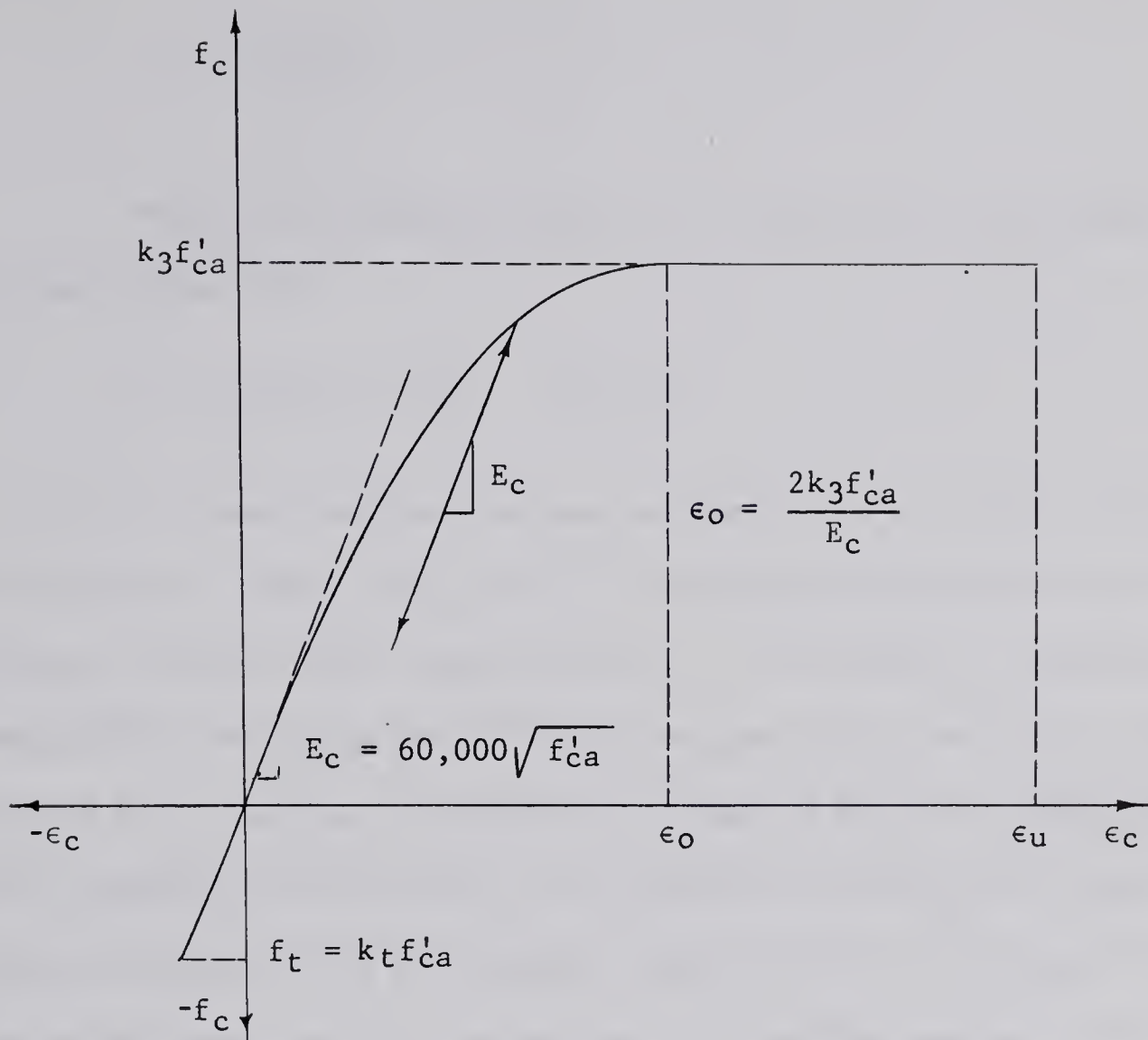


FIGURE 3.3
INSTANTANEOUS STRESS-STRAIN RESPONSE
FOR CONCRETE

The portion of the stress-strain curve from $\epsilon_c = 0$ to $\epsilon_c = \epsilon_0$ was chosen from the work of Hognestad (19). The curve is parabolic in shape and is defined by the equation

$$f_c = k_3 f'_{ca} \left(2 \frac{\epsilon_{IN}}{\epsilon_0} - \left(\frac{\epsilon_{IN}}{\epsilon_0} \right)^2 \right)$$

where

$$\epsilon_o = \frac{2k_3 f'_{ca}}{E_c}$$

The initial tangent modulus E_c was based on the expression derived by Pauw (31)

$$E_c = 60,000 \sqrt{f'_{ca}} \quad (\text{in psi})$$

The initial tangent modulus has been assumed to be a constant with time in this analysis. Washa and Fluck (48) have shown that the modulus of elasticity increases slightly under sustained load. This finding is supported by other investigators including Roll (38) who suggests that the higher strains produced on first loading of concrete, as compared to the strains produced on later unloading, could be due to the localized destruction of particle cohesion experienced by the concrete when initially resisting load. If this is the case, then the assumption of a constant modulus with time may not be in error for structural application, as initial loadings are produced by construction and not by the design loads.

The shape of the stress-strain curve between ϵ_o and ϵ_u was based on the work of Rasch (37) which showed that an increased resistance occurred in this zone under slow rates of straining. The strain rates which are associated with the redistribution of stress under sustained load are assumed to be slow strain rates.

For simplicity, the shape of the stress-strain curve between zero stress and the tensile strength of concrete was assumed to be identical to the initial portion of the compressive relationship.

Unloading and subsequent reloading of concrete are assumed to occur along a line parallel to the initial tangent modulus (5).

3.3.7 Concrete Shrinkage

The shrinkage-time curve derived by Troxell, Raphael, and Davis (44) was adopted for the analysis. This curve is shown in FIGURE 3.4 along with the shrinkage-time curves of several other investigators (12,35,43,47). The Troxell, Raphael, and Davis curve was derived under laboratory conditions which were similar to the conditions assumed in SECTION 3.3.1, and it has the advantage of depicting shrinkage strains up to 25 years.

3.3.8 Concrete Creep

Creep-stress-time relationships are generally determined from tests of specimens under constant sustained stress. Because the stresses in a structure under sustained load are constantly changing, this normal creep data is not directly usable for structural investigation. A method of computation is needed which can apply creep data obtained under constant stress to a variable stress problem.

The rate of creep method discussed by Ross (39) was used to determine creep strain under a varying stress. According to this method, the creep during any increment of time is dependent only on the stress during that increment and not on the previous stress history. The total creep strain after any duration of loading is then obtained by a summation of the creep increments up to that time. A limitation of this method is that no creep recovery occurs on removal of the load.

Although the calculation of creep by the rate of creep method implies a continuous integration of the stress-time function, the method

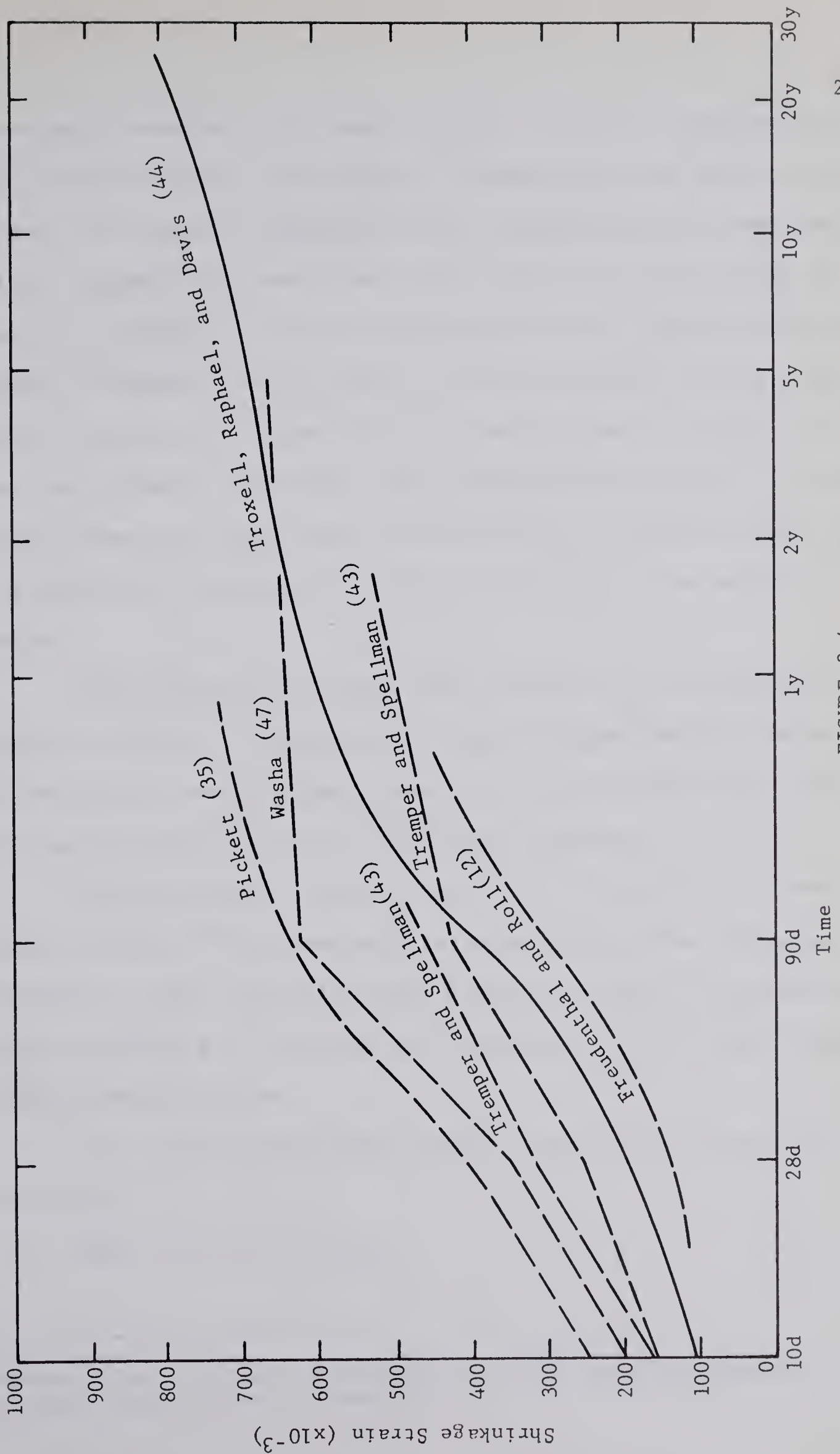


FIGURE 3.4
SHRINKAGE - TIME CURVES

is more easily adapted to the computer using a numerical integration procedure. This was done in this thesis by dividing the time under sustained load into finite time increments and then assuming that the stress during any time increment was constant and equal to the stress existing at the end of the increment. A study of the effects of this type of discretization was made in CHAPTER V and the results indicated that for long durations of loading (25 years), sufficiently accurate results can be obtained using three time increments. The three time increments were selected to divide the total creep into three equal divisions and thus the calculations apply to the approximate durations of loading of seven days, nine months, and 25 years.

Discretization using three time increments for a hypothetical duration of loading of 25 years implies that a reduced modulus approach will give satisfactory results after a duration of load of seven days. This has been shown by Green ⁽¹⁶⁾ to be a justifiable assumption.

The quantitative prediction of creep in this thesis was based on the work of Rusch ⁽⁴⁰⁾ who presented the stress-strain-time curves shown in FIGURE 3.5. These curves have been modified to apply to the conditions assumed in SECTION 3.3.1 and also to be compatible with the other assumptions of the preceeding sections.

The conditions under which Rüsç's curves were derived* are listed below:

1. age of loading = 56 days

*Information from a private communication with H. Hilsdorf, Research Associate, Munich Technical Institute.

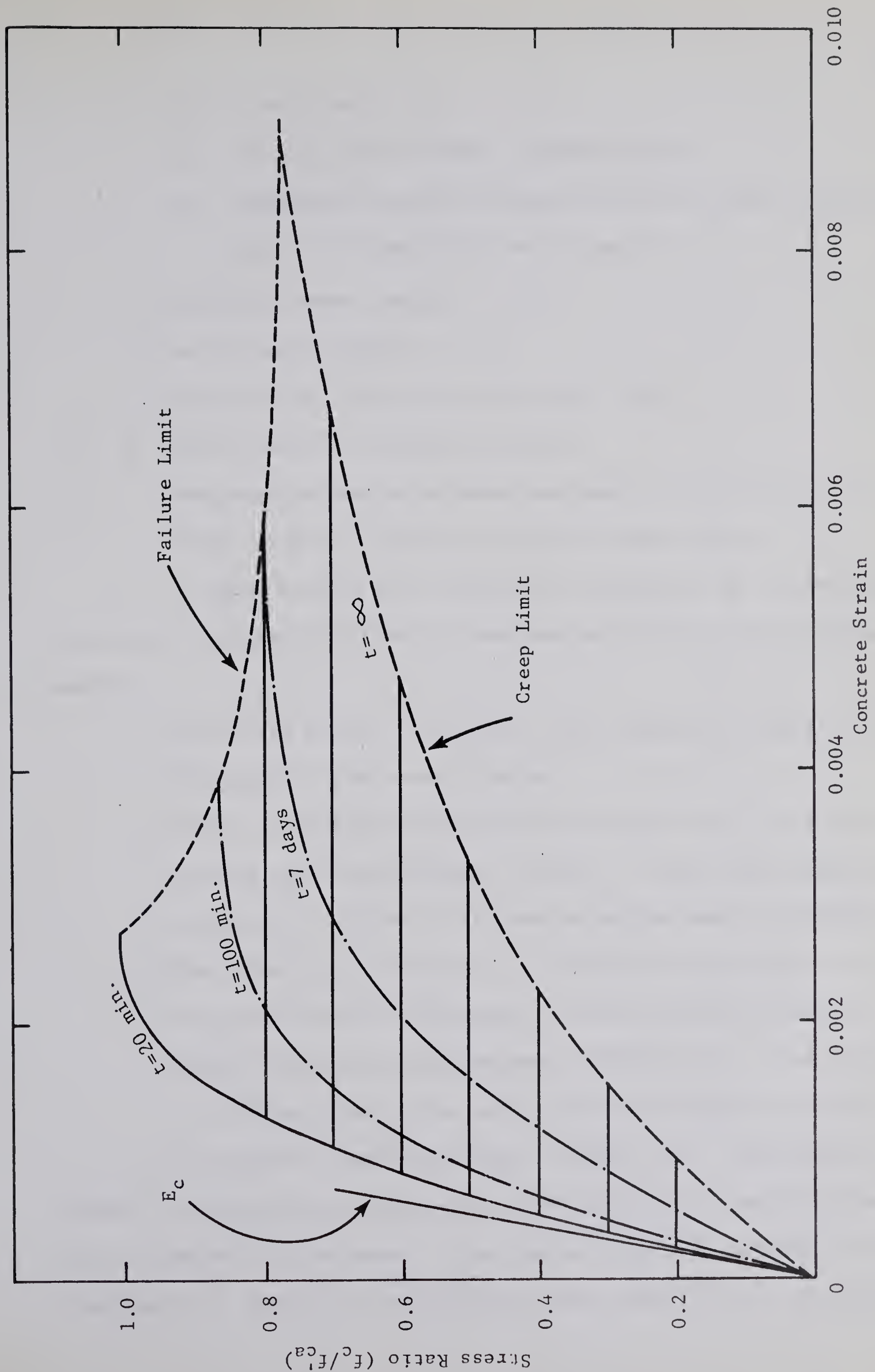


FIGURE 3.5

CONCRETE STRAIN vs STRESS/STRENGTH FOR TESTS BY RÜSCH (1960)

2. curing conditions:

- (a) 7 days at 20°C and 99% relative humidity
- (b) remainder of curing including the period under sustained load at 20°C and 65% relative humidity

3. aggregate/cement (weight) = 5.40

4. water/cement (weight) = 0.55

5. aggregate was Rhine gravel and quartz flour

6. cement was PZ275 (normal portland)

7. shrinkage strains on unloaded specimens were subtracted from total strains to obtain the reported creep strains.

In order to take into account the assumptions of the preceeding sections, the curves of FIGURE 3.5 have been modified in the following manner:

- 1. Short-time strains ($t = 20$ min) were subtracted from all strain abscissae to give creep strains.
- 2. Results were transformed vertically to be tangent to a horizontal failure limit line through $f_c/k_3f'_{ca} = 1.00$. This modification is made in conjunction with the assumption made in SECTION 3.3.4.
- 3. The creep strain abscissae were multiplied by a factor of 1.30 to account for the difference in curing conditions between Rusch's tests and those assumed in SECTION 3.3.1. The choice of 1.30 was based on the work of Troxell, Raphael, and Davis (44).

The modified curves are shown in FIGURE 3.6. Also shown in FIGURE 3.6 are the three creep curves which were used in applying the rate of creep method in this thesis. These curves have been obtained by fitting a mathematical equation to the modified creep limit line ($t = 25$ years)

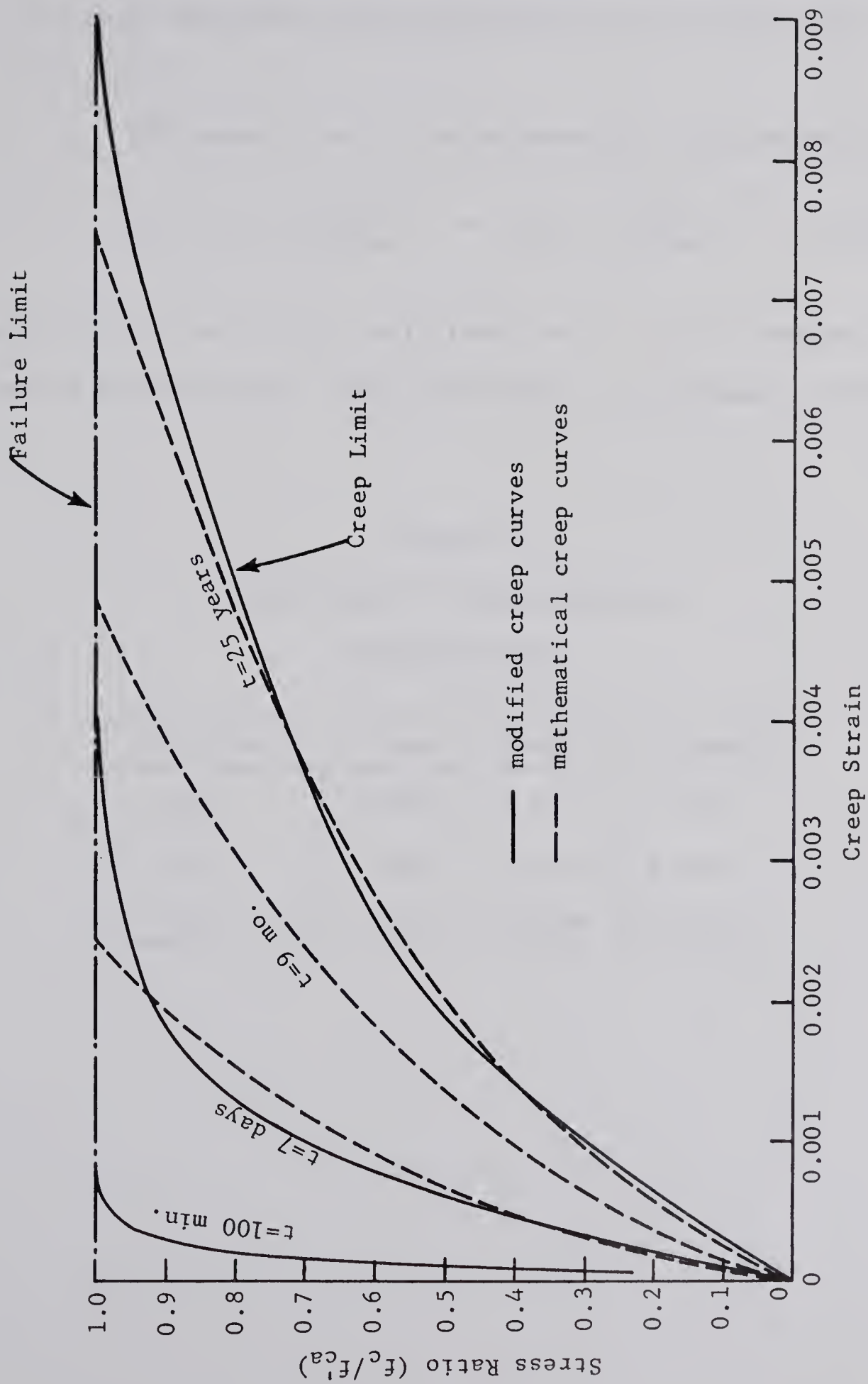


FIGURE 3.6
MODIFIED AND MATHEMATICAL CREEP CURVES

and then dividing the region between this line and the ordinate axis into three regions of approximately equal creep. The curves obtained correspond to the approximate durations of sustained load of seven days, nine months, and 25 years.

The general form of the mathematical creep equation is:

$$\epsilon_{CR} = F1(K) \left\{ \frac{f_c}{k_3 f'_{ca}} \right\}^3 + F2(K) \left\{ \frac{f_c}{k_3 f'_{ca}} \right\}^2 + F3(K) \left\{ \frac{f_c}{k_3 f'_{ca}} \right\}$$

where F1, F2, and F3 are coefficients and K is the reference to the time or loading stages. The coefficients are included in TABLE 3.1.

TABLE 3.1
COEFFICIENTS OF THE MATHEMATICAL
CREEP EQUATIONS

Coefficient	7 days	9 mon.	25 years
F1(K)	0.0009	0.0018	0.0028
F2(K)	0.0008	0.0016	0.0025
F3(K)	0.0007	0.0014	0.0021

When considering other than the three time increments used above, the coefficients of the mathematical creep equations can be evaluated from the following empirical formulae:

$$F1(K) = 0.0009 (0.64 \log_{10} t + 0.4)$$

$$F2(K) = 0.0008 (0.64 \log_{10} t + 0.4)$$

$$F3(K) = 0.0007 (0.64 \log_{10} t + 0.4)$$

where t = duration of loading in days.

A modification of the curves of FIGURE 3.6 to account for concrete strength has not been made. The creep relationships were assumed to be a function of the parameter $f_c/k_3f'_{ca}$ rather than the stress.

The proposed creep relations were also assumed to apply for concrete in tension. In this case, the absolute value of stress must be used in the cubic equations and the calculated result assigned a negative sign.

3.4 Conclusion

The properties of concrete and reinforcing steel outlined in this chapter have been formulated with the aid of many assumptions. These assumptions are limitations of the method of analysis developed in CHAPTER IV.

The variables discussed in CHAPTER III are assigned numerical values prior to their use in the thesis. Although some of the variables have been assigned numerical values in this chapter, these values apply specifically to only the frames investigated in this thesis. For a correlation of the analysis to existing tests, the values of the variables, particularly those associated with creep and shrinkage, must comply with

the actual conditions of the test rather than with the conditions assumed in SECTION 3.3.1. Transformation of creep data for this purpose can be made using the work of Neville and Meyers (28).

CHAPTER IV

METHOD OF ANALYSIS

4.1 Introduction

The method of analysis used in this thesis combines trial and error procedures and numerical integration to determine the equilibrium configurations of structural elements under load.

There are two possible combinations of loading stages considered in this thesis:

1. Short-time loading of a member. All loading stages in this case are associated with the application of increments of short-time load.
2. Short-time loading to a working load level, followed by a period of sustained load at this load level, followed by quick loading to failure. In this case, the first loading stage is associated with the application of short-time load to the level of working load. Up to three loading stages are then applied which are associated with the application of time increments under the level of sustained working load. Subsequent loading stages are again associated with the application of increments of quick load.

The analysis can be divided into four major parts:

1. the analysis of a fibre
2. the analysis of a cross-section composed of a number of fibres

3. the analysis of a member composed of a number of cross-sections
4. the analysis of a framework composed of a number of members.

The four stages of analysis are related to one another by the equilibrium and compatibility of the elements in the model being studied.

The following paragraphs include the assumptions, the sign convention, and a detailed description of the four stages of the analysis. The final section of this chapter emphasizes the limitations of the analysis.

The analysis has been adapted for use on the IBM 7040 digital computer at the University of Alberta. The computer flow diagrams of APPENDIX A are referenced in this chapter to facilitate the description of the analysis.

4.2 Assumptions of the Analysis

4.2.1 Assumptions of the Fibre Analysis

A concrete fibre is defined as the element of the cross-section obtained by passing two parallel planes through the section in a direction perpendicular to both the plane of the cross-section and the plane of principal bending.

The assumptions of fibre analysis are:

1. The material properties of CHAPTER III are applicable.
2. The fibre stress is constant under any loading stage. A loading stage is defined as either an application of an increment of external load (quick loading) or an application of a time increment in the case of sustained load.

4.2.2 Assumptions of Cross-Section Analysis

The following assumptions are made in analyzing a cross-section:

1. The cross-section is composed of a finite number of fibres equally spaced over the depth of the section.
2. Sections perpendicular to the axis of a member, that are plane before loading, remain plane after loading whether the loading is sustained or quick. The effect of shear on the strains, normal stresses, and deflections is thus considered as negligible.
3. Perfect bond exists between concrete and reinforcing steel at all times.
4. Numerical integration procedures satisfactorily predict the internal load and moment at a cross-section.
5. The cross-section is considered to have failed when one of the component fibres has failed in compression.
6. Bending of a cross-section occurs about one principal axis only. This implies that component fibres have a constant behavior over their width.
7. The area of the concrete displaced by the reinforcing steel is neglected.

4.2.3 Assumptions of Member Analysis

1. The member is composed of a finite number of cross-sections equally spaced over the length of the member.
2. Numerical integration procedures satisfactorily relate the internal behavior of the member to the external boundary conditions.
3. Deflections are small compared to the length of the member.

4.2.4 Assumptions of Frame Analysis

1. The end rotations of members at a common joint are equal to one another.
2. The unbalanced moment at a joint is distributed to the members according to their relative stiffnesses at the time under consideration.
3. The effect of axial deformations is negligible.

4.3 Sign Convention

The following sign conventions have been used in this analysis:

1. Compressive stresses and strains are positive.
2. A beam moment that causes compression in the top face of the beam is positive.
3. A column moment that causes compression in the right face of the column is positive. (It is assumed that the beam is located to the left of the column).
4. A positive curvature is associated with a positive moment.
5. Positive rotations and deflections are associated with positive values of curvature.

4.4 Analysis of a Fibre

The analysis of a fibre is the direct application of the material properties of CHAPTER III to the concrete of a structural member exposed to the various possible loading stages.

Each cross-section is divided into a number of fibres as shown in FIGURE 4.1. A fibre is analysed at its edge points L after each loading stage.

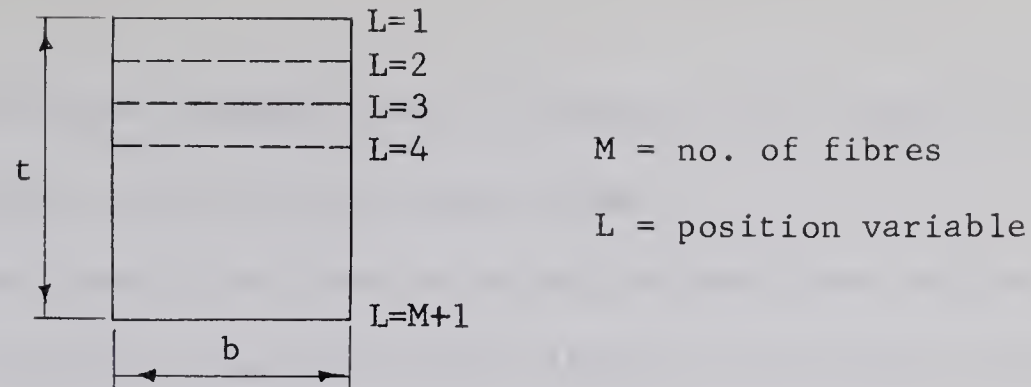


FIGURE 4.1

DIVISION OF A CROSS-SECTION INTO FIBRES

The analysis described in the following paragraphs is depicted diagrammatically by the flow diagram of APPENDIX A.2. The computer terminology is defined in APPENDIX A.1.

4.4.1 Establishment of Stress-Strain Compatibility

For a known value of strain at any point L , the compatible value of stress is determined by trial and error. Starting with an initial assumed value of stress, the total strain is computed and compared to the known value of strain. If agreement between strains is not obtained, the stress is incremented and the procedure is repeated until the computed strain and the known strain differ by a quantity less than a predetermined permissible variation in strain.

4.4.2 Initial Assumption of Fibre Stress

To facilitate convergence of the trial and error procedure, the initial assumed value of fibre stress should be as close as possible to the actual fibre stress.

For the first application of load, all fibre stresses were initially assumed to be zero. The initial assumption of fibre stress for

subsequent load stages, whether quick or sustained, was taken as the value existing at the end of the previous load stage.

If the stress in a fibre is calculated more than once during any load stage (as will occur when redistribution of moment is considered), the initial assumption of stress was that obtained in the previous calculation.

4.4.3 Calculation of Strain from Stress

Concrete strains are calculated using the following expression which has been discussed in SECTION 3.3.2.

$$\epsilon_T(K) = \epsilon_{SH}(K) + \epsilon_{IN}(K) + \epsilon_{CR}(K)$$

where K is the number of the loading stage

(a) Shrinkage component $\epsilon_{SH}(K)$

When sustained loading stages are considered, the shrinkage strain existing at the end of the time increment can be read directly from the curve of Troxell, Raphael and Davis ⁽⁴⁴⁾ in FIGURE 3.4.

The shrinkage component of strain for the quick loading stages which follow the sustained load stages is equal to the shrinkage strain at the end of the sustained load period.

(b) Instantaneous component $\epsilon_{IN}(K)$

The instantaneous component of total strain can be determined from the concrete stress-strain curve of FIGURE 3.3. Whether or not the unloading-loading branch is to be used is determined by a comparison of the fibre stress in the loading stage being considered to the corresponding fibre stresses in the previous loading stages.

(c) Creep component $\epsilon_{CR}(K)$

The creep component of total strain is calculated using the rate of creep method and the curves of FIGURE 3.6 as outlined in SECTION 3.3.8. For the quick loading stages following the sustained loading stages, the fibre retains the creep strain existing at the end of the sustained loading period.

4.4.4 Permissible Variation in Fibre Strain

The maximum permissible variation in fibre strain for any loading stage K is preset at a value of $DELE(K)$. $DELE(K)$ is the variation allowed in a fibre exposed to maximum stress. For fibres exposed to stresses less than the maximum value, the permissible variation is some fraction of $DELE(K)$ according to the following relationships.

$$\text{let } ZZ = \frac{\epsilon_{IN}(K)}{\epsilon_{max}(K=1)}$$

where $\epsilon_{IN}(K)$ = instantaneous component of total strain in the fibre under loading stage K .

$\epsilon_{max}(K=1)$ = strain in the fibre under short-time loading when the maximum stress is first reached

for $ZZ \leq 0.50$

$$\Delta\epsilon = \frac{DELE(K)}{4(1-ZZ)}$$

$$0.50 < ZZ \leq 1.00$$

$$\Delta\epsilon = DELE(K) * ZZ$$

and for $ZZ > 1.00$

$$\Delta\epsilon = DELE(K)$$

where $\Delta\epsilon$ = permissible variation in strain.

The permissible variation in strain is reduced for lightly stressed fibres to keep the associated stress error, which is generated by the allowable variation in strain, to a minimum. If the reduction is not made, the stress error can be high in lightly stressed fibres because of the non-linear nature of the stress-strain relationship.

4.4.5 Incrementing of Fibre Stress

The stress increment should not generate a strain increment greater than two times the allowable variation in strain. If this occurs, the trial and error procedure will not converge. Using the terminology of SECTION 4.4.4, the following stress increments were established by considering the non-linear stress-strain relationships.

for $ZZ \leq 0.50$

$$\Delta\sigma = \text{DELS}(K)$$

for $0.50 < ZZ \leq 1.00$

$$\Delta\sigma = 2\text{DELS}(K) (1-ZZ)$$

for $ZZ \geq 1.00$

$$\Delta\sigma = \text{DELS}(K)$$

where $\Delta\sigma$ = stress increment

$\text{DELS}(K)$ = maximum possible stress increment.

The quantity $\text{DELS}(K)$ need not be exactly preset. If the initial

choice of DELS(K) is too high to allow for convergence of the procedure, the computer analysis allows for incrementing of DELS(K) until convergence occurs.

4.4.6 Fibre Failure

A fibre fails according to the material property assumptions outlined in SECTION 3.3.3.

When a compression failure occurs, the fibre can no longer carry load of any type. However, when a fibre cracks due to tension it can no longer carry a tensile load but can carry a compression load if the need arises. Although tensile creep was included, a tensile crack was assumed to close immediately on stress reversal.

4.5 Analysis of a Cross-Section

The analysis of a cross-section is the direct application of the assumptions of SECTION 4.2.2 to the problem of determining an internal load and moment compatible with the known external load and moment acting on the cross-section.

The flow diagrams of APPENDIX A.3 give a diagrammatical representation of the analysis applied to a beam cross-section with no compression steel and a column cross-section with symmetrical reinforcement. The notation used in the computer flow diagrams and programs is defined in APPENDIX A.1.

4.5.1 Establishment of Load and Moment Compatibility

A trial and error procedure is used to determine the internal load and moment at a cross-section compatible with known values of applied load and moment.

A strain distribution is first assumed and the internal load and moment associated with it are calculated. The calculated load and moment are then compared to the applied load and moment. If the comparison is not favorable, the assumed strain distribution is incremented and the procedure repeated until the respective quantities differ by less than a prescribed permissible variation in load and moment.

4.5.2 Calculation of Internal Load and Moment

The cross-section of the beam or column was assumed to be composed of a finite number of discrete fibres as shown in FIGURE 4.1. For any linear strain distribution, the stress at the edge of each fibre can be calculated from the fibre analysis outlined in SECTION 4.4. FIGURE 4.2 shows the relationship between the fibre location and the stress and strain distributions.

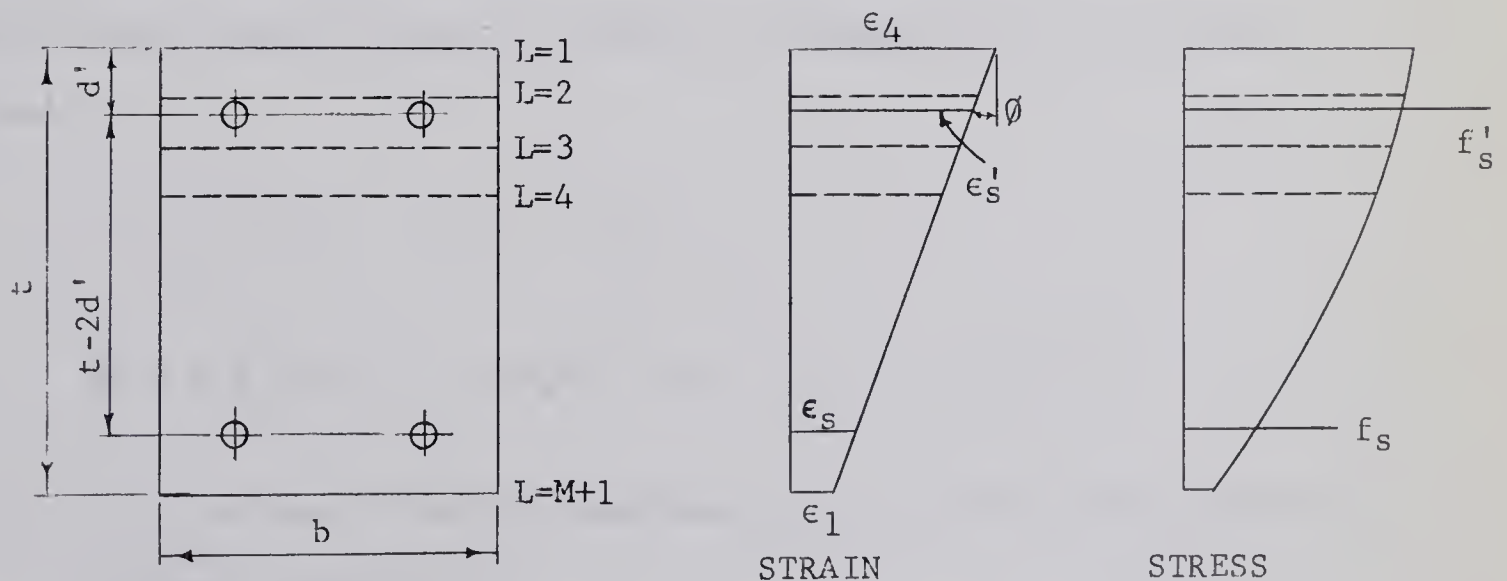


FIGURE 4.2

CROSS-SECTION UNDER LOAD AND MOMENT

The steel strains can be readily computed from the strain distribution.

$$\epsilon'_s = \epsilon_4 - \frac{d'}{t} \phi$$

$$\epsilon_s = \epsilon_4 - \frac{(t-d')}{t} \phi$$

where $\phi = \frac{(\epsilon_4 - \epsilon_1)}{t}$

The steel stresses are computed from the steel strains and the modulus of elasticity of steel. If the calculation of steel stress leads to a value greater than the yield stress, the corresponding steel stress is equated to the yield stress. Unloading of the steel is detected by a comparison of the steel stress in any loading stage to the corresponding steel stress in the previous loading stage.

The internal load and moment are computed from the steel and concrete stress distributions by numerical integration of the general formulae:

$$P = b \int_t f_c dy + A'_s f'_s + A_s f_s$$

$$BM = b \int_t f_c y dy + A'_s f'_s (\bar{y} - d') - A_s f_s (t - \bar{y} - d')$$

where \bar{y} = the distance from the compression face to the plastic centroid of the cross-section.

and y = distance from the plastic centroid to the fibre.

The numerical integration procedures used in this thesis are similar to those used by Newmark (29) . The total load on the concrete

of the cross-section is made up of a series of equivalent concentrated loads which act at the edges of each of the assumed fibres. The equivalent concentrated loads are calculated from the following formulae.

(a) $L = 1$ (top fibre)

$$R(L) = \frac{tb}{24M} \left\{ 7f_c(L) + 6f_c(L+1) - f_c(L+2) \right\}$$

(b) $L = M+1$ (bottom fibre)

$$R(L) = \frac{tb}{24M} \left\{ 7f_c(L) + 6f_c(L-1) - f_c(L-2) \right\}$$

(c) $1 < L < M+1$

$$R(L) = \frac{tb}{12M} \left\{ 10f_c(L) + f_c(L+1) + f_c(L-1) \right\}$$

where $R(L)$ = equivalent concentrated load at edge L

$f_c(L)$ = concrete stress at edge L .

The internal axial load is computed from

$$P = \sum_{L=1}^L R(L) + f'_s A'_s + f_s A_s$$

The internal moment is computed from

$$BM = \sum_{L=1}^L R(L) \left\{ y(L) \right\} + f'_s A'_s (\bar{y} - d') - f_s A_s (t - \bar{y} - d')$$

4.5.3 Initial Assumption of Strain Distribution

The initial assumption of strain distribution should be as close as possible to the actual strain distribution in order to reduce the time required for convergence of the analysis. In the first loading stage, the initial choice of strain distribution is computed from the applied load

and moment assuming linear elastic behavior of the concrete.

For the first computation cycle in each subsequent loading stage, the initial choice of strain distribution is the strain distribution existing after the preceeding loading stage.

For subsequent computation cycles within a loading stage, the initial choice of strain distribution is that existing after the preceeding cycle.

4.5.4 Incrementing of the Strain Distribution

It is necessary to increment the strain distribution if agreement is not obtained between the calculated internal load and moment and the applied load and moment. However, the choice of the increment in the strain distribution directly influences the permissible variation in load and moment and thus the permissible variation in curvature. For these reasons, the strain distribution increment should be kept as small as possible.

The strain distribution was incremented in this thesis by applying strain increments at the external faces of the cross-section. Using a procedure similar to that described in SECTION 4.4.5, the strain increment was made a function of the ratio of the compressive strain existing in the most highly stressed fibre to the approximate value of strain which would exist when the stress-strain curve first reaches the maximum stress. By applying increments in this manner, the load and moment increments which are generated are kept at a low value for all possible strain distributions. Using the notation of SECTION 4.4.5 and redefining ZZ as

$$ZZ = \frac{\epsilon_4(K)}{\epsilon_{\max}(K)}$$

for $ZZ \leq 0.50$

$$\Delta\epsilon = \frac{DELE(K)}{4(1-ZZ)}$$

for $0.50 < ZZ < 1.00$

$$\Delta\epsilon = DELE(K) * ZZ$$

and for $ZZ \geq 1.00$

$$\Delta\epsilon = DELE(K)$$

4.5.5 Permissible Variations in Load and Moment

The permissible variations in load and moment should be greater than two times the load and moment increments which are generated by incrementing the strain distribution. If this is not done, the trial and error procedure for cross-section analysis will not converge. The computer analysis does not require that the permissible variations in load and moment be exactly preset. The permissible variations may be preset at values which are too small to permit convergence and the computer will increment these values until convergence occurs.

4.5.6 Failure of a Cross-Section

The cross-section fails when one of the component fibres fails in compression.

4.6 Analysis of a Member

The analysis of a member is the direct application of the assumptions of SECTION 4.2.3 to the problem of determining the equilibrium

configuration of a loaded member which has known end conditions.

The formulation of a general method of analysis for all members is prevented by differences created by both the manner of loading and the end conditions of members. Three types of members are considered in this section.

1. A beam subjected to a uniform load having
 - (a) no axial load
 - (b) no end deflections
 - (c) symmetrical end restraints.
2. A column having
 - (a) no uniform load
 - (b) no end deflections
 - (c) symmetrical end restraints
3. A column fixed at one end and restrained at the other, having:
 - (a) no uniform load
 - (b) no end deflections

Flow diagrams depicting the analysis of all three types of members are included in APPENDIX A.4. The computer notation is defined in APPENDIX A.1.

4.6.1 Analysis of the Beam

The calculation of rotations and deflections is a straight forward procedure for a member having zero axial load since there are no second order deflections.

The beam is divided into a number of cross-sections as shown in FIGURE 4.3. The stresses and strains at each cross-section J are determined by the method of SECTION 4.5.

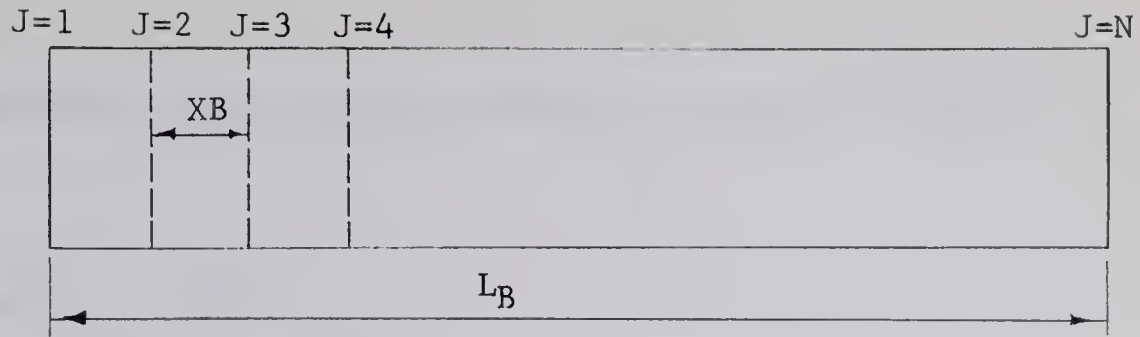


FIGURE 4.3
DIVISION OF A MEMBER

Numerical integration procedures are used to transform the discretized curvature distribution into a series of equivalent concentrated angle changes which are applied at the points J . These equivalent concentrated angle changes are calculated from the following expressions as used by Newmark (29) .

Let $\phi(J)$ = curvature at J

$RB(J)$ = equivalent concentrated angle change at J

1. $J=1$

$$RB(J) = \frac{XB}{24} (7\phi(J) + 6\phi(J+1) - \phi(J+2))$$

2. $J=N$

$$RB(J) = \frac{XB}{24} (7\phi(J) + 6\phi(J-1) - \phi(J-2))$$

3. $1 < J < N$

$$RB(J) = \frac{XB}{12} (10\phi(J) + \phi(J-1) + \phi(J+1))$$

The conjugate beam theory is used to calculate deflections and rotations at each point J . Under the action of the equivalent concen-

trated angle changes, the conjugate beam has the form of FIGURE 4.4.

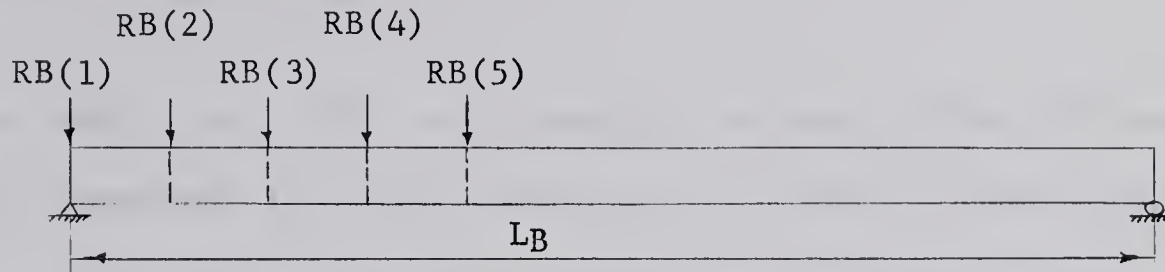


FIGURE 4.4

CONJUGATE BEAM FOR BEAM ANALYSIS

The rotations at the ends of the beam are equal to the reactions of the conjugate beam. They can be calculated from the following equations which take advantage of the beam symmetry.

$$\theta_B(J=1) = \theta(J=N) = \sum_{J=1}^N \frac{RB(J)}{2}$$

Applying the end rotations as reactions on the conjugate beam, the deflection at any point is computed as the bending moment in the conjugate beam, and the rotation at any point is computed as the shear force in the conjugate beam.

4.6.2 Analysis of the Column Bent in Symmetrical Single Curvature

The moment resisted at any point J of a column bent in symmetrical single curvature is obtained from the expression

$$BM(J) = BM(J=1) + PY(J)$$

where $BM(J)$ = moment at J

$BM(J=1)$ = end moment in the column

P = axial load

$Y(J)$ = deflection at J

Because $BM(J)$ and $Y(J)$ are dependent on one another, the analysis of the column bent in single curvature is a trial and error procedure.

The first step in the analysis is to assume a shape for the deflected column. This establishes a moment diagram for the column and by applying the beam analysis of SECTION 4.6.1, a new deflected shape is computed. The computed deflected shape is compared to the assumed deflected shape and if they do not agree, the computed deflected shape becomes the assumed deflected shape and the procedure is repeated until the two deflected shapes differ at any point J by less than a prescribed permissible variation in deflection. If the column is unstable, the analysis diverges. This is detected in the computer program by material failure in the column.

4.6.3 Analysis of the Fixed Ended Column

The moment resisted at any point J of the fixed ended column is obtained from the expression

$$BM(J) = BM(J=1) - \left\{ BM(J=1) - BM(J=N) \right\} * \frac{X(J)}{L_C} + P * Y(J)$$

where $BM(J)$ = moment at J

$BM(J=1)$ = end moment at $J = 1$

$BM(J=N)$ = end moment at $J = N$

$X(J)$ = distance along column from $J=1$ to $J=J$

L_C = column length

P = axial load

$Y(J)$ = deflection at J

The end moments at $J=1$ and $J=N$ are related by the requirement that the rotation and deflection at $J=N$ are zero and that the deflection at $J=1$ is also equal to zero. A trial and error procedure is used to establish this relationship and the remainder of the analysis is similar to that for the single curvature column although the conjugate beam has a different form.

For a known value of moment at $J=1$, assumptions are made of both the moment at $J=N$ and the deflected shape. A moment diagram is established from these assumptions. Following the analysis of SECTION 4.6.1 for the beam, equivalent concentrated angle changes, $RC(J)$, are calculated and applied to the conjugate beam of FIGURE 4.6. The fixed end of the real column is represented in the conjugate beam by a free end at which the shear and moment (rotation and deflection) are both equal to zero.

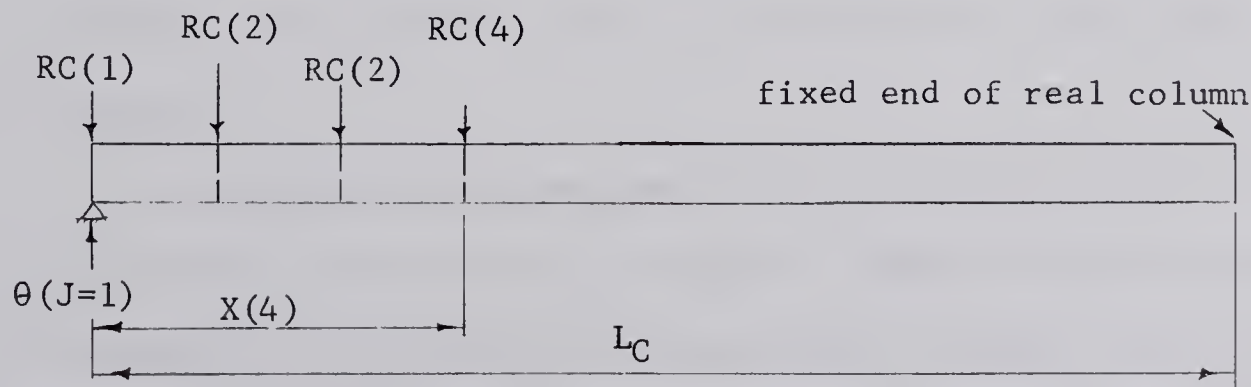


FIGURE 4.5

CONJUGATE BEAM FOR THE FIXED ENDED COLUMN

The rotation at $J=1$ is calculated from

$$\theta(J=1) = \sum_{J=1}^N RC(J)$$

The deflection at $J=N$ is calculated from

$$Y(J=N) = \theta(J=1)L_c - \sum_{J=1}^N (L_c - X(J))RC(J)$$

This deflection should be equal to zero or in other words, bending moment in the conjugate beam at $J=N$ should be zero.

The initial trial and error procedure of this analysis determines the bending moment required at $J=N$ to reduce the deflection at $J=N$ to approximately zero. The bending moment at $J=N$ is first assumed and the deflection at $J=N$ is computed. If the deflection at $J=N$ differs from zero by greater than a prescribed allowable variation, the bending moment at $J=N$ is incremented by ΔM_1 and the process is repeated to convergence.

When this first trial and error procedure has been satisfied, the equilibrium deflected shape is determined by the trial and error procedure of SECTION 4.6.2. The first trial and error procedure must always be satisfied before computations in the second trial and error procedure can commence.

To decrease the time required for solution, the two trial and error procedures were partially combined. When the bending moment at $J=N$ is incremented and the first trial and error procedure repeated, the assumed deflected shape became the deflected shape of the previous trial corrected to give zero deflections at the ends. Instability of the column is again

detected when non-convergence of the analysis leads to material failure in the column.

4.6.4 Permissible Variation in Deflection, ΔY , and the Moment Increment, $\Delta M1$

The permissible variation in deflection ΔY is used both in the comparison of two successive deflected shape trials for both column types and as a limit on the far end deflection, $Y(J=N)$, of the fixed ended column.

In its capacity as an allowable variation between two successive deflected shapes, the increment ΔY is of minor importance. Because of the nature of the analysis, if the additional moment generated by the increase in deflection between two successive deflected shape trials is less than the permissible variation in moment (SECTION 4.5.5), then the two deflected shape trials will be exactly the same. The permissible variation in moment thus has a greater influence on column equilibrium than does the permissible variation in deflection.

In its capacity as a limit on the deflection at the fixed end of the column in SECTION 4.6.3, the permissible variation in deflection is of prime importance. The magnitude of ΔY in this case is related to the magnitude of $\Delta M1$, the moment increment applied to $BM(J=N)$. The moment increment $\Delta M1$ should not generate a deflection increment at $J=N$ greater than ΔY . If this occurs the analysis will not converge.

The value of $\Delta M1(K)$ was calculated in this thesis as a function of the permissible variation in column moment, the permissible variation in deflection, and the calculated value of deflection at $J=N$. Application

of a moment increment $\Delta M_1(K)$, equal in magnitude to the permissible variation in column moment, will generate a change in $Y(J=N)$ equal to some multiple of the permissible variation in deflection. By comparing this multiple to the calculated end deflection $Y(J=N)$, a moment increment can be calculated that will reduce the end deflection to zero. If this procedure is not sufficient to allow convergence after a preset number of tries, the computer will increment the permissible variation in deflection until convergence occurs.

4.6.5 Initial Assumptions of Column Deflected Shape and Moment at the Fixed End of Column

The time required to converge the column trial and error procedures is reduced if the initial assumption of column deflected shape is as close as possible to the equilibrium deflected shape. The deflections are initially assumed to be zero in the trial and error procedures of the first loading stage. In subsequent loading stages, the initial assumption of deflected shape is the deflected shape of the preceeding loading stage.

The initial assumption of bending moment at the fixed end of the column for the first loading stage was chosen as -0.50 times the moment at the restrained end. For subsequent loading stages, the initial choice of moment at the fixed end was the moment existing at the end of the preceeding loading stage.

4.7 Analysis of a Framework

The analysis of a framework is the direct application of the assumptions of SECTION 4.2.4 to the problem of obtaining the equilibrium configuration of a framework under load. The framework is made up of

a number of members which have been analysed separately and which must now be joined together. The final analysis must define the structure such that the loads are in equilibrium and the deformations are compatible in all the members at all the joints.

Flow diagrams depicting the analysis of the model frameworks considered in CHAPTERS VII and VIII are included in APPENDIX A.5. The computer terminology is defined in APPENDIX A.1. The discussion of this chapter pertains to frameworks in general of which the frameworks of the flow diagrams are an example.

4.7.1 Establishment of Equilibrium and Compatibility at a Joint

The equilibrium at a joint in a framework is established by trial and error. The end moment of a beam at the joint is first assumed and the corresponding end rotation of the beam is calculated by the methods of SECTION 4.6. If a second beam is present at the joint, its end moment is incremented by $\Delta M_2(K)$ until its end rotation and the end rotation of the first beam differ by less than a prescribed permissible variation in end rotation. The undistributed moment at the joint can now be computed and divided among the columns. This division of moment to the columns constitutes another trial and error procedure which is culminated when the column end rotations differ from each other by less than the permissible variation in end rotation. The column end rotations are now compared to the beam end rotations. If all rotations are not within the permissible variation in rotation, the end moment of the first beam is incremented by ΔM_2 and the process is repeated to convergence.

4.7.2 The Permissible Variation in Rotation

The permissible variation in rotation was preset at values which would give negligible errors in the attainment of joint equilibrium. If the choice of variation proved to be too small and the analysis would not converge, the computer program would increment the variation until convergence occurred.

4.7.3 The Moment Increment $\Delta M_2(K)$

The moment increment, $\Delta M_2(K)$, in this thesis varied with the degree of incompatibility at the joint and was calculated as a function of the permissible variation in beam moment and the calculated discrepancy in rotation. Application of a moment increment, $\Delta M_2(K)$, which was equal to the permissible variation in beam moment, to the members at the joint will generate a change in the joint rotation. This change in joint rotation is then divided into the calculated discrepancy in rotation at the joint and the ratio formed by this division is multiplied by the permissible variation in beam moment to obtain the moment increment $\Delta M_2(K)$.

4.7.4 Initial Assumption of Beam End Moment

The beam end moments in the first loading stage can be initially predicted by linearly elastic moment distribution.

The beam end moments for subsequent loading stages are initially assumed equal to the values existing at the end of the preceeding loading stages.

4.7.5 Frame Failure

A frame may fail either through material failure or instability.

Both forms of failure are detected in the analysis when the instantaneous component of total strain exceeds ϵ_u .

If material failure is detected during the course of analysis of a frame or a member, section or fibre within the frame, the frame does not instantly fail. The computer will attempt to prevent failure by redistributing moments in the frame before declaring a frame to have failed. The form of redistribution is a reduction in joint moment in the case of material failure in the column and an increase in joint moment in the case of material failure in the beam. If redistribution of this form prevents an equilibrium configuration from being attained, the frame has failed. The computer program will increment the column load in the loading stage in which failure occurs to a value which is just below the failure load. The information on the behavior near failure was obtained with this procedure.

The flow diagrams of APPENDIX A.5 depict the analysis applied to the investigation in this thesis. As it is the purpose of this thesis to study the behavior of columns in frameworks, the redistribution of moment was stopped before failure occurred in the beam. For the actual members being analysed, a convenient stopping point was when the unbalanced moment at the joint reached a value of zero because at this point column failure was imminent. For a general evaluation of framework behavior, this specific procedure would not be incorporated.

4.8 Conclusion

The description of the analysis of frameworks in SECTION 4.7 is general and does not apply to any specific framework. For a specific

application, such as presented in CHAPTER VII of this thesis, the analysis must be modified to satisfy the specific boundary conditions.

The extent of application of the analysis is limited by computer capacity, the time required by the computer for analysis, and possibly by the accuracy of the analysis. The accuracy of the analysis is discussed in CHAPTER V.

CHAPTER V

ERRORS OF THE ANALYSIS

5.1 Introduction

Errors in the analysis could result from three sources:

1. The material property assumptions.
2. The necessity of dividing the structure into discrete elements and the duration of loading into discrete time increments for the purposes of numerical integration.
3. The permissible variations in the convergence of the trial and error procedures.

The first possible source of errors will not be discussed because the exact material behavior is unknown. However, it should be noted that the analysis can be applied for material properties other than those assumed in CHAPTER III.

The second possible source of errors is discussed by comparing the results obtained by varying the number of fibres, panels, and time increments for both a beam and a column.

The third possible source of errors can only be discussed qualitatively as the exact structural behavior is unknown.

The analysis will be compared to test results in CHAPTER VI.

5.2 Errors Resulting from Discreteness in the Analysis

Cross-sections, members, and duration of sustained load have

been divided into discrete divisions, and numerical integration procedures have been used in the analysis. The accuracy of the numerical integration is dependent on the number of discrete divisions considered.

Discreteness was investigated by comparing the changes in the predicted behavior which resulted from varying the numbers of panels, fibres, and creep stages for both a beam and a column. The beam and column variables were chosen so as to investigate the effect of discreteness within the approximate range of application in the original investigation.

The beam was simply supported, twenty feet in length, and carried a uniform sustained load of three kips per foot. The cross-section and material properties were the same as for the beams described in CHAPTER VII. The behavior properties calculated and used for comparison were the mid-span deflection, the end rotation, the steel stress at mid-span, and the maximum concrete stress at mid-span; all existing after a hypothetical duration of sustained load of 25 years.

The column was simply supported, twenty feet in length, twelve inches square, and carried a sustained load of 225 kips acting through equal end eccentricities of 0.75 inches ($e/t = 0.0625$). The cross-section and material properties were the same as for the columns of CHAPTER VII. The behavior properties calculated and used for comparison were the centre-line deflection, the end rotation, the tensile steel stress at the centre-line, the maximum concrete stress at the centre-line, and the maximum moment; all existing after a duration of sustained load of 25 years.

5.2.1 Comparison of the Effects of Discreteness

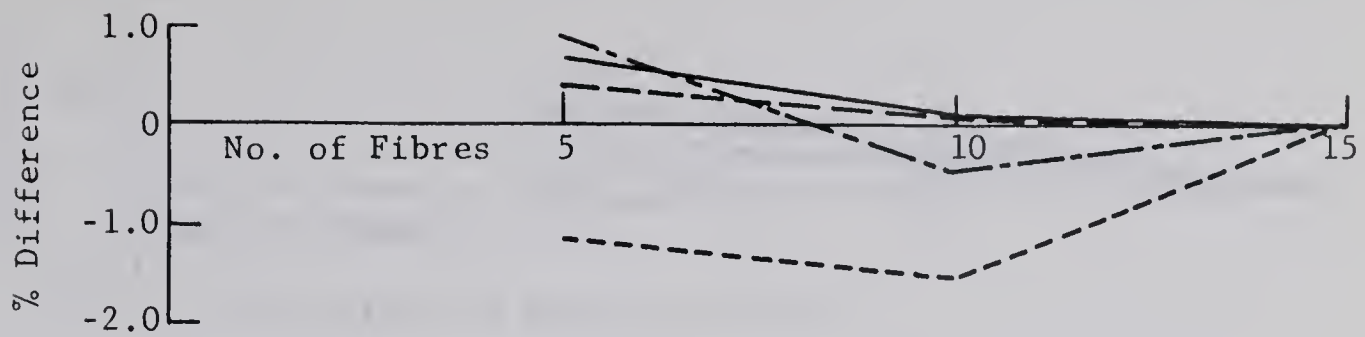
The magnitudes of the quantities calculated for comparison are shown in TABLES B.1 and B.2 of APPENDIX B for the beam and column respective-

ly. The calculations were made considering all combinations of 5, 10, or 15 fibres; 6, 10, or 20 panels; and 1, 3, 5, or 7 creep stages in the beam and 1, 2, 3, 5, or 7 creep stages in the column.

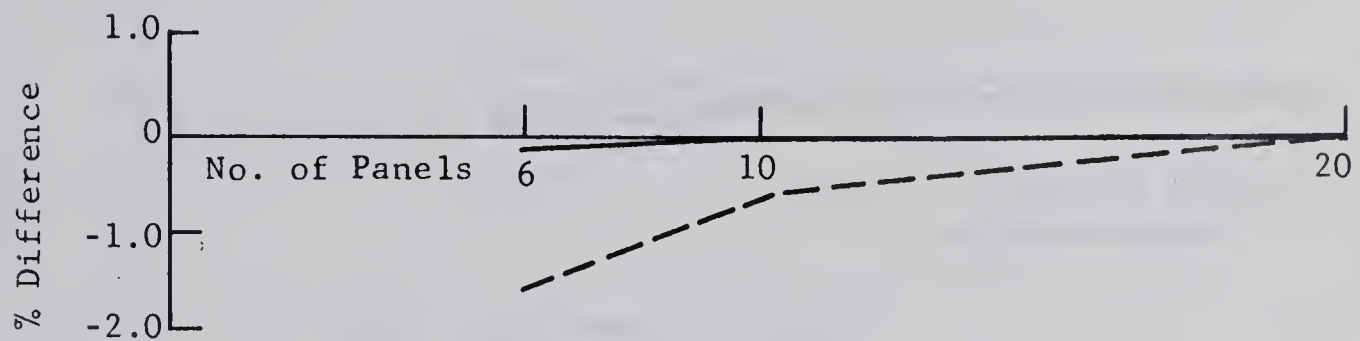
The results in TABLES B.1 and B.2 have been reduced to the graphs of FIGURES 5.1 and 5.2. These graphs show a percentage comparison for each type of discreteness. In plotting the graphs, it was assumed that the results based on the largest number of increments most nearly approached the truth. Accordingly, the values obtained by considering 15 fibres, 20 panels, or 7 creep stages were taken as the correct values. The trends existing in FIGURES 5.1 and 5.2 were somewhat influenced by errors resulting from the permissible variations of closure in the trial and error procedures. This source of errors is discussed in the following section.

For the range of discreteness considered, the effect on the beam results of the number of fibres and the number of panels was negligible. The maximum percent variation produced in either case was less than two percent. The maximum percent variation produced by considering a varying number of creep stages was five percent. There were no significant trends in the accuracy of the beam results as the number of fibres, panels, and time increments was varied. This indicates that the errors are at least partly due to errors produced by the permissible variations of convergence of the trial and error procedures.

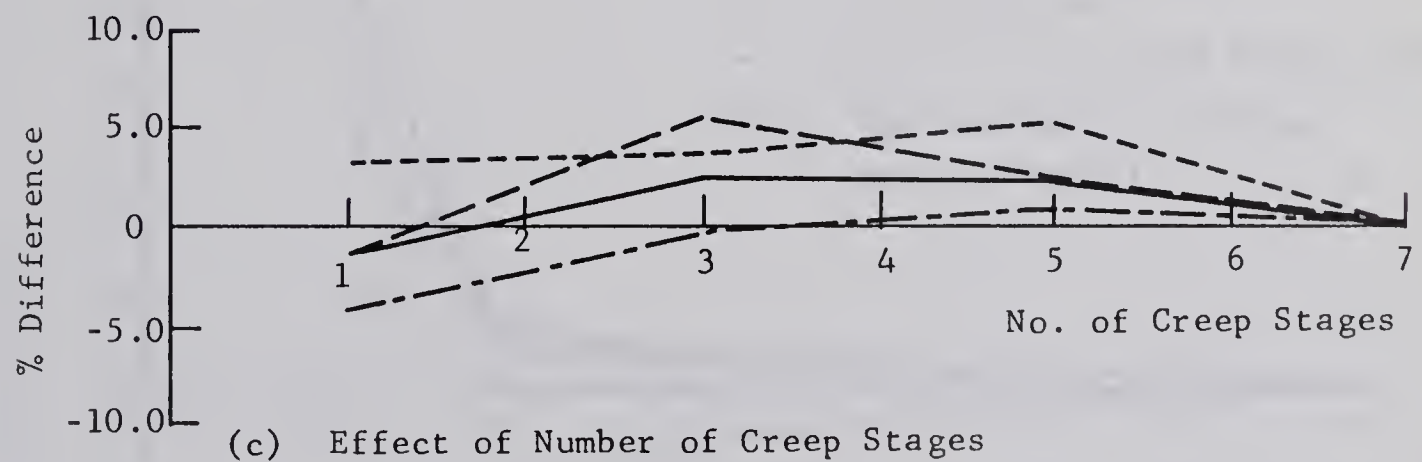
For the range of discreteness considered, the effect on the column results of the number of fibres and the number of panels was also negligible. The maximum variation produced in either case was less than one-half percent. However, a definite trend was exhibited by the column



(a) Effect of Number of Fibres



(b) Effect of Number of Panels



(c) Effect of Number of Creep Stages

- Centre-Line Deflection
- - - End Rotation
- · - Steel Stress at Centre-Line
- - - Maximum Concrete Stress

FIGURE 5.1

EFFECT OF ANALYSIS DISCRETENESS ON BEAM RESULTS

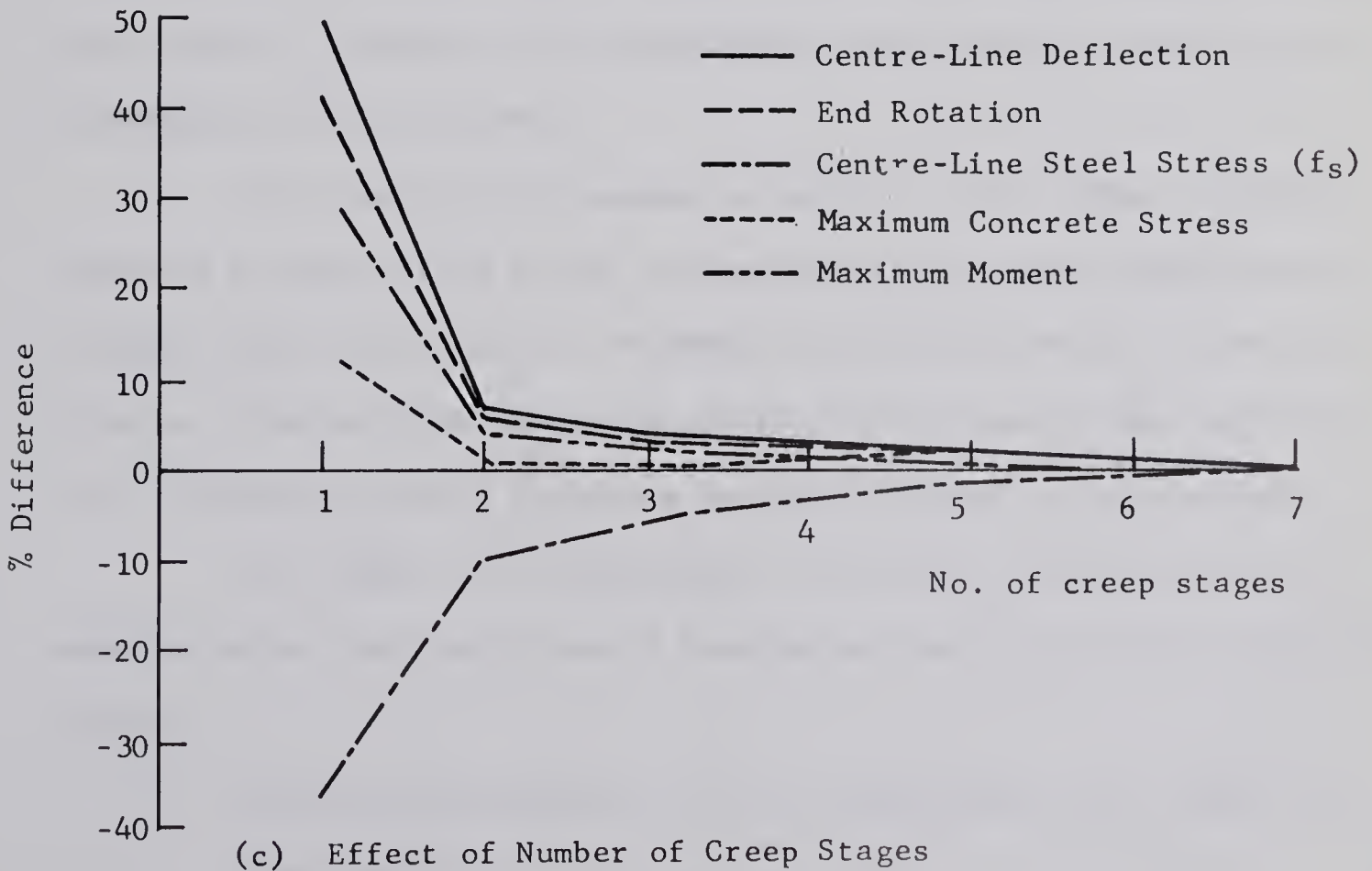
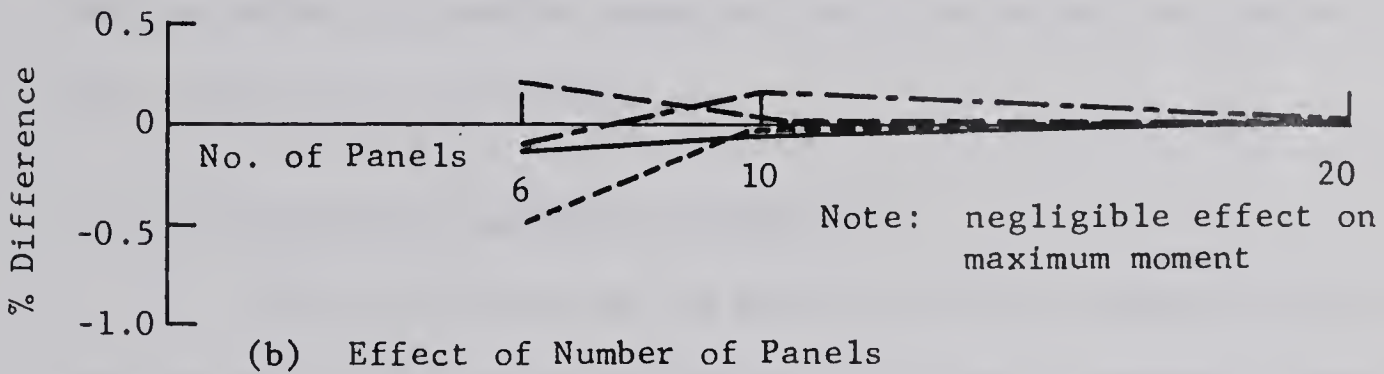
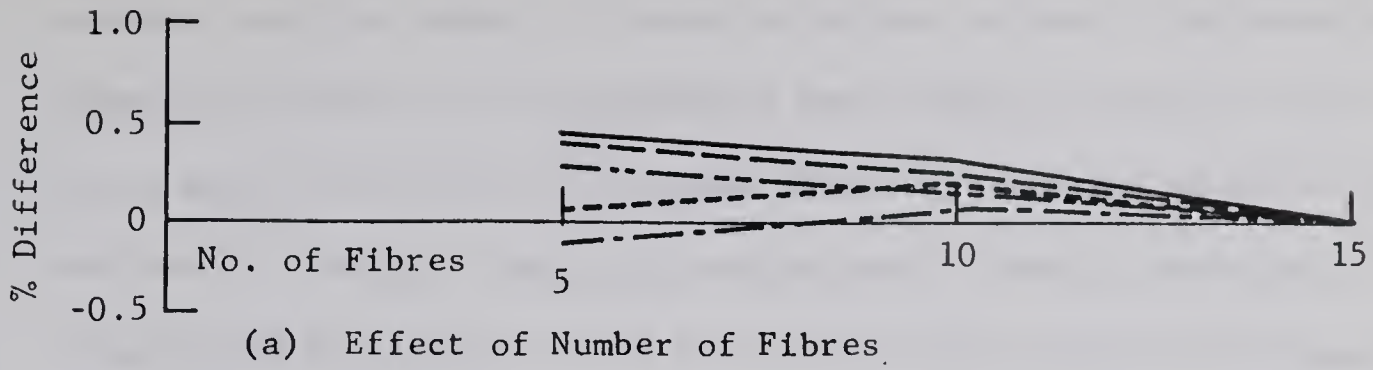


FIGURE 5.2

EFFECT OF ANALYSIS DISCRETENESS ON COLUMN RESULTS

results when the number of creep stages was varied. This behavior shows the importance of considering the changing stresses in the concrete and steel as the time passes when computing the behavior for long periods of loading. The large variations in results using only one creep stage would be similar to the variations which would be produced using a reduced modulus approach with the reduced modulus based on ultimate creep. However, for small durations of loading, Green (16) has shown that an effective modulus based on the actual creep function will give a good prediction of behavior.

5.2.2 Conclusions Regarding Discreteness

The conclusions on the effect of discreteness are valid only for the small range of investigation considered. However, there is no indication that trends will be more or less significant for other beams and columns. Therefore, the conclusions were assumed to apply to all investigation in this thesis.

The choice of the number of panels or the number of fibres appeared to have little effect on the results for either the beam or column, located near the two extremes of the cross-section interaction diagram. However, the use of ten fibres and ten panels was instituted in this thesis in order to have a margin of safety in calculations.

The number of creep stages to be used in the calculation of behavior after long durations of loading was set at three for the following reasons:

1. The maximum variations in the investigation were less than five percent.

2. The variations in the end rotations of both the beam and the column were both approximately five percent on the high side. Since the error is similar for both members, the error in the calculation of the equilibrium joint moment in a frame should be negligible.
3. If the number of creep stages is limited to three, sufficient computer capacity is still available for investigation of the effect of quick load following the sustained load.

5.3 Errors Resulting from Permissible Variations in the Trial and Error Procedures

Accidental or round-off errors are the result of allowing the trial and error procedures to converge within a permissible range of variation. These errors may be positive or negative and their overall effect for a large number of calculations should not be significant. The magnitudes of the errors were controlled in the analysis by using small increments and then letting the computer establish the permissible variation of closure at a value just large enough to prevent continuous looping in the analysis.

5.4 Conclusion

The sources of errors are difficult to discuss quantitatively since absolutely correct answers do not exist because of the non-homogeneous nature of concrete. However, the correlation with test results in the following chapter suggests that these errors are within satisfactory limits.

CHAPTER VI

APPLICATION OF THE ANALYSIS TO EXISTING TESTS

6.1 Introduction

Experimental and analytical results are compared in this chapter in an attempt to verify the applicability of the method of analysis described in CHAPTER IV. The experimental investigations include those by

1. Washa and Fluck (49) on the sustained loading of reinforced concrete beams containing various amounts of compressive reinforcement,
2. Martín and Olivieri (23) on the short-time loading of reinforced concrete columns bent in double curvature,
3. Furlong (13) on the short-time loading of rectangular reinforced concrete frames containing columns bent in symmetrical single curvature,
4. Furlong and Ferguson (14) on the sustained loading of a reinforced concrete rectangular frame with subsequent quick loading to failure after a duration of sustained load of 100 days,
5. Green (16) on the sustained loading of eccentrically loaded reinforced concrete columns.

Deformation characteristics have been used as the basis of comparison in this chapter as it is these characteristics which influence the redistribution of load in a frame.

For the sustained load investigations in this chapter, the creep

and shrinkage properties of concrete outlined in CHAPTER III have been modified where necessary to apply to the specific conditions of each test. This was not done for the Washa and Fluck investigation because of the similarity in conditions between their tests and those assumed in SECTION 3.3.1.

The remaining sections of this chapter present individual comparisons of the test results and analytical results of each investigation. The final section in this chapter discusses the effectiveness of the method of analysis in predicting the behavior.

6.2 Beam Tests Under Sustained Load - Washa and Fluck

Washa and Fluck (49) have investigated the effect of compressive reinforcement on the plastic flow of reinforced concrete beams. Their test series comprised 34 specimens subjected to a sustained uniform load of 2 1/2 years duration. Thirty of the specimens were used to investigate various combinations of beam sizes and amounts of compressive reinforcement. The remaining four specimens contained either air entraining cement or expanded slag aggregate and are outside the scope of the analysis.

The 30 specimens consisted of 15 pairs of beams; each pair representing one combination of the five beam sizes and the three conditions of compressive reinforcement investigated. The details of the beams are summarized in TABLE 6.1.

The beams were all tested in a simply supported condition.

The deformation characteristics used for comparison were:

1. Centre-line deflections under short-time loading and after various durations of sustained load up to 2 1/2 years.

TABLE 6.1
DETAILS OF THE BEAMS TESTED BY WASHA
AND FLUCK UNDER SUSTAINED LOADS

Beam	Width b_B (in)	Depth t_B (in)	Span L_B (ft)	f'_{ca} (ksi)	f_y (ksi)	$\frac{d'}{t_B}$	Unif. load #/ft	Reinforcing	
								A_s (in ²)	A'_s (in ²)
A1-A4	8.0	12.0	20	3.63	50.9	0.156	378	1.32	1.32
A2-A5	8.0	12.0	20	3.63	50.9	0.156	378	1.32	0.62
A3-A6	8.0	12.0	20	3.63	50.9	0.156	378	1.32	0
B1-B4	6.0	8.0	20	3.00	47.0	0.227	107	0.62	0.62
B2-B5	6.0	8.0	20	3.00	47.0	0.227	107	0.62	0.31
B3-B6	6.0	8.0	20	3.00	47.0	0.227	107	0.62	0
C1-C4	12.0	5.0	20.8	2.94	51.0	0.200	82	0.80	0.80
C2-C5	12.0	5.0	20.8	2.94	51.0	0.200	82	0.80	0.40
C3-C6	12.0	5.0	20.8	2.94	51.0	0.200	82	0.80	0
D1-D4	12.0	5.0	12.5	2.92	51.0	0.200	229	0.80	0.80
D2-D5	12.0	5.0	12.5	2.92	51.0	0.200	229	0.80	0.40
D3-D6	12.0	5.0	12.5	3.22	51.0	0.200	229	0.80	0
E1-E4	12.0	3.0	17.5	2.99	56.2	0.229	38	0.44	0.44
E2-E5	12.0	3.0	17.5	2.99	56.2	0.229	38	0.44	0.22
E3-E6	12.0	3.0	17.5	2.99	56.2	0.229	38	0.44	0

2. Centre-line strains at the level of the compressive steel under short-time loading and after various durations of loading up to 2 1/2 years.

6.2.1 Comparison of the Results of Washa and Fluck's Beam Tests with the Results of the Analysis

FIGURE 6.1 shows the actual and the computed centre-line deflections for the Washa and Fluck beams and FIGURE 6.2 shows the actual and the computed centre-line strains at the compressive steel level. In these figures, the observed deformations have been connected by continuous solid curves. The calculated deformations have been connected by straight dashed lines because time was not a continuous variable in the analysis. The calculated deformations apply for short-time loading and after durations of sustained loading of seven days, nine months, and 25 years.

Errors may have occurred in transferring the observed data from the published curves to FIGURES 6.1 and 6.2. The published curves used an arithmetic time scale and were considerably smaller in size than the two figures in this chapter.

In general, a good correlation was obtained with all tests except those of E series where the computed quantities tended to be low. The beams of this series had a three inch overall depth and a very large length to depth ratio compared to the beams of the other series. Because of the higher sensitivity in the beams of E series, an exact measurement of the parameters is needed before a good correlation with the analysis can be obtained.

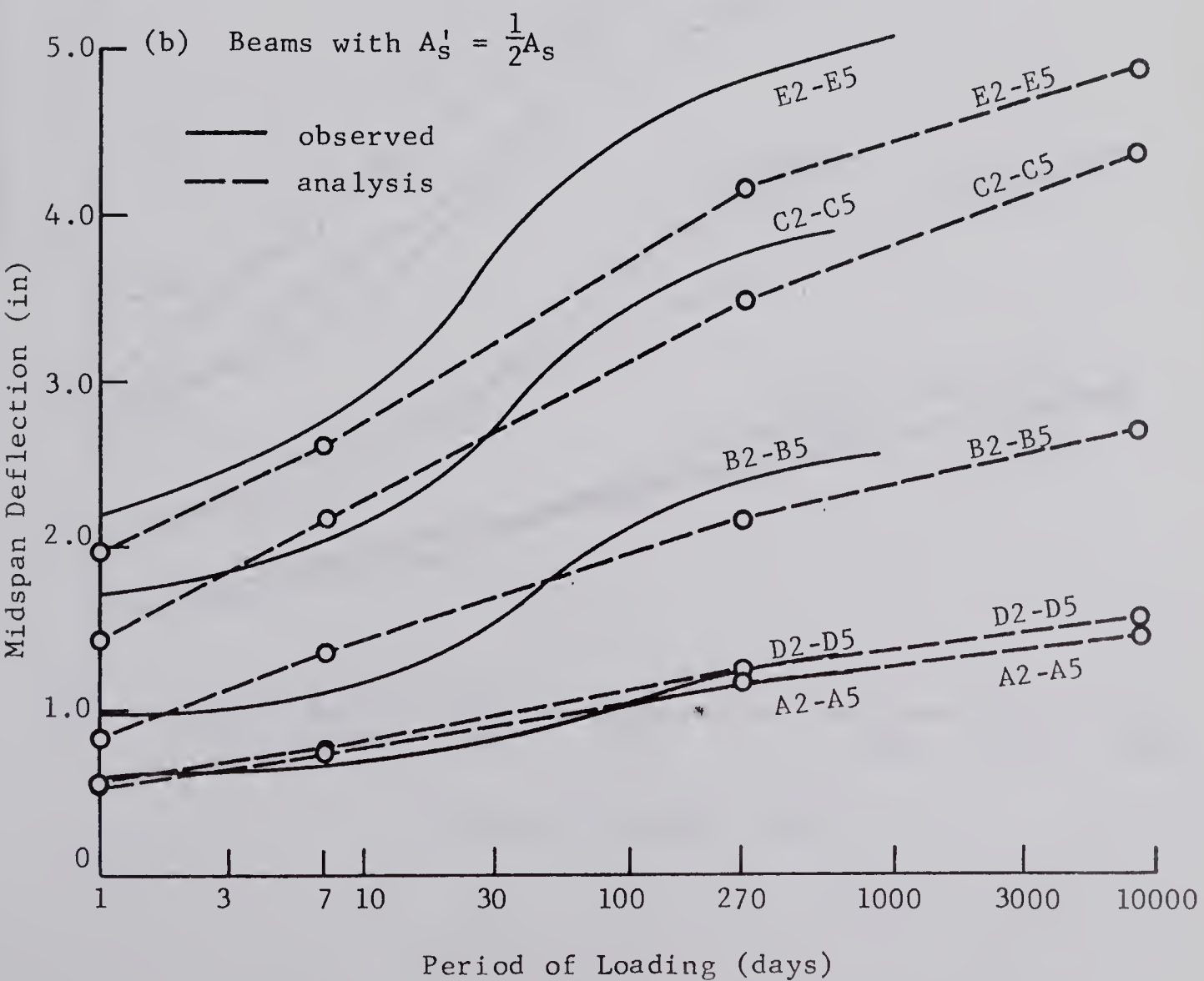
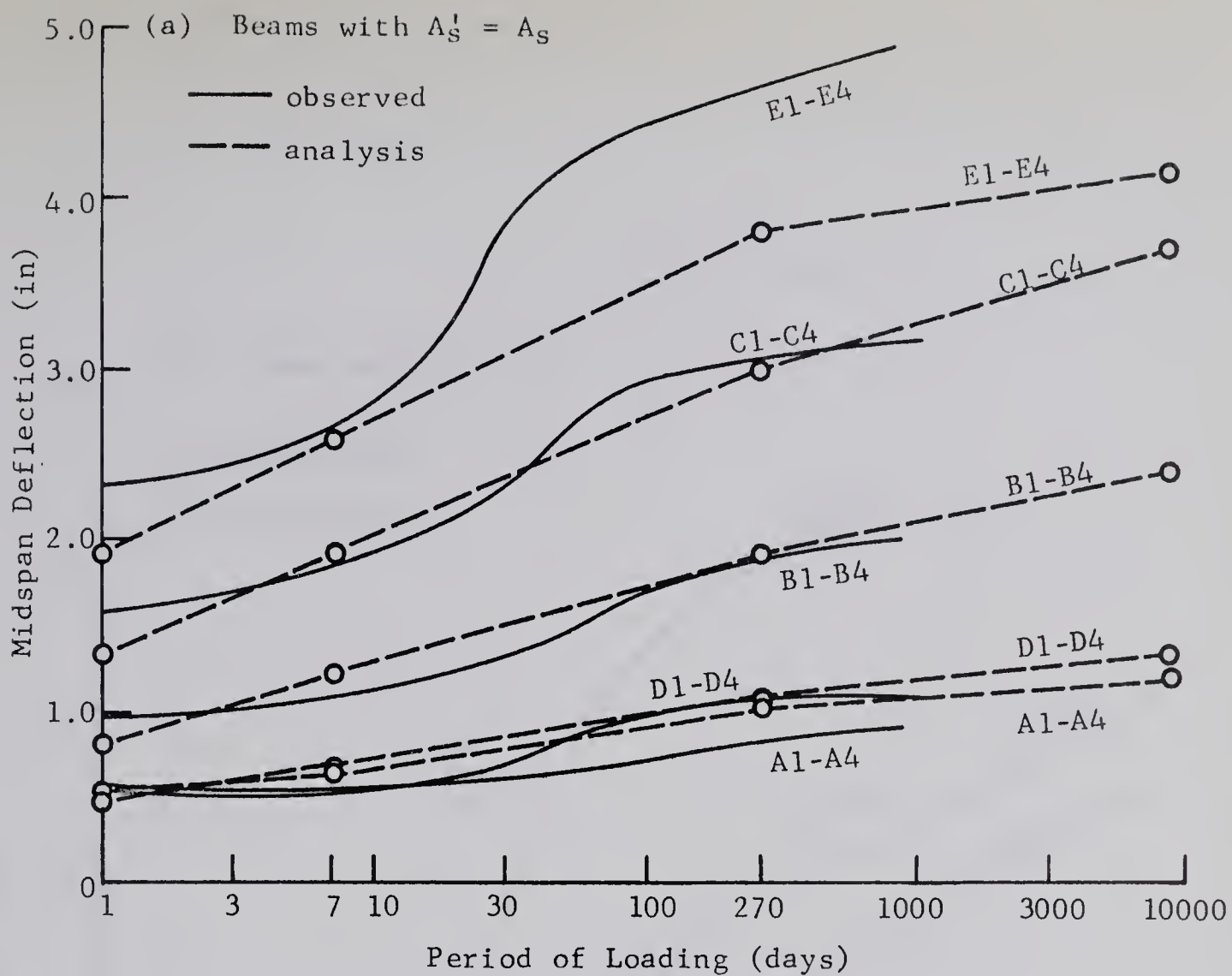
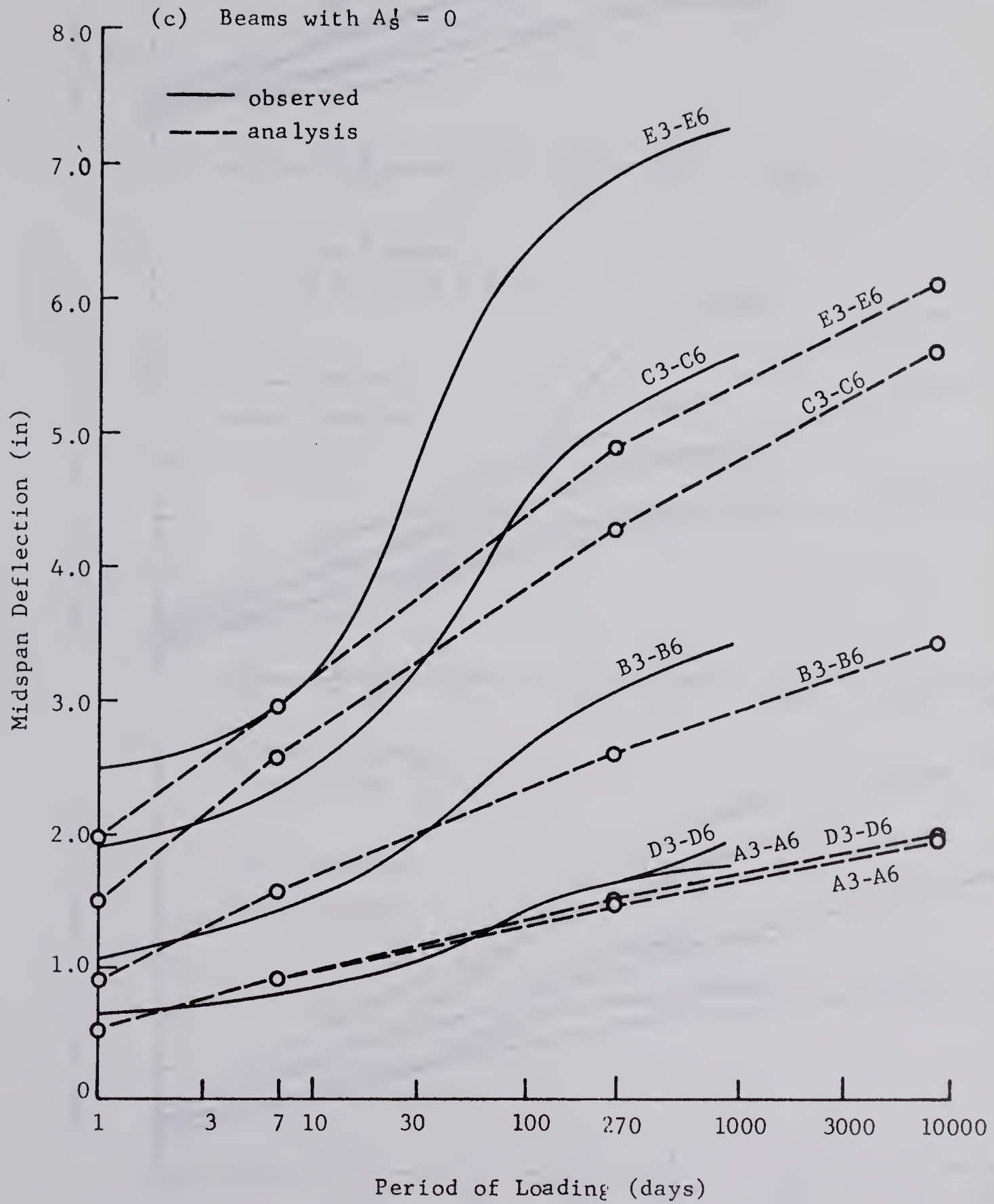


FIGURE 6.1

ANALYSIS APPLIED TO THE WASHA AND FLUCK
BEAM TESTS. PART 1. MIDSPAN DEFLECTIONS



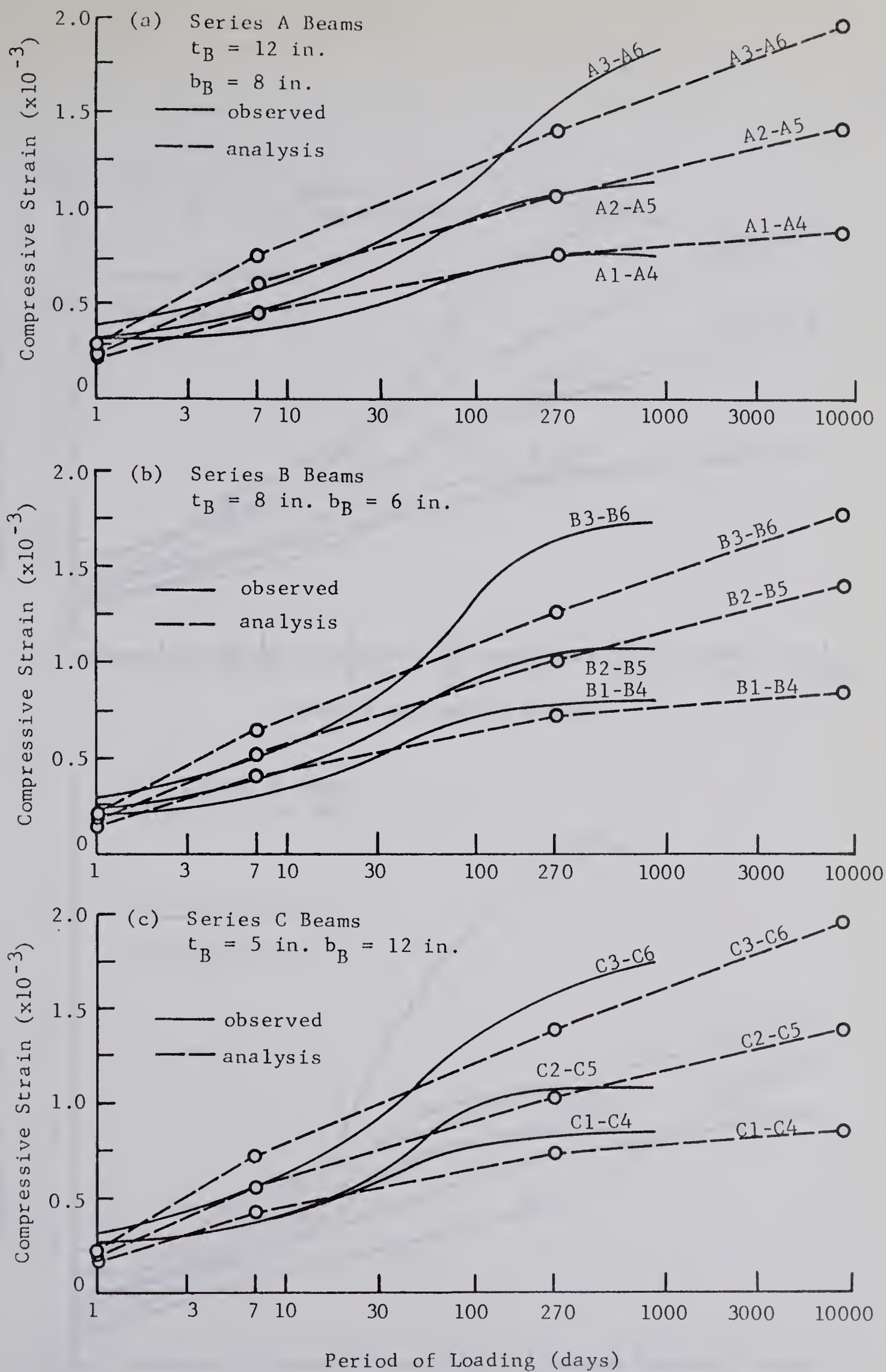
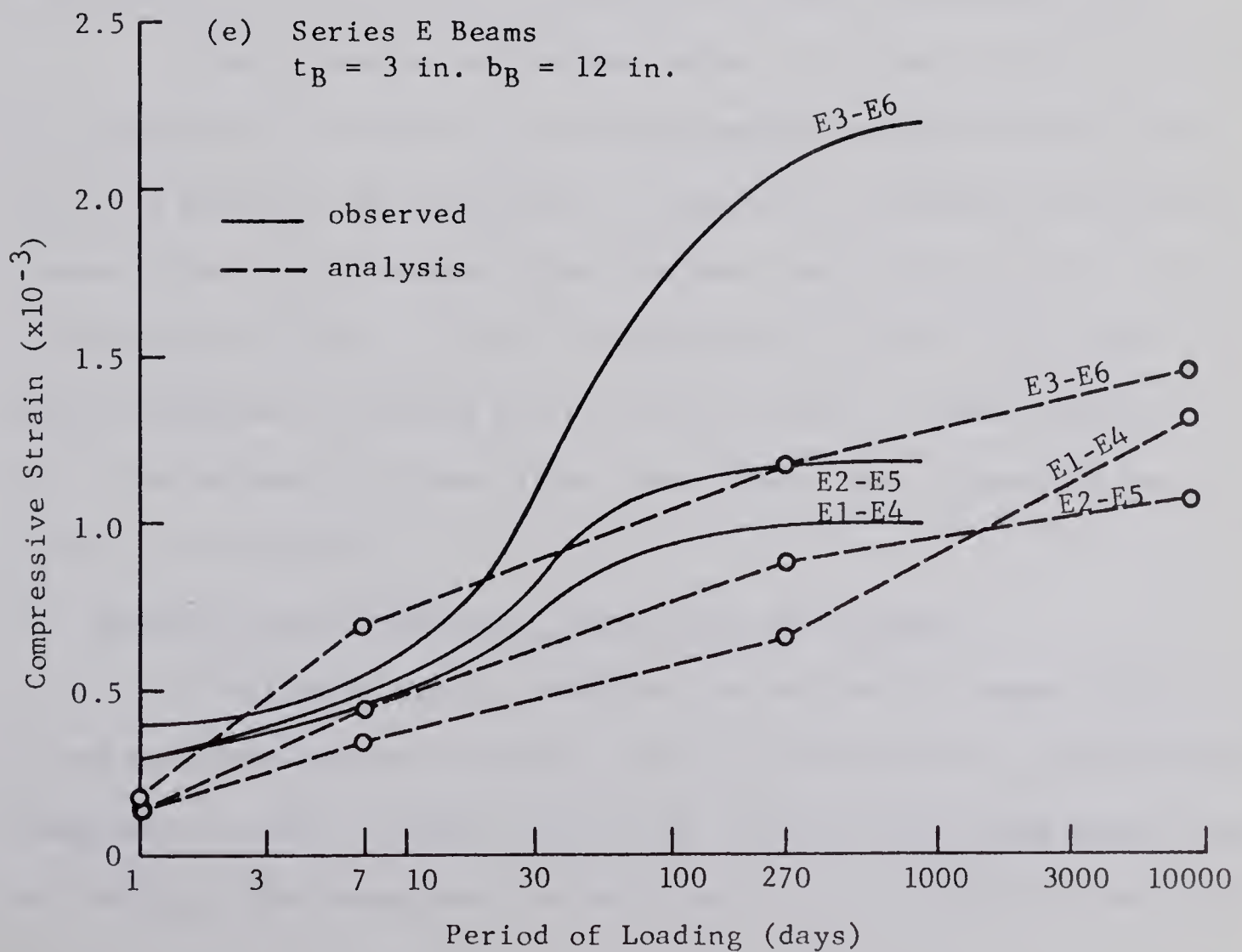
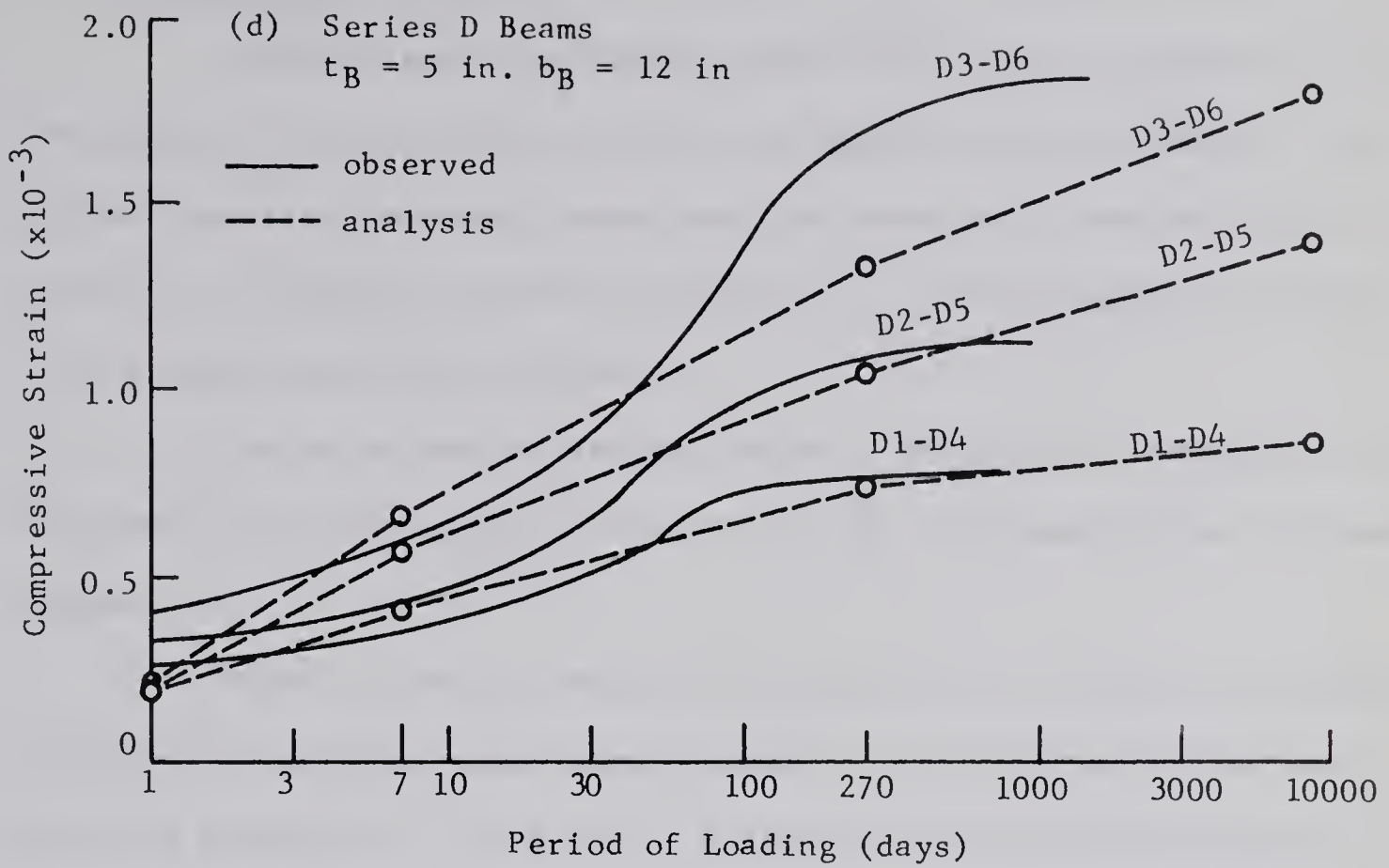


FIGURE 6.2

ANALYSIS APPLIED TO THE WASHA AND FLUCK BEAM TESTS:
 PART 2 - STRAINS AT THE COMPRESSIVE STEEL LEVEL



1. Centre-Line Deflections

The calculated deflections under short-time loading were all in the range of ten to twenty per cent less than the measured values. The reason for this trend could have been the presence of some sustained load effect in the measured values or could lie in the assumption of perfect bond between concrete and steel.

The calculated deflections after a duration of loading of seven days were all in the range of zero to ten per cent greater than the measured values.

After nine months duration of loading the calculated deflections exhibited no definite trend when compared to the observed deflections. With the exception of the beams of E series, the difference between the measured and the calculated values was less than fifteen per cent.

The calculated deflections after 2 1/2 years duration of loading also exhibited no definite trend when compared to the observed values. With the exception of the beams of E series, the difference between the measured and the calculated values was less than twenty per cent. The calculated values in this case were extrapolated from the results after nine months duration of loading and the results after 25 years duration of loading. The extrapolation was along the straight line connecting the two points in the figures.

2. Strains at the Compressive Steel Level at Mid-Span

The trends which existed for the deflection comparison also existed for the compressive strains with the exception that the calculated compressive strains tended to be on the low side after nine months duration of loading. The comparison for the beams in the E series was not good.

6.3 Short-Time Tests of Slender Hinged Columns - Martín and Olivieri

Martín and Olivieri (23) have investigated the short-time load behavior of slender reinforced concrete columns bent in double curvature. Their test series comprised eight reinforced concrete columns with a geometric slenderness ratio of forty. Two of the columns were concentrically loaded and the remaining six columns were loaded through an eccentricity ratio of $e_1/e_2 = -1/2$. Loads were applied in successive stages to failure. The comparison in this chapter considers only the eccentrically loaded columns. The details of these columns are summarized in TABLE 6.2.

The deformation characteristics used for comparison were the deflected shapes of the columns at various levels of load.

6.3.1 Comparison of the Results of Martín and Olivieri's Column Tests with the Results of the Analysis

FIGURES 6.3 (a to f) show the comparison between the measured and computed deflected shapes of the Martín and Olivieri Test Columns. The observed deflections along the column length have been connected by solid lines and the deflections of the analysis have been connected by dashed lines. The comparison has been made at only a few levels of load for each column as this was deemed sufficient to indicate trends.

The correlation between the measured and the computed deflected shapes was good for columns 412-1 and 422-2. For the remaining four columns of the investigation, the correlation was not good. A comparison of the results, however, seems to indicate that perhaps the actual eccentricity in the tests did not correspond with the desired eccentricity. Columns 412-2 and 432-1 show observed deflected shapes which are larger than the

TABLE 6.2
 DETAILS OF THE HINGED ENDED COLUMNS TESTED BY
 MARTIN AND OLIVIERI UNDER SHORT-TIME LOADS

Column	Width b_c (in)	Depth t_c (in)	Length L_c (in)	f'_{ca} (ksi)	f_y (ksi)	$\frac{d'}{t_c}$	e_2 (in)	e_1 (in)	Reinforcing A_s (in ²)	
412-1	5.0	3.54	141.7	4.88	40.0	0.20	0.748	-0.374	0.22	0.22
412-2	5.0	3.54	141.7	3.63	40.0	0.20	0.748	-0.374	0.22	0.22
422-1	5.0	3.54	141.7	5.06	40.0	0.20	1.375	-0.688	0.22	0.22
422-2	5.0	3.54	141.7	3.73	40.0	0.20	1.375	-0.688	0.22	0.22
432-1	5.0	3.54	141.7	5.41	40.0	0.20	0.999	-0.500	0.22	0.22
432-2	5.0	3.54	141.7	3.83	40.0	0.20	0.999	-0.500	0.22	0.22

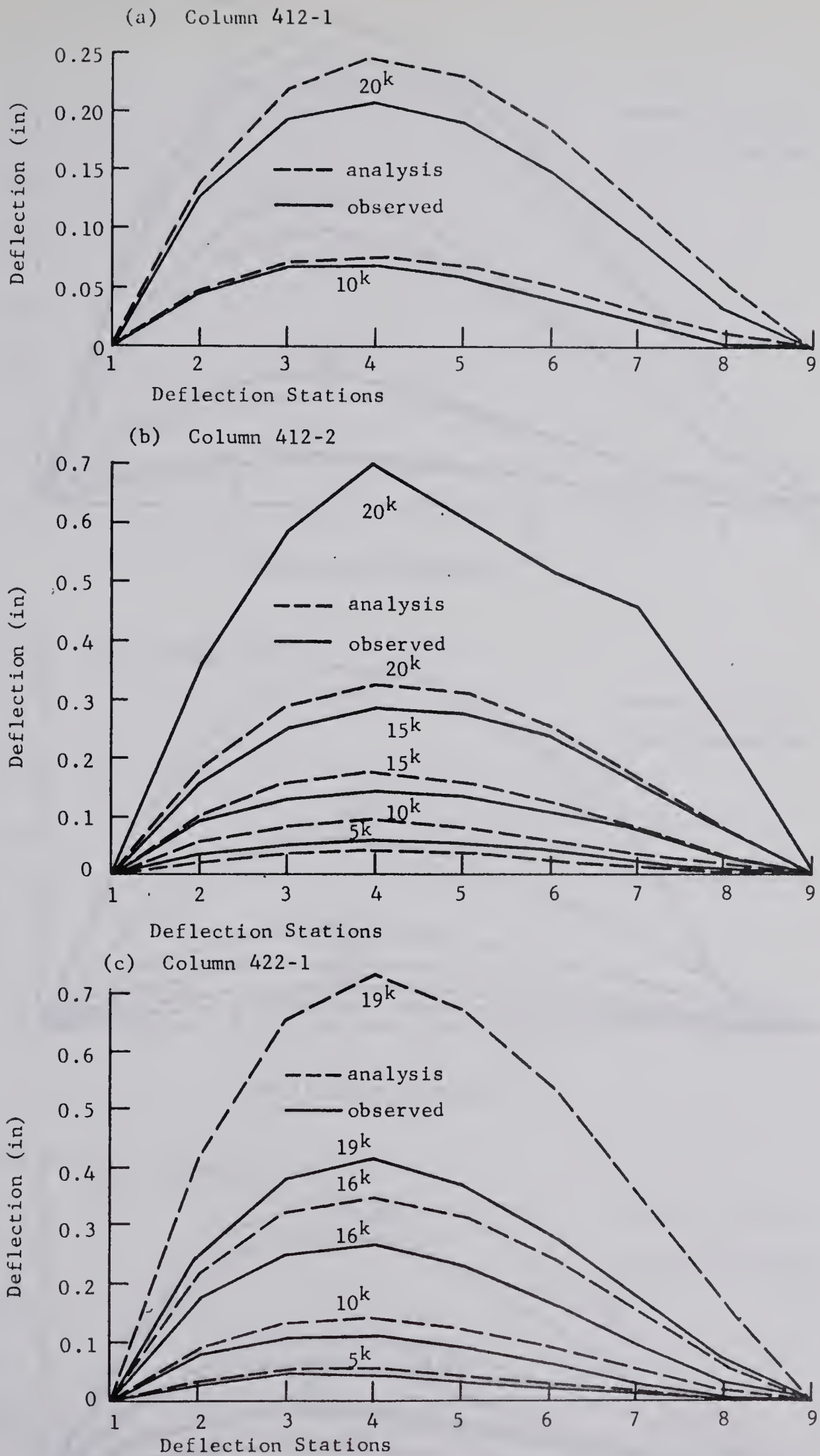
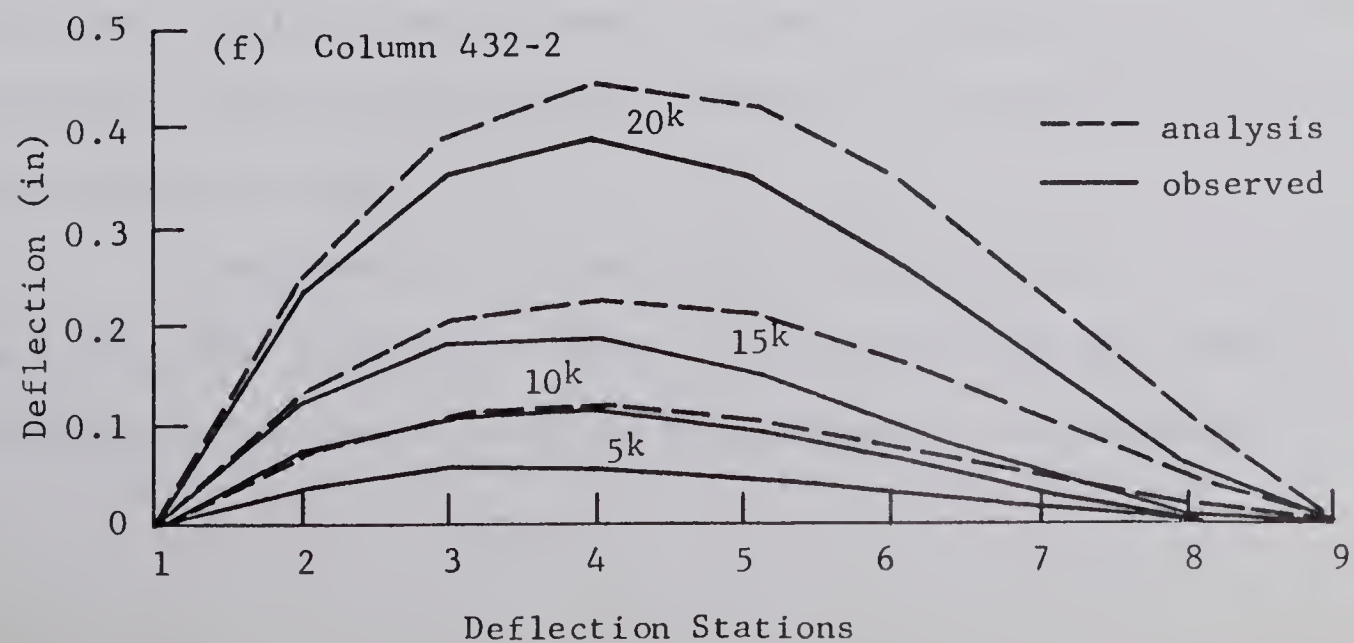
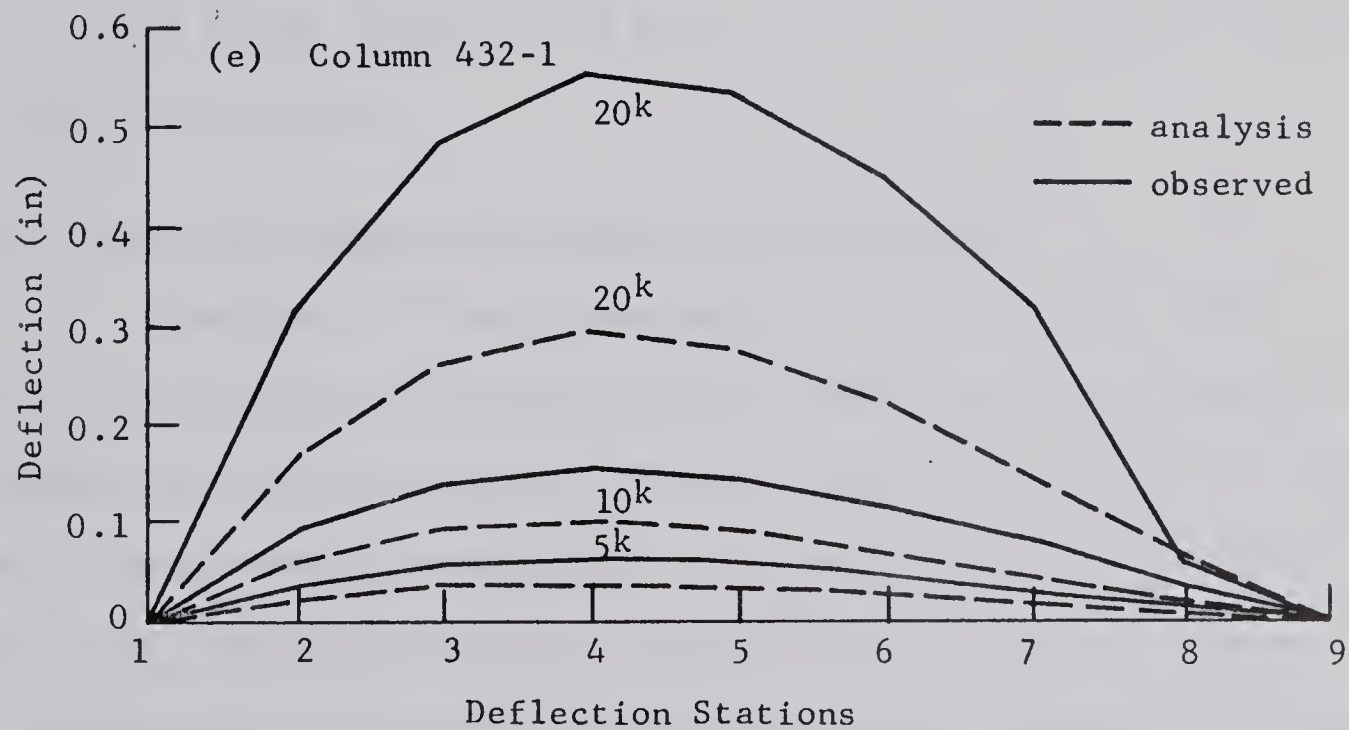
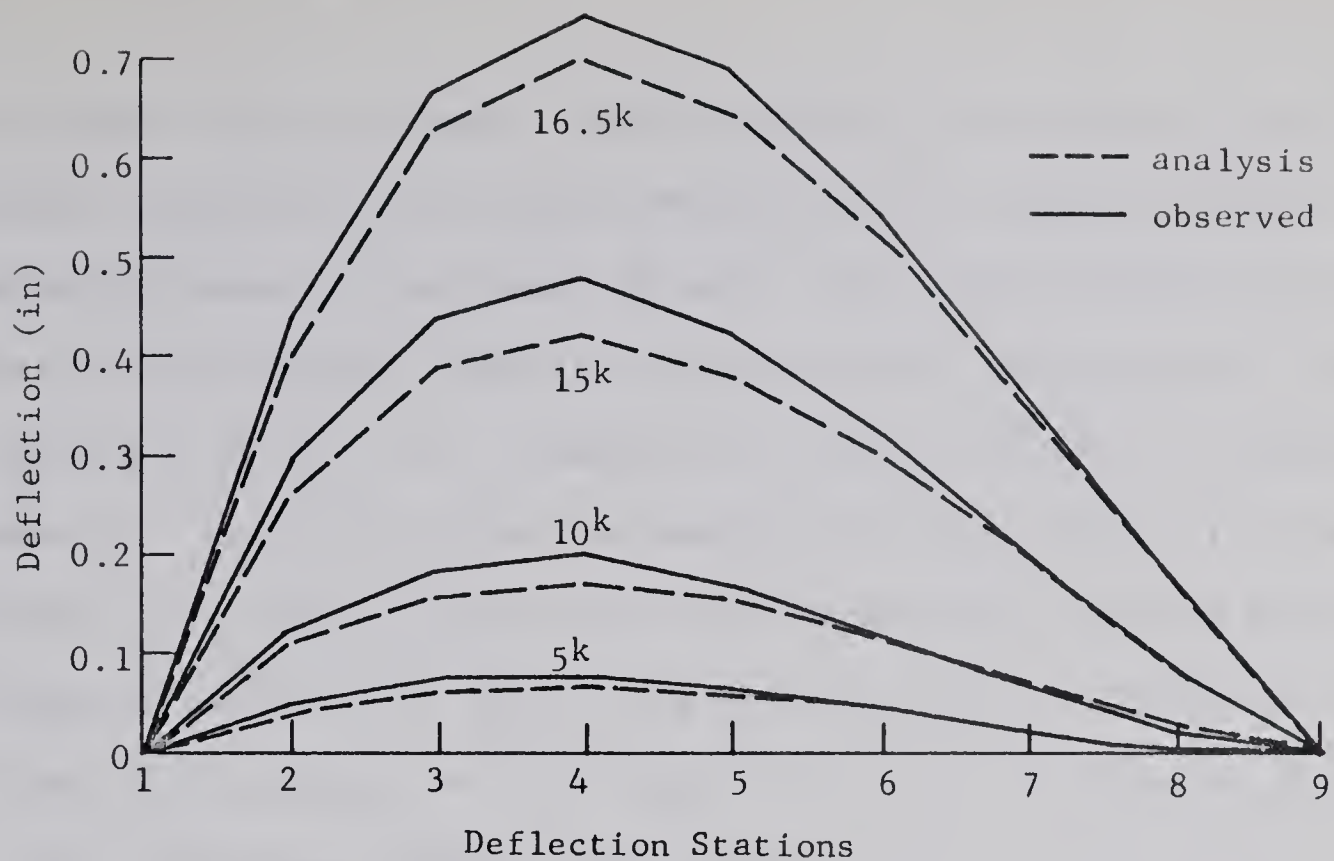


FIGURE 6.3

ANALYSIS APPLIED TO COLUMN TESTS OF MARTIN AND OLIVIERI

(d) Column 422-2

78



calculated deflected shapes. There appears to be a greater amount of double curvature in the computed deflected shapes than in the observed deflected shapes at each level of load. This would indicate that the ratio of observed end eccentricities was greater (more positive) than the reported value of $-1/2$. Columns 422-1 and 432-2 exhibit the opposite behavior. These cases show that computed deflected shapes are larger and exhibit less double curvature than the corresponding observed deflected shapes at each level of load. This would indicate that the ratio of observed eccentricities was less (negatively) than the reported value of $-1/2$. The slender columns of the investigation are quite sensitive to load and a slight change in end eccentricity could result in a large change in deflection.

6.4 Short-Time Tests of Columns in Frames-Furlong

Furlong ⁽¹³⁾ has investigated the behavior under short-time loading of rectangular reinforced concrete frames containing columns bent in symmetrical single curvature. The test series consisted of six frames in which three nominal values of e/t were considered by varying the column stiffness, the beam stiffness, and the manner of loading. Frames 1 and 5 were not included in this comparison because in Frame 1, the columns were not identical, and in Frame 5, trouble developed with the loading apparatus midway through the test. Details of Frames 2R, 3R, 4, and 6 are included in TABLE 6.3.

The frames were loaded by applying axial loads to the columns, and two, point loads to the beams. These beam loads were applied at a distance "X" on each side of the beam mid-span. The parameter "X" is

TABLE 6.3

DETAILS OF FURLONG'S TESTS ON RECTANGULAR

FRAMES WITH COLUMNS BENT IN SINGLE CURVATURE

Frame	L _c in	L _B in	t _B =t _c in	b _B =b _c in	X in	Nom. e/t	$\frac{d'}{t_B} = \frac{d'}{t_c}$	E _s ksi x 10 ³	f' _{ca} ksi	f _y ksi	$\frac{L_B}{L_c}$	reinf. (in ²)	
												beam A _S =A _S '	col. A _S =A _S '
2R	80	120	4.0	6.0	20	0.106	0.20	28.4	4.30	57.0	1.48	0.80	0.22
3R	80	120	4.0	6.0	20	0.337	0.20	29.5	3.34	58.5	1.48	0.80	0.22
4	80	64	4.0	6.0	16	0.222	0.20	30.2	3.24	54.0	0.81	0.80	0.22
6	60	144	4.0	6.0	20	0.320	0.20	29.7	3.55	53.0	2.31	0.80	0.22
7*	60	144	4.0	6.0	20	0.141	0.20	29.7	4.80	50.7	2.31	0.80	0.22

*Sustained load test reported by Furlong and Ferguson (14)

also included in TABLE 6.3.

6.4.1 Comparison of the Results of Furlong's Frame Tests with the Results of the Analysis

FIGURES 6.4 to 6.7 show the comparisons between the measured and computed column deformation characteristics. Part (a) of each figure shows load-rotation curves and part (b) of each figure shows load-deflection curves. No differentiation, other than symbolic, has been made as to the location of the observed readings. Load-deformation curves computed at the University of Texas have also been included in the figures.

The correlation was good in all cases between the analytical and the observed results. The analysis of this thesis appears to give better results than does the analysis developed at the University of Texas. The reason for this can be attributed to the differences in the assumptions of the instantaneous stress-strain properties of concrete. The analysis of the University of Texas uses a value of k_3 of 1.00 and credits the concrete with no tensile strength, while the analysis of this thesis was applied using a k_3 value of 0.85 and crediting the concrete with a tensile resistance. The total range of concrete resistance is approximately the same in both cases. However, for the frameworks of Furlong's investigation, the loading produced larger tensile forces in the beams than in the columns. Consequently, by using the Texas analysis, the relative stiffnesses of the beams were underestimated and the predicted column moments and deformations were larger than did actually occur. Another point of difference between the two methods of analysis is that the Texas analysis considers concrete to be a non-linear elastic material and the analysis of this thesis does

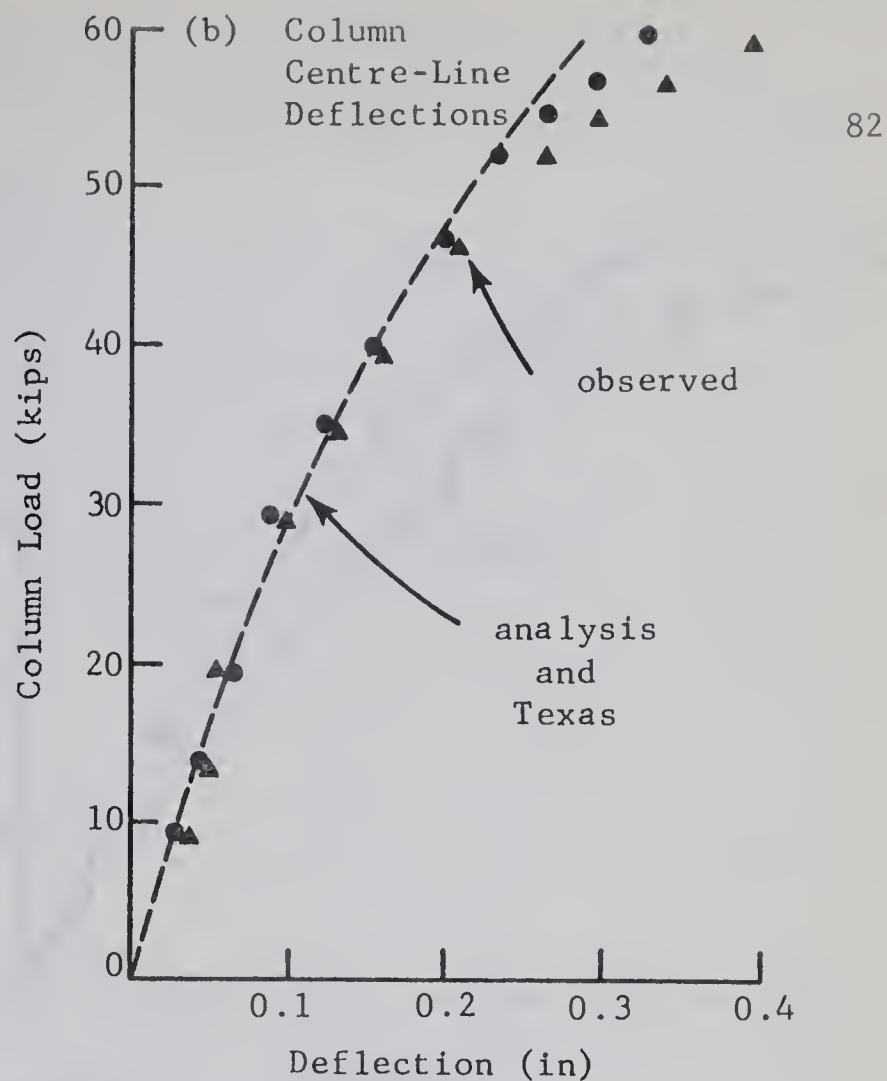
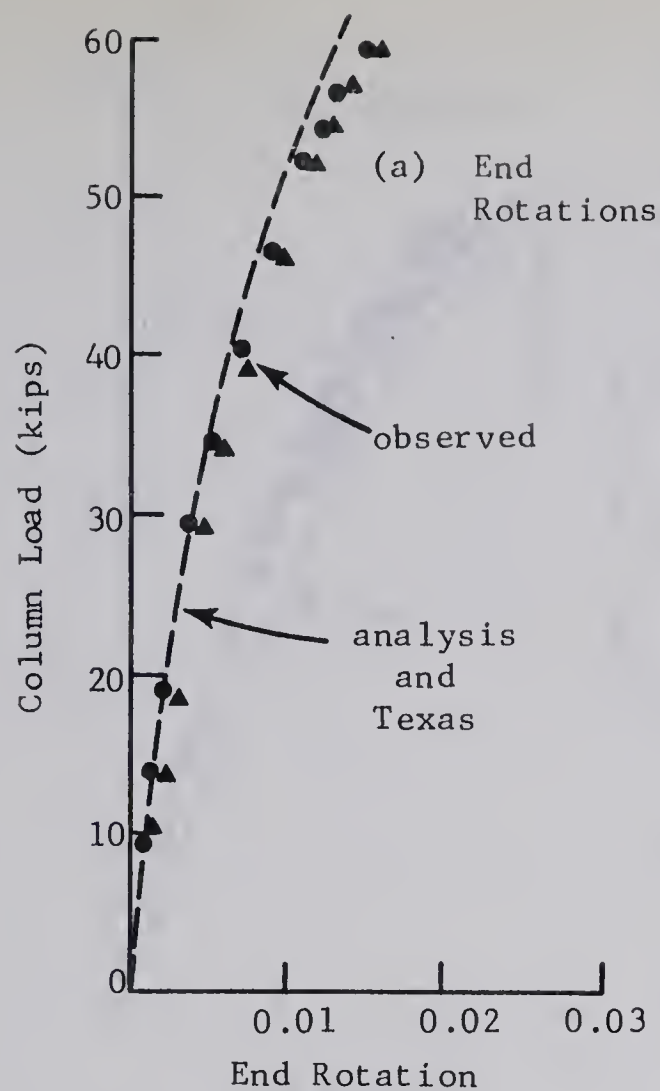


FIGURE 6.4
ANALYSIS APPLIED TO FURLONG TEST FRAME NO. 2R

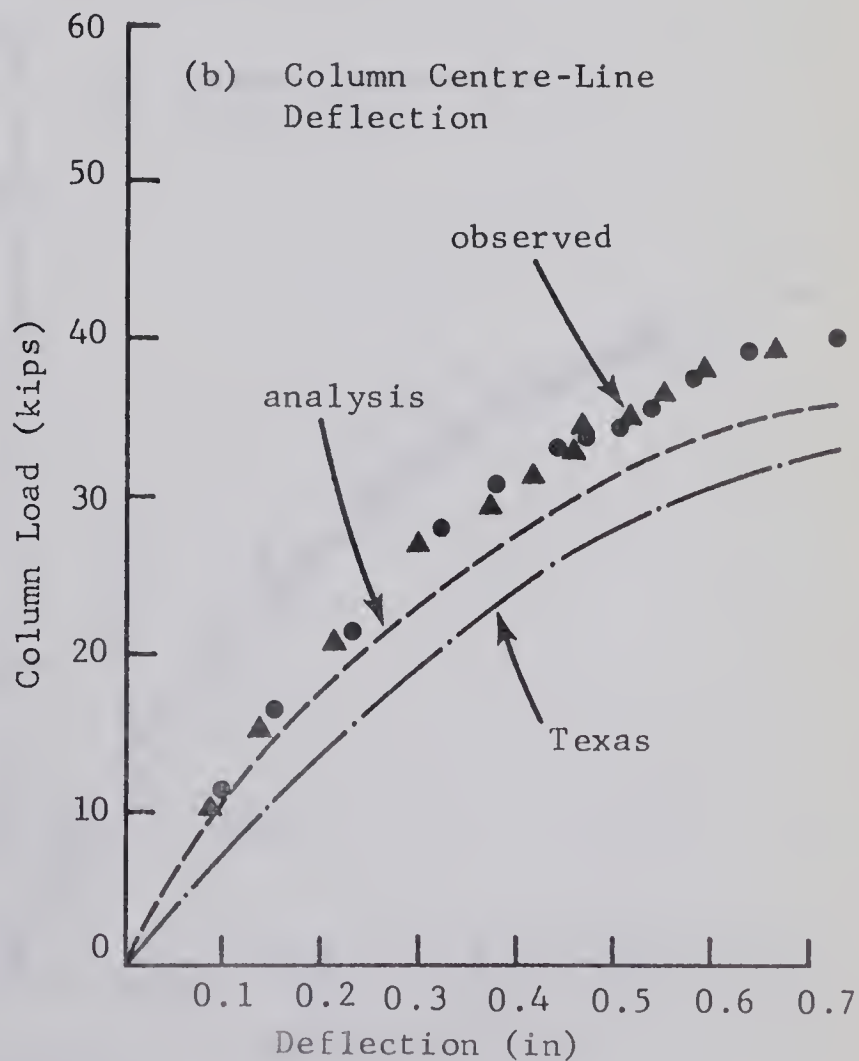
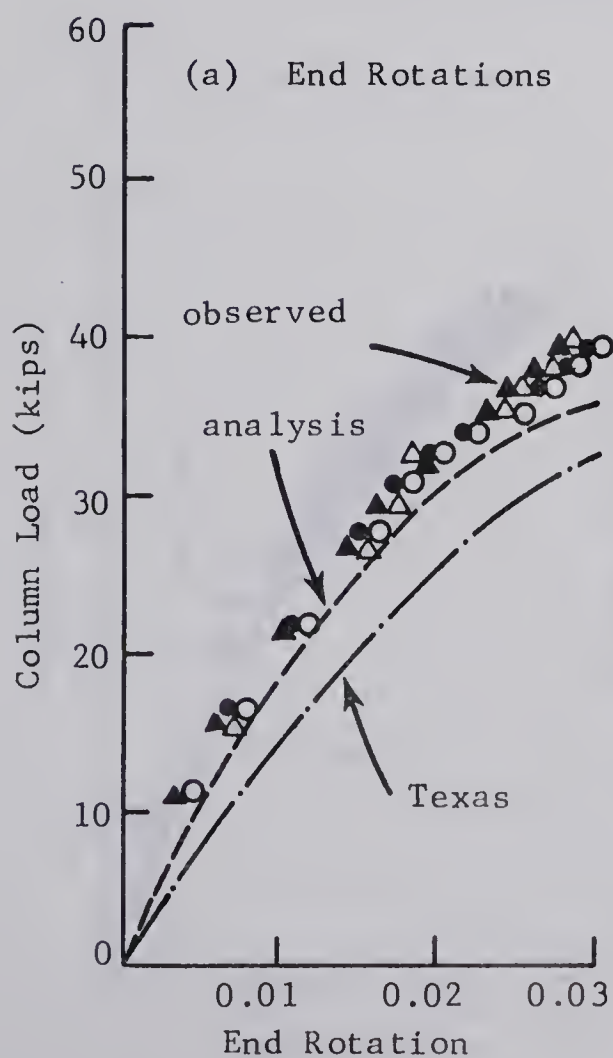


FIGURE 6.5
ANALYSIS APPLIED TO FURLONG TEST FRAME NO. 3R

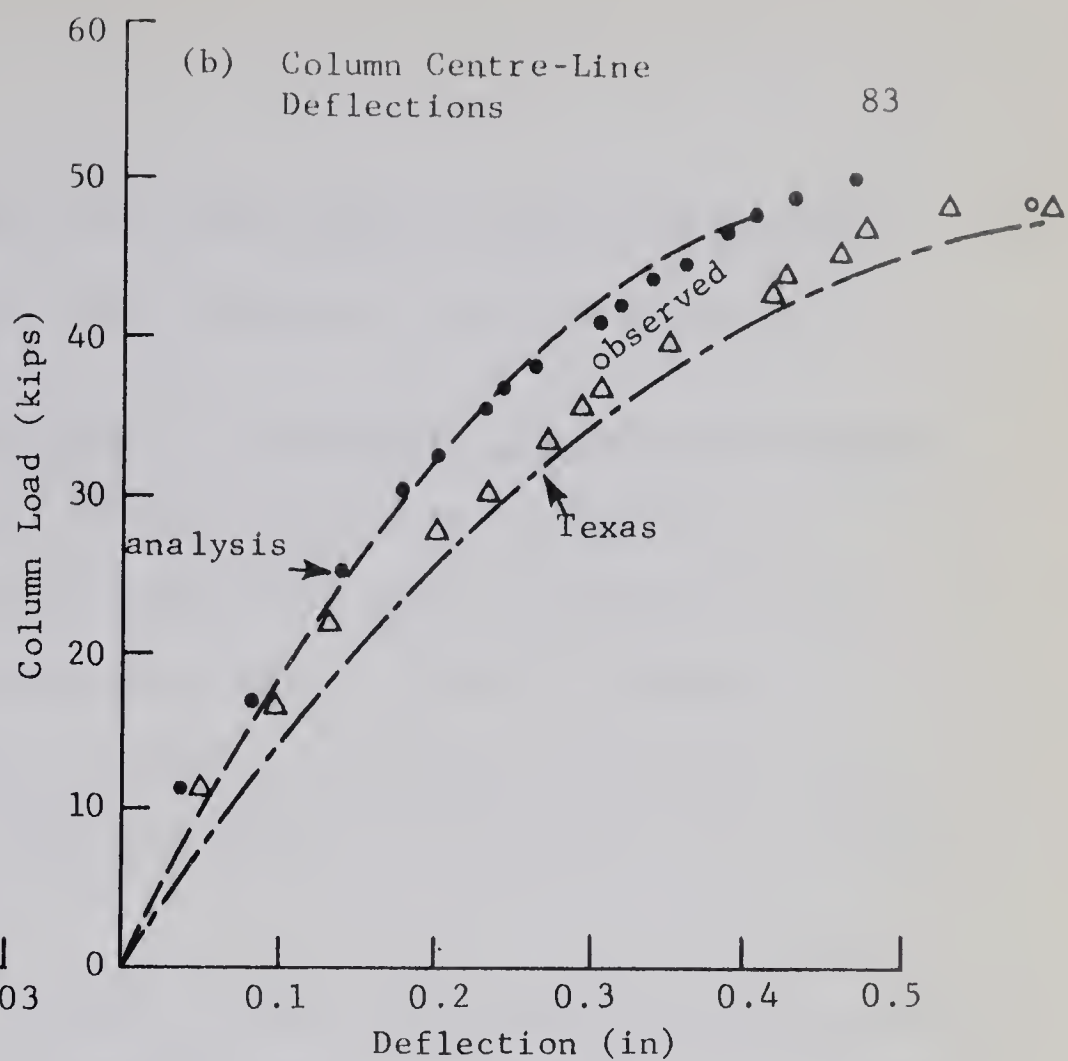
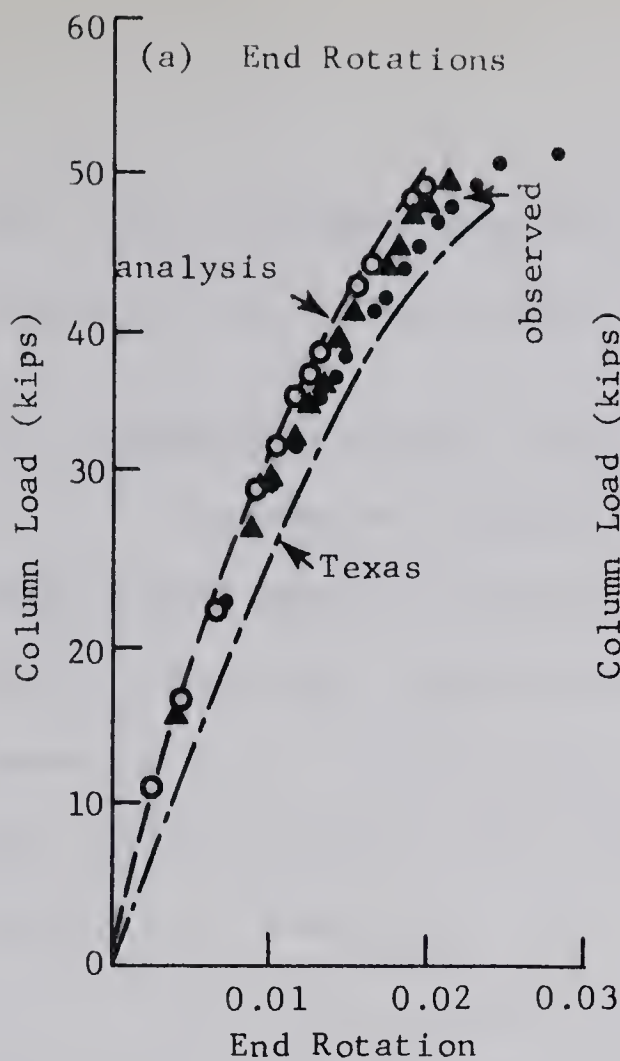


FIGURE 6.6
ANALYSIS APPLIED TO FURLONG TEST FRAME No. 4

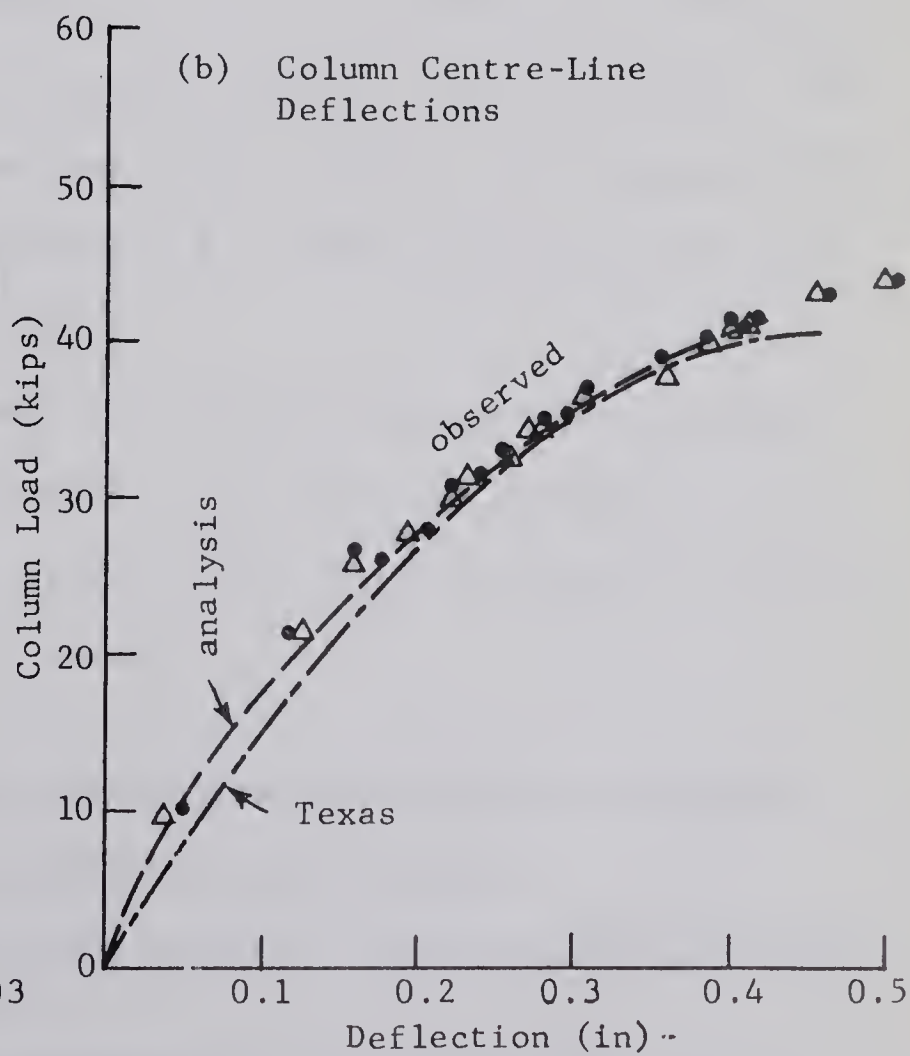
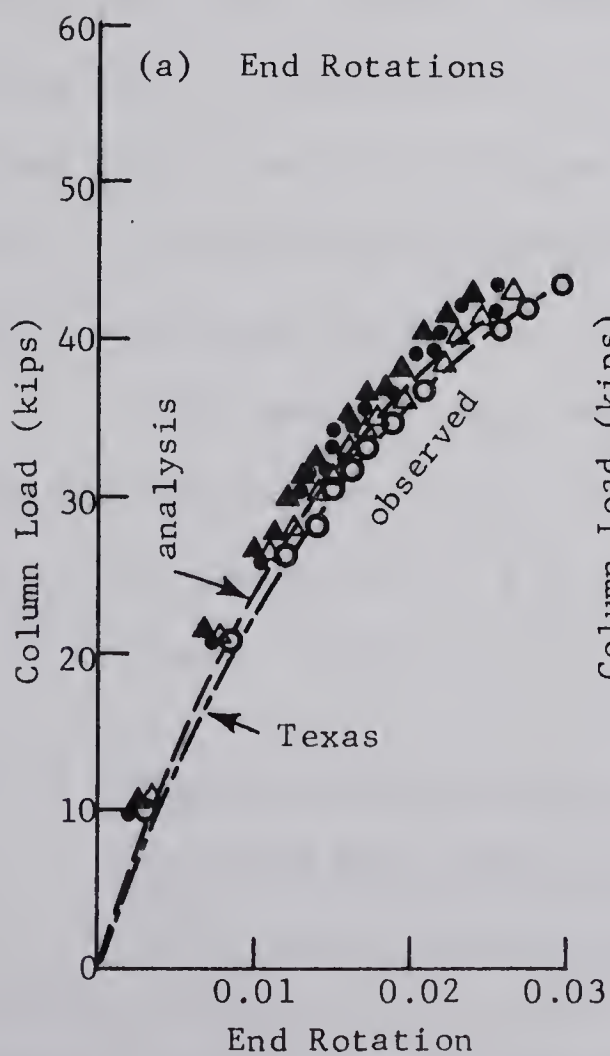


FIGURE 6.7
ANALYSIS APPLIED TO FURLONG TEST FRAME No. 6

not. This difference apparently had little effect because the unloading of sections was not significant until the failure load was approached.

6.5 Sustained Load Test of Columns in a Framework - Furlong and Ferguson

Furlong and Ferguson ⁽¹⁴⁾ have reported on the testing of a rectangular, reinforced concrete, closed frame under a sustained load of 100 days duration. The frame was quick loaded to failure following the sustained load. This test was conducted as a continuation of the original test series by Furlong ⁽¹³⁾, and the details* of the specimen are included as Frame 7 in TABLE 6.3.

The creep strains in FIGURE 3.6 have been modified through division by 1.30 to account for the fact that the frame was cured under more favorable conditions than assumed in SECTION 3.3.1. This modification reduces the creep data to approximately the values originally derived by Rüschi. The creep coefficients for the equations of the analysis were determined from the approximate equations of SECTION 3.3.8. These equations were also modified through division by 1.30.

The variable k_3 , which reflects the similarity in strength between the specimen and the companion cylinders, was assigned a value of 1.00 in the analysis. A previous analysis with $k_3 = 0.85$ did not produce as good a correlation with results.

6.5.1 Comparison of the Results of Furlong and Ferguson's Sustained Load Frame Test with the Results of the Analysis

The results of Furlong and Ferguson's sustained load frame test

*Details and test results were supplied through private communication with R.W. Furlong, Associate Professor of Civil Engineering, University of Texas.

are compared to the analytical results in FIGURE 6.8. The column load has been plotted against the centre-line deflections for both the beams and the columns. In this form, the deflection curves under sustained load show up as horizontal lines at the level of sustained load. The durations of loading considered were 44 hours, 285 hours, and 100 days, and the analysis and experimental results corresponding to these times are shown in FIGURE 6.8.

The analytical deflections were higher than the observed deflections under the initial short-time loading. However, under the short-time load which was sustained, the error was not appreciable, particularly for the east column and the south beam.

Under sustained load, a good correlation existed between the analysis and the observed deflections for the east column. The deflections for the west column were lower than those predicted by the analysis. For the beams, the correlation was relatively good for all durations of loading considered. The computed deflection corresponds approximately to the observed deflection for the south beam after 100 days under sustained load.

For the application of quick load following the sustained load, deflections predicted by the analysis were higher than the observed deflections. However, the correlation was reasonably good for the west column and the north beam, and very good for the east column and the south beam.

The curves showing analytical behavior were terminated at 70 kips because the computer would not calculate deflections at the failure load of approximately 73 kips. The observed failure load was 78.5 kips.

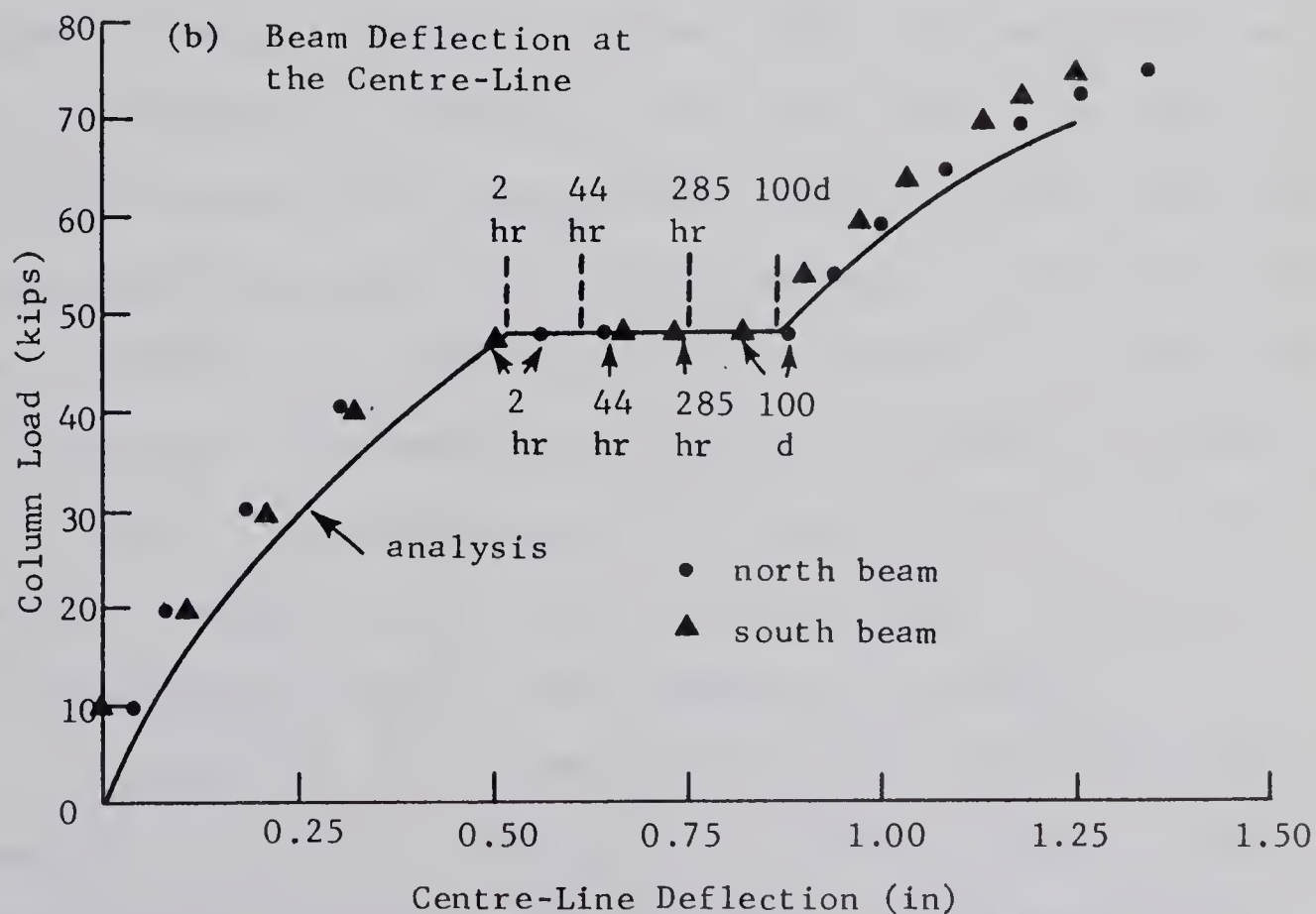
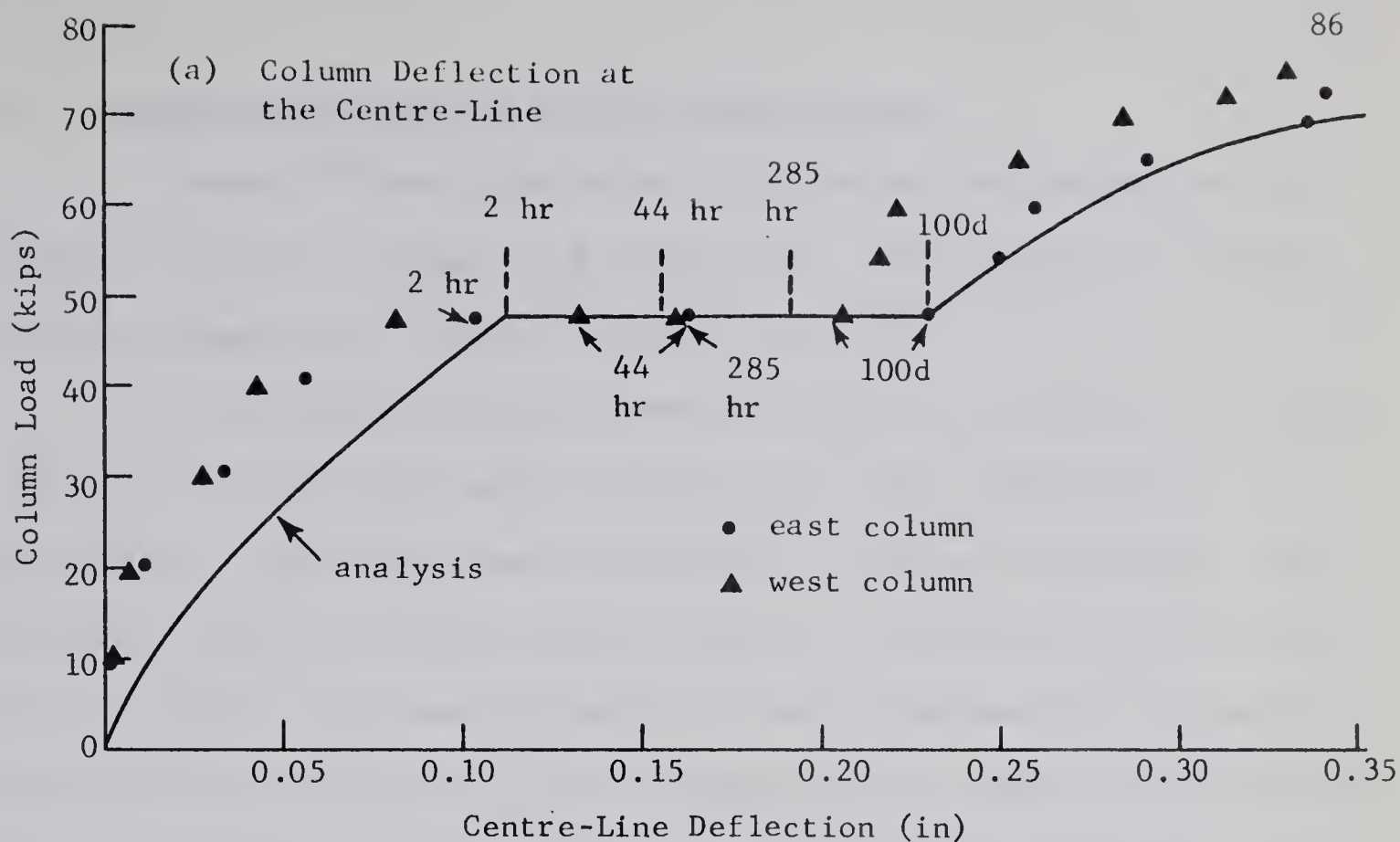


FIGURE 6.8

ANALYSIS APPLIED TO THE TEST FRAME
OF FURLONG AND FERGUSON

6.6 Sustained Load Tests of Hinged Columns - Green

Green (16) has reported on the sustained load testing of ten reinforced concrete columns with hinged ends. The properties of these column specimens are contained in TABLE 6.4.

The columns were moist cured for five to six days and then were stored in the laboratory until the day of the test, approximately six weeks later. The curing conditions during the period of sustained load fluctuated about an average relative humidity of 75% and an average temperature of 64.5°F. The average monthly difference between the 5th and 95th percentile temperatures and relative humidities was approximately 20°F and 35%, respectively. An estimation of creep under these conditions is difficult since according to Neville and Meyers (28), the creep under a varying relative humidity will be higher than that which would occur under a constant humidity equal to the average value. For this reason, even though the curing conditions appear to be better for Green's columns than those assumed in SECTION 3.3.1, the creep curves of FIGURE 3.6 have been used for the comparison. The approximate equations of SECTION 3.3.8 have been used to determine the coefficients of the creep equation at various durations of loading. A minimum of three creep stages was used in the analysis to predict the behavior under the longer durations of loading.

The value of k_3 was set at 0.75 for the calculations using the analysis of this thesis. Because little is known of the concrete quality, this value was based on the parameters used by Green in his analysis. In Green's analysis, the strength gain was assumed to be complete and k_3 varied from 0.95 to 0.82 with duration of loading, but the concrete was credited with no tensile strength. Therefore, to keep the

TABLE 6.4

DETAILS OF GREEN'S HINGED END COLUMNS

TESTED UNDER SUSTAINED LOAD

Column	Sust. load (k)	Ecc. (in)	t_c (in)	b_c (in)	L_c (in)	E_s (ksi x 10 ³)	f_y (ksi)	f'_{ca} (ksi)	$A'_s = A_s$ (in ²)
S-1	53.0	0.15	4.02	5.94	75.0	29.2	65.5	4.00	0.246
S-2	27.5	1.00	4.06	6.03	76.0	29.2	60.2	5.50	0.240
S-3	42.5	0.15	4.09	6.00	75.0	29.2	58.1	5.50	0.240
S-4	42.0	0.725	4.06	6.00	75.0	29.2	56.0	4.00	0.238
S-5	41.5	0.425	4.09	6.00	75.0	29.2	58.4	3.96	0.243
S-6	36.5	0.63	4.05	6.07	75.0	29.2	64.2	3.32	0.242
S-7	29.0	0.60	4.06	6.00	77.0	29.2	58.7	3.96	0.238
S-8	30.0	1.10	4.09	6.00	75.0	29.2	59.7	4.10	0.244
S-9	30.0*	1.70	4.03	6.00	75.0	29.2	63.5	4.10	0.243
S-10	18.0	1.70	4.03	6.00	75.0	29.2	65.4	3.45	0.242

*Failed under a short-time load of 31.0^k.

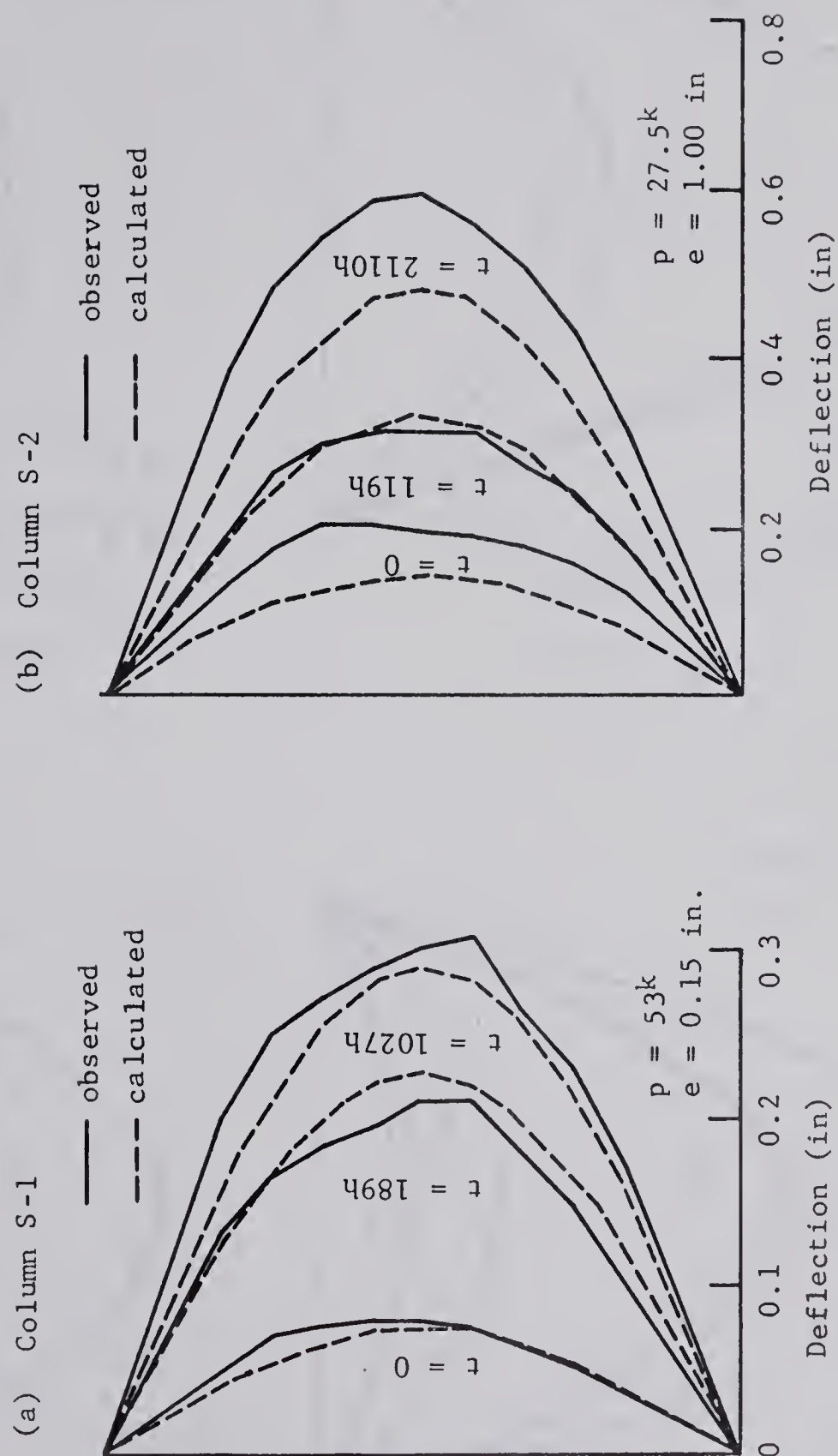
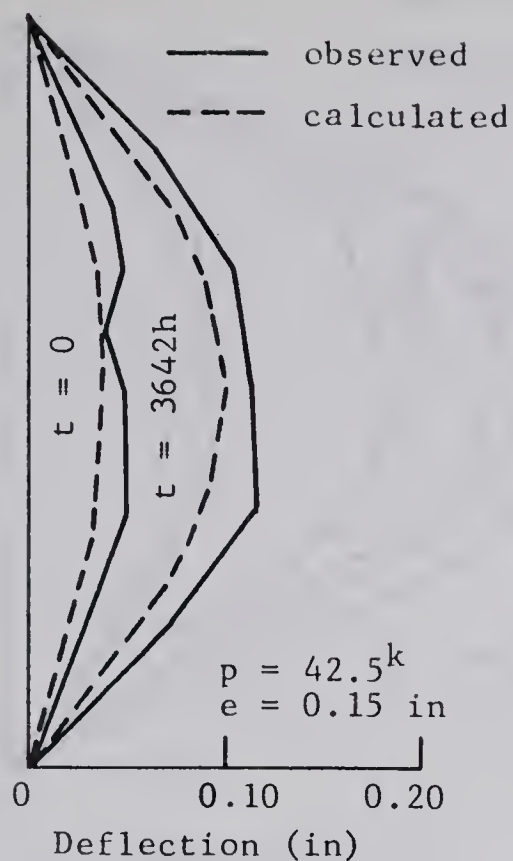
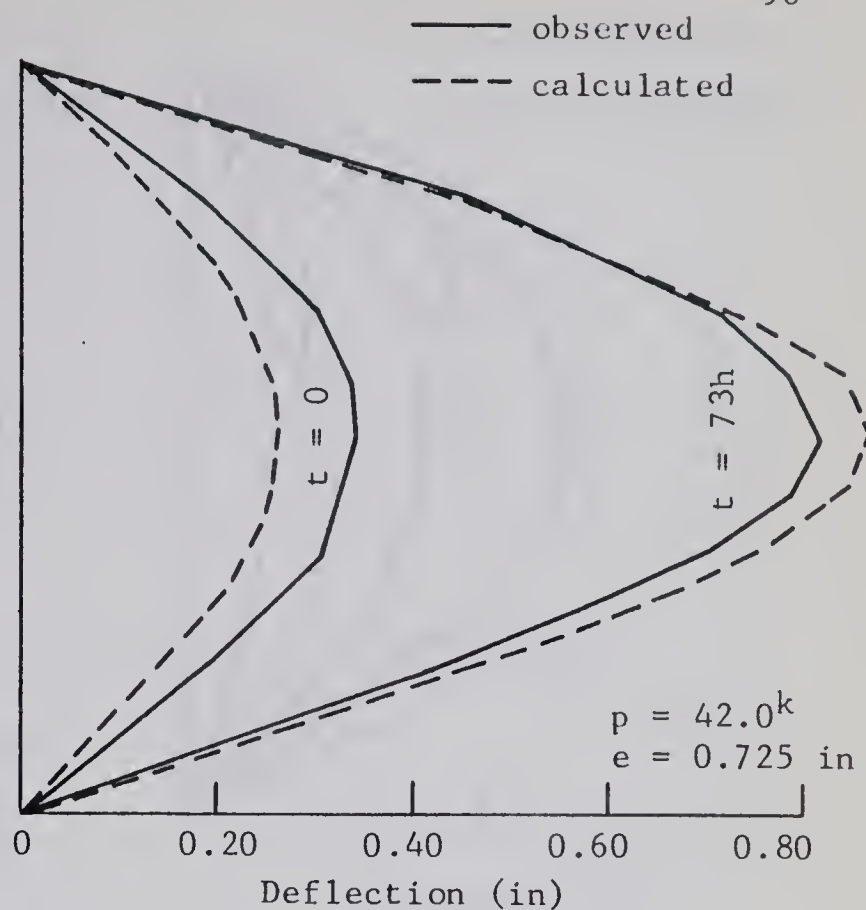


FIGURE 6.9

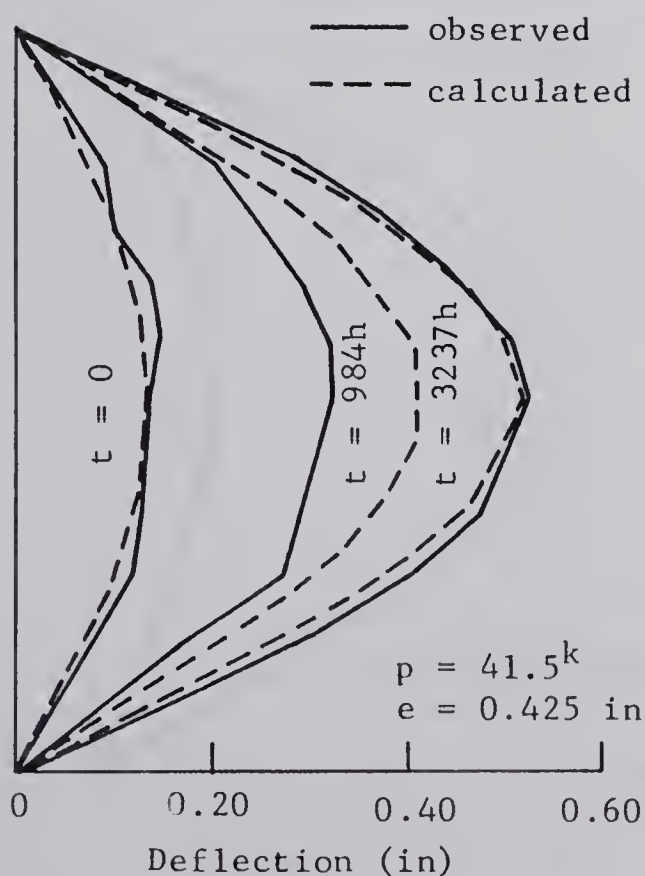
THE ANALYSIS APPLIED TO THE COLUMN
TESTS OF GREEN



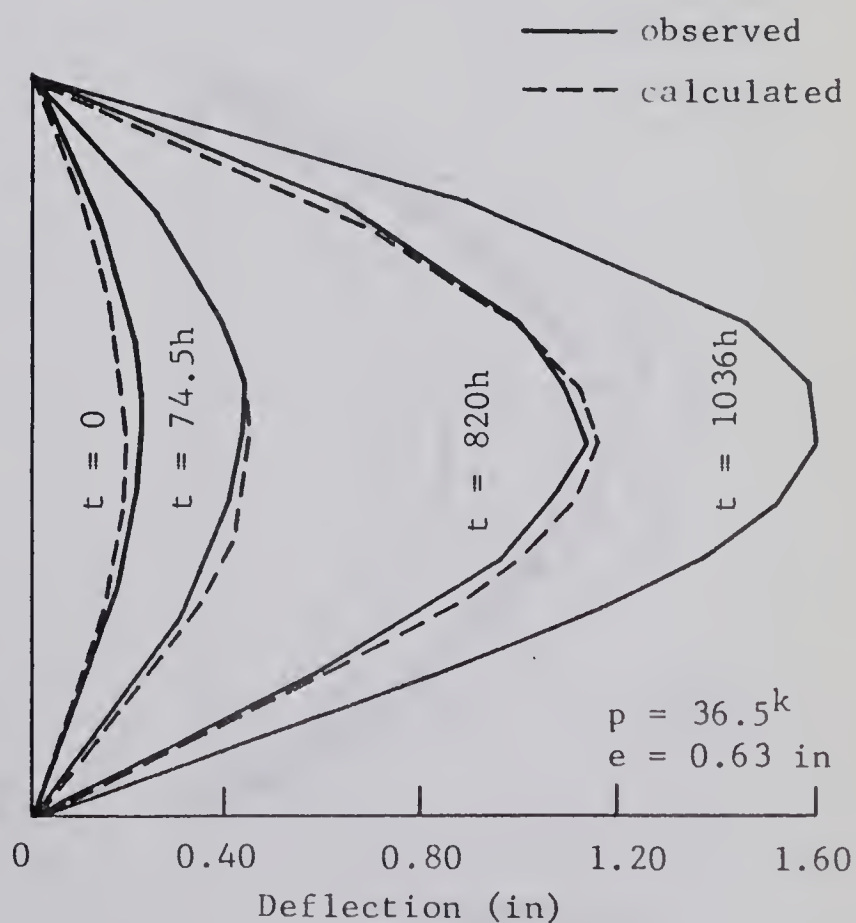
(c) Column S-3



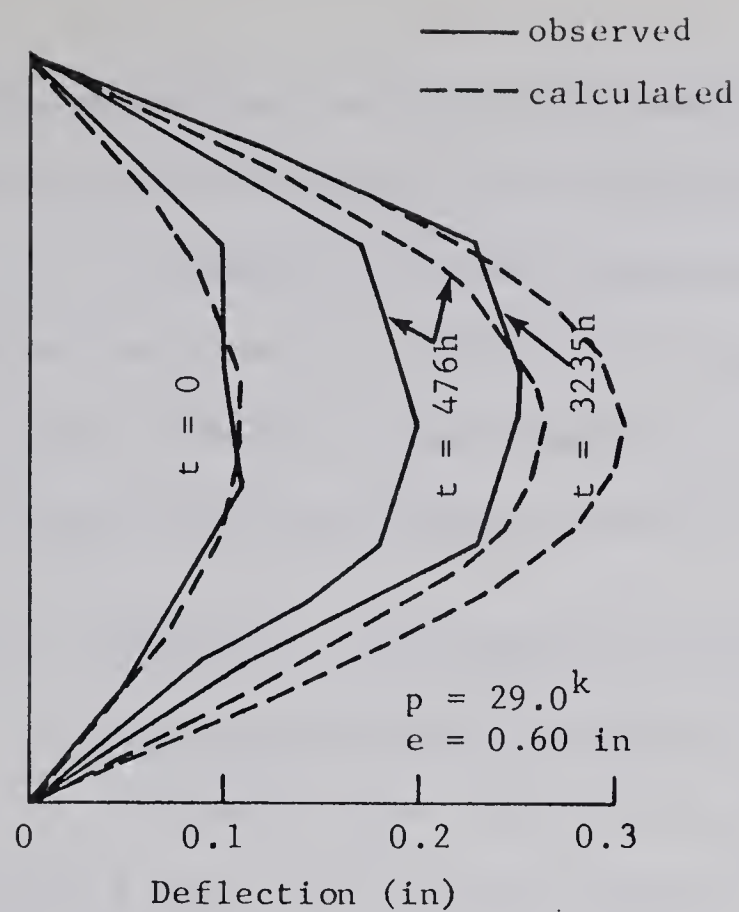
(d) Column S-4



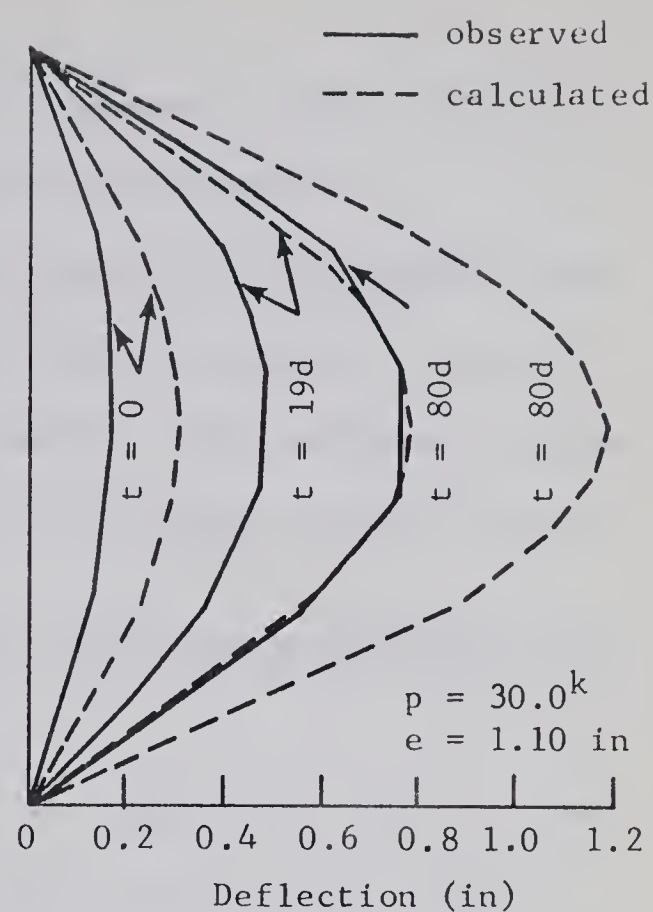
(e) Column S-5



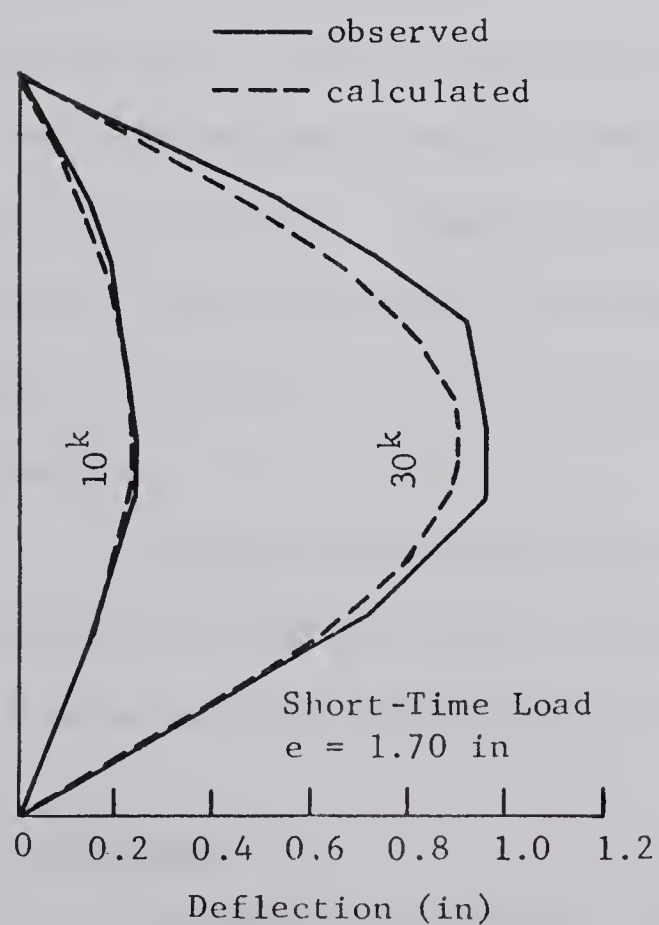
(f) Column S-6



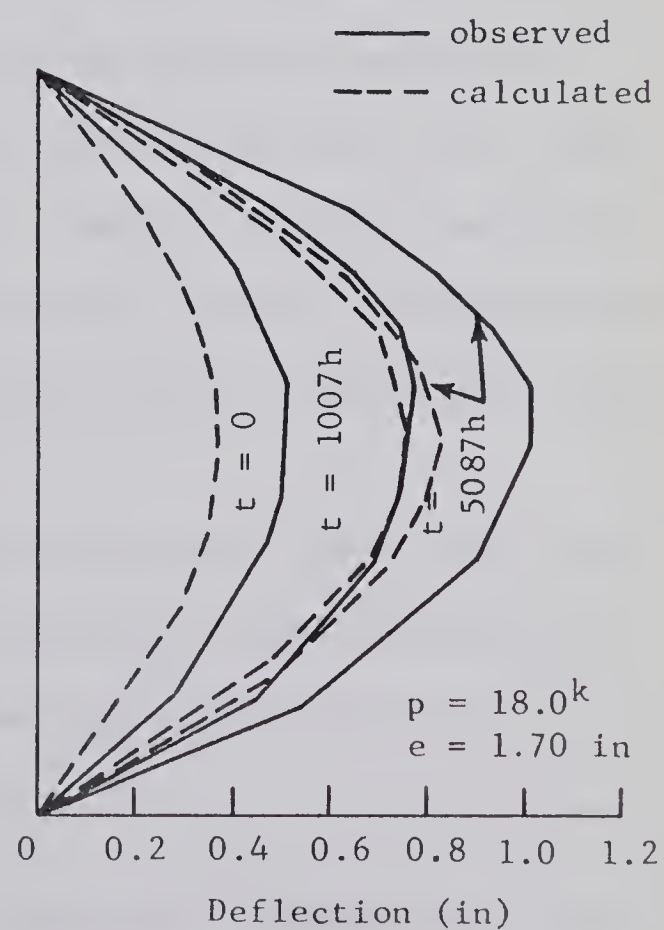
(g) Column S-7



(h) Column S-8



(i) Column S-9



(j) Column S-10

range of concrete resistance approximately the same in both analyses, k_3 was set at 0.75 for use with the analysis of this thesis.

Although the column lengths were reported as 75 inches, each end of the column was stiffened by a considerable increase in section size over a length of approximately 11.5 inches. The stiffness of these end blocks was approximated as infinite in the analysis of this thesis.

6.6.1 Comparison of the Results of Green's Sustained Load Column Tests with the Results of the Analysis

FIGURES 6.9(a) to 6.9(f) show the computed and actual column deflected shapes after various periods under sustained load. The durations of loading in hours have been noted on the curves.

The correlation between the measured and the computed deflected shapes was reasonably good for most of the columns. Columns S-2 and S-10 show calculated deflected shapes which were considerably smaller than the observed deflected shapes under short-time loading and at the longest duration of loading. Columns S-7 and S-8, however, exhibited calculated deflected shapes which were considerably larger than the observed deflected shapes. For column S-6, the analysis column failed at the longest duration of loading.

Although Green's analytical results have not been shown, his correlation between the actual and the observed mid-height deflections was similar to that achieved using the analysis of this thesis.

6.7 Conclusion

The method of analysis, for the most part, showed a good correlation with the results of experimental investigations. However, only one

of these investigations involved sustained loading of a frame. As this is within the field of application of the method of analysis, it would be desirable to correlate with more frame investigations as they become available.

Before the analysis could be applied to the experimental investigations, the material properties for the concrete had to be determined for the particular test conditions. Generally, all the influencing factors are not reported on by the investigators, and a determination of the material properties becomes partly intuitive. This is especially true in the determination of the value of k_3 to be used. Usually the only information available is the value of k_3 used by the investigators in the analyses applied to their own tests.

CHAPTER VII

DESCRIPTION OF THE INVESTIGATION OF LONG COLUMNS IN FRAMEWORKS

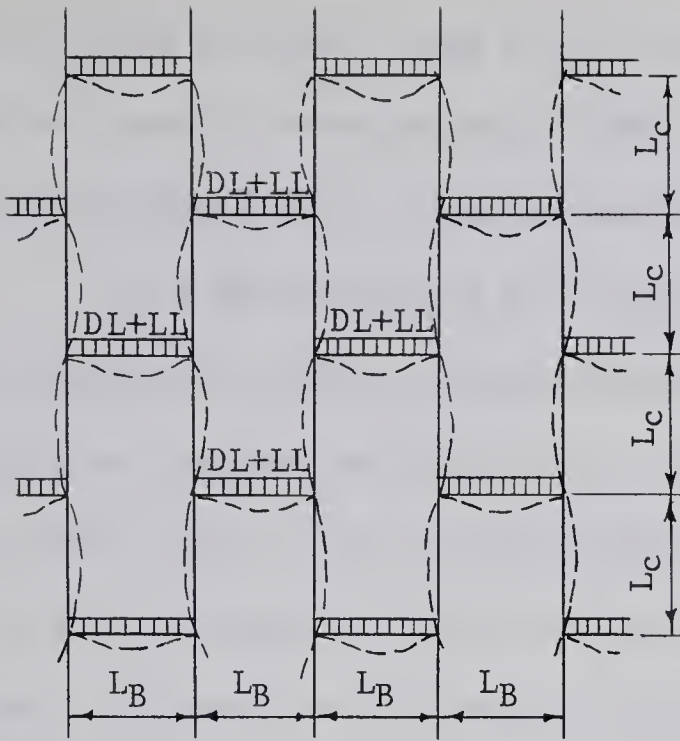
7.1 Introduction

The analysis developed in CHAPTERS III to VI of this thesis has been applied to an investigation of the effect of sustained load on the behavior of long, reinforced concrete columns in a number of selected frameworks. The columns were bent in either symmetrical single curvature or double curvature with one end of the column fixed. The major variables in the investigation were the column slenderness ratio and the level of the sustained load.

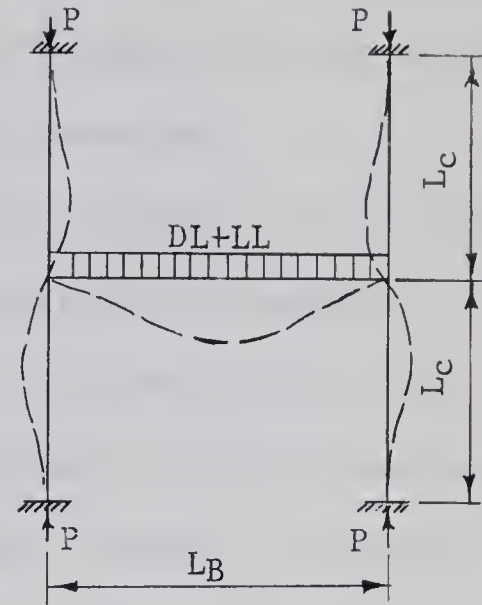
This chapter provides a description of the frameworks, the assumptions used in the analysis of the frameworks, the scope of the analysis, and the data used in the analysis. The final section discusses the choice of the frameworks.

7.2 Description of the Frameworks

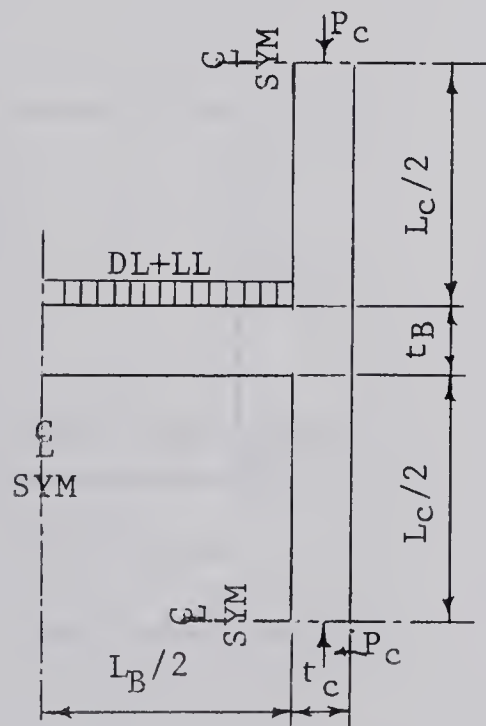
The columns of the investigation were included in the frameworks shown in FIGURES 7.1(a) and 7.1(b). FIGURE 7.1(a) shows the column bent in symmetrical single curvature and FIGURE 7.1(b) shows the column fixed at one end and bent in double curvature. Because of the symmetry present in the frameworks, the investigation of column behavior can be carried out by analysis of the partial frameworks of FIGURES 7.1(c) and 7.1(d). FIGURE



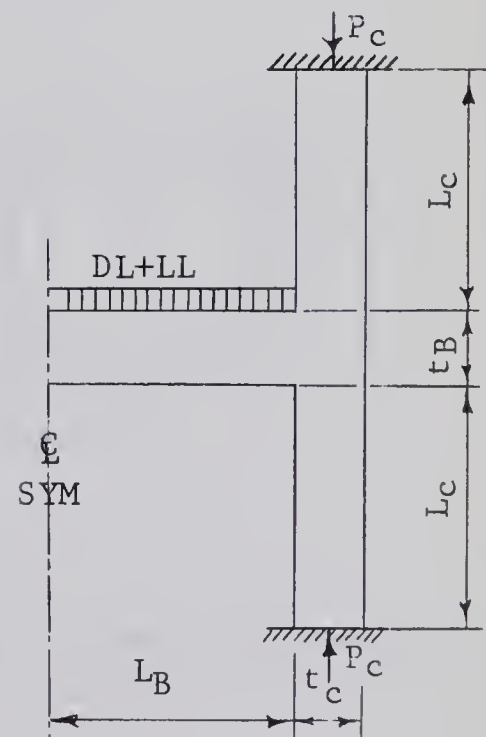
(a) The Column in Symmetrical Single Curvature



(b) Column Bent in Double Curvature



(c) Model for the Analysis of the Columns Bent in Symmetrical Single Curvature



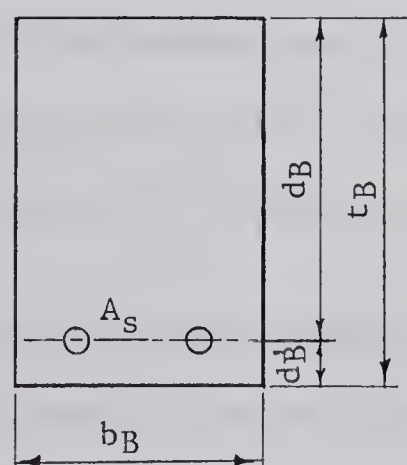
(d) Model for the Analysis of the Columns Bent in Double Curvature

FIGURE 7.1

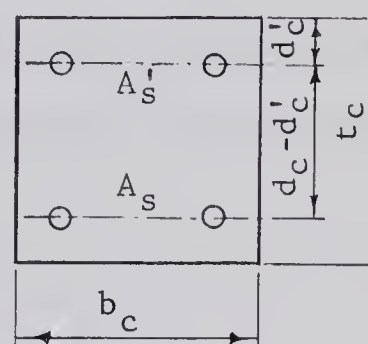
FRAMEWORKS OF THE ANALYSIS

7.1(c) shows the model used in the analysis of the columns bent in symmetrical single curvature and FIGURE 7.1(d) shows the model for the analysis of the columns fixed at one end and bent in double curvature.

The properties of all the beams were kept constant in the column investigations. These included the geometric properties, the material properties, and the uniform load. A typical beam cross-section is shown in FIGURE 7.2(a). The corresponding column properties with the exception of length and level of sustained load were also kept constant. A typical column cross-section is shown in FIGURE 7.2(b).



(a) Beam Cross-Section



(b) Column Cross-Section

FIGURE 7.2

MEMBER CROSS-SECTIONS

The following assumptions have been made to simplify the analysis of the frameworks:

1. All columns in any particular framework are identical in every respect except length.
2. The columns have a constant cross-section over their length.
The beams have reinforcement only on the tension face regardless of variations in the location of the point of contraflexure.
3. The members are initially straight.
4. The ends of the members do not deflect vertically or laterally.
5. The uniform load on the beams is constant and is sustained indefinitely.
6. The column loads are applied axially at the column ends. They may be either sustained or increased in stages.
7. In the models used for analysis (FIGURES 7.1(c) and (d), the additional axial load in the lower column due to the uniform load on the beam has been ignored.

7.3 Scope of the Investigation

A total of twelve frameworks have been analysed for this thesis. Six of the frameworks contained columns bent in symmetrical single curvature and six of the frameworks contained columns fixed at one end and bent in double curvature. Each group of six frameworks was formed by considering geometrical slenderness ratios of $L_c/t_c = 10, 16, 22, 28, 34,$ and 40 .

Six different loading sequences were applied to the columns in each of the twelve frameworks. Initially, the short-time failure load was obtained by successive incrementation of the column axial load. The five

remaining load sequences were formed by applying to the columns, sustained axial loads equal to 30%, 40%, 50%, 60%, and 70% of the short-time failure load. The duration of sustained load was 25 years with intermediate calculations being made at seven days and nine months based on the creep properties assumed in SECTION 3.3.8. If failure did not occur during the period of sustained load, increments of short-time axial load were then applied to produce failure.

A maximum of eight loading stages were used in applying each loading sequence to the single curvature columns and seven loading stages in applying each loading sequence to the double curvature columns. Each loading stage represented either an increment of load in the case of short-time loading or an increment of time in the case of sustained loading. The sustained load stages were preceded by a short-time loading stage to the value of the sustained load.

7.4 Data for the Analysis

The numerical data have been divided into four categories:

1. dimensions and loads
2. material properties
3. increments to attain convergence of the trial and error procedures
4. permissible variations in the convergence of the trial and error procedures.

7.4.1 Dimensions and Loads

The same beam was used in all the frames analyzed. This beam is described in TABLE 7.1.

TABLE 7.1
BEAM DIMENSIONS AND LOAD

Uniform load (k/ft)	Length L_B (ft)	Depth t_B (in)	Width b_B (in)	$\frac{d'}{t_B}$	Steel $\frac{A_s}{b_B t_B}$ (%)
4.0	20.0	17.5	12.0	0.100	3.0

The uniform load on the beam of 4k/ft represents 64% of the failure load of an identical simply supported beam.

The column data held constant in the analyses are listed in TABLE 7.2.

TABLE 7.2
CONSTANT COLUMN DIMENSIONS

Depth t_c (in)	Width b_c (in)	$\frac{d'}{t_c}$	Tension steel $A_s/b_c t_c$ (%)	Comp. steel $A'_s/b_c t_c$ %
12.0	12.0	0.100	1.00	1.00

Column designations, lengths, slenderness ratios, and levels of sustained load are included in TABLES 7.3 and 7.4 for the columns bent in single curvature and the columns bent in double curvature respectively. The actual values of load considered in each loading stage of each loading sequence are dependent on the results of the analysis of the columns loaded

TABLE 7.3

VARIABLE DATA FOR THE COLUMNS BENT

IN SYMMETRICAL SINGLE CURVATURE

Column	Length (ft)	$\frac{L_c}{t_c}$	Sustained load	Column	Length (ft)	$\frac{L_c}{t_c}$	Sustained load
S-10.ST	10.0	10	--	S-28.ST	28.0	28	--
S-10.30	10.0	10	0.30 PULT	S-28.30	28.0	28	0.30 PULT
S-10.40	10.0	10	0.40 PULT	S-28.40	28.0	28	0.40 PULT
S-10.50	10.0	10	0.50 PULT	S-28.50	28.0	28	0.50 PULT
S-10.60	10.0	10	0.60 PULT	S-28.60	28.0	28	0.60 PULT
S-10.70	10.0	10	0.70 PULT	S-28.70	28.0	28	0.70 PULT
S-16.ST	16.0	16	--	S-34.ST	34.0	34	--
S-16.30	16.0	16	0.30 PULT	S-34.30	34.0	34	0.30 PULT
S-16.40	16.0	16	0.40 PULT	S-34.40	34.0	34	0.40 PULT
S-16.50	16.0	16	0.50 PULT	S-34.50	34.0	34	0.50 PULT
S-16.60	16.0	16	0.60 PULT	S-34.60	34.0	34	0.60 PULT
S-16.70	16.0	16	0.70 PULT	S-34.70	34.0	34	0.70 PULT
S-22.ST	22.0	22	--	S-40.ST	40.0	40	--
S-22.30	22.0	22	0.30 PULT	S-40.30	40.0	40	0.30 PULT
S-22.40	22.0	22	0.40 PULT	S-40.40	40.0	40	0.40 PULT
S-22.50	22.0	22	0.50 PULT	S-40.50	40.0	40	0.50 PULT
S-22.60	22.0	22	0.60 PULT	S-40.60	40.0	40	0.60 PULT
S-22.70	22.0	22	0.70 PULT	S-40.70	40.0	40	0.70 PULT

TABLE 7.4

VARIABLE DATA FOR THE COLUMNS

BENT IN DOUBLE CURVATURE

Column	Length (ft)	$\frac{L_c}{t_c}$	Sustained load	Column	Length (ft)	$\frac{L_c}{t_c}$	Sustained load
D-10.ST	10.0	10	--	D-28.ST	28.0	28	--
D-10.30	10.0	10	0.30 PULT	D-28.30	28.0	28	0.30 PULT
D-10.40	10.0	10	0.40 PULT	D-28.40	28.0	28	0.40 PULT
D-10.50	10.0	10	0.50 PULT	D-28.50	28.0	28	0.50 PULT
D-10.60	10.0	10	0.60 PULT	D-28.60	28.0	28	0.60 PULT
D-10.70	10.0	10	0.70 PULT	D-28.70	28.0	28	0.70 PULT
D-16.ST	16.0	16	--	D-34.ST	34.0	34	--
D-16.30	16.0	16	0.30 PULT	D-34.30	34.0	34	0.30 PULT
D-16.40	16.0	16	0.40 PULT	D-34.40	34.0	34	0.40 PULT
D-16.50	16.0	16	0.50 PULT	D-34.50	34.0	34	0.50 PULT
D-16.60	16.0	16	0.60 PULT	D-34.60	34.0	34	0.60 PULT
D-16.70	16.0	16	0.70 PULT	D-34.70	34.0	34	0.70 PULT
D-22.ST	22.0	22	--	D-40.ST	40.0	40	--
D-22.30	22.0	22	0.30 PULT	D-40.30	40.0	40	0.30 PULT
D-22.40	22.0	22	0.40 PULT	D-40.40	40.0	40	0.40 PULT
D-22.50	22.0	22	0.50 PULT	D-40.50	40.0	40	0.50 PULT
D-22.60	22.0	22	0.60 PULT	D-40.60	40.0	40	0.60 PULT
D-22.70	22.0	22	0.70 PULT	D-40.70	40.0	40	0.70 PULT

to failure under short-time loads.

7.4.2 Material Properties

The reinforcing steel was assumed to have a yield point of 50 ksi and modulus of elasticity of 30,000 ksi.

The concrete stress-strain properties independent of sustained load are included in TABLE 7.5. The concrete stress-strain curve had the shape shown in FIGURE 3.3.

TABLE 7.5
CONCRETE PROPERTIES INDEPENDENT
OF SUSTAINED LOAD

f'_{ca28} (ksi)	k_3	k_t	ϵ_u
4.0	0.85	-0.15	0.0038

The sustained load properties of concrete are listed in TABLE 7.6. The shrinkage values were obtained from FIGURE 3.4 ⁽⁴⁴⁾ and the creep coefficients from TABLE 3.1.

TABLE 7.6
SUSTAINED LOAD PROPERTIES OF CONCRETE

Variable	Duration of Loading		
	7 days	9 months	25 years
$\epsilon_{SH}(K)$	0.0002	0.0006	0.0008
F1(K)	0.0009	0.0018	0.0028
F2(K)	0.0008	0.0016	0.0025
F3(K)	0.0007	0.0014	0.0021

7.4.3 Incrementing Data

The variables listed in this section are used either directly as increments to converge the trial and error procedures of the analysis or indirectly in the calculation of these increments as outlined in CHAPTER IV. The incrementing variables have identical numerical values for both forms of column restraint. These values are included in TABLE 7.7.

The moment increments $\Delta M1(K)$ (SECTION 4.6.4) and $\Delta M2(K)$ (SECTION 4.7.3) are not listed in this section because their magnitudes are directly dependent on the error of closure in their respective trial and error procedures.

TABLE 7.7
INCREMENTING DATA

Variable	Framework Columns	Loading Stage K							
		1	2	3	4	5	6	7	8
DELE(K) (in/in x 10^{-3})	All columns	4.0	4.0	4.0	4.0	4.0	4.0	4.0	4.0
DELS(K) (psi)	Column 1 in each series	60	60	60	60	60	60	60	60
	Columns 2-6 in each series	60	30	15	12	60	60	60	60
$\epsilon_{\max}(K)$ in/in x 10^{-3}	Column 1 in each series	1.8	1.8	1.8	1.8	1.8	1.8	1.8	1.8
	Columns 2-6 in each series	1.8	4.4	7.2	10.0	10.0	10.0	10.0	10.0

7.4.4 Permissible Variations

The permissible variations constitute allowable errors in the closure of the trial and error procedures of the analysis. The numerical values reported in this section are used either directly as permissible variations or indirectly in the calculation of permissible variations as outlined in CHAPTER IV.

The values listed in TABLE 7.8 were preset prior to computer calculation. They were all subject to increase by the computer if an endless calculation loop resulted and the analysis would not converge. This was not a frequent occurrence but did occur when the columns became unstable and exhibited a high sensitivity to a change in load. The values most often affected were $\Delta Y(K)$ for the columns bent in double curvature and $\Delta \theta(K)$ for the columns bent in single curvature.

The less restrictive incrementing data used for the frames containing the columns bent in double curvature was necessary to reduce the time required for computer solution.

TABLE 7.8
PERMISSIBLE VARIATION DATA

Variable Frames	$\Delta P_B(K)$ (kips)	$\Delta P_C(K)$ (kips)	$\Delta M_B(K)$ (in k)	$\Delta M_C(K)$ (in k)	DELE(K) in/in $\times 10^{-5}$	$\Delta Y(K)$ (in)	$\Delta \theta(K)$ rad.
Single Curvature	7.50	4.0	30.0	10.0	4.0	0.005	0.0002 to 0.0004
Double Curvature	7.50	5.0	40.0	15.0	4.0	0.005 to 0.020	0.0002

7.5 General Comments

The frames described in this chapter were chosen to limit the analysis to a consideration of only two members. This limitation was necessary because of the restrictions imposed by both the memory capacity of the computer and the time required for computer analysis.

CHAPTER VIII

RESULTS OF THE INVESTIGATION OF LONG COLUMNS IN FRAMEWORKS

8.1 Introduction

The results of the investigation of long columns in frameworks under sustained load are presented in this chapter along with a discussion of the trends which appeared to exist.

The results have been presented in graphical form. The ordinate and abscissa parameters of the graphs have a dimensional form so that it is not implied that all cases which satisfy the appropriate non-dimensional parameters will exhibit the same behavior.

A section is included in this chapter on the analysis of the frames by first order theory so as to provide a reference point for the interpretation of the results.

The remaining sections of the chapter present results on:

1. Load-moment behavior of the columns.
2. Maximum column deflections.
3. Maximum concrete stresses.
4. Maximum and minimum steel stresses.
5. Joint rotations.
6. Failure loads.

It should be noted that in all cases the eccentricity of the axial load applied to the columns was small according to a first order

analysis.

8.2 Analysis Using First Order Theory

The first order theory used in this thesis was elastic moment distribution. Member stiffnesses were assessed using the gross concrete section and neglecting the effect of reinforcement. First order theory does not consider the effects of secondary moments in the columns.

The results of the first order analysis are listed in TABLES 8.1 and 8.2 for the single curvature frames and the double curvature frames respectively.

TABLE 8.1

FIRST ORDER ANALYSIS OF THE FRAMES CONTAINING
THE COLUMNS BENT IN SINGLE CURVATURE

Frame	L_B (ft)	L_c (ft)	Unif. Load k/ft	FEM ft.k	I_c/L_c Column in ³	I_B/L_B Beam in ³	D.F. Column	D.F. Beam	Mend Column ft.k	Mend Beam ft.k
S-10	20	10	4.0	133.3	14.40	22.33	0.282	0.437	37.5	75.1
S-16	20	16	4.0	133.3	9.00	22.33	0.223	0.554	29.8	59.5
S-22	20	22	4.0	133.3	6.55	22.33	0.185	0.630	24.6	49.3
S-28	20	28	4.0	133.3	5.14	22.33	0.158	0.685	21.0	42.0
S-34	20	34	4.0	133.3	4.24	22.33	0.138	0.725	18.3	36.7
S-40	20	40	4.0	133.3	3.60	22.33	0.122	0.756	16.3	32.5

TABLE 8.2
FIRST ORDER ANALYSIS OF THE FRAMES CONTAINING
THE COLUMNS BENT IN DOUBLE CURVATURE

Frame	L_B (ft)	L_C (ft)	Unif. Load (k/ft)	FEM (ft.k)	I_C/L_C Column in ³	I_B/L_B Beam in ³	D.F. Column	D.F. Beam	$M_{Col.}$ ft.k	M_{Beam} ft.k
D-10	20	10	4.0	133.3	14.40	22.33	0.360	0.279	48.0	96.1
D-16	20	16	4.0	133.3	9.00	22.33	0.309	0.383	41.1	82.3
D-22	20	22	4.0	133.3	6.55	22.33	0.270	0.461	36.0	72.0
D-28	20	28	4.0	133.3	5.14	22.33	0.240	0.521	32.0	63.9
D-34	20	34	4.0	133.3	4.24	22.33	0.216	0.569	28.8	57.5
D-40	20	40	4.0	133.3	3.60	22.33	0.196	0.608	26.1	52.3

8.3 Load-Moment Behavior

The load-moment behavior of the columns in the frameworks is illustrated in FIGURES 8.1 to 8.17. The behavior of the single curvature columns and the behavior of the double curvature columns are discussed separately in the following sections.

8.3.1 Load-Moment Behavior of the Columns Bent in Single Curvature

The load-moment behavior of the columns bent in single curvature is shown in FIGURES 8.1 to 8.9. These curves are of three types:

1. FIGURES 8.1 to 8.6 show the relationship between load and moment for the various loading sequences applied to each frame.

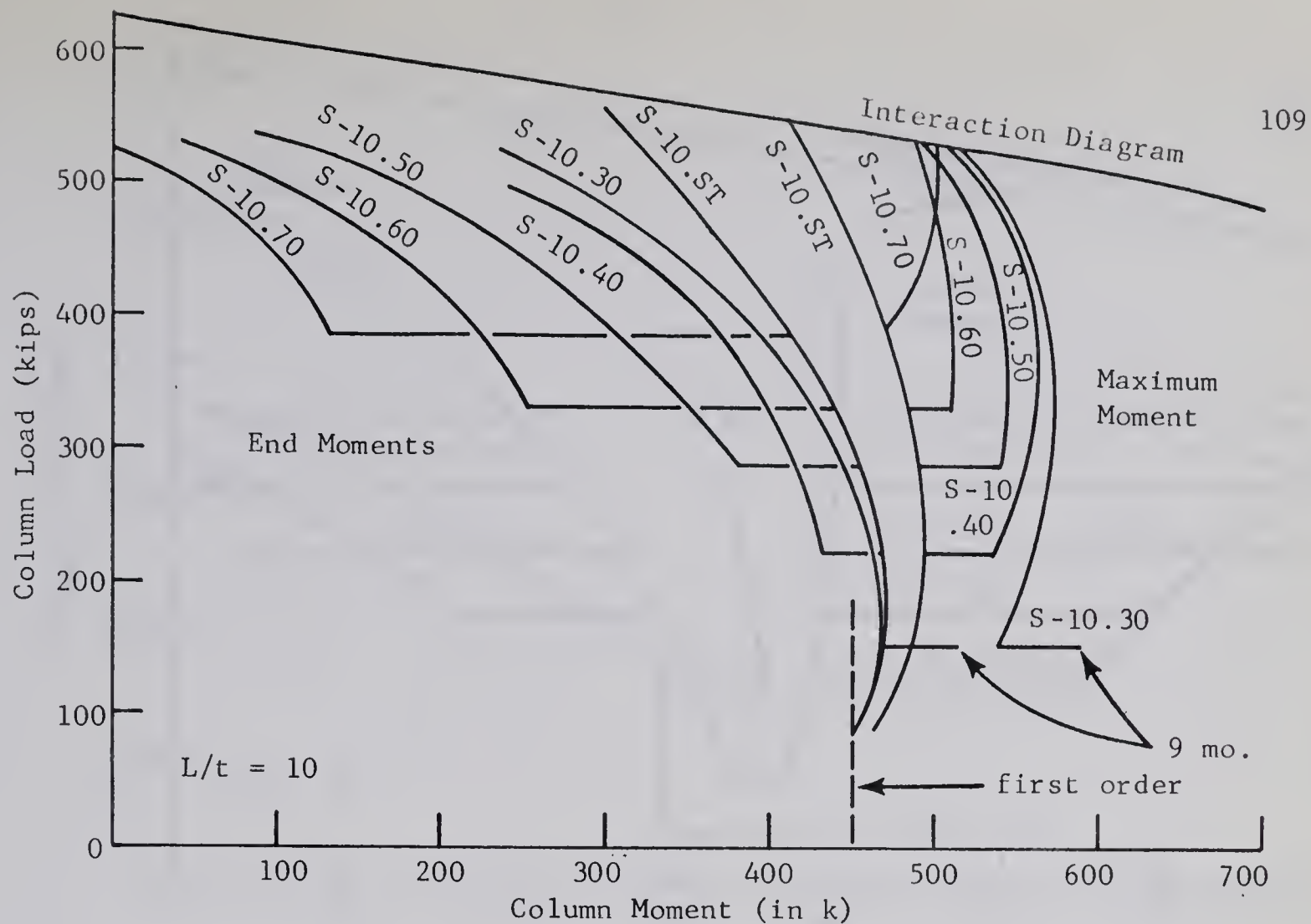


FIGURE 8.1
LOAD-MOMENT BEHAVIOR OF COLUMNS S-10

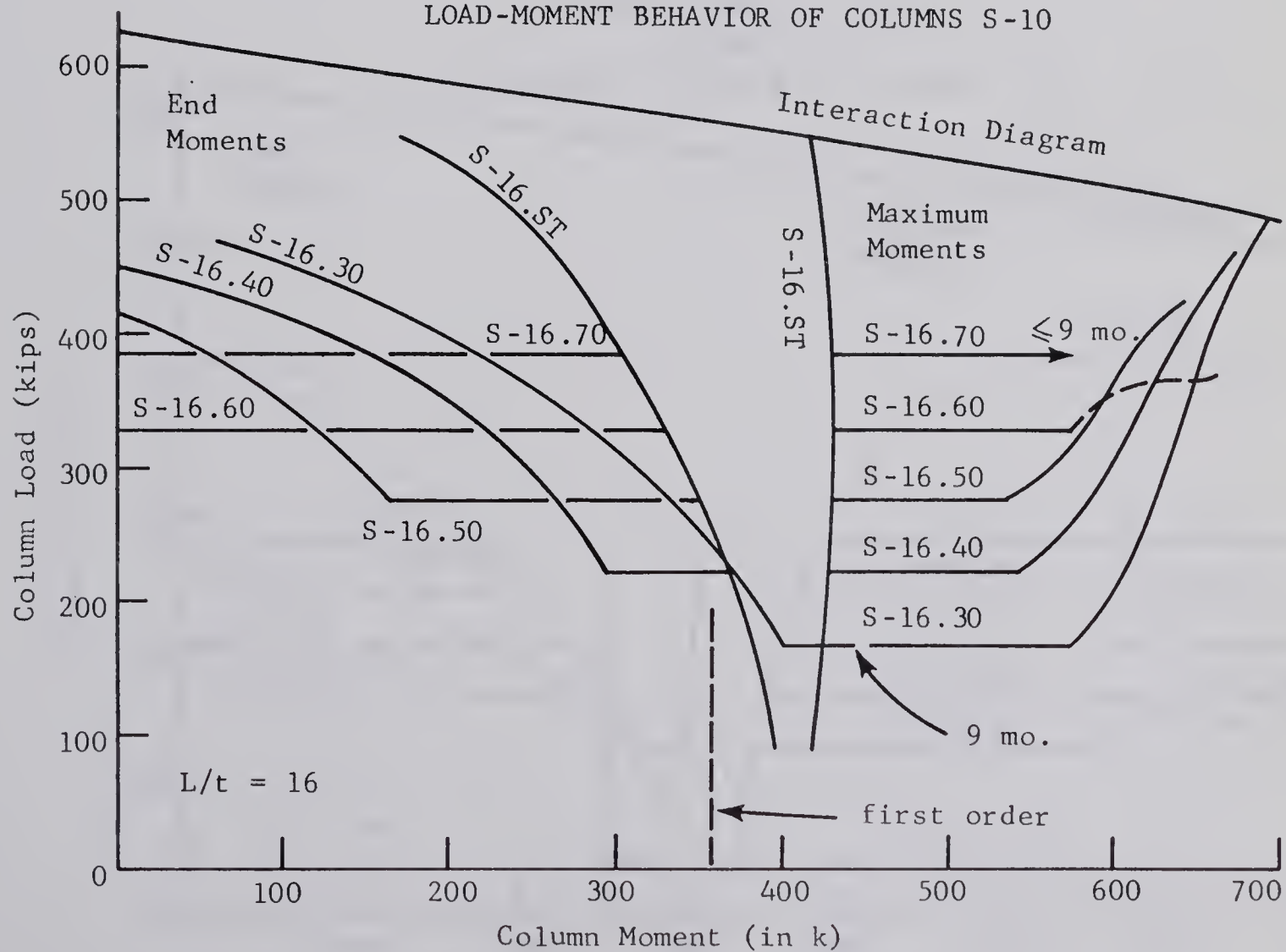


FIGURE 8.2
LOAD-MOMENT BEHAVIOR OF COLUMNS S-16

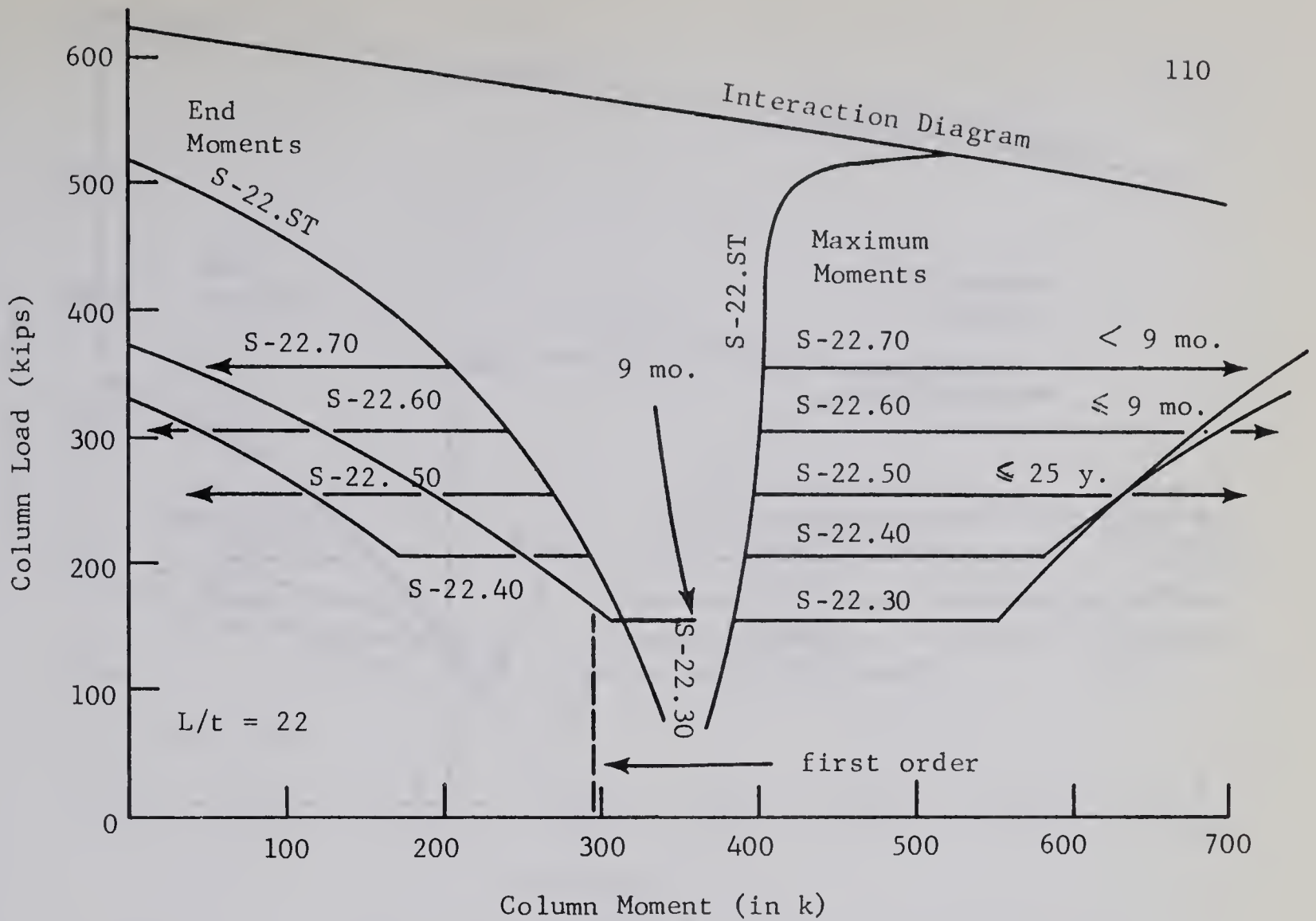


FIGURE 8.3

LOAD-MOMENT BEHAVIOR OF COLUMNS S-22

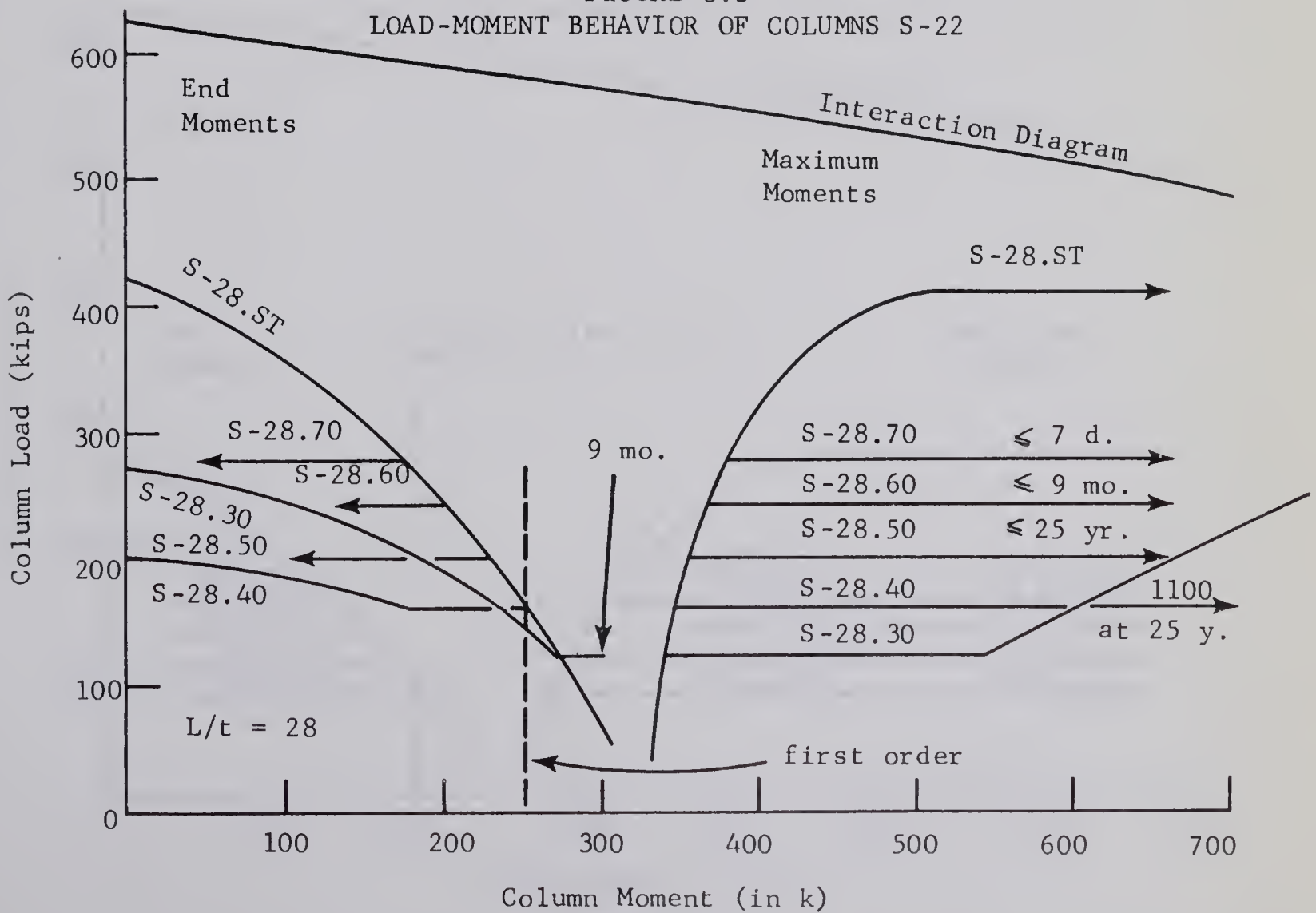


FIGURE 8.4

LOAD-MOMENT BEHAVIOR OF COLUMNS S-28

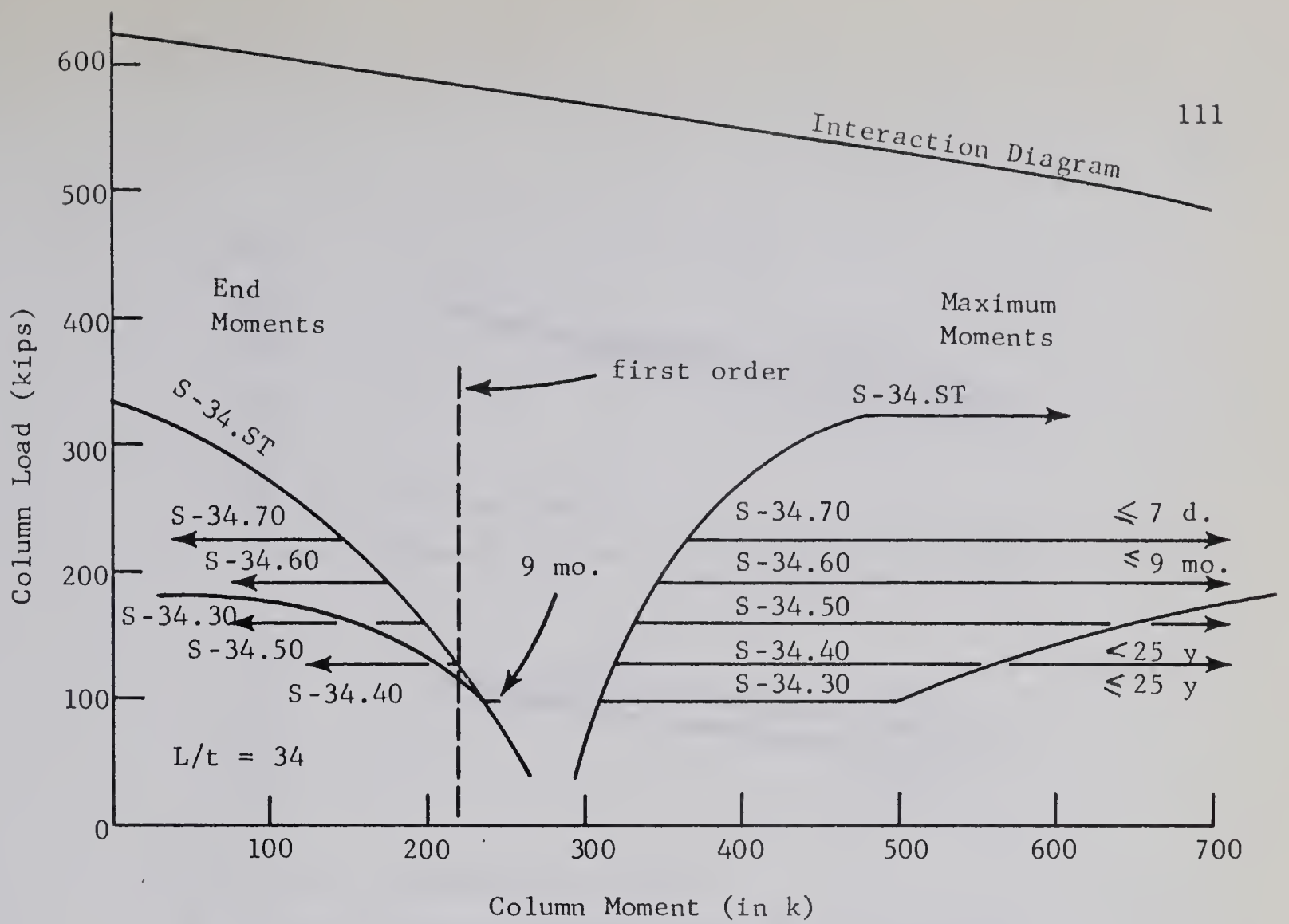


FIGURE 8.5
LOAD-MOMENT BEHAVIOR OF COLUMNS S-34

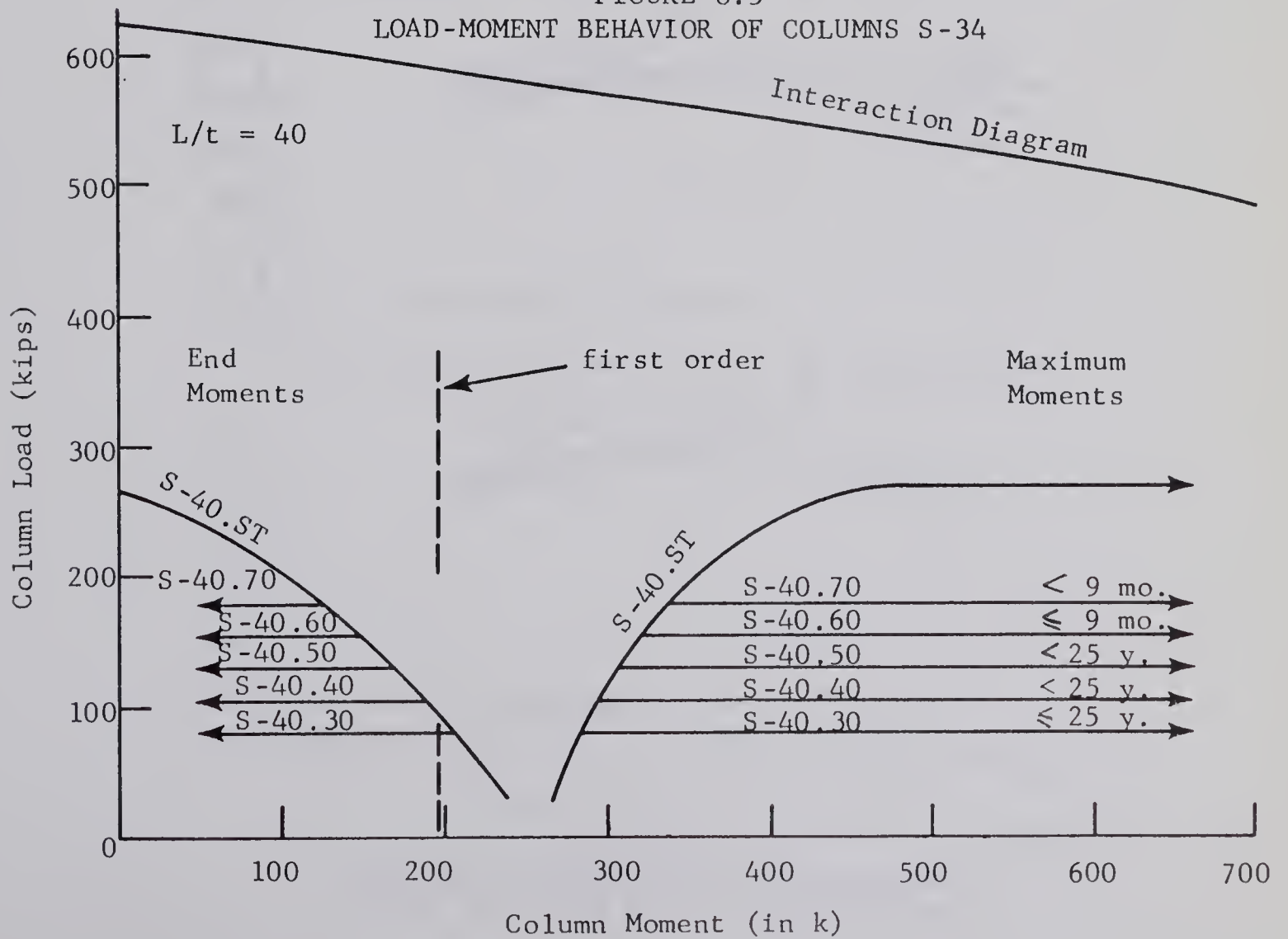


FIGURE 8.6
LOAD-MOMENT BEHAVIOR OF COLUMNS S-40

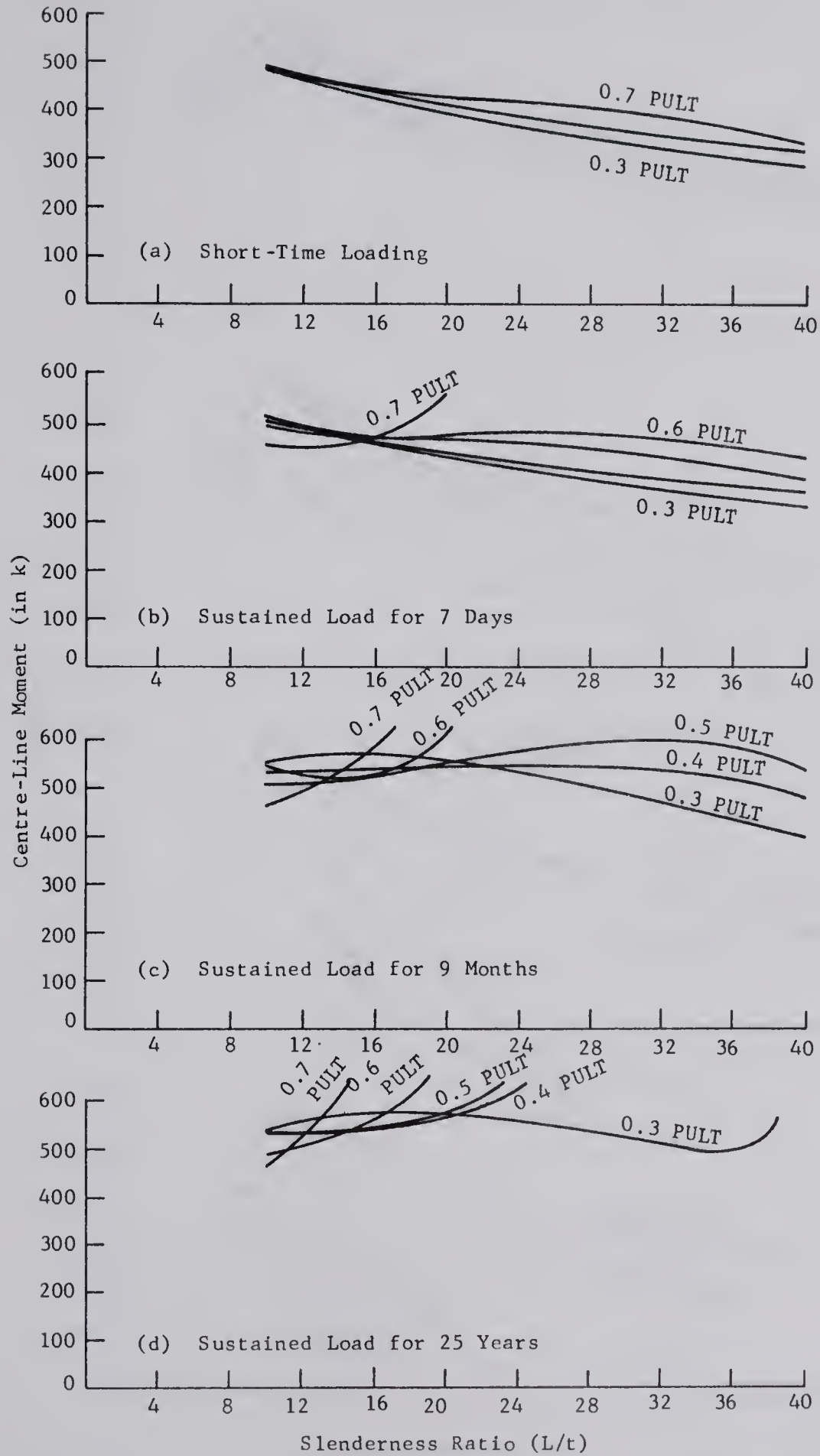


FIGURE 8.7
VARIATION IN MAXIMUM MOMENT WITH SLENDERNESS
RATIO FOR THE COLUMNS BENT IN SINGLE CURVATURE

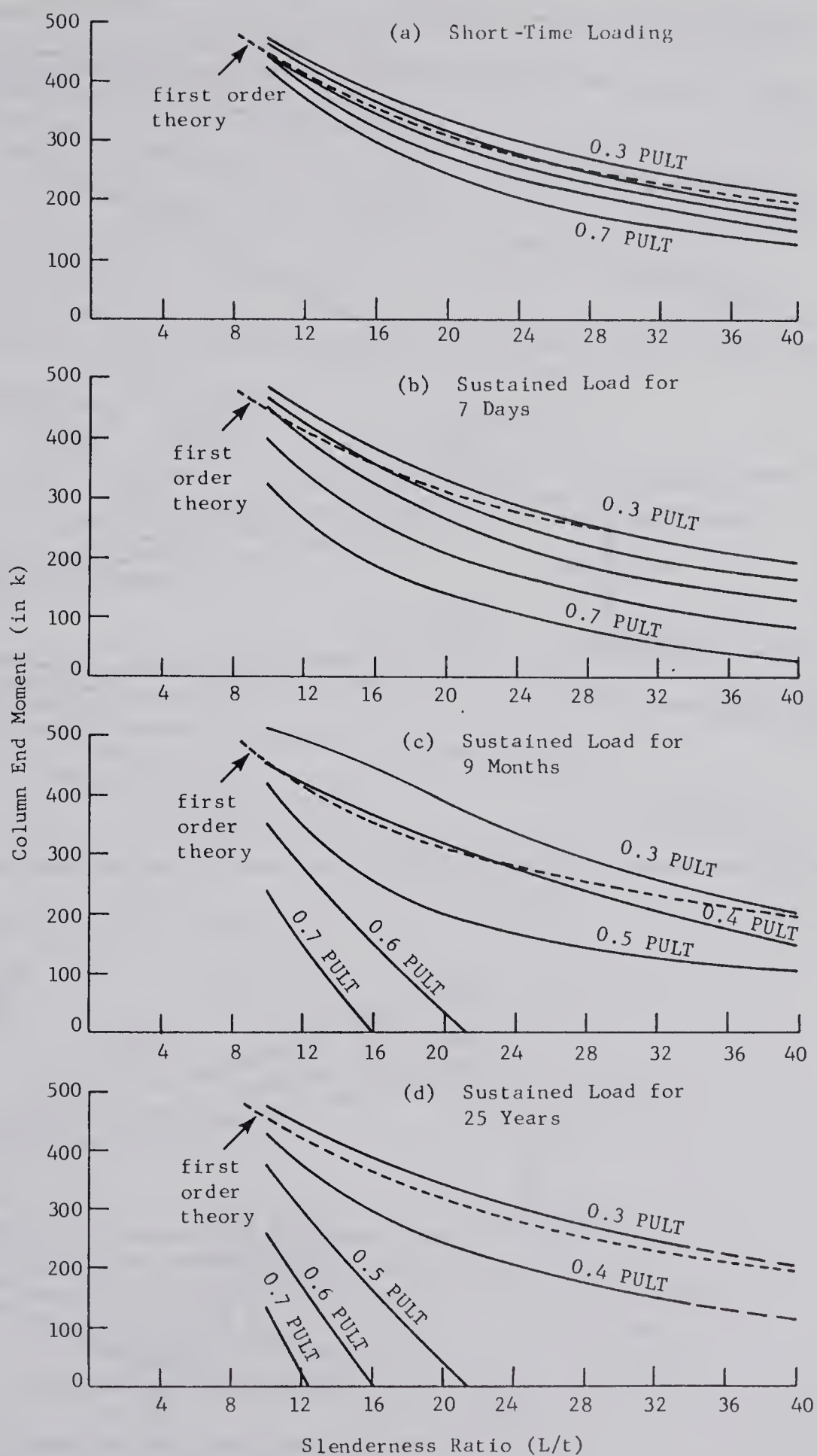


FIGURE 8.8
VARIATION IN COLUMN END MOMENT WITH SLENDERNESS
RATIO FOR THE COLUMNS BENT IN SINGLE CURVATURE

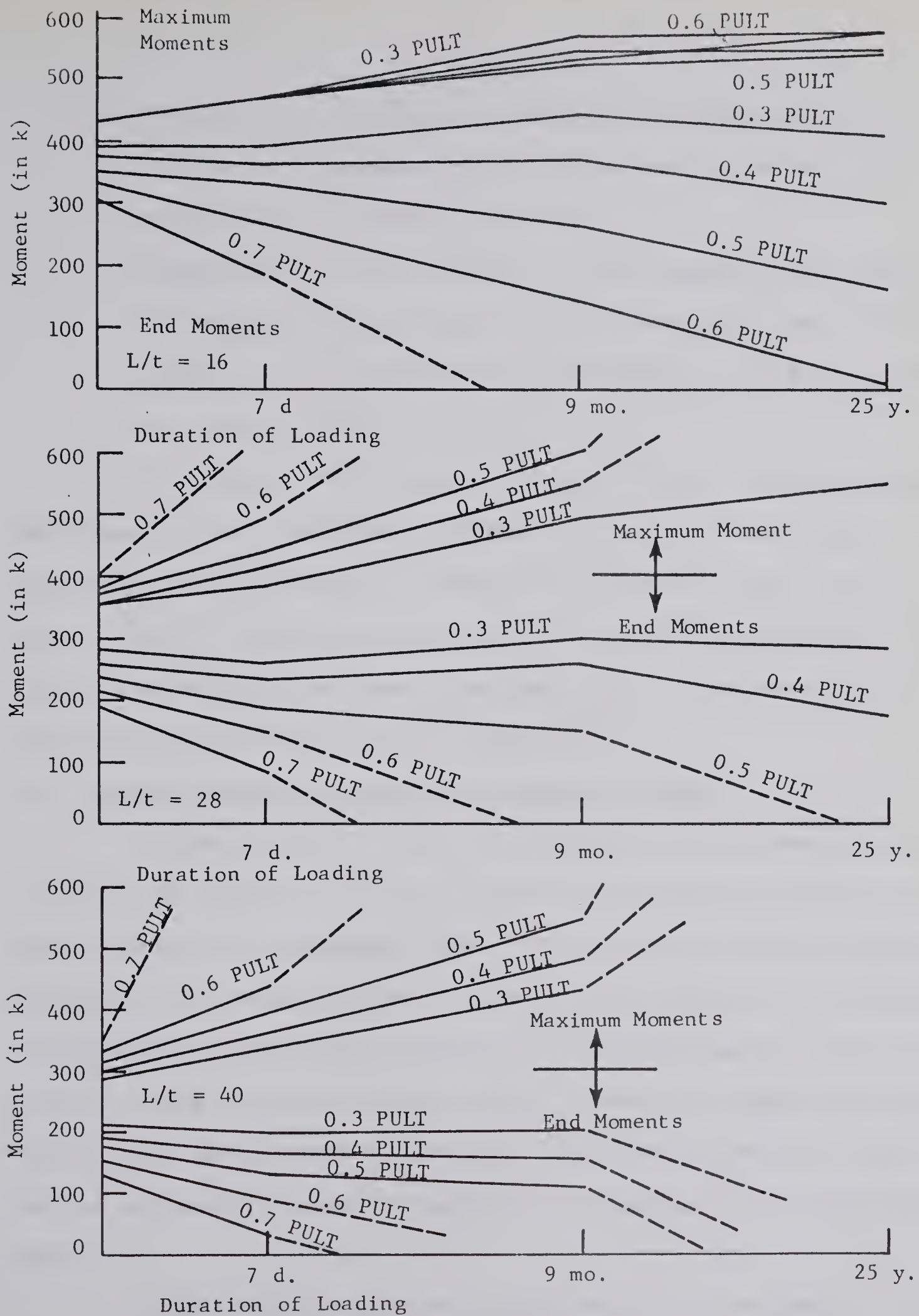


FIGURE 8.9

VARIATION IN SINGLE CURVATURE COLUMN MOMENTS WITH TIME

2. FIGURES 8.7 and 8.8 show the maximum and minimum moments as a function of slenderness ratio for the various levels of sustained load and durations of loading.
3. FIGURE 8.9 shows the variation in column moments with time for the various levels of sustained load. The three parts of this figure are cross-sections through FIGURES 8.7 and 8.8 at slenderness ratios of 16, 28, and 40.

The behavior of the single curvature columns under increasing axial load is best illustrated by FIGURES 8.1 to 8.6. These figures also illustrate the total changes in moment under sustained load. The upper line in each of these figures represents the interaction diagram for the column cross-section under short-time loads. The column moment by first order theory is also included as a reference.

(a) Columns Subjected to Short-Time Loading to Failure

Columns S-10.ST to S-40.ST of FIGURES 8.1 to 8.6 were subjected to short-time loading to failure. The short-time failure loads decreased with an increase in slenderness ratio. This decrease in failure load was only slight from column S-10.ST to column S-16.ST because of the absence of instability. For further increases in slenderness ratio, however, instability under short-time loading became increasingly apparent and the failure loads were reduced considerably. The failure loads under short-time loading were used to assess the magnitude of sustained load in each load level.

Column S-10.ST exhibited unusual behavior at low levels of load. In this range, the relative stiffness of the column increased with increasing load as evidenced by the increase in end moment. This behavior

was due to a reduction in tensile cracking with an increase in load. The other columns under short-time load did not exhibit this behavior because the moments distributed to them were of a smaller order.

The relative stiffness of columns S-10.ST to S-40.ST decreased with either an increase in load or an increase in slenderness ratio because of the development of the deflection moment which is the product of the axial load and the deflection. The development of the deflection moment also produced changes in the maximum moment. However, whether the increase in deflection moment resulted in increases or decreases in the maximum moment depended on the effect of the deflection moment on the stiffness of the column. For shorter columns the deflections are small, but an increase in the deflection has a large effect on the stiffness of the column. As a result, the relative stiffness of a short column in a frame will decrease at a faster rate than the deflection moment increases. The net effect is a reduction in the maximum moment in the column as was exhibited by column S-10.ST. Columns S-28.ST, S-34.ST, and S-40.ST all exhibited increases in maximum moment with increasing deflection moment throughout the complete range of loading. The increasing deflection moments also caused reductions in the relative column stiffness and column end moments, but the mid-height moments increased more rapidly than the end moments decreased. Columns S-16.ST and S-22.ST exhibited behavior between that of S-10.ST and S-28.ST.

The non-linear stress-strain diagram for concrete also had an influence on the behavior of the columns under short-time loading. For the shorter columns, a "hinge" developed at the mid-height of the column near failure and the relative stiffness of the column decreased rapidly. For the longer columns, this hinge did not develop because the failure was due

to instability. However, as the failure load was approached, the behavior of the longer columns was influenced by non-linear rotation at the centre-line of the beam. With a reduction in the relative stiffness of the column, the mid-span or maximum moment in the beam was increased through the redistribution of moment. When the end moment in the column had reduced almost to zero, the response of the beam to a change in end moment deviated from the linear behavior it had exhibited up until then. As a result, some of the moment was redistributed back to the column. This behavior hastened the change from stable to unstable behavior in the longer columns.

(b) Columns Subjected to a Sustained Load Followed by Quick Loading to Failure

Columns .30 to .70 in each series illustrate the frame behavior under various levels of sustained axial load in the columns. The behavior of these columns was similar to the behavior under short-time loading although the length effects were amplified by the deflections caused by the dimensional instability of the concrete under sustained load.

At the lowest level of sustained load (0.30 PULT), all the columns except S-40.30 exhibited an increase in relative column stiffness with up to nine months under sustained load. This was due to the action of the compression steel* in the column in reducing the amount of creep. Under a sustained load, the stiffness of a structural concrete member is reduced with time because of the increase in the curvatures due to creep. However, when compression steel is present, the stress in the compression zone is redistributed from the concrete to the steel, and since creep is stress

*Although the reinforcing steel may be in compression in both column faces, the term compression steel is used to refer the reinforcing in the concave side of the column.

dependent, this retards the loss in stiffness with time. In the frames of the investigation, the beams did not have compression steel, and at low levels of load, the stiffness of the beam reduced at a faster rate with time than did the stiffness of the column. The net effect of this was an increase in the relative stiffness of the column and a resulting increase in the column moments. The increase in relative stiffness at the low levels of load was only exhibited up to nine months duration of loading. From this time up to 25 years under load, the relative stiffness of the columns decreased because the compression reinforcement had yielded and thus was no longer effective in accepting stress from the concrete in the redistribution process. Thus, a "softer" column resulted. The compression steel also retarded the decrease in the stiffness of the columns at the higher load levels. The effect, however, was not as noticeable because of the increased importance of the deflection moment and because the compression steel yielded after shorter durations of loading.

The deflection moments were increased considerably under sustained load. As was the case under short-time load, the increasing deflection moments caused large decreases in the relative stiffness of the shorter columns with only slight increases in maximum moment. However, because the deflection moments were larger than under short-time loading, the contribution of deflection moment to increases in maximum moment was more noticeable at lower values of slenderness ratio than under short-time load. In other words, the effect of sustained load was to produce a marked increase in the tendency of the columns to become unstable. Unstable behavior under sustained load was exhibited by column S-16.70 which failed after a duration of loading of approximately nine months. For larger slenderness

ratios, the level of sustained load required to produce instability decreased. For the columns with a slenderness ratio of 40, instability was exhibited under all levels of sustained load except the lowest one (0.3 PULT).

The columns which did not fail under sustained load were quick loaded to failure following the period of sustained load. More long column behavior was exhibited under this quick loading than under the short-time loading without the sustained load phase. This behavior was due to the increase in the column deflections under the sustained load and also due to the compression steel, which after having yielded under sustained load, was no longer effective in resisting increases in load.

For all of the columns except those with a slenderness ratio of 10, the failure load under the subsequent quick load decreased as the level of the sustained load increased. This behavior was not exhibited by columns S-10.30 to S-10.60 because the increases in deflection moment were manifested as decreases in the relative column stiffness rather than as increases in maximum moment. The maximum moment in these columns decreased with an increase in the deflection moment as the failure load was approached. Column S-10.70 did not fall into the above generalization as it approached instability at failure.

The non-linear behavior of concrete had a greater influence on the behavior of the columns subjected to sustained load than it did on the columns which were subjected to only short-time load. The combination of non-linearity in both the instantaneous and the time dependent stress-strain responses resulted in very little linear behavior being exhibited by the structural members. For the columns investigated, the net effect of sus-

tained load was an increase in the "hinging" in both the columns and the beams over that exhibited under short-time loading. The hinging in the columns caused rapid decreases in the relative stiffness of columns S-10.30 to S-10.60 as the failure load was approached. Columns S-10.70 and S-16.30 to S-16.60 show the effects of hinging in the restraining beam. These columns became unstable with only a small increase in the quick load following the sustained load. This resulted from moment being distributed from the beam back to the column as a result of hinging in the beam. For higher slenderness ratios, the effect of this hinging was minor compared to the influence of the deflection moments.

(c) Variation in Column Moments and Stiffnesses with Time

FIGURES 8.7 and 8.8 show the effect of slenderness ratio on the maximum and end moments in the columns under the different levels of sustained load and for different durations of loading.

Under short-time loading, FIGURE 8.7(a) shows that the maximum moments in the columns decreased with an increase in slenderness ratio for the levels of load considered. This was due to the decrease in the magnitude of the load in each load level with an increase in slenderness ratio and also to the absence of instability at these load levels.

The behavior after a duration of sustained load of seven days is shown in FIGURE 8.7(b). At the highest level of load, the compression steel had yielded in all the columns and the influence of increasing slenderness ratio on instability was apparent. At the lower levels of sustained load, the compression steel had yielded only in the shorter columns and as a result there was no trend towards instability for the higher slenderness ratios. Since none of the compression steel had yielded at the lower levels

of sustained load in the more slender columns, behavior was similar to that under short-time loading.

The behavior after nine months duration of loading is shown in FIGURE 8.7(c). At the two higher load levels, the compression steel had yielded in all of the columns and the instability of the "softer" columns at high slenderness ratios was apparent. At the lower levels of load, the compression steel had not yet yielded in columns S-40.50, S-40.40, S-40.30, S-34.40, S-34.30, or S-28.30. (See FIGURE 8.23). The influence of this factor on the change in maximum moment with slenderness ratio is apparent from the curves.

The behavior at the end of 25 years under load is shown in FIGURE 8.7(d). The compression steel in all the columns had yielded by this time. At the four higher load levels the trend towards instability was apparent. At the lowest level of load, however, the magnitude of load was only large enough to cause unstable behavior in column S-40.30.

FIGURE 8.8(a) illustrates the effect of the slenderness ratio and the level of load on the relative stiffness of the columns under short-time loading. The stability of these columns is shown by the similarity in shape between these curves and the first order theory line.

The relative stiffnesses of the columns after a duration of sustained load of seven days is illustrated in FIGURE 8.8(b). The columns exhibited the stable behavior shown under short-time loading, but the decrease in the relative stiffness was larger as the load level was increased. This decrease was the same for the short and long columns indicating the greater effect of increasing deflections on the stiffness of the short columns. The increased deflections in the shorter columns at the two

higher load levels were the result of yielding in the compression steel.

After longer periods of sustained loading, FIGURES 8.8(c) and (d) show the increasing influence of yielding of the compression steel on relative column stiffness. The relative stiffness decreased rapidly with slenderness ratio once the compression steel had yielded, but again the decrease in relative stiffness was retarded at higher slenderness ratios because of the delay in the yielding of the compression steel.

The curves of FIGURE 8.9 best illustrate the changes in the maximum moment and the end moment which occurred with an increase in the duration of loading. At the higher load levels, the influence of yielding in the compression steel is evidenced by sharp changes in both relative stiffness or end moment and maximum moment. The changes were not as pronounced at the lower load levels because of the small magnitudes of axial load. The increases in the relative stiffnesses of columns S-16.30 and S-28.30 over the values under short-time loading are also shown in FIGURE 8.9.

8.3.2 Load-Moment Behavior of the Double Curvature Columns

The load-moment behavior for the double curvature columns of the investigation is shown in FIGURE 8.10 to 8.18. These curves are of four types:

1. FIGURES 8.10 to 8.15 show the load vs. moment curves for the various loading sequences applied to each frame.
2. FIGURE 8.16 shows the effect of slenderness ratio and level of sustained load on the maximum and joint moments after various periods of sustained load.

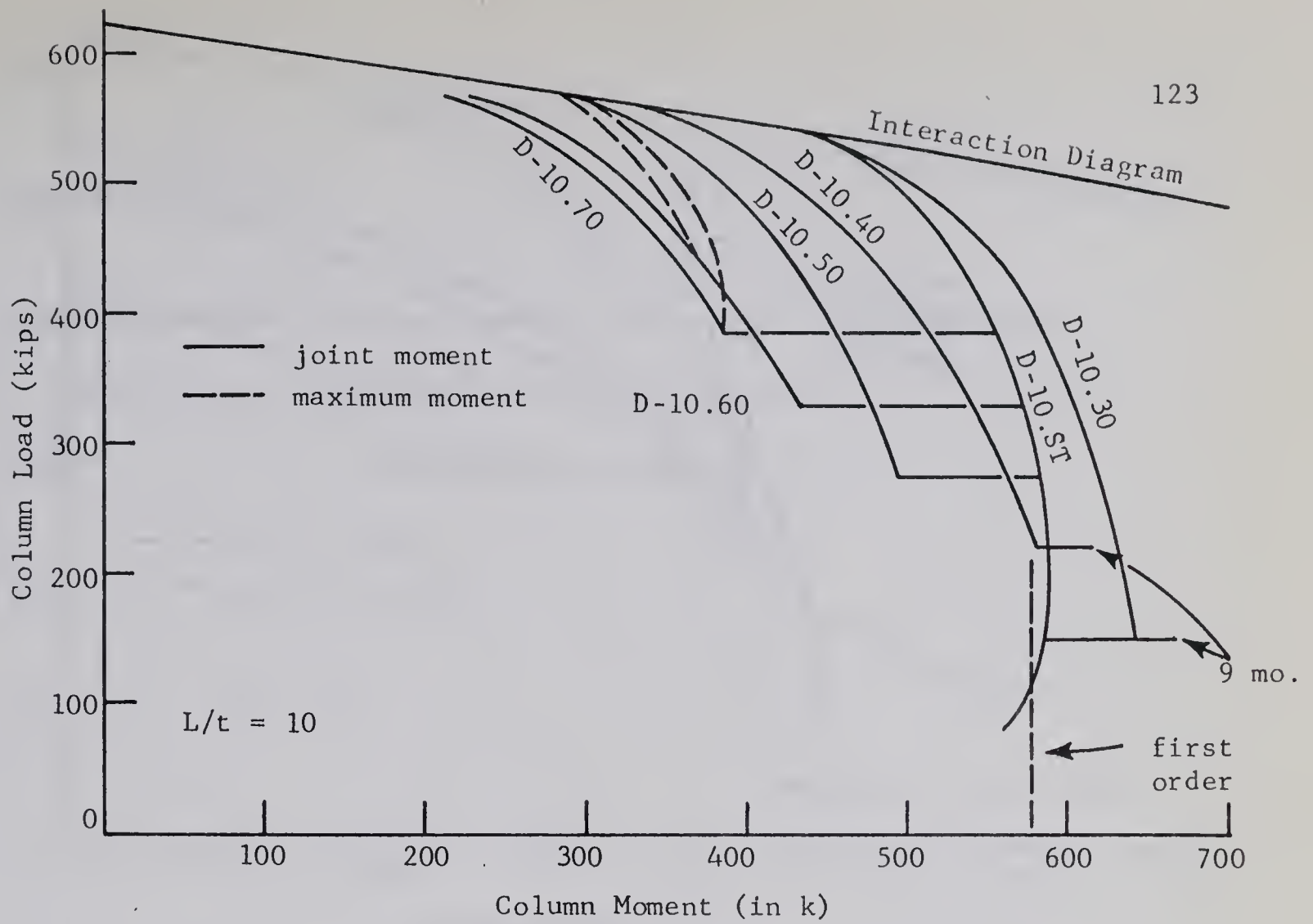


FIGURE 8.10
LOAD-MOMENT BEHAVIOR OF COLUMNS D-10

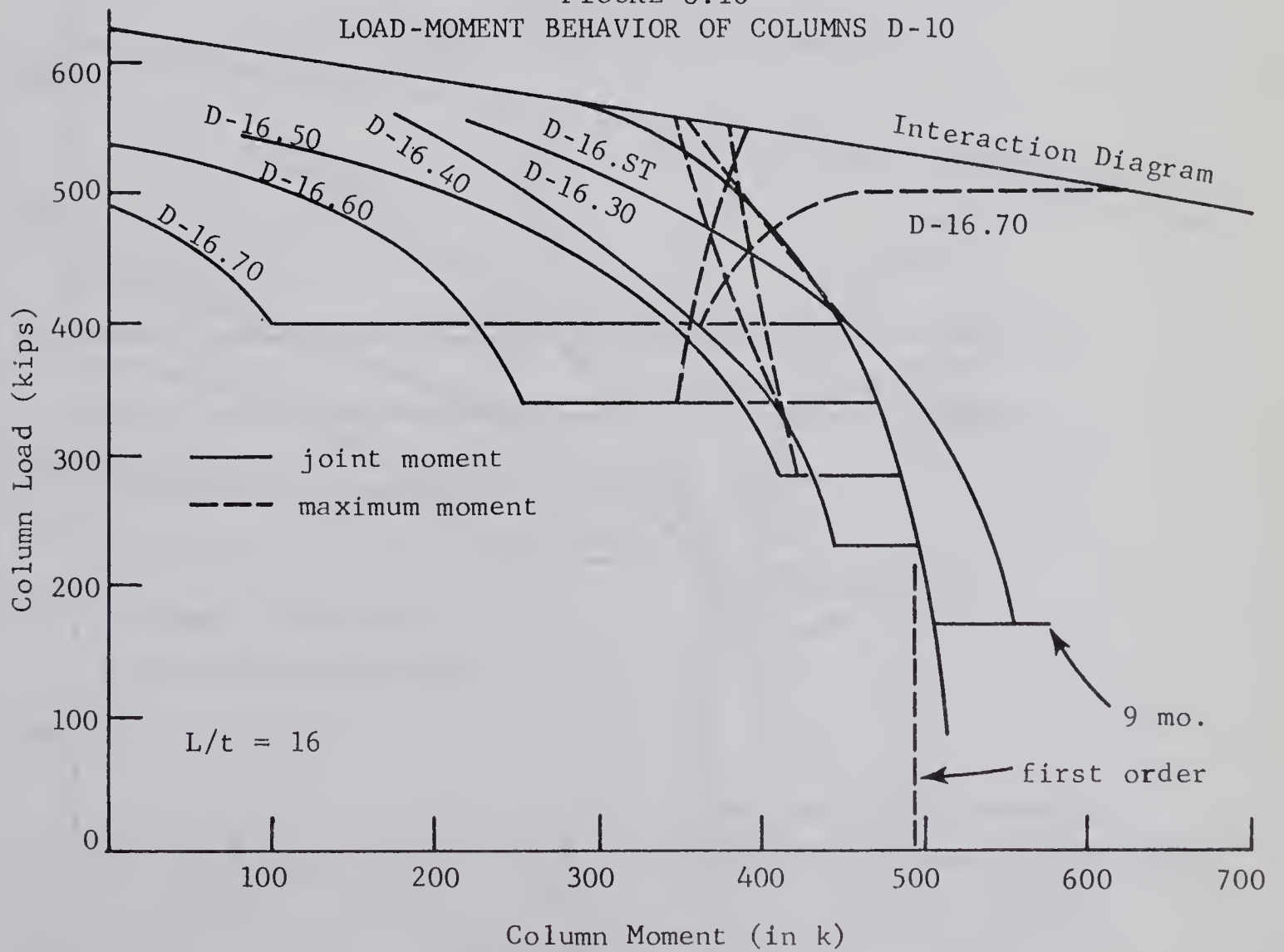


FIGURE 8.11
LOAD-MOMENT BEHAVIOR OF COLUMNS D-16

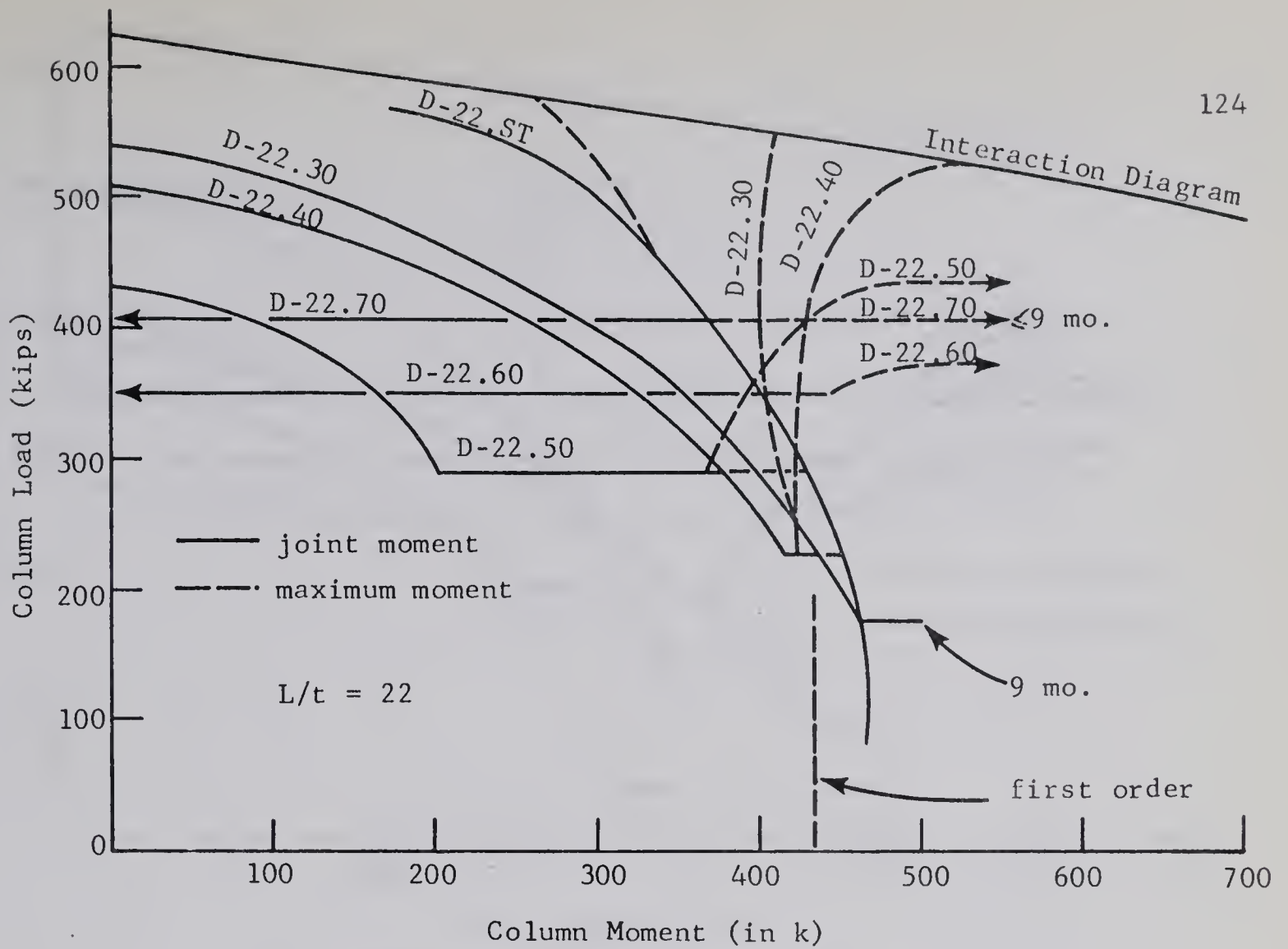


FIGURE 8.12
LOAD-MOMENT BEHAVIOR OF COLUMNS D-22

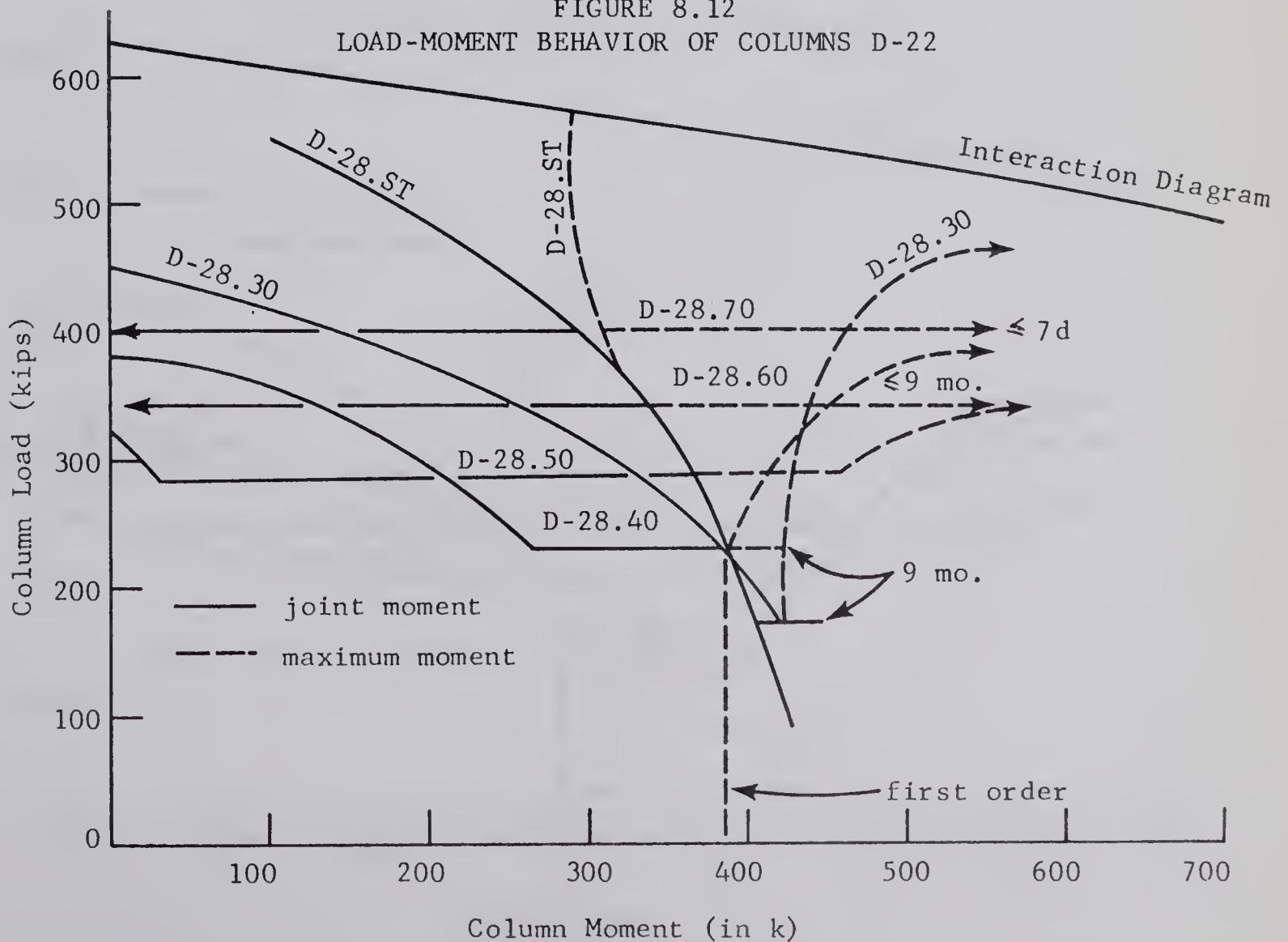


FIGURE 8.13
LOAD-MOMENT BEHAVIOR OF COLUMNS D-28

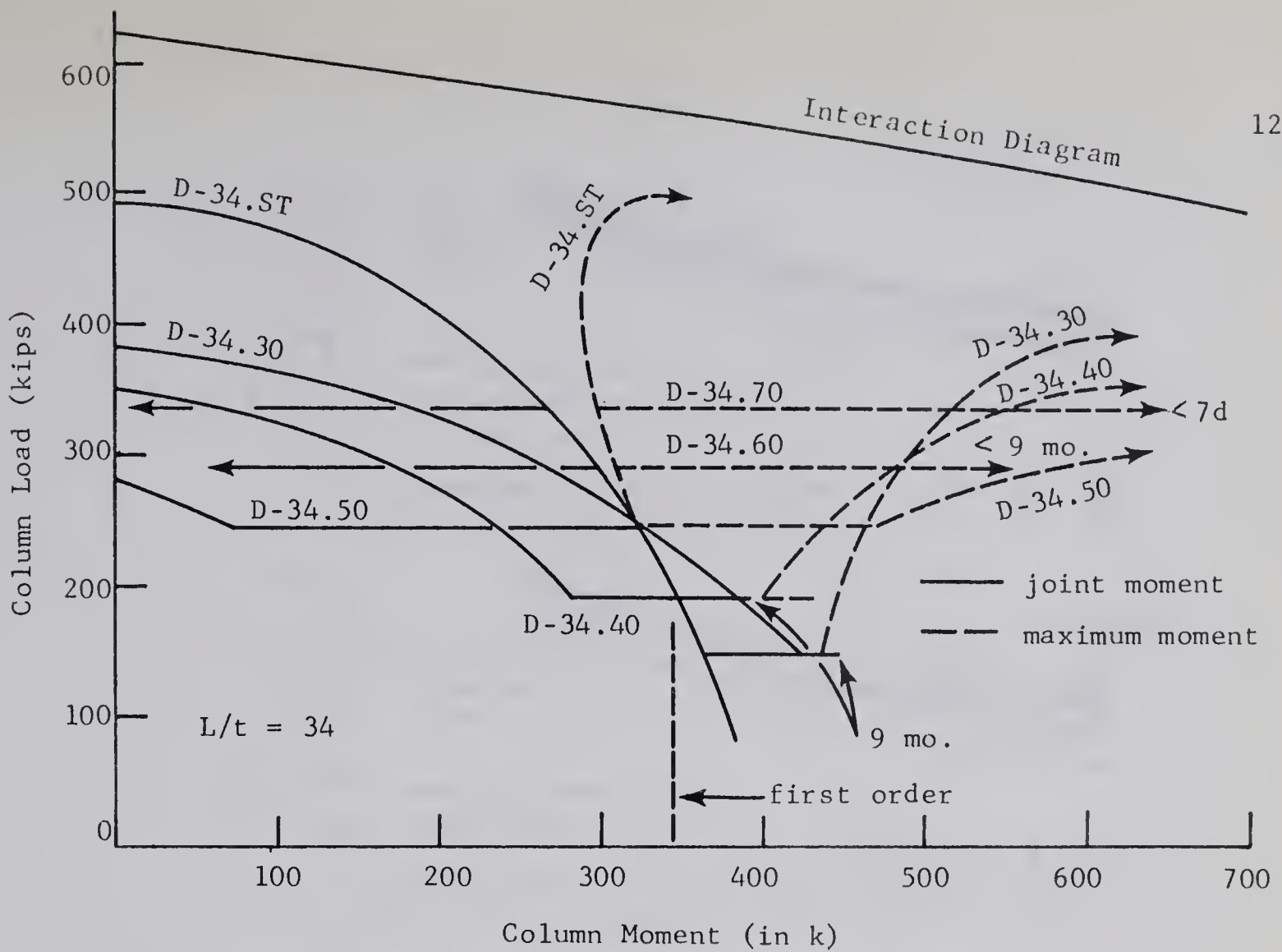


FIGURE 8.14

LOAD-MOMENT BEHAVIOR OF COLUMNS D-34

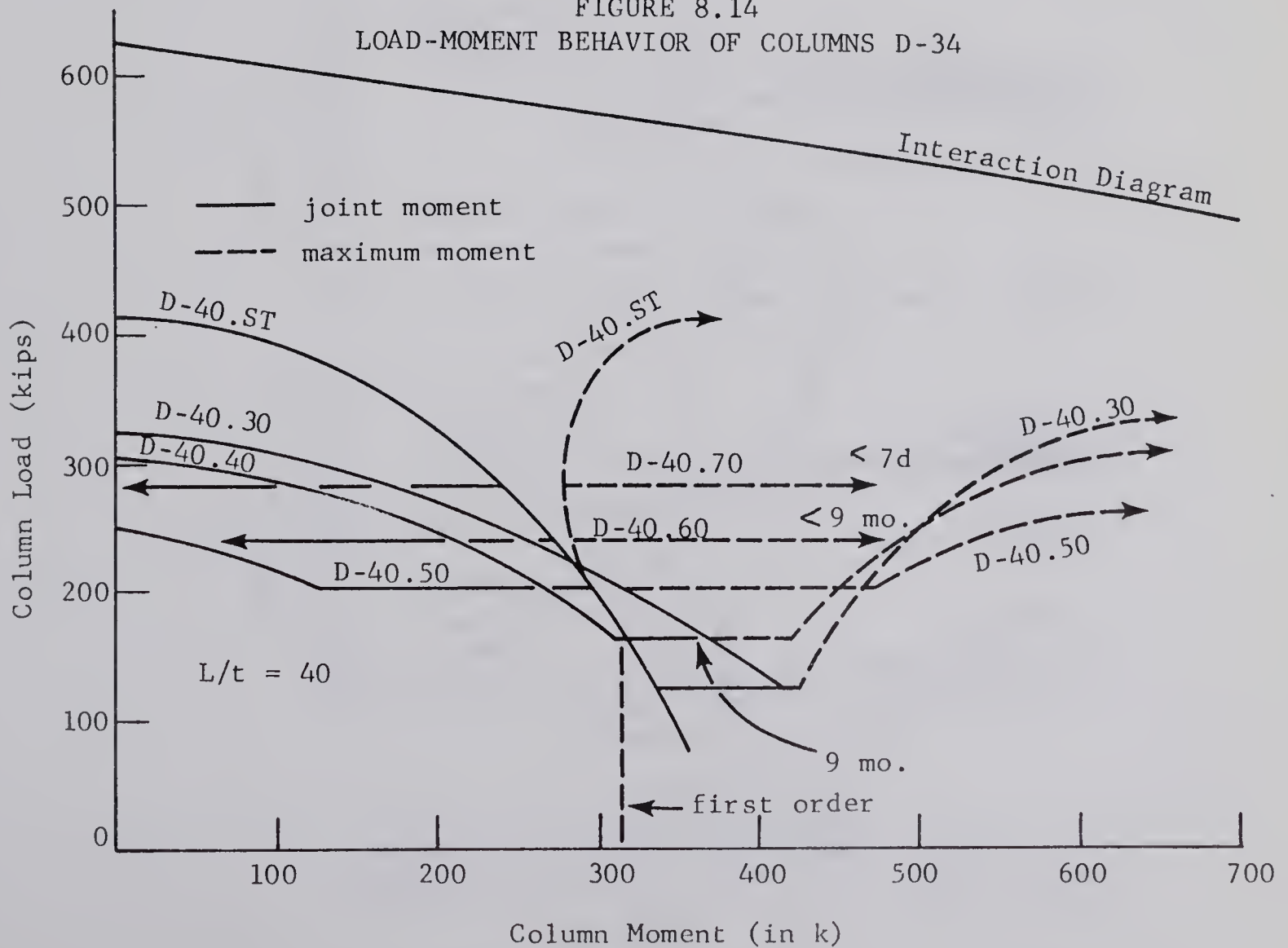


FIGURE 8.15

LOAD-MOMENT BEHAVIOR OF COLUMNS D-40

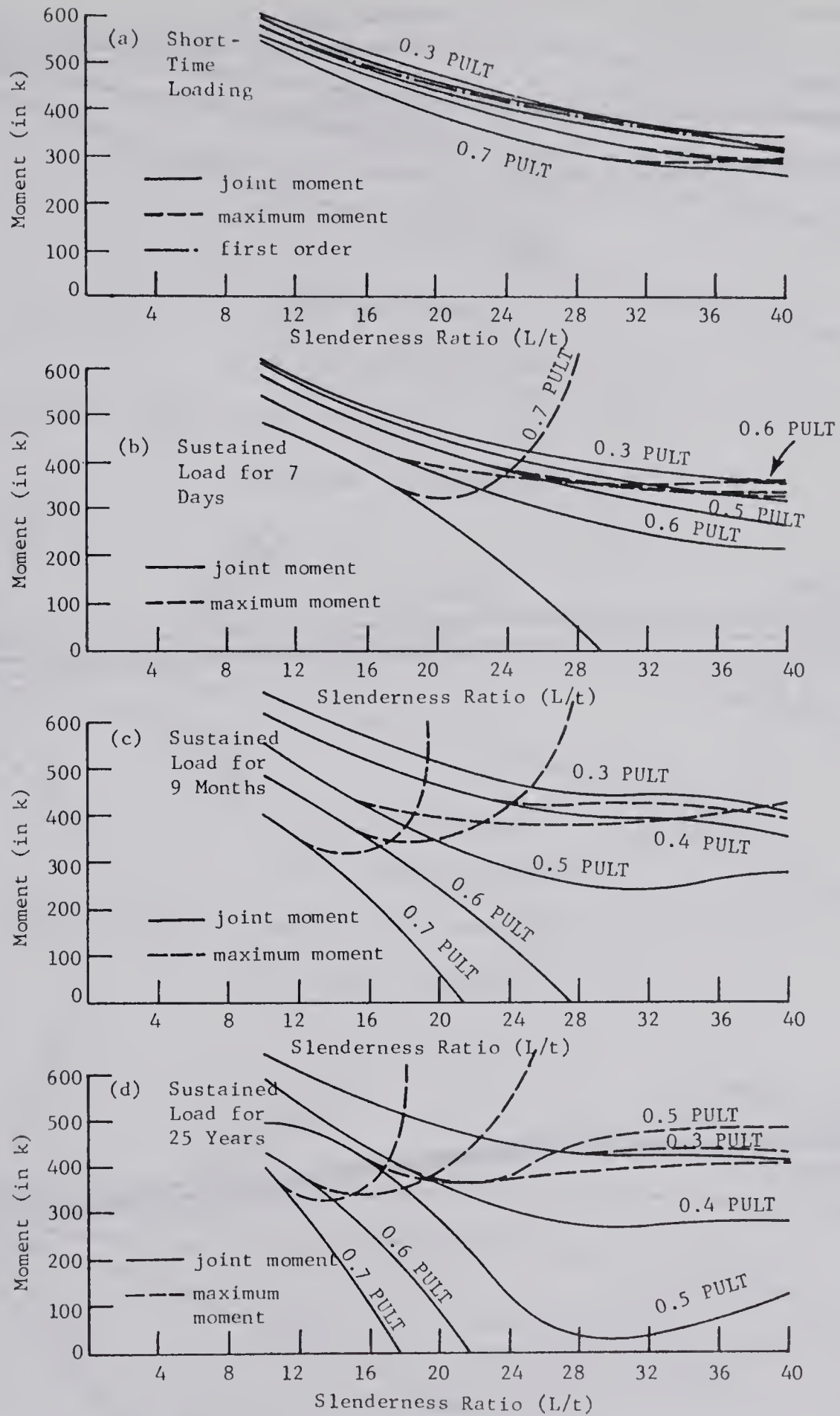


FIGURE 8.16

VARIATION IN JOINT MOMENT AND MAXIMUM MOMENT WITH SLENDERNESS RATIO FOR THE COLUMNS BENT IN DOUBLE CURVATURE

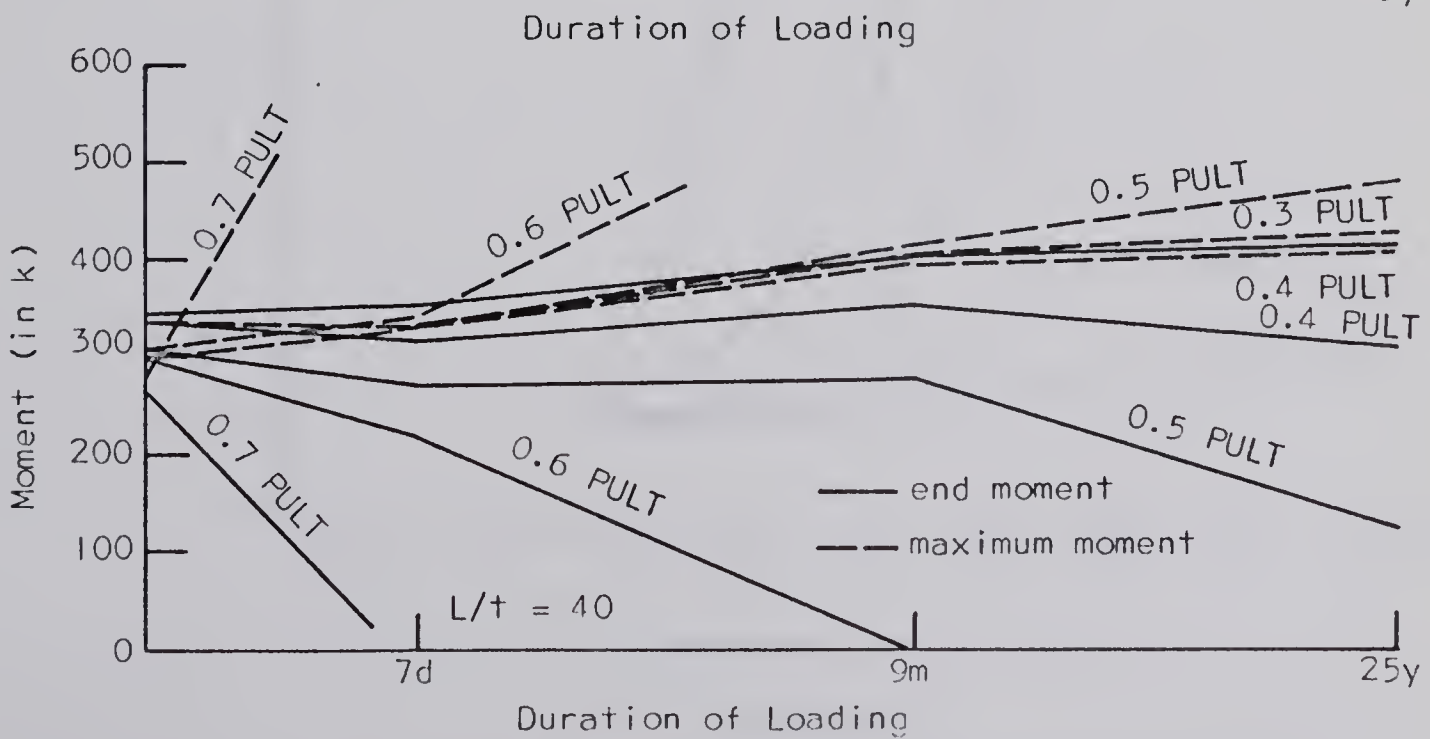
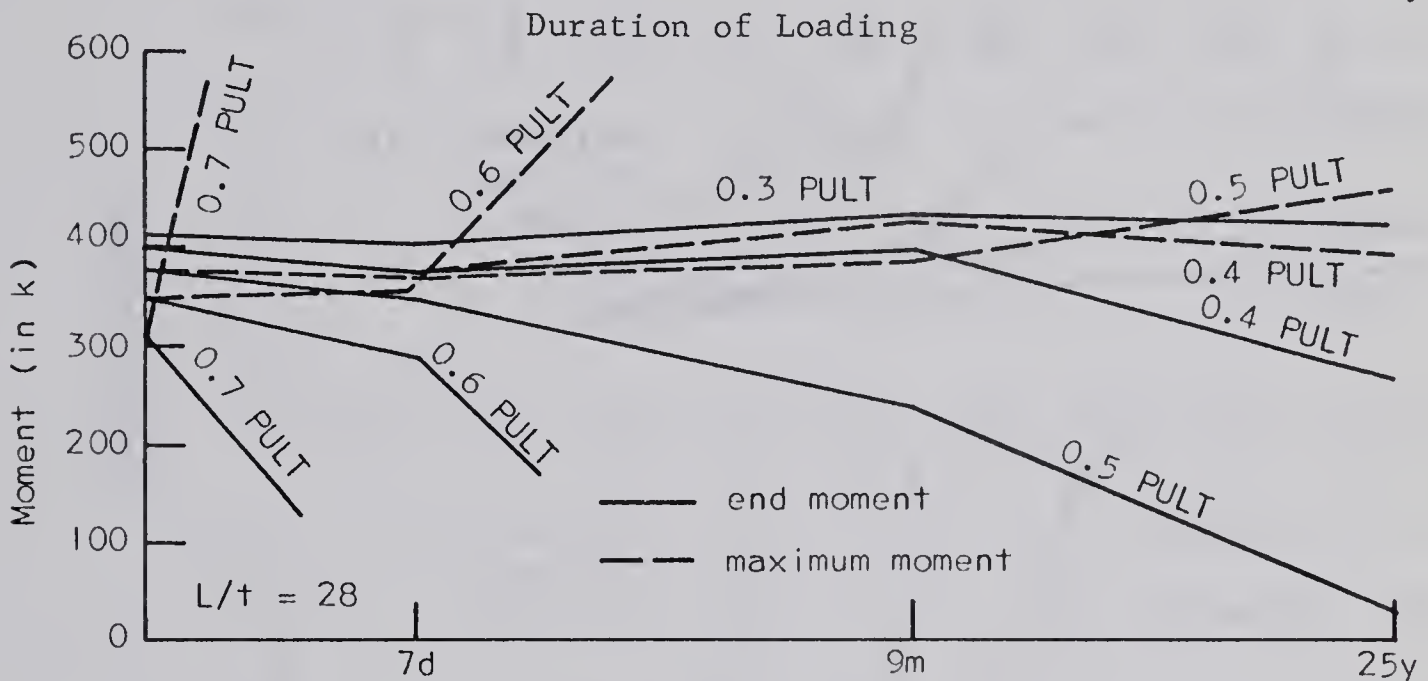
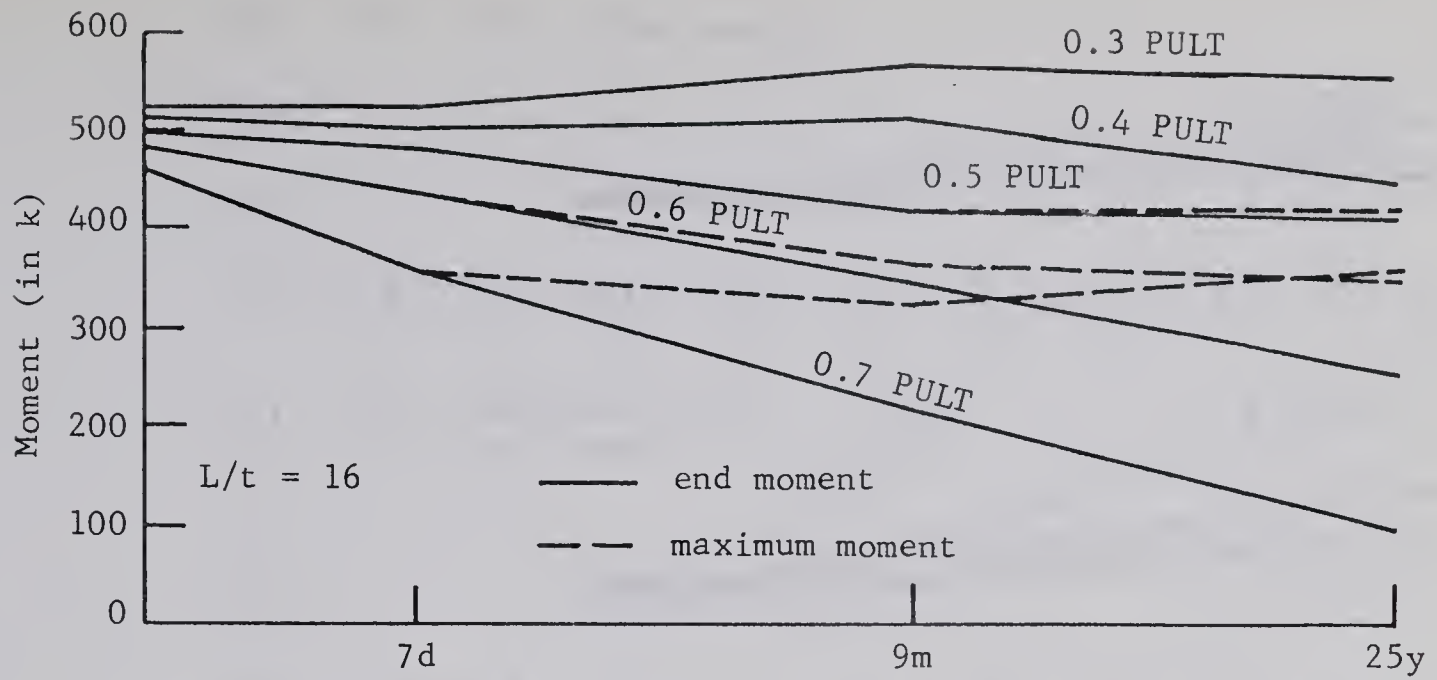


FIGURE 8.17

VARIATION IN DOUBLE CURVATURE COLUMN
MOMENTS WITH TIME

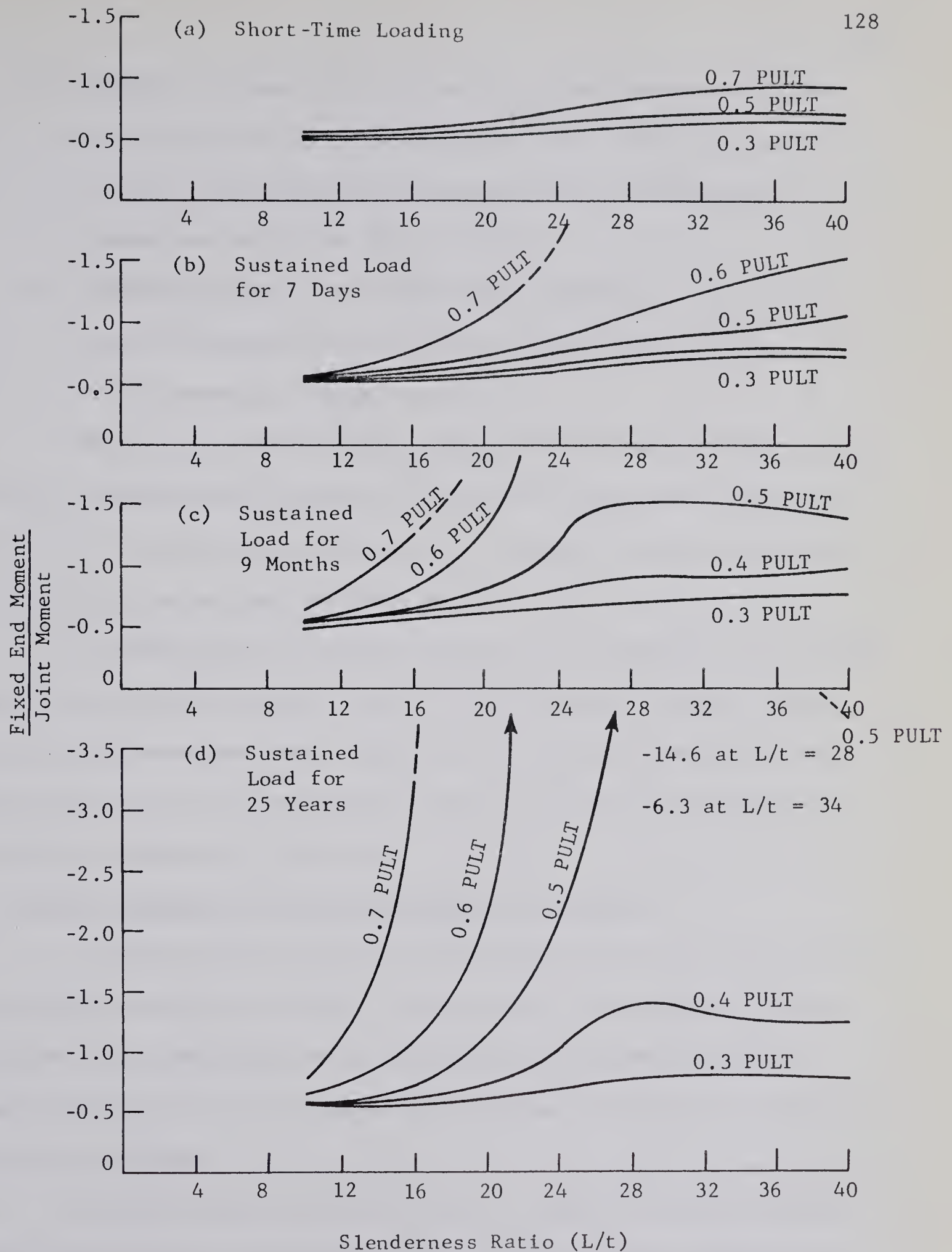


FIGURE 8.18

EFFECT OF SUSTAINED LOAD ON THE RATIO OF
FIXED END MOMENT TO JOINT MOMENT FOR
THE COLUMNS BENT IN DOUBLE CURVATURE

3. FIGURE 8.17 shows the variation in column moments with time for the various levels of sustained load. The three parts of this figure are cross-sections through FIGURE 8.16 at slenderness ratios of 16, 28, and 40.
4. FIGURE 8.18 shows the effect of the slenderness ratio and level of sustained load on the carry-over factors after various durations of sustained load.

Many of the factors which influenced the behavior of the single curvature columns also influenced the behavior of the double curvature columns. As a result, the explanations of behavior are not as detailed in this section as in the preceeding section.

FIGURES 8.10 to 8.15 best illustrate the behavior of the columns under increasing load and also show the total changes in moment which occurred under sustained load. Again, the interaction diagram for the cross-section and the column moment computed by first order theory are included as references to behavior.

(a) Columns Subjected to Short-Time Loading to Failure

Columns D-10.ST to D-40.ST of FIGURES 8.10 to 8.15 were subjected to short-time loading to failure. The increase in the relative column stiffness with increasing load at low levels of load was apparent in column D-10.ST just as in column S-10.ST and again was due to a reduction in tensile cracking.

With the fixed end restraint and the double curvature configuration, an increase in the deflection moment had a primary effect on relative column stiffness and only a secondary effect on maximum moment. As a result, the moment at a point away from the joint exceeded the joint

moment due to deflection moment only after considerable long column behavior had been exhibited. No long column action was exhibited by columns D-10.ST and D-16.ST. In column D-16.ST, the point of maximum moment had just begun to move away from the joint at the time of failure. Columns D-22.ST and D-28.ST exhibited noticeable long column action with column D-28.ST being on the verge of instability at failure. Columns D-34.ST and D-40.ST exhibited unstable failures.

The failure loads under short-time loading increased with an increase in slenderness ratio up to column D-22.ST. This behavior was the direct result of the decrease in the relative column stiffness due to the increasing deflection moment. The failure load of column D-28.ST was only slightly less than that of column D-22.ST, but because of the instability exhibited in columns D-34.ST and D-40.ST, the failure loads decreased substantially as the slenderness ratio was increased beyond 28. The behavior and failure loads under short-time loading had a decided influence on the behavior of the models studied under sustained load because the magnitudes of sustained load were based on the short-time failure loads. The ratio of the failure load under sustained load to the failure load under short-time loading was a minimum at a slenderness ratio of approximately 28 (see FIGURE 8.28). As a result, by basing the magnitude of sustained load on the short-time failure load, the columns with intermediate values of slenderness ratio exhibited more unstable behavior under sustained load than the columns with the higher values of slenderness ratio. This behavior is noticeable in all the behavior curves for the double curvature columns.

The non-linear behavior of concrete influenced the short-time

failure loads of the double curvature columns in much the same way as it influenced the single curvature columns. The formation of a "hinge" at the joint in columns D-10.ST, D-16.ST, and D-22.ST caused large reductions in the relative column stiffness with increasing load as the failure load was approached, and as a result, the failure loads were substantially increased. Columns D-34.ST and D-40.ST were influenced by the slight "hinging" of the beam. This is evidenced by the sudden change from stable to unstable behavior as the relative column stiffness approached zero. Column D-28.ST appears to have been influenced by both types of hinging, but the column hinge appeared to be more dominant.

(b) Columns Subjected to a Sustained Load Followed by Quick Loading to Failure

The columns numbered .30 to .70 in each series were subjected to a hypothetical sustained load followed by a quick loading to failure if they did not fail under the sustained load. The behavior under sustained load was influenced considerably by the magnitude of the sustained load.

As was the case with the single curvature columns, the relative stiffness of the double curvature columns at the lower load levels showed an increase with time up to nine months duration of loading. This behavior, which was limited to the lowest load level (0.30 PULT) in the single curvature columns, was exhibited by some of the double curvature columns at 0.40 PULT. Again the behavior was due to the relief in concrete stress through transfer to the compression steel, and was more noticeable in the double curvature columns because of the smaller deflection moments at any load level.

The long column action under sustained load increased noticeably

from that exhibited under short-time loading except in columns D-10.30 to D-10.70 where sustained loading produced no long column action. Although the columns D-16.50 to D-16.70 exhibited considerable long column action under sustained load, the maximum moments were not increased beyond the values reached under short-time loading. Columns D-22.40 to D-22.70 all exhibited long column action under sustained load with column D-22.70 becoming unstable after approximately nine months duration of loading. Column D-22.60 was on the verge of instability after 25 years of sustained load and also showed an increase in maximum moment over the short-time value. Columns .30 to .70 of the remaining series all exhibited long column action under sustained load to the extent that all of the maximum moments after 25 years duration of loading exceeded the corresponding short-time values. Columns .60 and .70 in series D-28, D-34 and D-40 became unstable and failed during the period of sustained load.

The shorter columns, when subjected to quick load following the sustained load, exhibited primarily stable failures. An exception to this was column D-16.70 which exhibited an unstable failure. Columns D-16.60 and D-22.30 were both on the verge of instability at failure, and the remaining columns exhibited stable failures.

The relative stiffnesses of the double curvature columns decreased rapidly with load as the quick load was applied following the sustained load. Again this behavior was due to the increase in the deflections and the yield of the compression steel under sustained load.

The double curvature columns which were subjected to sustained load were more influenced by the non-linear behavior of concrete than were the corresponding single curvature columns. This occurred because the

relative stiffness of a double curvature column decreased without a significant increase in the maximum moment. As a result, most of the columns were relatively stable when their relative stiffness approached zero. After this condition was reached, however, further redistribution of moment was incomplete as beam "hinging" caused some of the moment to be distributed back to the column. This resulted in a rather sudden change from stable to unstable behavior in the column. Column "hinging" also occurred in the shorter columns which exhibited a stable failure. This is shown by the large decrease in the relative stiffness of each column as the load approached failure.

(c) Variation in Column Moments and Stiffnesses with Time

FIGURE 8.16 shows the effect of slenderness ratio and the level of sustained load on the maximum moment and the joint moment or relative stiffness in the columns after various durations of sustained load.

The behavior under short-time loading is shown in FIGURE 8.16(a). For the load levels considered, the columns were relatively stable as evidenced by the similarity in shapes between the first order theory curve and the end moment curves. The slenderness ratio at which long column action occurred decreased as the level of load increased.

The behavior after seven days under sustained load is shown in FIGURE 8.16(b). The compression steel had yielded over a portion of the length in all of the columns at the highest load level. This resulted in large decreases in the relative column stiffness as the slenderness ratio was increased and also had a large effect on the development of long column action. The shorter columns under sustained loads of 0.50 PULT and 0.60 PULT also had experienced some yielding of the compression steel, but

the tendency to become unstable had only increased slightly over that exhibited under short-time loading.

The behavior after nine months duration of loading is shown in FIGURE 8.16(c). The compression steel had yielded in all the columns except D-34.30, D-40.30, and D-40.40, and the effect of this on the results was apparent. The instability with increasing slenderness ratio was very noticeable at the higher load levels. At the lower sustained load levels, the columns with an intermediate value of slenderness ratio exhibited the most unstable behavior. This was the result of the fact that the short-time load capacity and thus the magnitude of the sustained load at each load level were higher for the short and intermediate length columns than for the long columns.

The behavior after 25 years under sustained load is shown in FIGURE D.16(d). All of the compression steel had yielded by this time. The behavior was similar, only amplified, to that exhibited after nine months under sustained load.

FIGURE 8.17 shows the variation in column moments with time under the various levels of sustained load for the columns with slenderness ratios of 16, 28, and 40. The effect of the yielding of the compression steel on the column stiffness is quite apparent in these figures. The rate of change of the maximum moment and the end moment changed when the compression steel had yielded.

FIGURE 8.18 shows the effect of slenderness ratio, level of sustained load, and duration of loading on the carry-over factors of the columns bent in double curvature. Under short-time loading, the shorter columns exhibited very little unstable or non-linear behavior and the

carry-over factors were very close to the first order value of -0.5. With an increase in the slenderness ratio and/or an increase in the level of load, the columns became more unstable and the carry-over factors decreased (became more negative). After the load had been sustained for seven days, the effect of instability on the carry-over factors became very apparent at high levels of load where the compression steel had yielded. This trend continued with longer durations of loading. After long durations of loading, the carry-over factors under a sustained load of 0.50 PULT reached a minimum at the intermediate slenderness ratio of 28 and then increased for larger slenderness ratios. This behavior was again due to the higher magnitude of sustained load for intermediate slenderness ratios than for large slenderness ratios.

Although the large carry-over factors, which occurred when the columns became unstable, appear to indicate large magnitudes for the fixed end moment, in actual fact, the major reason for the large carry-over factors was the decrease in the column end moment or relative stiffness. The fixed end moment achieved a magnitude slightly less than the maximum moment at the most critical points.

The fixed end restraint in the model frame is an approximation of the restraint given by a very stiff beam or by a footing in an actual frame. In an actual frame this type of restraint would not completely restrict the rotation of the joint and as a result, the assumption of a completely fixed end will probably result in an overestimation of the carry-over factors and also the column capacity.

8.4 Maximum Column Deflections

8.4.1 Maximum Deflections of the Columns Bent in Single Curvature

FIGURE 8.19 shows the maximum or mid-height deflections of the columns bent in single curvature. These curves show the effect of the level of sustained load, the slenderness ratio, and the duration of loading on the maximum deflections.

The behavior under short-time loading is illustrated in FIGURE 8.19(a). For the levels of load considered, the deflections increased with an increase in either the slenderness ratio or the level of load. For the low levels of load, the relationship between the maximum deflection and the slenderness ratio was almost linear. This was due to the stability of the columns at these levels of load.

The behavior after a duration of sustained load of seven days is shown in FIGURE 8.19(b). The columns were still relatively stable except at the highest load level (0.70 PULT) where the compression steel had yielded and the resulting "softer" columns rapidly became unstable with increasing slenderness ratio.

FIGURES 8.19(c) and (d) show the behavior after nine months and 25 years under sustained load. After nine months duration of loading, the compression steel had yielded in all of the columns at the two higher load levels and had yielded in only the shorter columns at the lower load levels. At the higher load levels, the deflections increased very rapidly with slenderness ratio due to the unstable behavior of the columns once the compression steel had yielded. After a duration of loading of 25 years, all the compression steel had yielded and as a result, unstable behavior was exhibited at all load levels as the slenderness ratio increased.

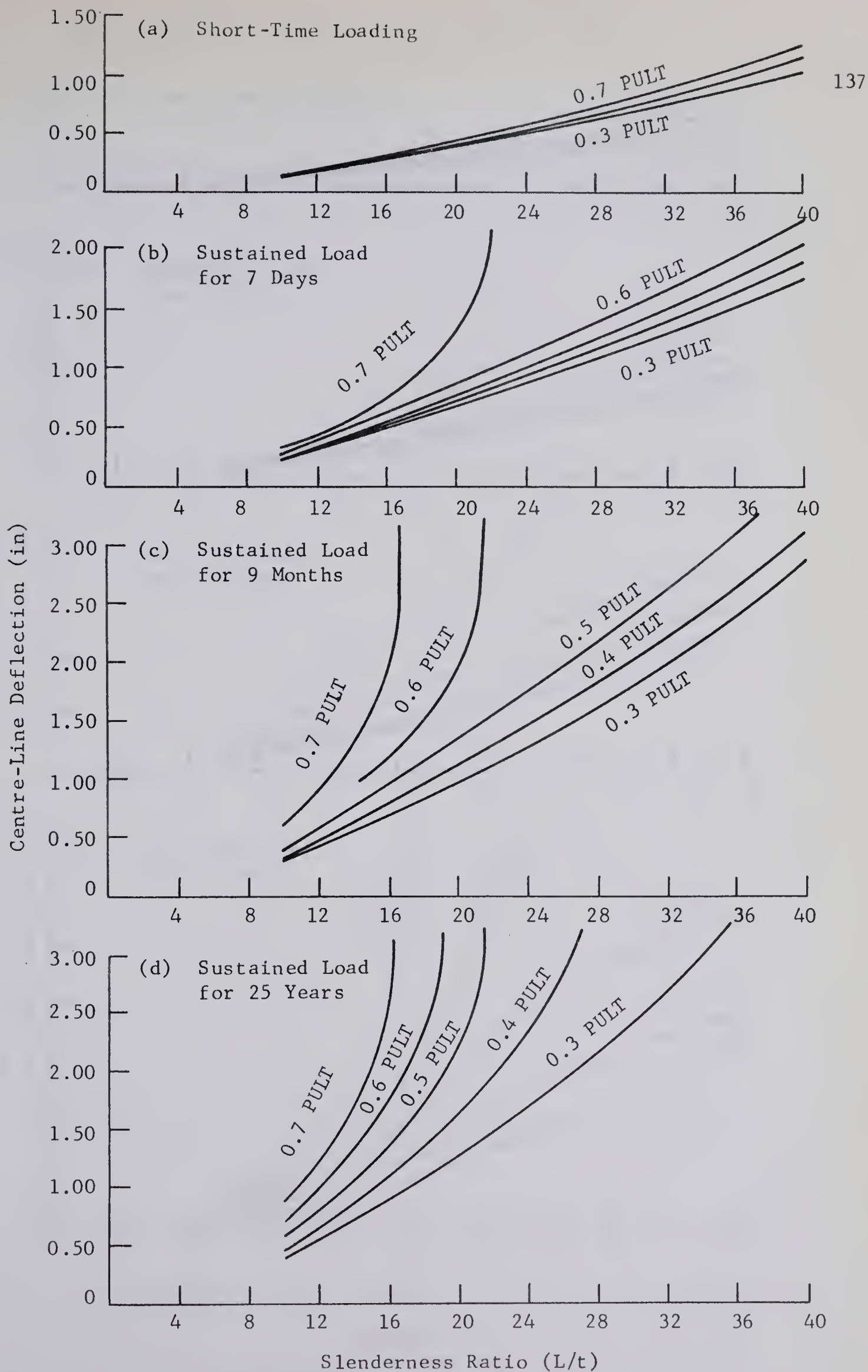


FIGURE 8.19
EFFECT OF SUSTAINED LOAD ON THE MAXIMUM
DEFLECTION OF THE COLUMNS BENT IN SINGLE CURVATURE

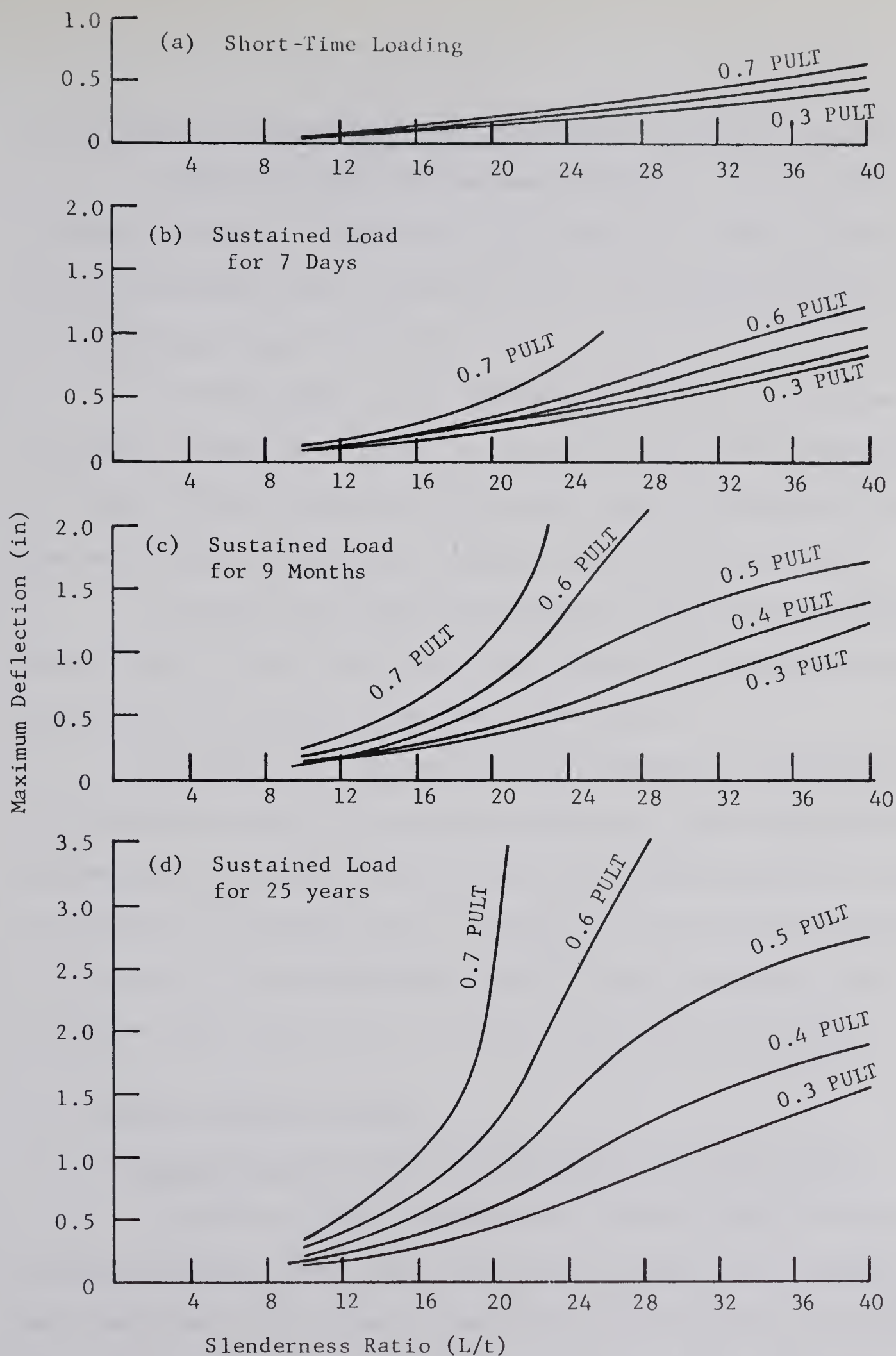


FIGURE 8.20

EFFECT OF SUSTAINED LOAD ON THE MAXIMUM DEFLECTIONS
OF THE COLUMNS BENT IN DOUBLE CURVATURE

8.4.2 Maximum Deflections of the Columns Bent in Double Curvature

FIGURE 8.20 shows the maximum deflections of the columns bent in double curvature. These curves show the effect of the parameters of level of sustained load, slenderness ratio, and duration of sustained load on the maximum column deflections.

The development of the maximum deflections in the columns bent in double curvature was similar to the development in the columns bent in single curvature except that the double curvature deflections were smaller because of the greater restraint offered to the columns.

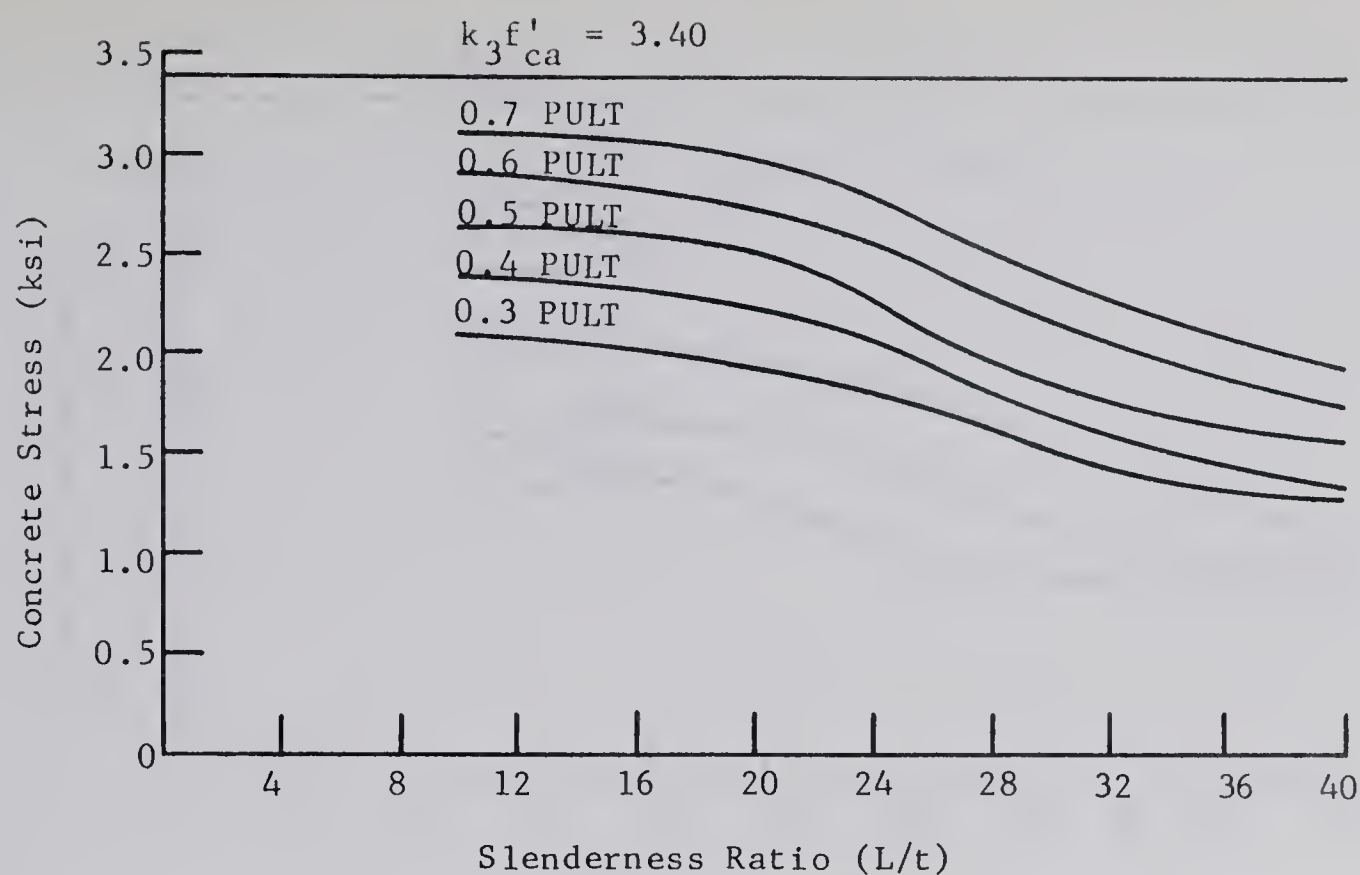
The position of maximum deflection varied from approximately 30 per cent to 45 per cent of the column length away from the column joint depending on the degree of the long column effect.

The fact that the most critical combination of parameters occurred at intermediate values of slenderness ratios was also demonstrated by the maximum deflections, particularly after the longer durations of loading. As pointed out previously, this primarily resulted from the high short-time capacity of the intermediate length columns and the fact that the sustained loads were chosen as a ratio of the short-time capacity.

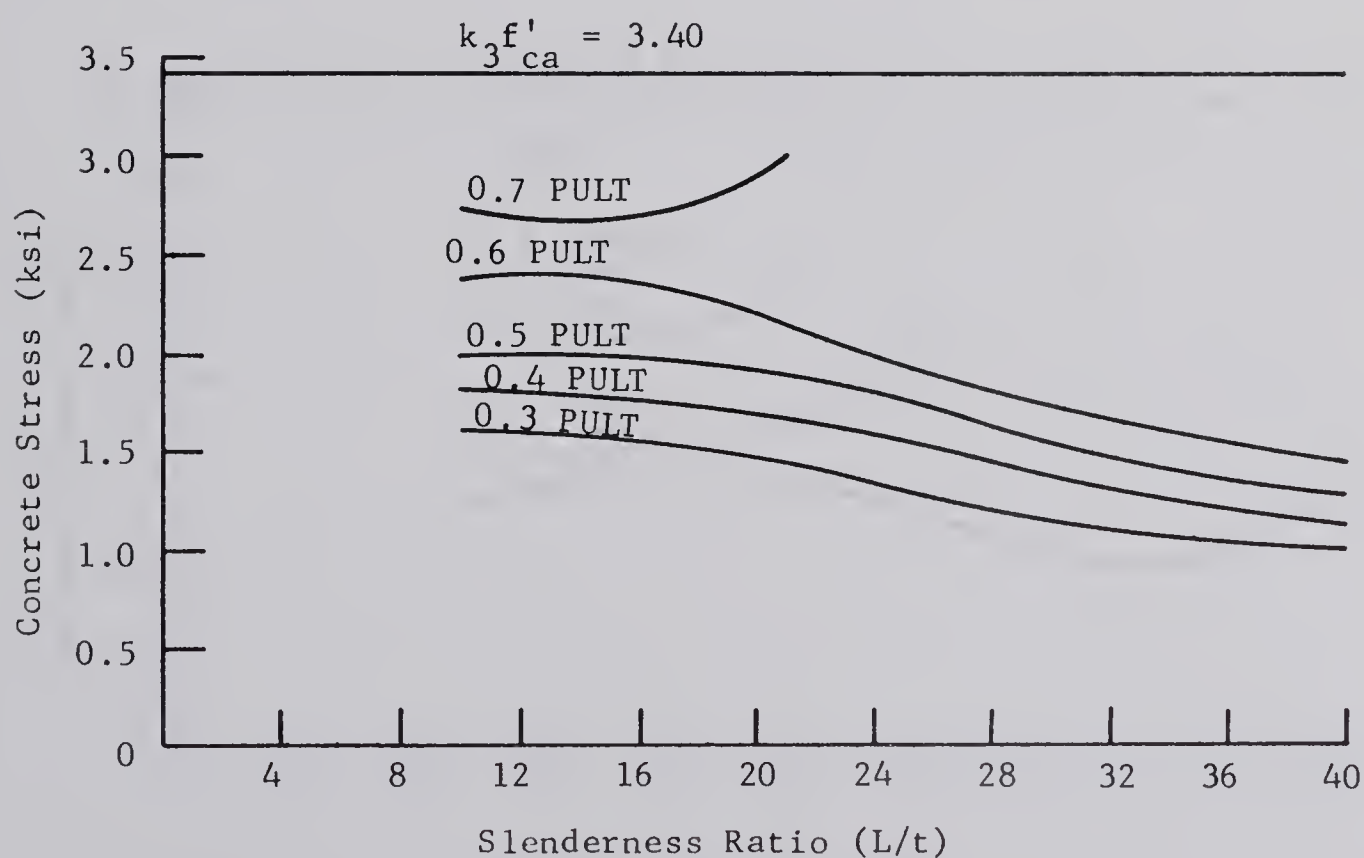
8.5 Maximum Concrete Stresses

8.5.1 Maximum Concrete Stresses in the Single Curvature Columns

FIGURE 8.21 shows the effect of sustained load on the maximum concrete stresses in the single curvature columns. The variables considered are slenderness ratio, level of sustained load, and duration of sustained load. For short-time loading, as shown in FIGURE 8.21(a), maximum concrete stresses decreased with decreasing level of load and with increasing slender-



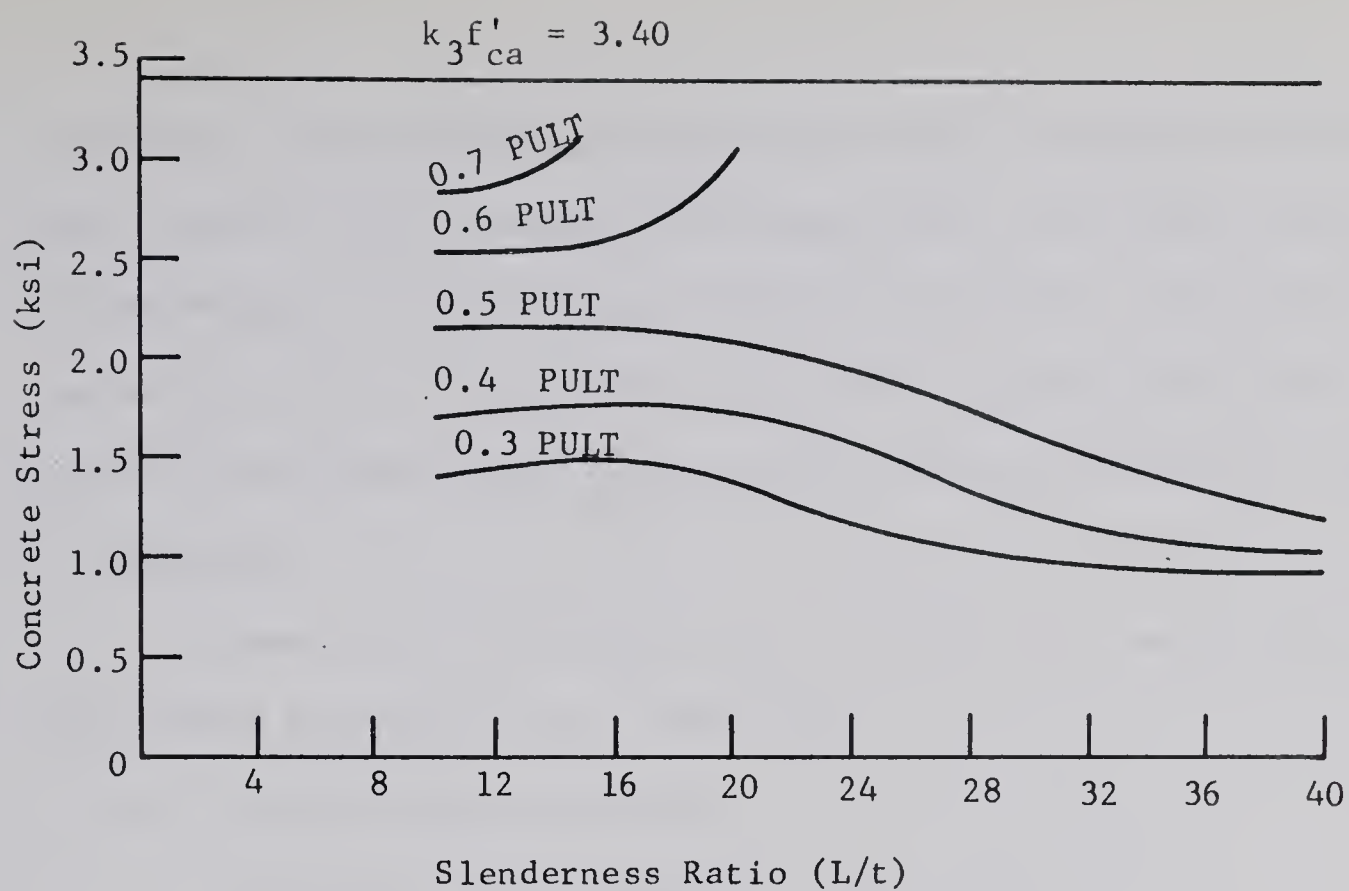
(a) Short-Time Loading



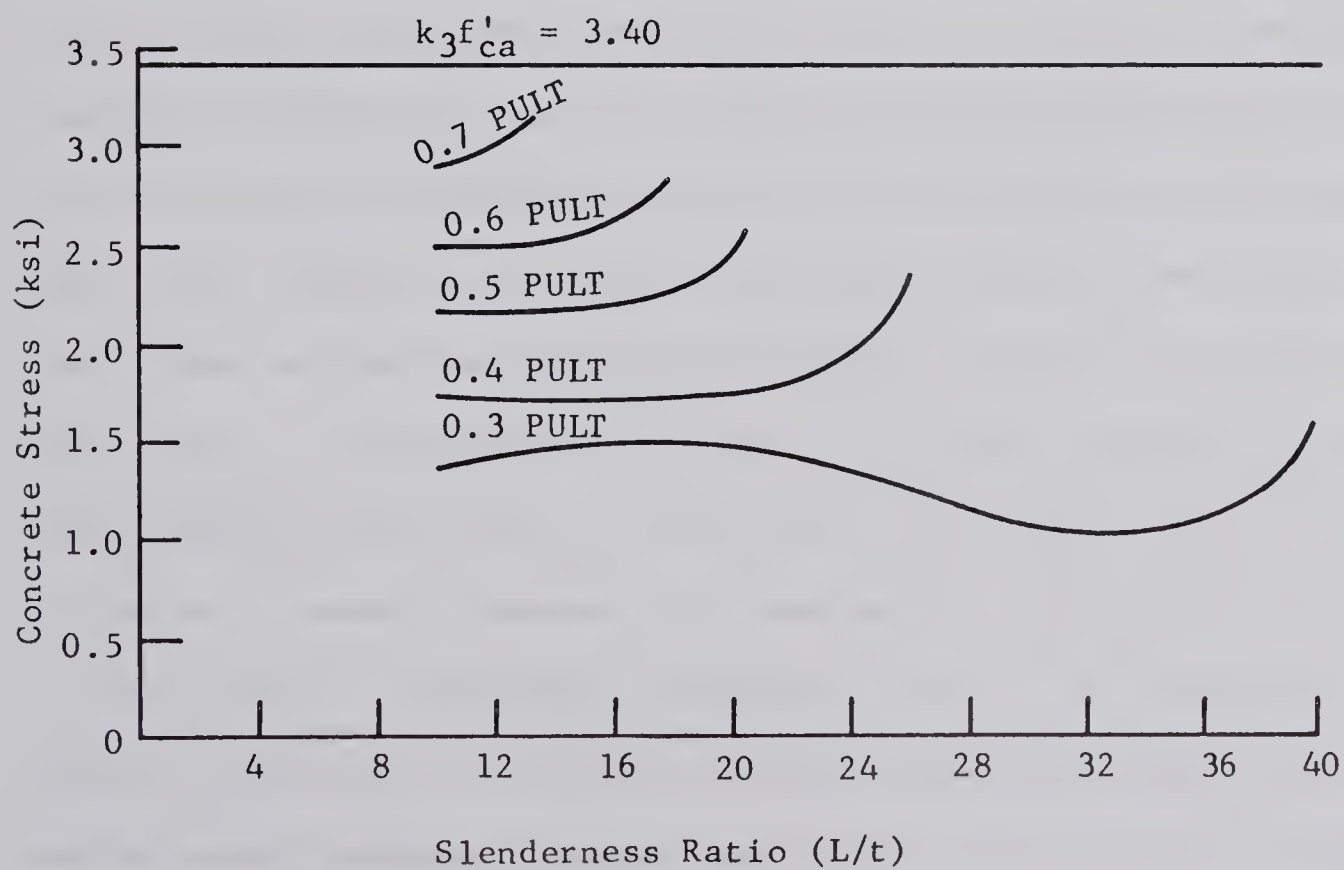
(b) Sustained Load for 7 Days

FIGURE 8.21

EFFECT OF SUSTAINED LOAD ON THE MAXIMUM CONCRETE
STRESS IN THE COLUMNS BENT IN SINGLE CURVATURE



(c) Sustained Load for 9 Months



(d) Sustained Load for 25 Years

ness ratio. The decrease in maximum stress with slenderness ratio was a direct result of the decrease in the magnitude of the load at each level of load because of the decrease in short-time failure load with increasing slenderness ratio. Stresses did not increase substantially with increasing level of load because very little unstable behavior occurred at the levels of load shown.

There are three factors which influence the maximum concrete stress under sustained load. These are:

1. redistribution of stress
2. yielding of the compression steel, and
3. changes in maximum moment.

Under sustained load, stress redistributes from the concrete to the steel because of the dimensional instability of the concrete and the dimensional stability of the steel. If the changes in maximum moment are small and if the compression steel does not yield, the maximum concrete compression stress will decrease with time. This general behavior was exhibited by all the columns at the lower load levels after a duration of sustained load of seven days. At the highest load level (0.7 PULT), however, the compression steel yielded during the first seven days resulting in "softer" columns and large increases in moment and consequently, large increases in maximum concrete stress at the higher slenderness ratios. At the lower slenderness ratios, yielding of the compression steel resulted in small decreases in maximum moment because of larger decreases in the relative stiffness and thus the maximum concrete stress was reduced even more.

The behavior after a sustained load duration of nine months is shown in FIGURE 8.21(c). The compression steel had yielded at the lower

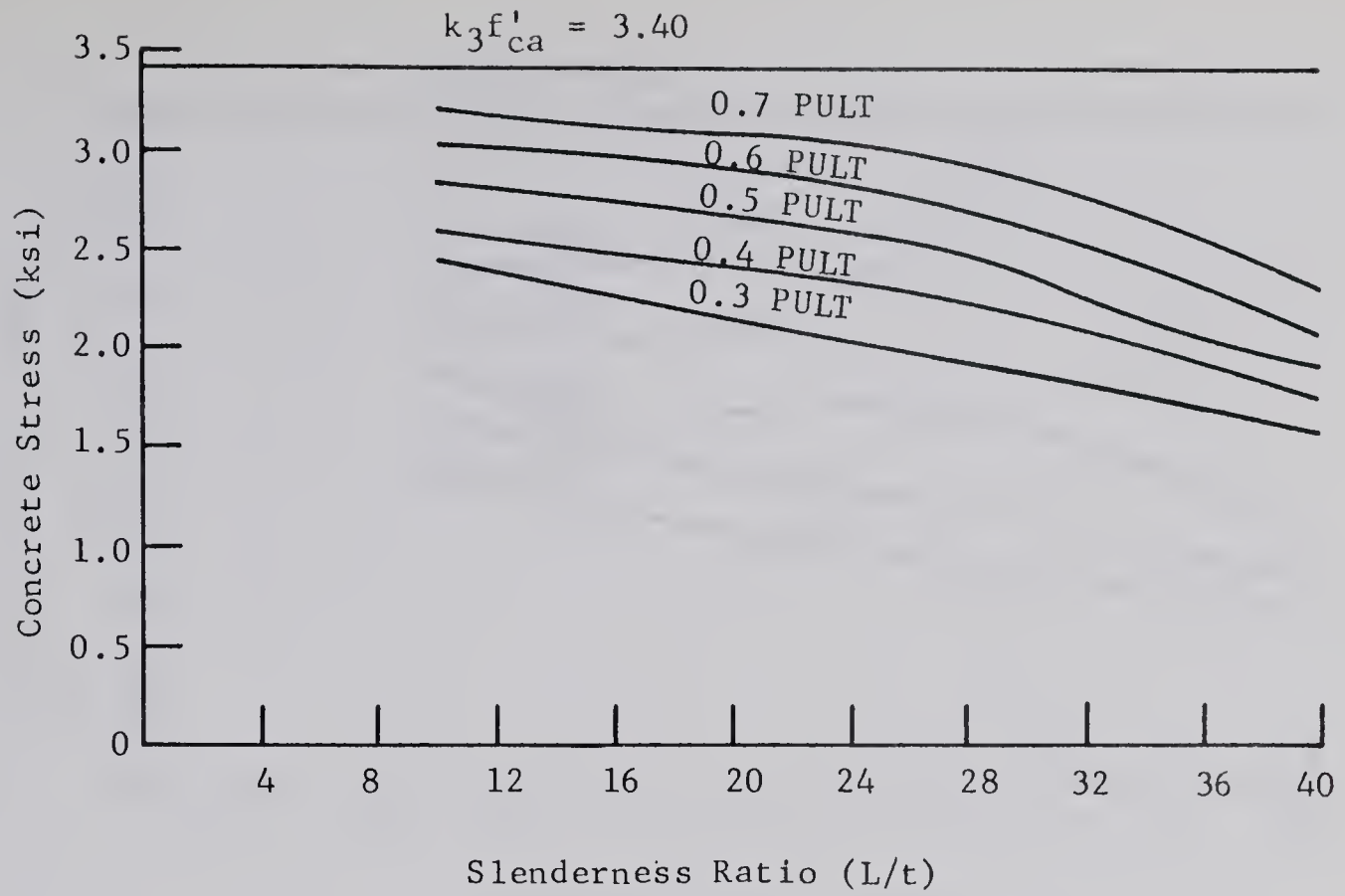
slenderness ratios, but the effect of this on maximum concrete stress was only noticeable at the higher load levels where instability developed. At the lower load levels, further changes in maximum concrete stress from seven days duration of loading were small because changes in maximum moment were small. At higher slenderness ratios, the maximum concrete stresses continued to decrease with time at the lower load levels where compression steel had not yet yielded. For these cases, the increases in maximum moment were not as influential on maximum concrete stress as was the redistribution of stress from concrete to steel.

The behavior after 25 years duration of loading is shown in FIGURE 8.21(d). All the compression steel had yielded by this time and, as a result, the majority of maximum concrete stresses showed an increase over the values at nine months because of the increases which resulted in the maximum moments. At the lowest level of load (0.3 PULT), the shorter columns showed no significant change because the maximum moments were not materially affected. At the maximum value of slenderness ratio considered, the maximum concrete stress increased noticeably because of instability.

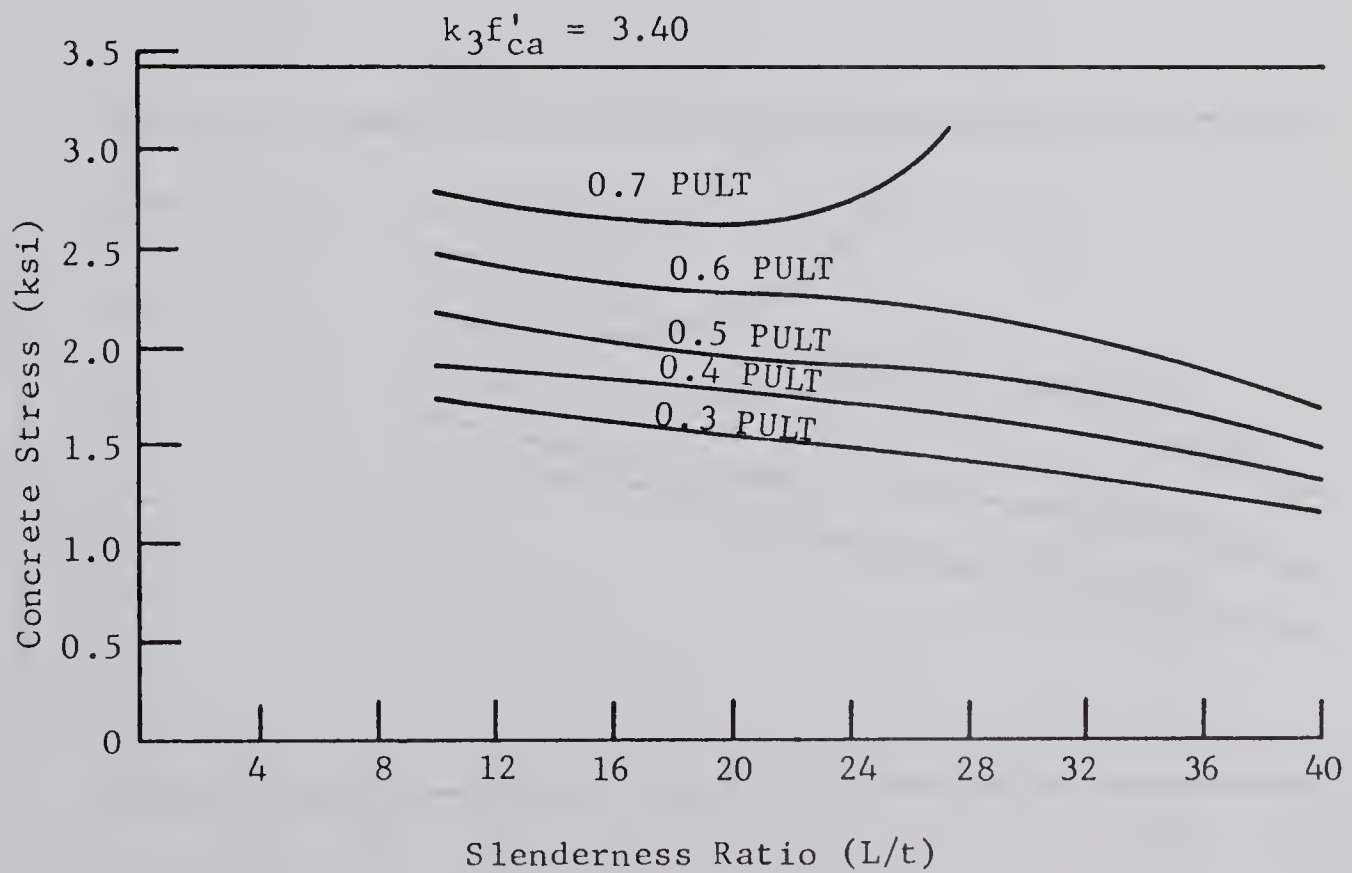
8.5.2 Maximum Concrete Stresses in the Double Curvature Columns

FIGURE 8.22 shows the effect of sustained load on the maximum concrete stress in the columns bent in double curvature. The variables considered are level of sustained load, slenderness ratio, and duration of sustained load.

The changes in maximum concrete stress in the double curvature columns were influenced by the same factors as for the single curvature columns. However, the increases in maximum stresses due to increasing



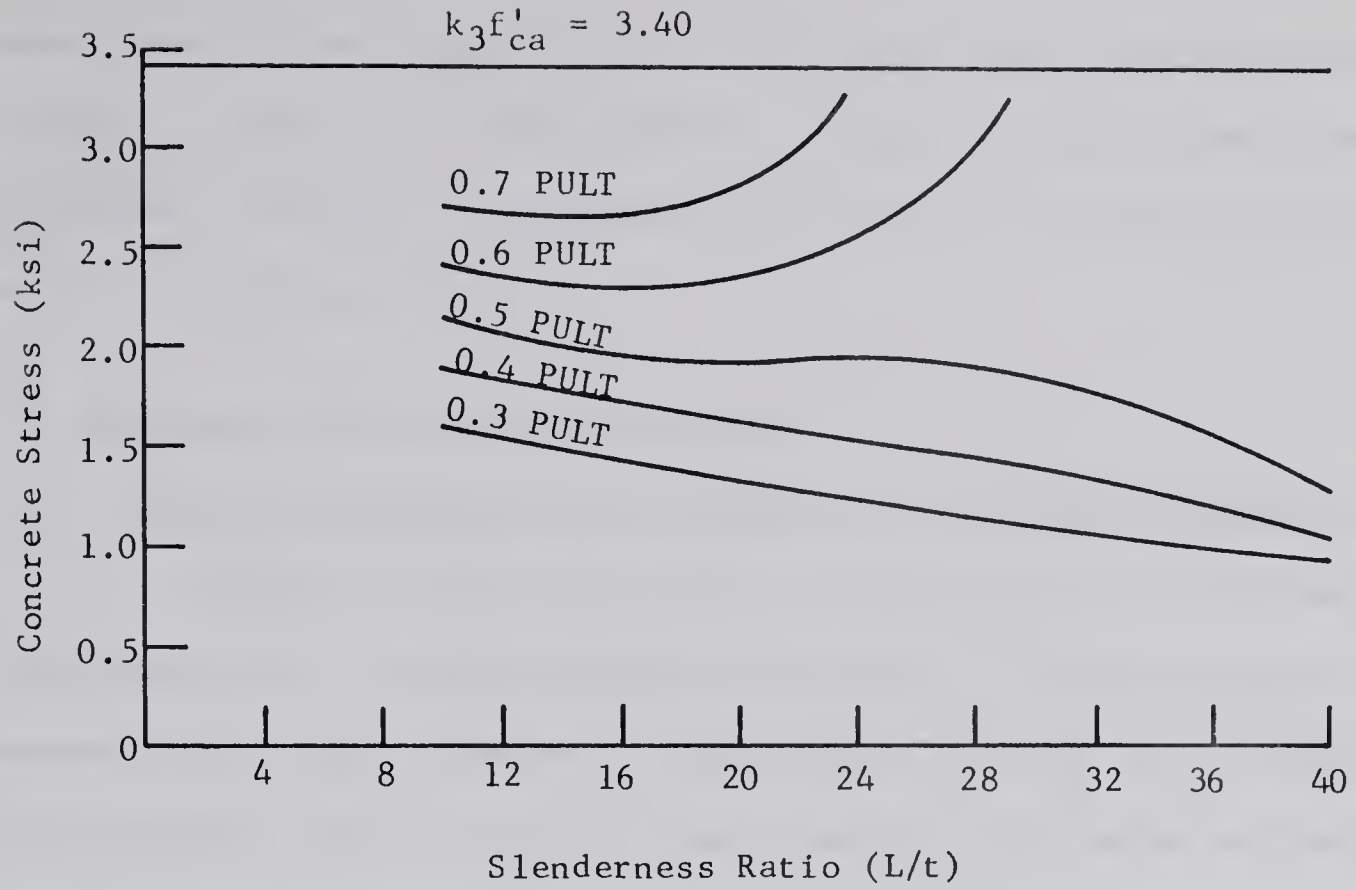
(a) Short-Time Loading



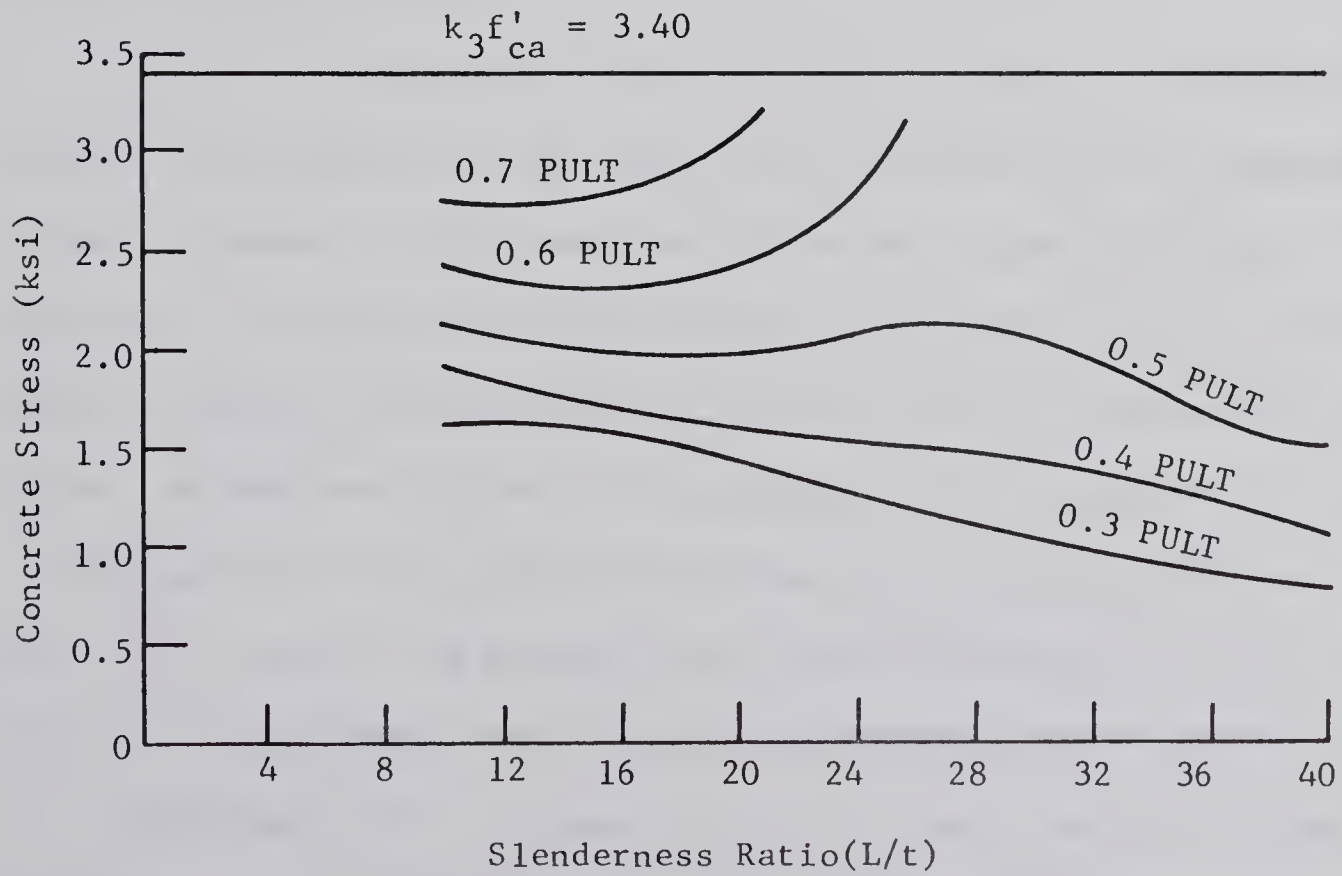
(b) Sustained Load for 7 Days

FIGURE 8.22

EFFECT OF SUSTAINED LOAD ON THE MAXIMUM CONCRETE STRESS IN THE COLUMNS BENT IN DOUBLE CURVATURE



(c) Sustained Load for 9 Months



(d) Sustained Load for 25 Years

moment were not as pronounced due to the lower tendency of the double curvature columns to become unstable. Maximum concrete stresses were yet another indicator of the more critical state of loading at the intermediate slenderness ratios.

8.6 Maximum and Minimum Steel Stresses

8.6.1 Maximum and Minimum Steel Stresses in the Single Curvature Columns

FIGURE 8.23 shows the effect of sustained load on the maximum and minimum steel stresses in the columns bent in single curvature. The maximum steel stress occurred in the compression steel at the point of maximum moment and the minimum stress occurred in the steel on the other face, also at the point of maximum moment. The variables considered in the curves are the level of sustained load, the slenderness ratio, and the duration of sustained load.

The steel stresses under short-time loading are shown in FIGURE 8.23(a). The behavior can be explained by considering the combined effects of load and moment on the cross-section at the column mid-height. For the load levels considered, both the maximum or mid-height moment and the magnitude of sustained load decreased with an increase in slenderness ratio. However, at the lower values of slenderness ratio considered, the decrease in the magnitude of the loads with an increase in slenderness ratio was small. As a result, the maximum steel stress decreased, but the minimum steel stress increased, with increasing slenderness ratio up to a value of L/t of approximately 20. Beyond this point, the decrease in the magnitudes of the sustained loads was larger with an increase in slenderness ratio. As a result, both the maximum and minimum steel stresses decreased with

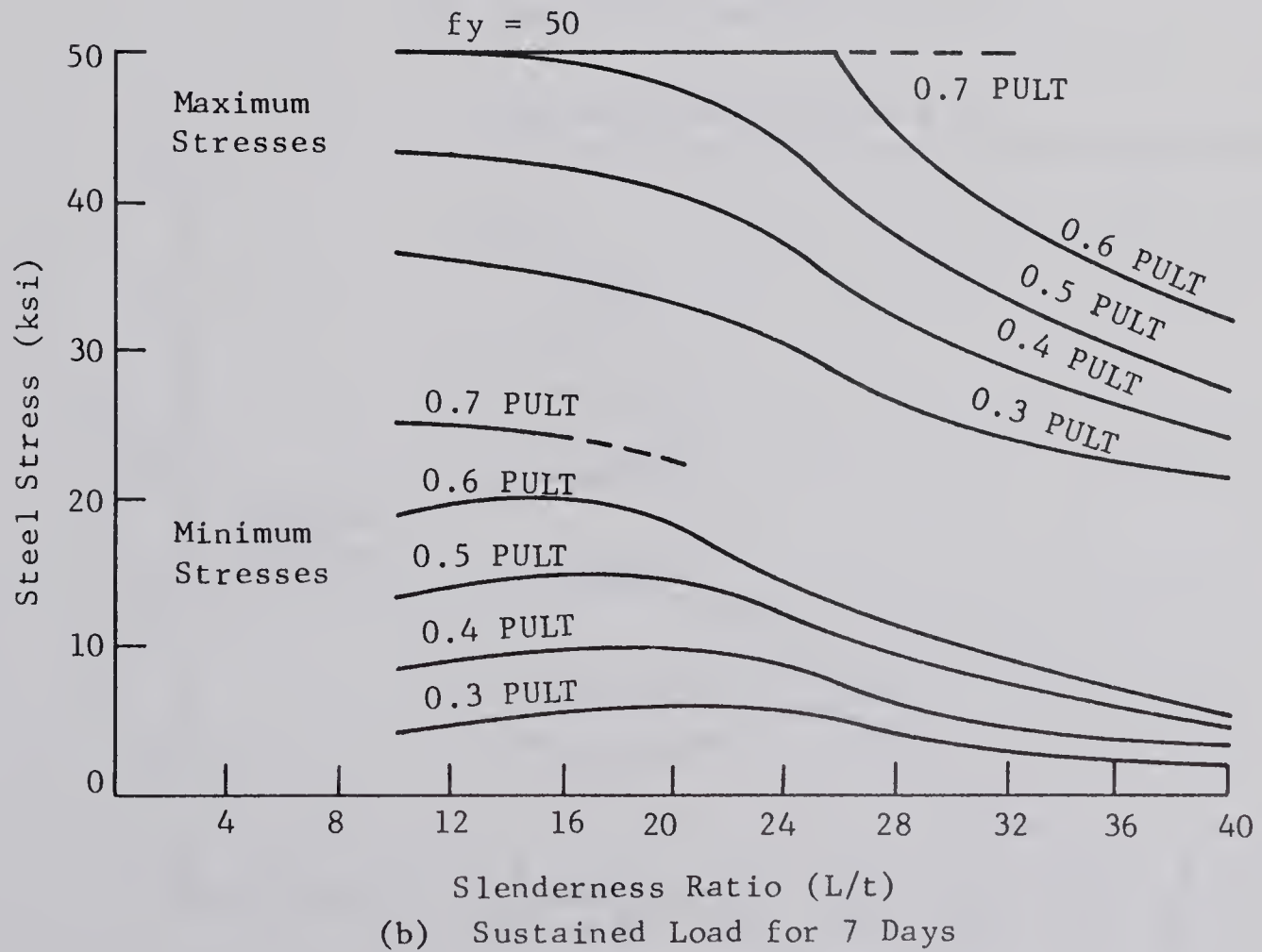
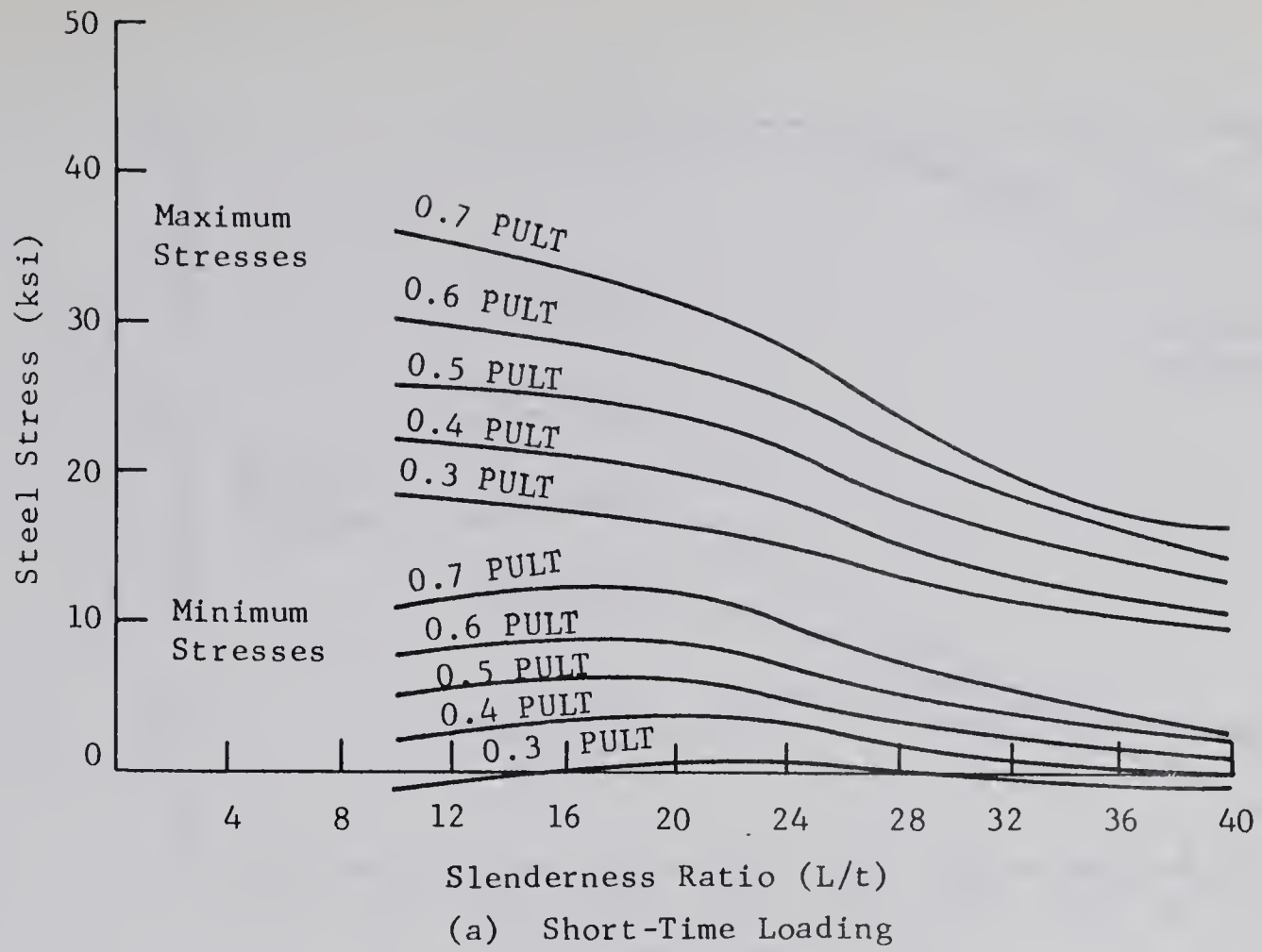
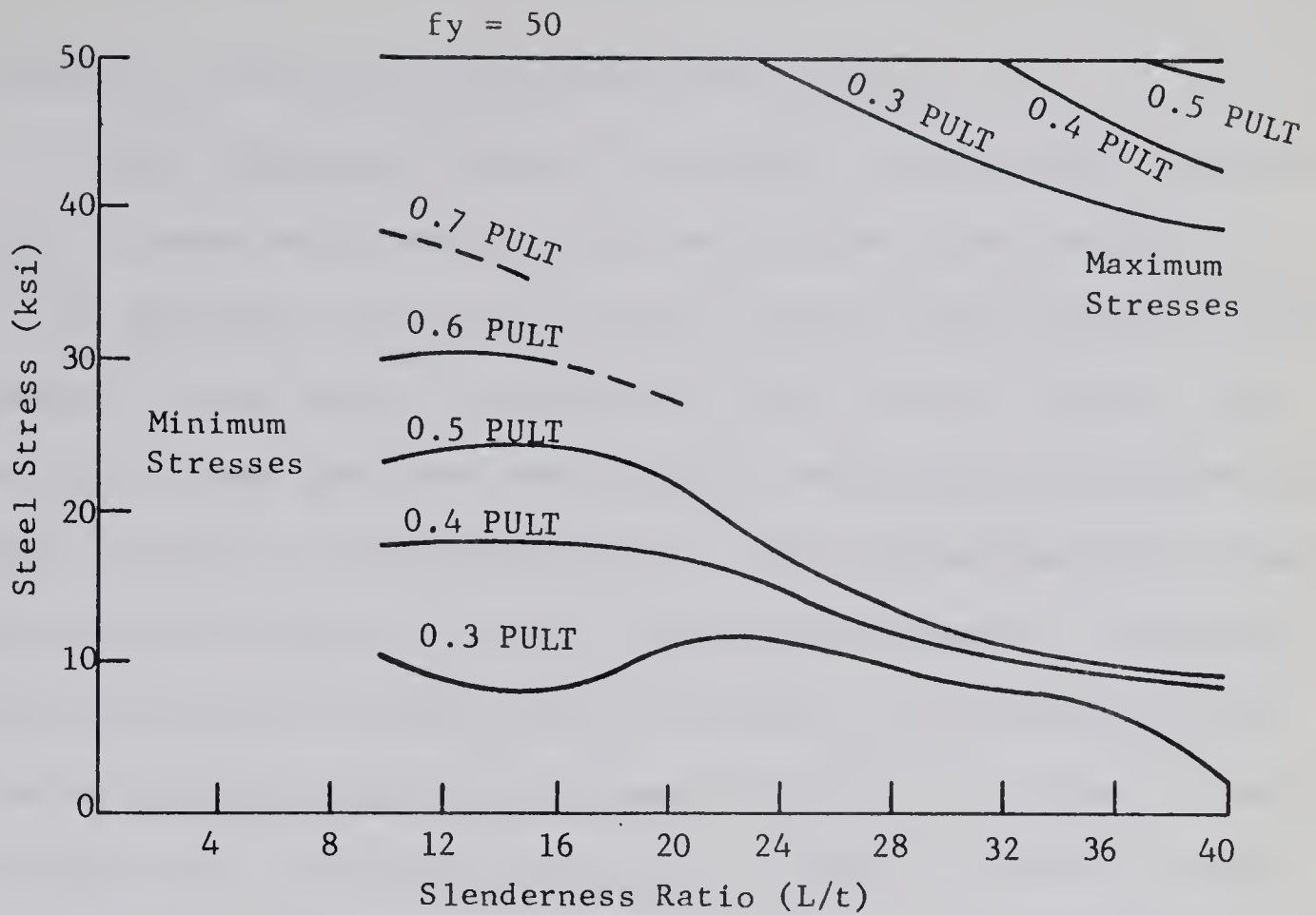
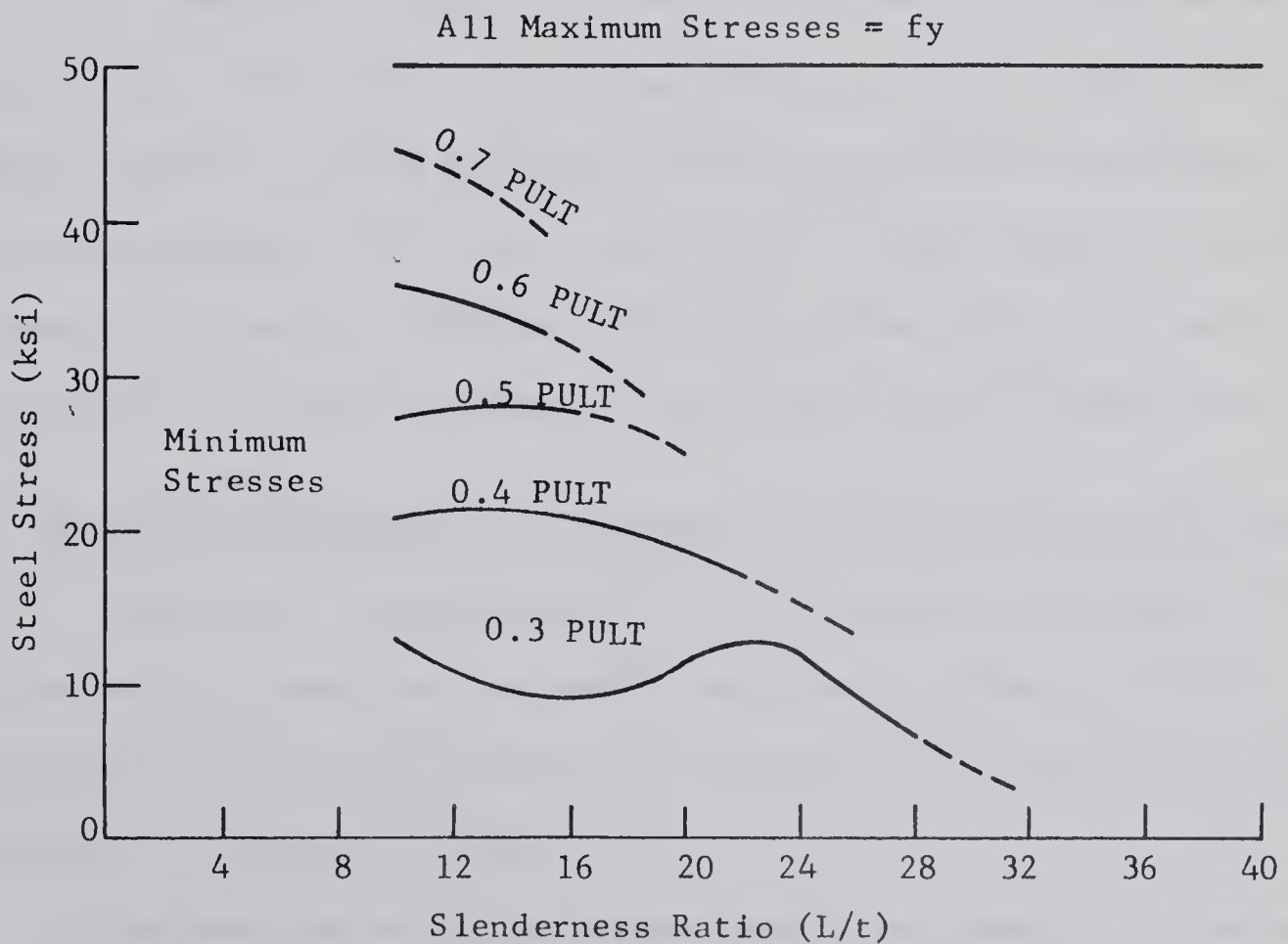


FIGURE 8.23

EFFECT OF SUSTAINED LOAD ON MAXIMUM AND MINIMUM STEEL STRESSES IN THE COLUMNS BENT IN SINGLE CURVATURE



(c) Sustained Load for 9 Months



(d) Sustained Load for 25 years

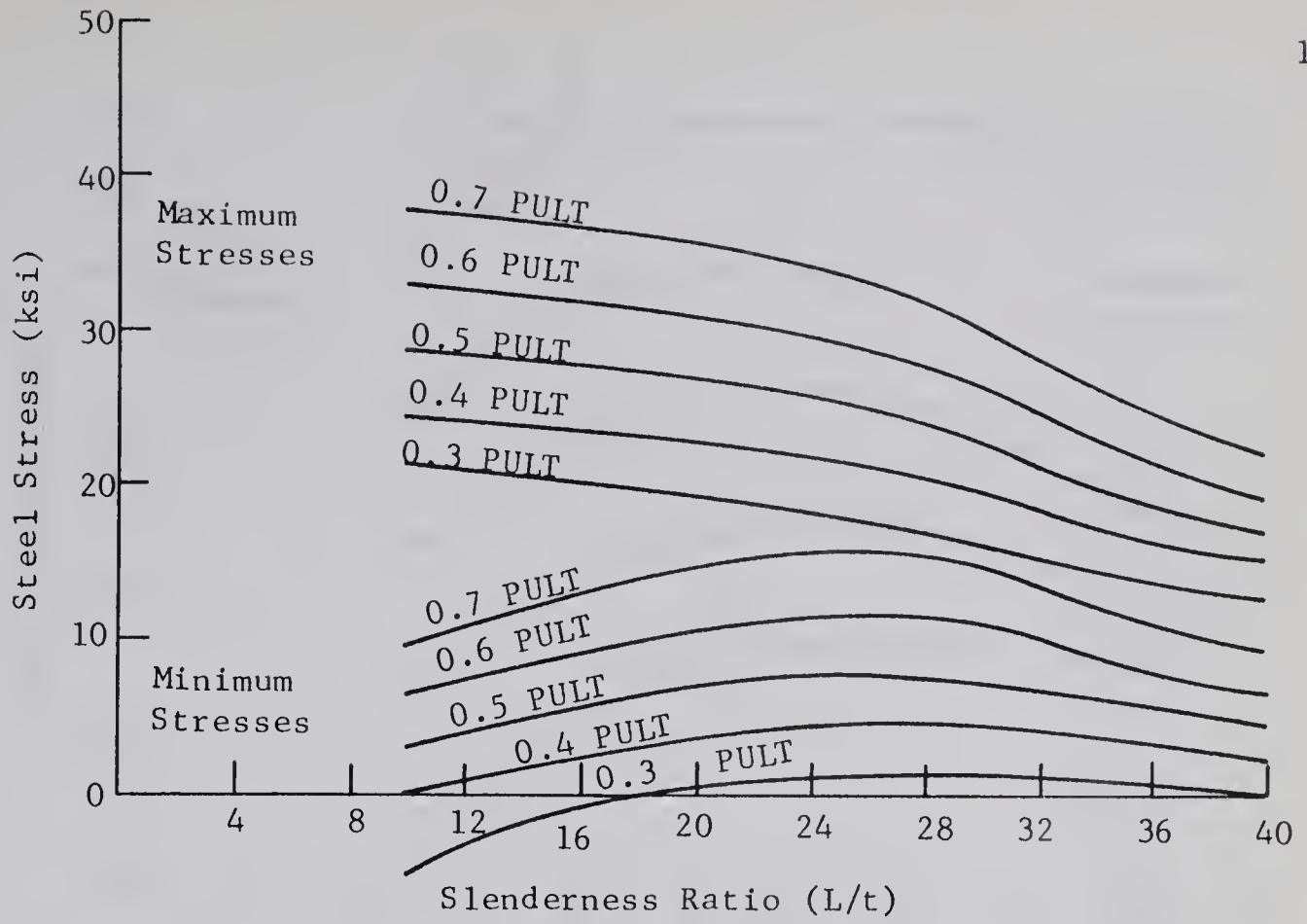
an increase in slenderness ratio beyond about twenty.

Under sustained loading, the principal factors which influenced the steel stresses were the redistribution of stress from concrete to steel, the magnitude of the sustained load, and the magnitude of the maximum moment. At low values of slenderness ratio, the magnitudes of sustained load at each load level were high and redistribution of stress from concrete to steel was the dominant factor. Both the maximum and minimum steel stresses increased with time. The rate of increase of the maximum stresses was greater than the rate of increase of the minimum stresses because the maximum moment also increased with time. At higher values of slenderness ratio, the compression steel was slower in yielding because of the decrease in the magnitude of sustained load with increasing slenderness ratio. The steel stresses increased with time until the compression steel yielded. When this occurred, the tendency of the columns to become unstable increased and the minimum steel stresses began to decrease. The shape of the minimum steel stress curve at the lowest level of load after the longer durations of loading reflects the larger effect of compression steel on relative column stiffness at this level than at higher load levels.

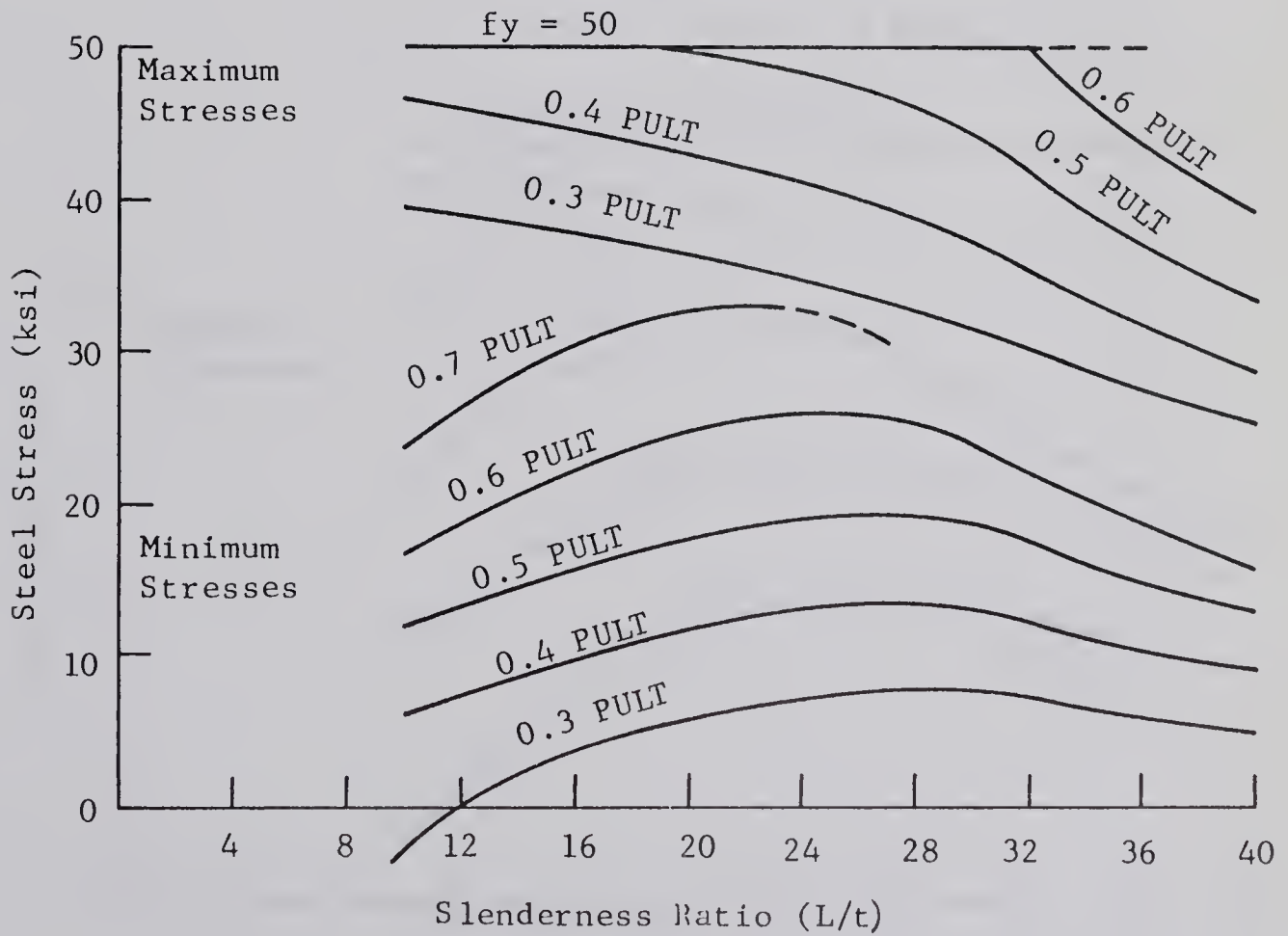
8.6.2 Maximum and Minimum Steel Stresses in the Double Curvature Columns

The effect of sustained load on the minimum and maximum steel stresses in the columns bent in double curvature is shown in FIGURE 8.24. The variables considered are level of sustained load, slenderness ratio and duration of sustained load.

The behavior under short-time loading was similar to that exhibited by the single curvature columns. In the case of the short columns, the



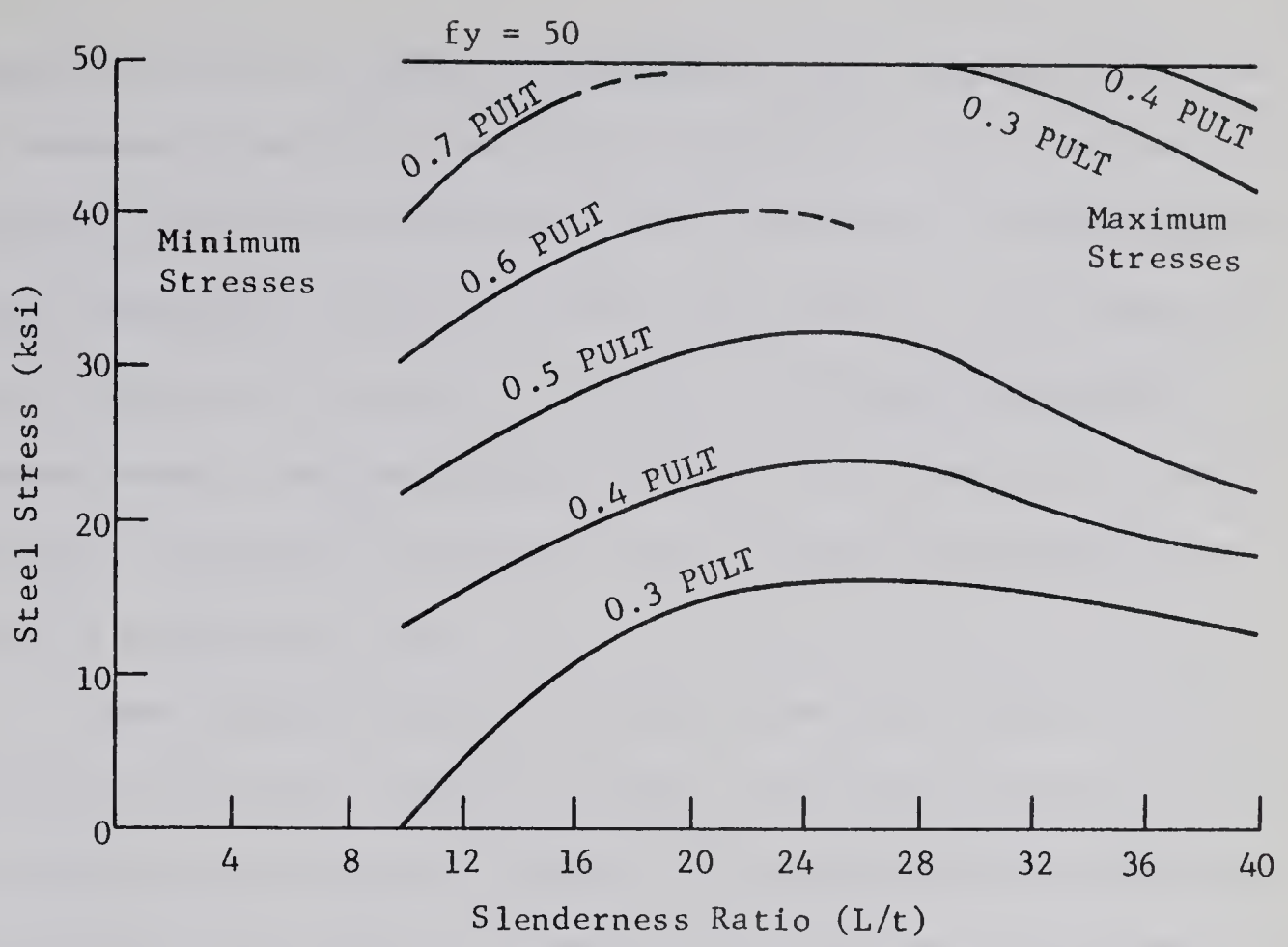
(a) Short-Time Loading



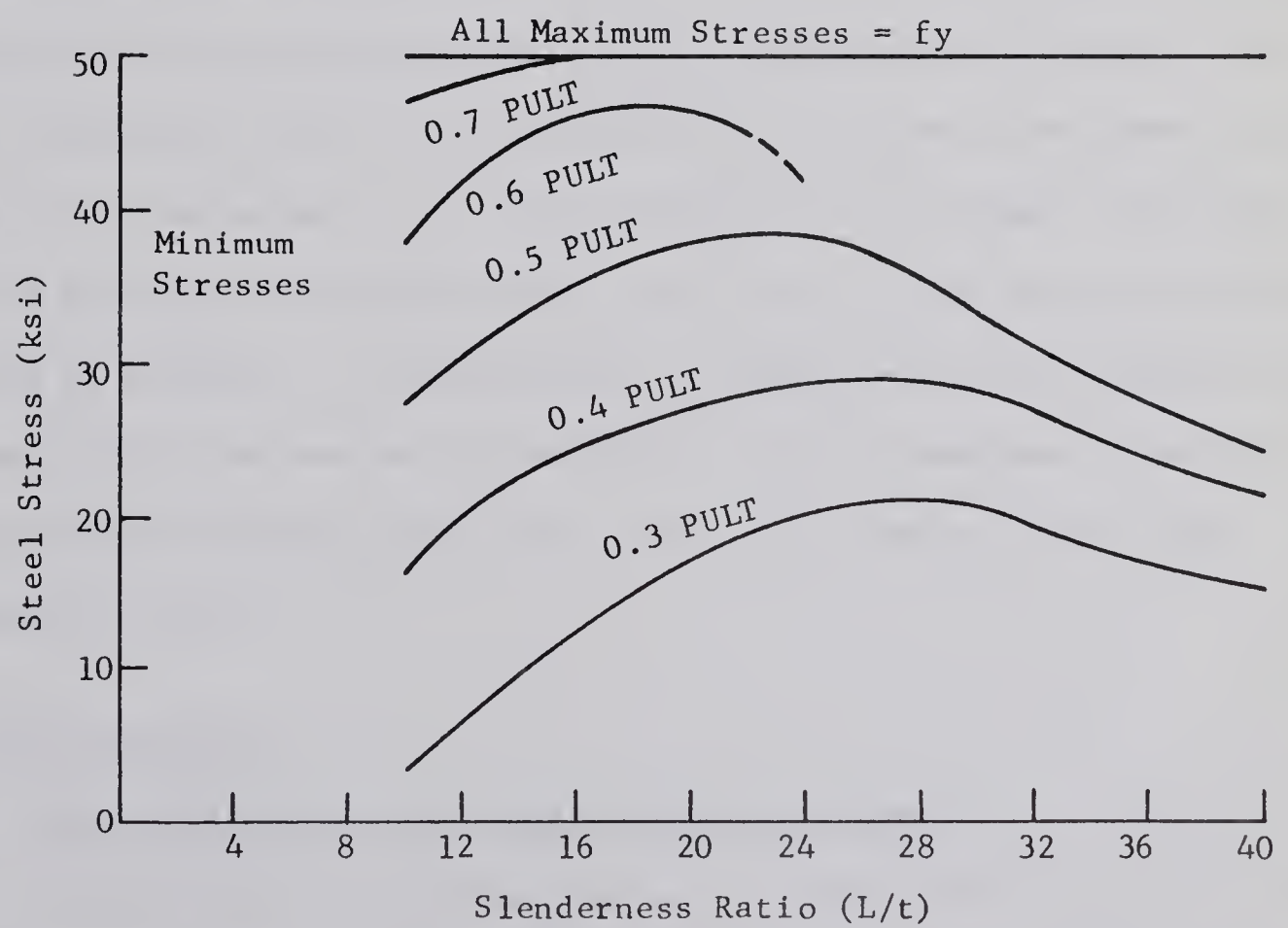
(b) Sustained Load for 7 Days

FIGURE 8.24

EFFECT OF SUSTAINED LOAD ON THE MAXIMUM AND MINIMUM STEEL STRESSES IN THE COLUMNS BENT IN DOUBLE CURVATURE



(c) Sustained Load for 9 Months



(d) Sustained Load for 25 Years

magnitude of the load at each level remained almost constant while the moment decreased; both with increasing slenderness ratio. As a result, the maximum steel stresses decreased and the minimum steel stresses increased. At higher slenderness ratios, the reverse was true; as the slenderness ratio was increased the magnitude of load at each level decreased and the maximum moment remained almost constant. As a result, for slender columns both the maximum and minimum steel stresses decreased with an increase in slenderness ratio.

Under sustained load, the behavior was also similar to that exhibited by the single curvature columns. The redistribution of stress from concrete to steel was the dominant factor which led to increasing steel stresses with duration of loading. The increases with time for the minimum stresses were greater for lower slenderness ratios than for higher slenderness ratios because maximum moments decreased with time for the lower slenderness ratios. This behavior was not true at the lower levels of load where increases in relative stiffness of the columns with time produced increases in maximum moment with time at least up to nine months duration of loading. At higher values of slenderness ratio, maximum moments increased with time because of instability. This prevented the minimum stresses from increasing at as fast a rate with time as at the lower slenderness ratios.

8.7 Joint Rotations

8.7.1 Joint Rotations in the Single Curvature Columns

The effect of sustained load on the joint rotations of the columns bent in single curvature is shown in FIGURE 8.25. The variables considered

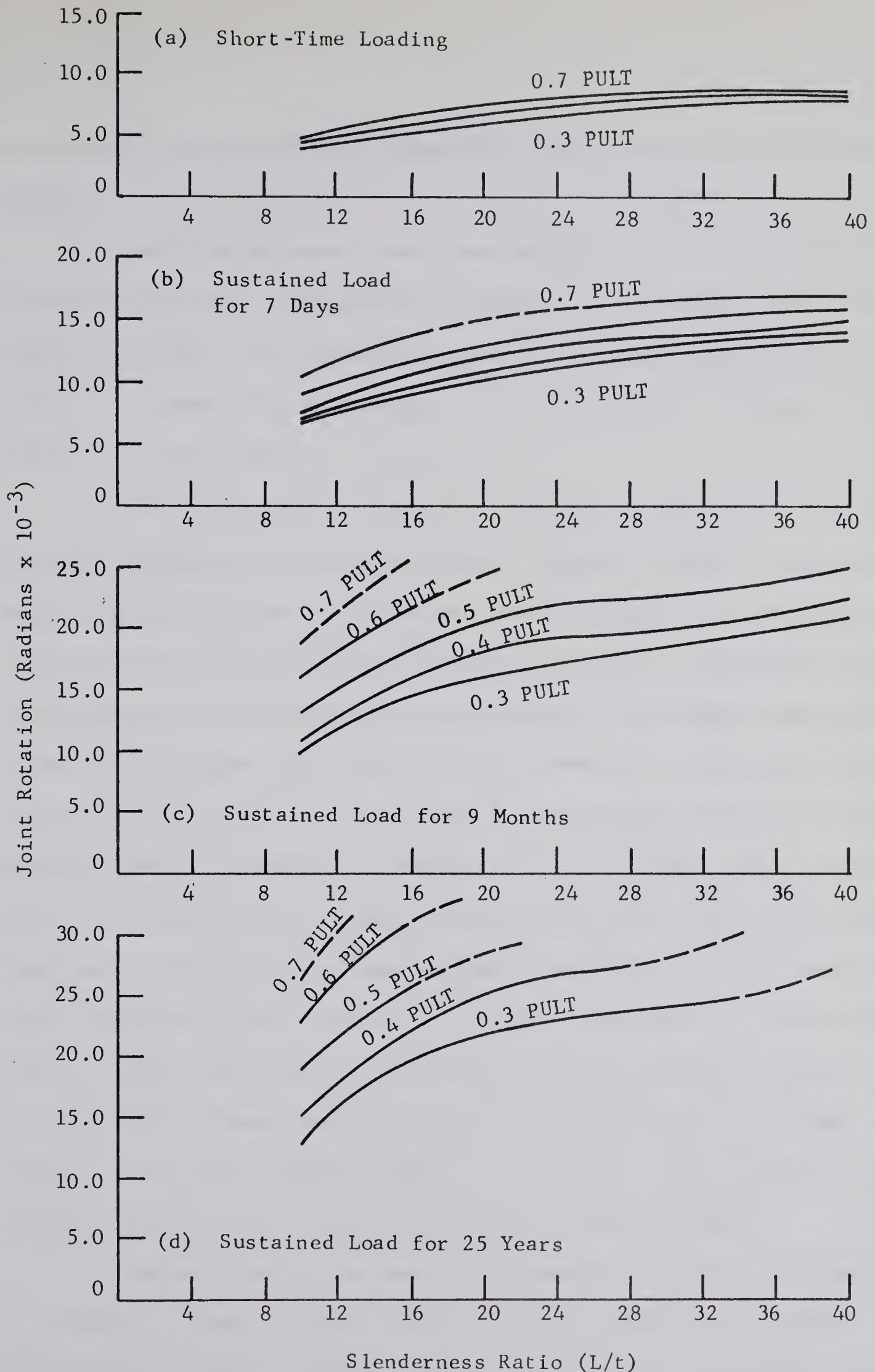


FIGURE 8.25

EFFECT OF SUSTAINED LOAD ON THE JOINT ROTATION
OF THE COLUMNS BENT IN SINGLE CURVATURE

are level of sustained load, slenderness ratio, and duration of sustained loading.

The behavior under short-time loading is shown in FIGURE 8.25(a). The curves show that end rotation increases at a decreasing rate with slenderness ratio. This behavior was due to the decreasing magnitude of load at each level with slenderness ratio and also to the absence of instability at the load levels considered.

After seven days of sustained loading, the joint rotations plotted in FIGURE 8.25(b) show the same trends as computed for short-time loading. Again this behavior can be attributed to the decrease in magnitude of sustained load at each load level with an increase in slenderness ratio. The increase in rotations with time were greater for higher slenderness ratios and for higher load levels. At low levels of load and low slenderness ratios, the compression steel had a significant influence on column stiffness and as a result, the increases in end rotation with time were small. At higher levels of load and low slenderness ratios, the compression steel had yielded and the column stiffness was reduced. This resulted in larger increases in end rotation with time. The stiffness of the very slender columns was reduced at a greater rate with time than was the case for the shorter columns even though the compression steel was slower in yielding in the more slender columns. As a result, the increases in end rotation with time were greater than for the shorter columns.

The behavior of the restraining beam had a greater influence on the increase in end rotations with time for the more slender columns than it did for the shorter columns. The stiffness of the restraining beam decreased at a faster rate with time for large slenderness ratios because

of the larger percentage of the total moment carried by the beam in this case and the non-linear response of the beam to this moment.

FIGURES 8.25(c) and (d) illustrate the behavior after longer loading periods. At lower values of slenderness ratio, the shape of the curves was still influenced by the decrease in the magnitude of sustained load at each level of load with an increase in slenderness ratio. For the higher values of slenderness ratio, the rate of increase in end rotation with time was still greater than at low slenderness ratios for low levels of load; again reflecting the more rapid decrease in column stiffness with time at the higher slenderness ratios. At the higher load levels, the effect of the reduction in column stiffness due to yielding of the compression steel became very noticeable and the end rotations increased rapidly with time.

8.7.2 Joint Rotations in the Double Curvature Columns

The effect of sustained load on the end rotations of the columns bent in double curvature is shown in FIGURE 8.26. The variables considered are level of sustained load, slenderness ratio, and duration of sustained load.

The factors which influenced the behavior of the double curvature columns were similar to those which influenced the behavior of the single curvature columns. The end rotations of the double curvature columns were generally smaller than those of the single curvature columns because of the difference in the deflected shapes produced by the change in the mode of column restraint.

For the levels of load considered, the end rotations were higher

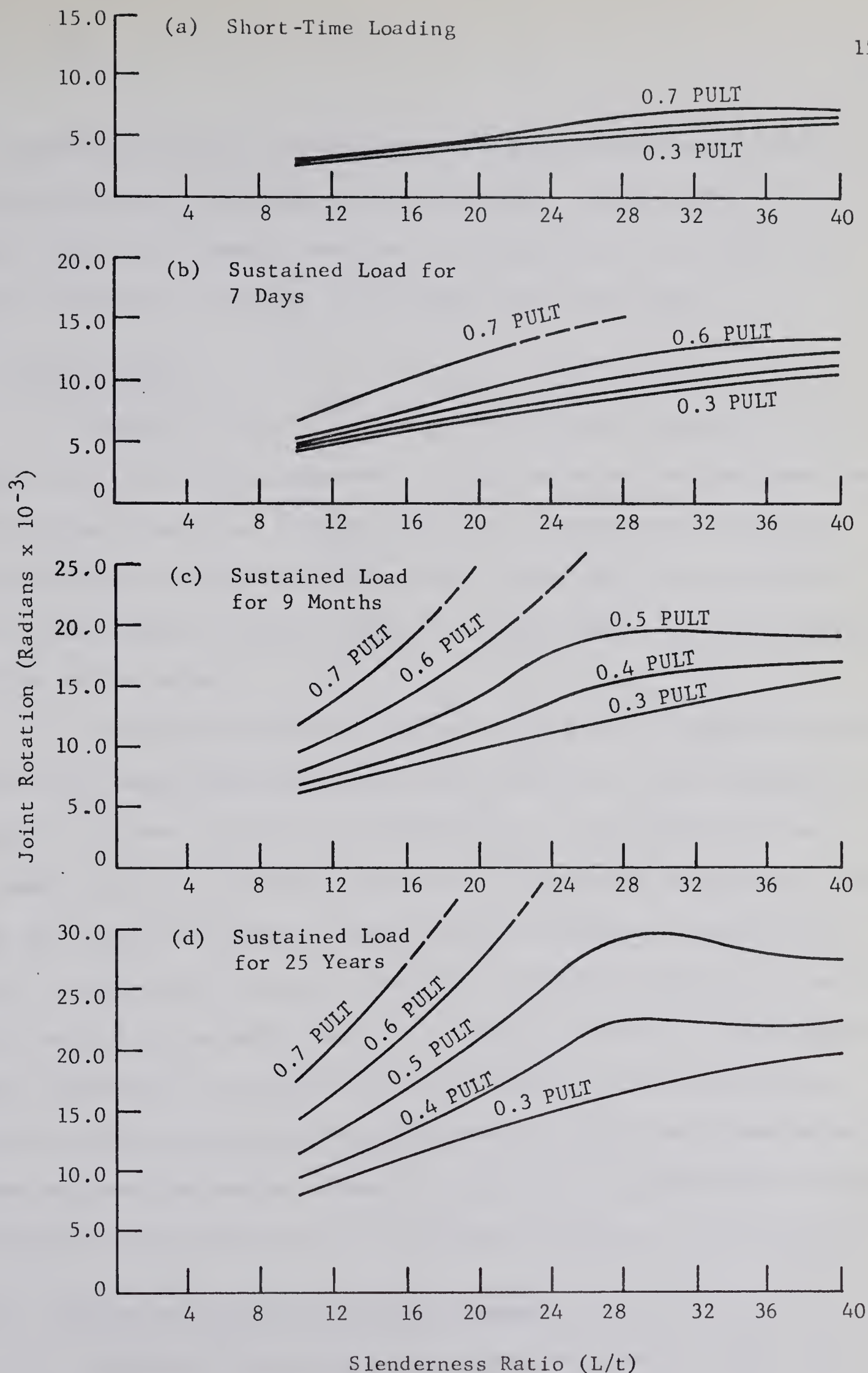


FIGURE 8.26

EFFECT OF SUSTAINED LOAD ON THE JOINT ROTATION
OF THE COLUMNS BENT IN DOUBLE CURVATURE

at intermediate values of slenderness ratio than at the larger values of slenderness ratio, particularly after the longer periods under sustained load. Again, this behavior was due to the magnitude of sustained load being assessed as a fraction of the short-time failure load.

8.8 Failure Loads

FIGURES 8.27 and 8.28 show the failure loads obtained for the frames containing the columns bent in single curvature and the frames containing the columns bent in double curvature. The failure loads have been reported as failure loads for frames rather than as failure loads for columns because in actual fact, it was the frame that failed through failure in the column.

The figures are bounded on the top by a curve showing the failure loads under short-time loading and on the bottom by a curve showing the loads, which when sustained, produced failure at a hypothetical time of 25 years. The set of solid failure curves which cross the enclosed region were obtained by analytically subjecting the columns to sustained loads equal to various percentages of the short-time failure loads for a period of 25 years and then quick loading the columns to failure. Also shown in these figures are two dashed curves which represent the loads causing failure under sustained load after hypothetical durations of loading of seven days and nine months. These two curves are only approximations because the duration of loading was not a continuous variable in the analysis.

8.8.1 Failure of the Single Curvature Columns

FIGURE 8.27 shows the failure loads obtained by analysis for the frames containing columns bent in single curvature. The significant

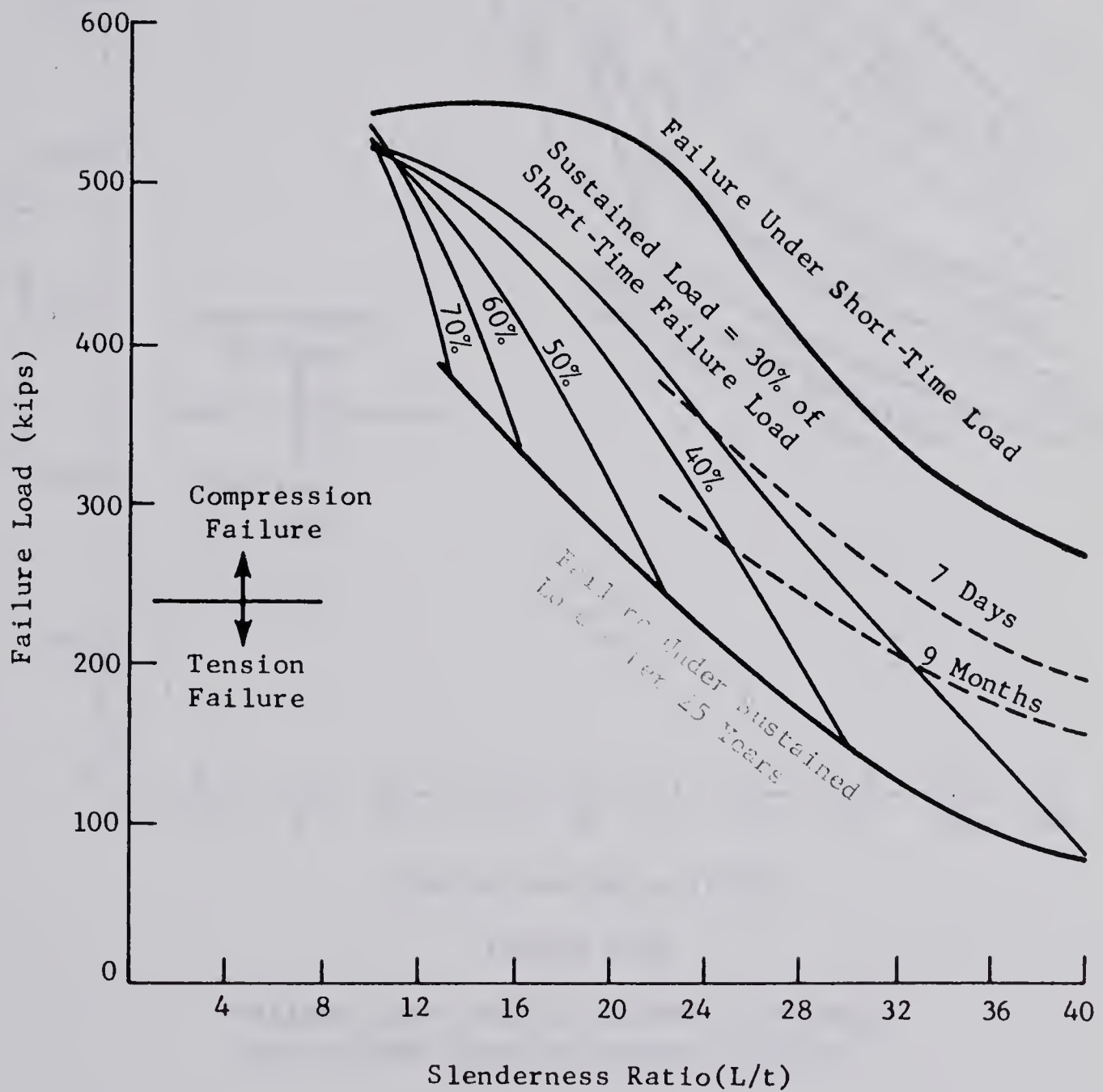


FIGURE 8.27

FAILURE LOADS FOR THE FRAMES CONTAINING
THE COLUMNS BENT IN SINGLE CURVATURE

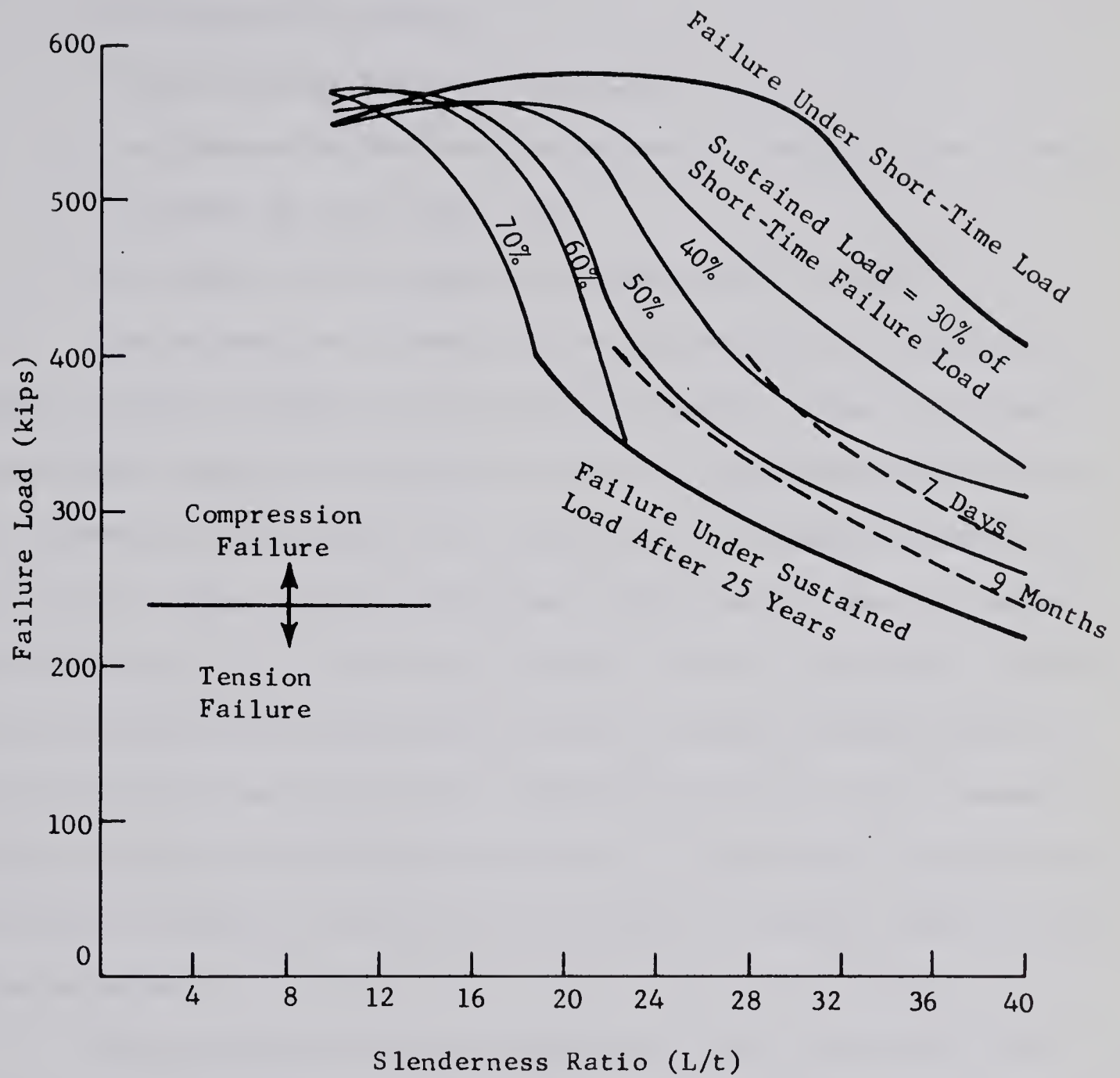


FIGURE 8.28

FAILURE LOADS FOR THE FRAMES CONTAINING
THE COLUMNS BENT IN DOUBLE CURVATURE

factors affecting the failure loads were:

1. the level of sustained load
2. the duration of loading
3. the slenderness ratio of the columns
4. the response of the restraining beam to changes in the relative stiffness of the columns, and
5. the effect of the compression steel in the column .

The failure loads under short-time loading were influenced by changes in the stiffnesses of both the beam and the column. The shorter columns were stable up to the time of failure. The variation in strength with increasing slenderness ratio in this range was small because of the reduction in column stiffness and moment which resulted from an increase in slenderness ratio. For the more slender columns, instability occurred, and the failure load-slenderness ratio curve assumes a shape similar to that of the Euler buckling curve. The position of the curve, however, differs from that of the Euler curve because of the action of the restraining beams and because concrete does not exhibit a linearly elastic stress-strain behavior.

The presence of a restraining beam causes a reduction in the effective length of a column and thus increases the column failure load. For a constant restraint, as considered in this thesis, the percentage increase in failure load above that of an unrestrained column, should increase with slenderness ratio because the effective length factor for the restrained column decreases with an increase in slenderness ratio.

The effect of the non-linear stress-strain behavior of concrete is to reduce both the column and the beam stiffnesses from the values pre-

dicted from linearly elastic theory. The decrease in the column stiffness will affect the failure loads in two ways. First of all, a decrease in the stiffness of an isolated column causes a direct decrease in the failure load according to stability theory. However, when the column is restrained, a reduction in the stiffness of the column relative to the beam causes a decrease in the effective length of the column and thus an increase in the failure load. Neither of these effects were significant for the columns which exhibited an unstable behavior under short-time loading because the concrete response was almost linear when the columns became unstable. The decrease in the beam stiffness with increasing slenderness ratio had a significant effect on the failure load in that it caused a reduction in the failure loads through an increase in the effective length of the columns.

The effect of the sustained load was to reduce the stiffnesses of both the beams and the columns. Subsequent applications of quick load to the columns resulted in rapidly decreasing column stiffnesses because of the larger deflections produced by sustained load and because the compression steel was generally no longer effective in resisting the increasing load. For any value of slenderness ratio, the decrease in beam stiffness with increasing load was also greater than under short-time loading because the rate of transfer of the undistributed moment to the beam had increased. As a result of this combination of factors, the failure loads under quick loading after a period of sustained loading were lower than the values under short-time loading only. The reduction in the failure loads increased as the level of sustained load was increased. The effect of the compression steel was to retard the loss in column stiff-

ness with time and thus increase the failure load for any particular column. The failures which occurred during the sustained load period were instability failures. This is evidenced by the similarity in shape between the failure curves and an Euler curve and by the computed deformations.

8.8.2 Failure of the Double Curvature Columns

FIGURE 8.28 shows the failure loads obtained by analysis for the frames containing the columns bent in double curvature. The factors which affected these failure loads were similar to the factors which affected the failure loads of the frames containing the columns bent in single curvature.

The failure loads under short-time loading show that the frames remained relatively stable up to high values of slenderness ratio. Very little long column action was exhibited up to a slenderness ratio of approximately 22, and as a result, the failure loads were increased with an increase in slenderness ratio in this region through decreases in the relative stiffnesses of the columns. At intermediate values of slenderness ratio, the long column effect became more apparent and the relative stiffness of the column decreased at a greater rate with increasing slenderness ratio. The increase in the amount of redistribution of moment with an increase in slenderness ratio also caused the beam stiffness to decrease with slenderness ratio. The combined effect of column instability and decreasing beam stiffness produced a rapid decrease in the failure load with increasing slenderness ratio at the high values of slenderness ratio.

The effect of sustained load on failure was less pronounced for the columns bent in double curvature than for the columns bent in single curvature. Under the quick loading which followed the sustained load, the

columns showed a stable failure up to intermediate values of slenderness ratio. As the level of sustained load increased, the value of slenderness ratio beyond which instability failures occurred, decreased.

The curves which show the failures under sustained loading indicate through their shape that these failures were of an unstable nature. This was also borne out by the computed deformations. The effect of increasing length on failure load, for sustained loads, was not as pronounced as with the single curvature columns nor was it as pronounced as for short-time loading. The reason for this behavior was that the stiffness of the fixed end restraint did not decrease under sustained load or with the amount of moment which it had to carry. Therefore, any factor which tended to decrease the stiffness of the column or of the restraining beam was not as efficient in reducing the strength of the frame because of the redistribution of moment to the fixed end restraint. In other words, the potential decrease in strength with an increase in slenderness ratio or with the sustaining of load was reduced by the action of the fixed end restraint. Because of this effect, the ratio of the failure load after 25 years of sustained loading to the short-time failure load reached a minimum value at an intermediate value of slenderness ratio. As this ratio was the basis of choosing the sustained load at each load level, the frames with an intermediate value of slenderness ratio exhibited the most critical behavior.

CHAPTER IX

DISCUSSION OF THE ANALYSIS AND ITS APPLICATION TO LONG COLUMNS IN FRAMEWORKS

9.1 Introduction

A resume of the effects of the variables considered in the investigation of restrained reinforced concrete long columns is given in this chapter. This discussion is limited to the range of behavior investigated in this thesis. In other words, it is limited to tied columns with small but practical eccentricity ratios, e/t .

The failure loads obtained by analysis are compared to the failure loads predicted by various methods of design. A discussion is included of the applicability of the design methods to columns under sustained load.

The limitations of the method of analysis are also discussed, and the final section gives a discussion of other methods of analysis presently in use.

9.2 Resume of the Present Investigations

The range of this investigation was limited to only a small number of practical cases. The columns were laterally restrained in all cases with the modes of column restraint considered being:

1. symmetrical single curvature bending, and;
2. double curvature bending with one end of the column fixed.

Other constants of the investigation included the properties of the restraining beam, the cross-section properties of the column, and the undistributed moment at the joint. The nominal e/t values considered were small and decreased with length from 0.0749 ($L/t = 10$) in the single curvature columns and from $e/t = 0.103$ ($L/t = 10$) in the double curvature columns.

A general discussion of the results pertaining to the variables considered is included in the following sections.

9.2.1 Effect of Sustained Load

Sustained load produced significant decreases in both column stiffness and beam stiffness. The net result was usually a decrease in the relative stiffness of the column except at low levels of sustained load where the compression steel retarded the decrease in column stiffness with time to the extent that the relative stiffness of the column was increased.

The column stiffness decreased at a faster rate with increasing axial load in the subsequent loading to failure of a column subjected to sustained load than it did under short-time loading only. This behavior occurred because the sustained load increased the column deflections and because the compression steel yielded under sustained load through redistribution of stress.

Sustained load caused a marked increase in the tendency of the columns to become unstable. This behavior resulted in substantial decreases in the failure loads of the more slender columns from the corresponding values under short-time loading. For shorter columns, where instability is not a problem, the failure loads under sustained loading may actually be increased from the corresponding values under short-time loading because

of reductions in relative column stiffness due to sustained loads.

Changes in the level of sustained load were also influential in producing changes in both deformations and failure loads either during or after the period of sustained load. In general, as the level of sustained load was increased, the deflections increased and the failure loads decreased.

9.2.2 Effect of the Restraints

The action of the restraints in all cases was to increase the failure loads over those which would be obtained by removing the column from the structure. In the region near failure, whether under sustained load or under increasing axial load, the net redistribution of moment was from the column to the beam because of the decreasing relative stiffness of the column at high loads. This redistribution of moment, which increases the column safety, cannot be considered if restraints are not considered.

The behavior of the restraining beam under the changes in moment resulting from redistribution was also a factor in determining the behavior of the columns. If the columns were relatively stiff, the amount of the redistribution was small and the response of the restraining beam was approximately linearly elastic. If the amount of redistribution required was large, the response of the beam was no longer linear. The stiffness of the beam decreased and as a result, moment was redistributed back to the column with a resultant reduction in the column failure load. This form of behavior in the restraining beam became more important as the slenderness ratio of the column was increased, because of the increased sensitivity of the column.

The fixed end restraint had a considerable effect on the behavior of the columns. The major contribution was a decrease in the sensitivity of the column to load through the introduction of a point of inflection into the deflected shape. The increased column stiffness resulted in decreased deformations and increased failure loads compared to the corresponding single curvature columns. For the shorter columns, the increase in strength was due to the fact that increases in deflection caused decreases in column stiffness without significantly contributing to an increase in maximum moment. For the longer columns, the increase in strength was due to a decrease in the unstable behavior through a decrease in the effective length of the column.

A minor contribution of the fixed end restraint to the behavior of the columns resulted from the fact that the stiffness of this restraint did not change with an increase in the amount of moment redistributed to it. As a result, the fixed end was more important in reducing column failure as the stiffness of the restraining beam decreased.

9.2.3 Effect of Slenderness Ratio

The major contribution of the increase in the slenderness ratio of the column to the column behavior resulted from the decrease in column stiffness and the increase in long column action which accompanied the increase in slenderness ratio. The presence of a sustained load amplified the behavior from that produced under short-time loading.

The increase in the amount of unbalanced moment carried by the beam also increased as the slenderness ratio of the columns was increased. As a result, the stiffness of the beam also decreased as the slenderness

ratio of the column increased. This behavior added to the increase in the sensitivity of the columns which resulted from an increase in the slenderness ratio.

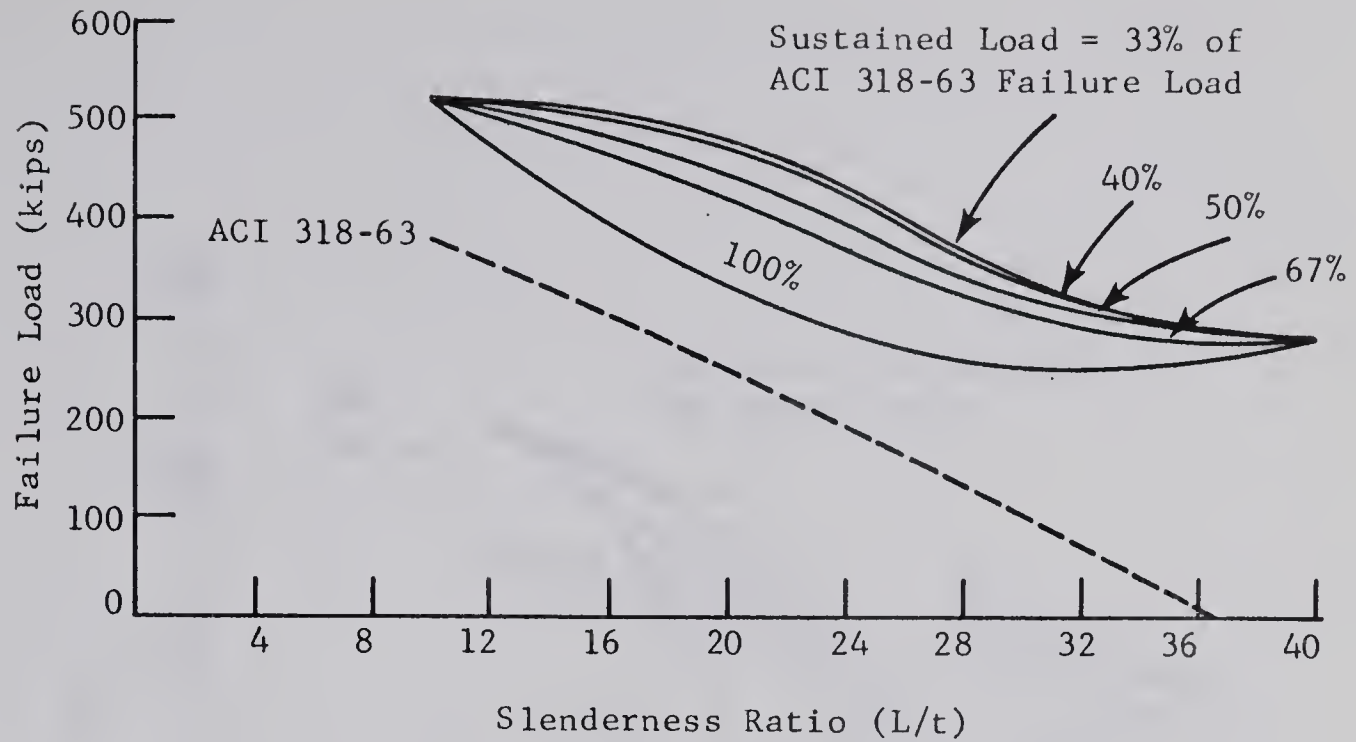
9.3 Applicability of Long Column Design Formulae to Columns Subjected to Sustained Load

FIGURES 9.1 and 9.2 compare the column strengths obtained by analysis with the strengths predicted by the ACI Building Code ⁽¹⁾, the 1965 National Building Code of Canada ⁽²⁶⁾, and the Recommendations of the CEB ⁽¹¹⁾. The basis of comparison for the curves has been taken as the condition which would exist if the columns were subjected to sustained loads for a period of 25 years and then quick loaded to failure. The sustained loads were taken as various percentages of the failure strengths recommended by the codes. The percentages used were chosen to simulate the nominal column load factors 3.0, 2.5, 2.0, 1.5, and 1.0. The analysis strengths under these assumed loading conditions were obtained by linear interpolation of the curves of FIGURE 8.27 and 8.28.

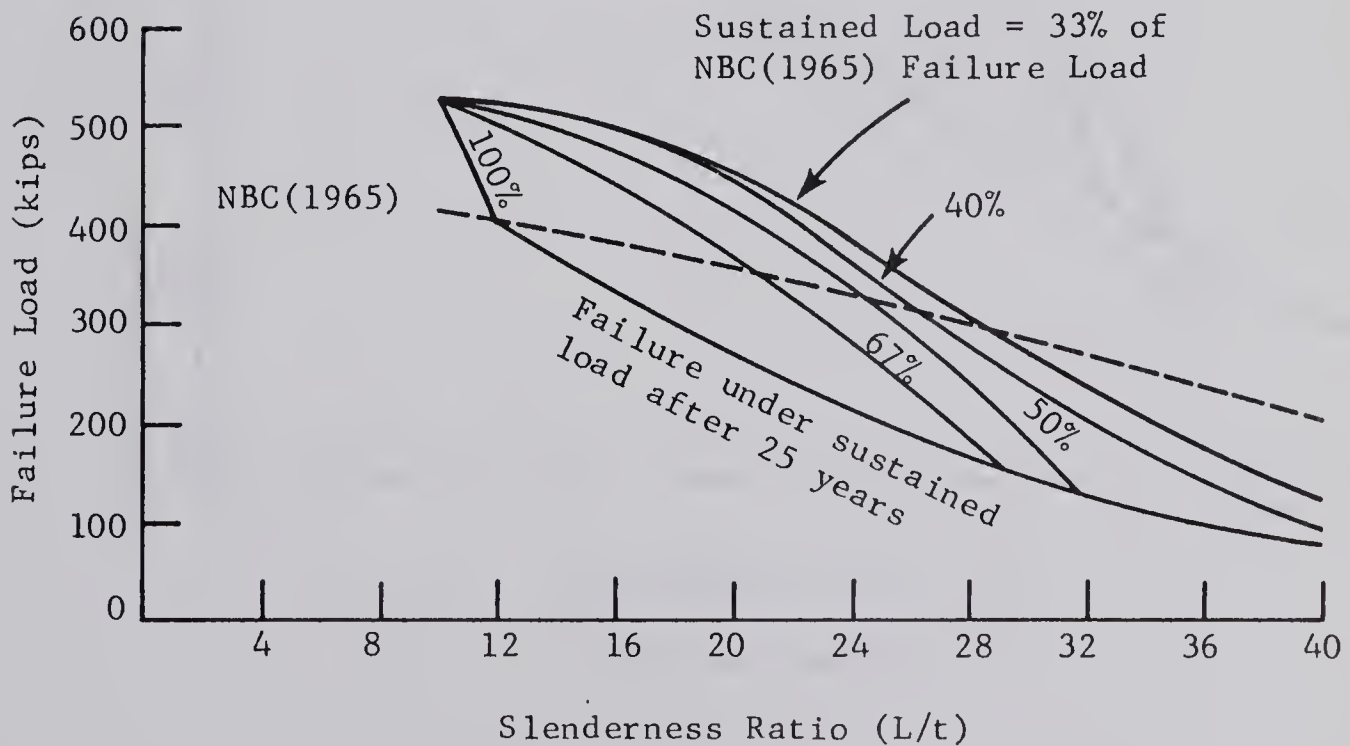
9.3.1 Comparison for the Single Curvature Columns

1. ACI Building Code

FIGURE 9.1(a) shows the comparison between the analysis strengths and the strengths predicted by the ACI Building Code, ACI 318-63 ⁽¹⁾, for the columns bent in single curvature. The curves show that the factor of safety predicted by the analysis is much higher than the nominal factor of safety in all cases, particularly for very slender columns. In this particular comparison much of the extra margin of safety resulted from the fact that the ACI 318-63 long column reduction formula does not take



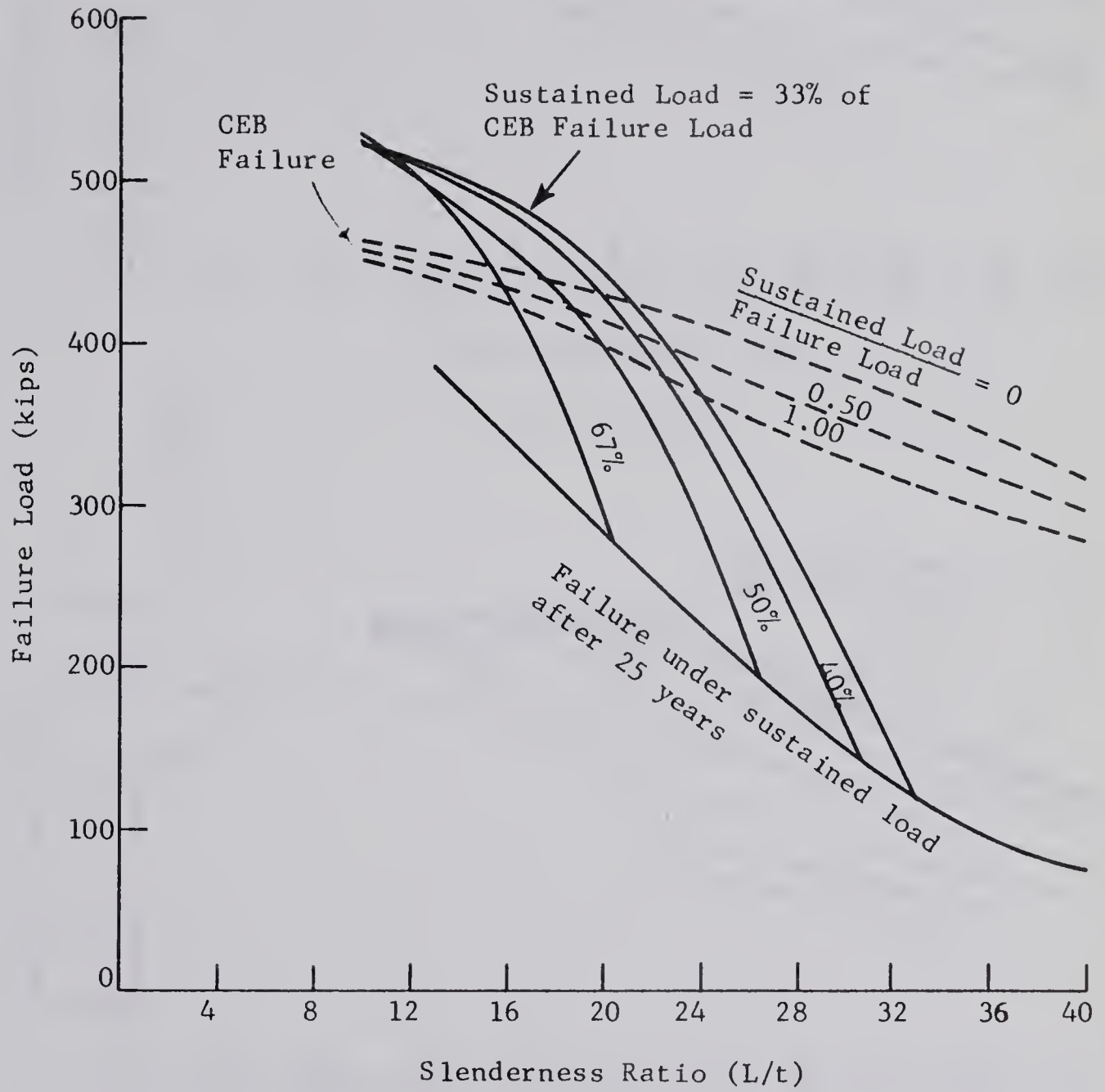
(a) ACI 318-63



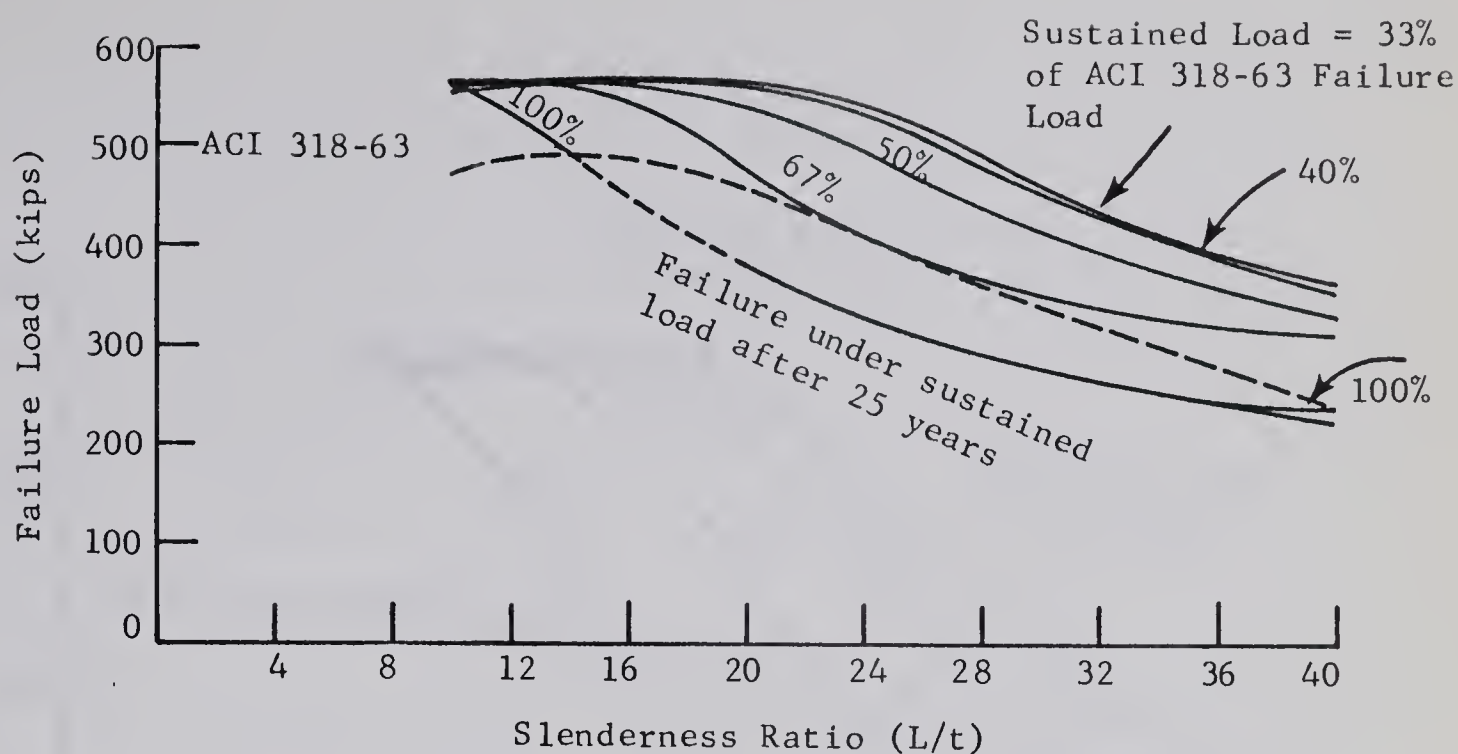
(b) National Building Code (1965)

FIGURE 9.1

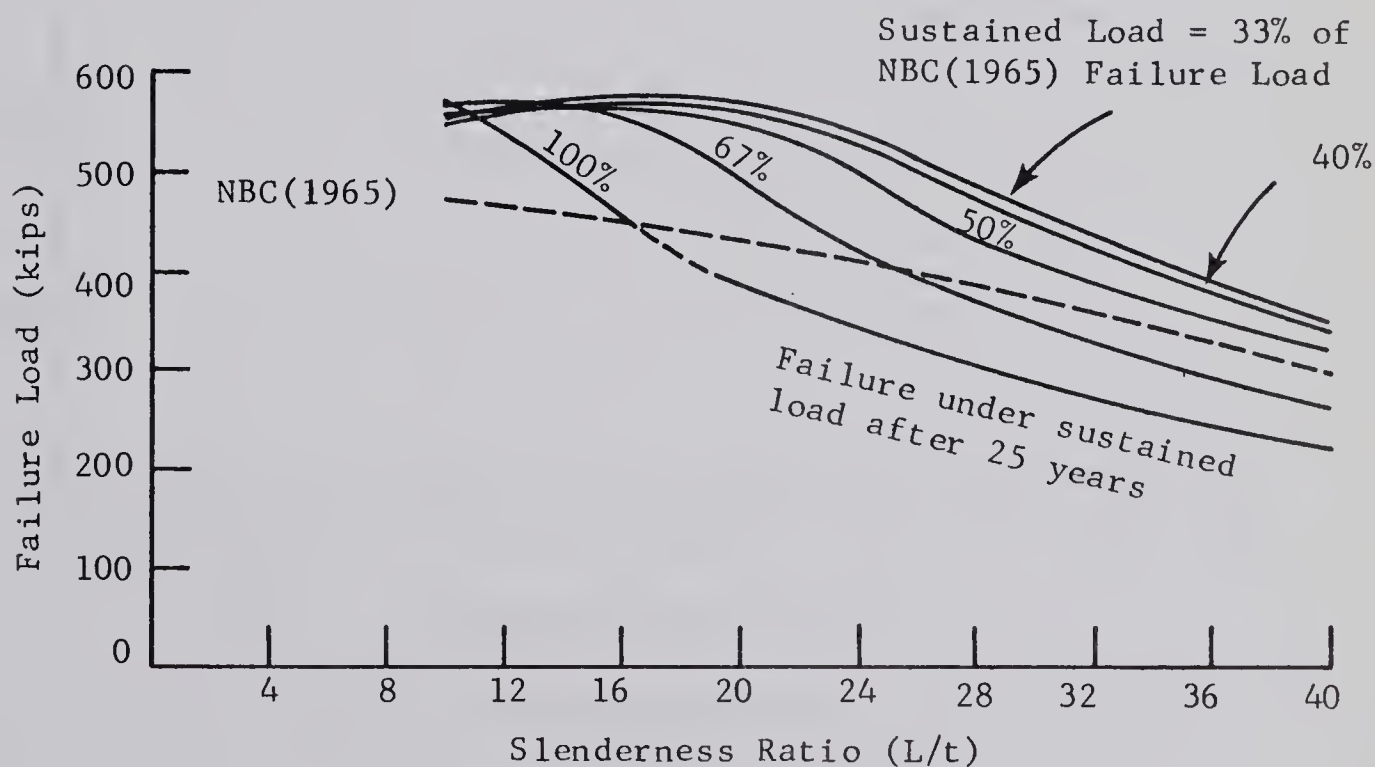
COMPARISON OF ACTUAL FAILURE LOADS WITH PREDICTED
FAILURE LOADS AFTER 25 YEARS UNDER SUSTAINED LOAD
FOR THE SINGLE CURVATURE COLUMNS



(c) CEB Recommendations



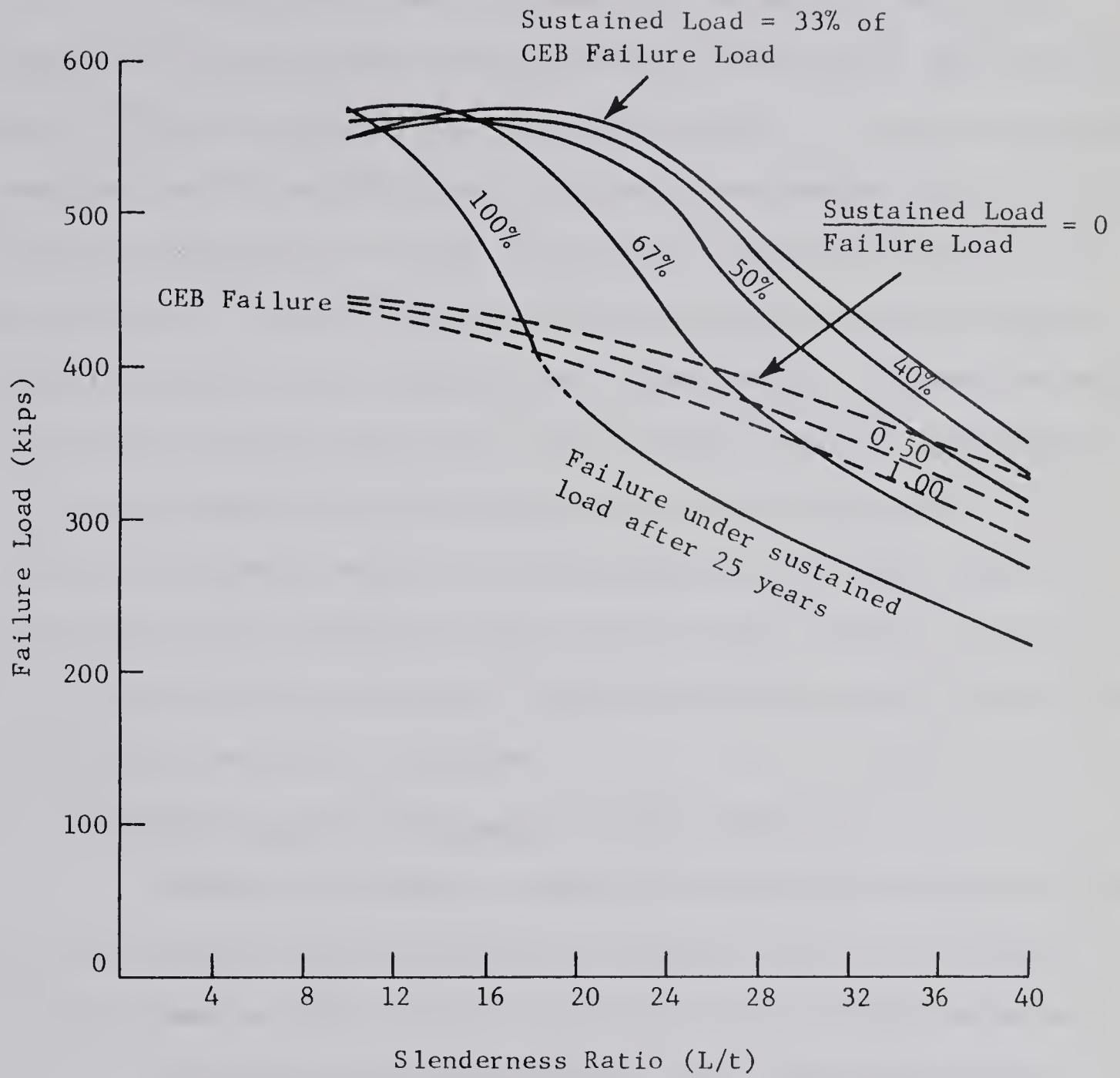
(a) ACI 318-63



(b) National Building Code (1965)

FIGURE 9.2

COMPARISON OF ACTUAL FAILURE LOADS WITH PREDICTED
FAILURE LOADS AFTER 25 YEARS UNDER SUSTAINED LOAD
FOR THE DOUBLE CURVATURE COLUMNS



(c) CEB Recommendations

into account the influence of the restraining beams.

2. National Building Code of Canada (1965)

FIGURE 9.1(b) shows the comparison between the analytical strengths and the strengths predicted by the 1965 National Building Code of Canada (26) for the columns bent in single curvature. For these particular examples, the National Building Code gives a more realistic prediction of failure strength after a period of sustained load of 25 years than does the ACI Code. The more realistic prediction is due to the inclusion of effective length factors into the long column formula. However, by basing the effective length factors on a linear elastic analysis, the changes in failure loads due to non-linear behavior are not accounted for. This resulted in an underestimation of failure loads for the lower values of slenderness ratio considered because of non-linear behavior in the column, and an overestimation of failure loads for the more slender columns because of non-linear behavior in the beam.

3. Recommendations of the European Concrete Committee

FIGURE 9.1(c) shows the comparison between the analytical strengths and the strengths predicted using the recommendations of the European Concrete Committee (CEB) (11) for the columns bent in single curvature.

Because the CEB Recommendations do not specifically outline design procedures, the manner of interpretation of the procedures is outlined below.

- (a) The complementary moment to be added to the first order moment was computed from the formula.

$$M_c = \frac{PULT (t_c + e_o) \left(\frac{kL_c}{r}\right)^2}{3300 \pi^2} (1 + \psi_c)$$

where M_c = complementary moment

P_{ULT} = ultimate failure load

t_c = depth of column

e_o = column end eccentricity at failure

kL_c = effective length of column

r = radius of gyration of the column cross-section

ψ = creep coefficient

ϵ = ratio of sustained load to ultimate load

- (b) The recommended value of $\psi = 1/3$ was used.
- (c) The cross-section interaction diagram formulae used were from ACI-318-63 (1).
- (d) The column effective length factors, k , were taken from the nomographs based on linear elastic theory included in the National Building Code (1965) (26). The comments in the CEB Recommendations include the column effective length factors in the parameter ρ . The ρ values recommended by the CEB correspond to $k = 0.87$ for symmetrical single curvature columns and $k = 0.69$ for double curvature columns fixed at the far end (for columns in multistory frames). By using the NBC nomographs, k varied from 0.80 to 0.63 for the single curvature columns and from 0.63 to 0.56 for the double curvature columns.
- (e) No maximum or minimum limits of kL_c/r were used.

The addition of a complementary moment to the moment of the first order analysis, as recommended by the CEB, is a more realistic approach to the failure of a long column than that afforded by the ACI Code or the

National Building Code. However, the comparison does not appear to be much better for the columns of the investigation than that given by the National Building Code.

The use of elastically derived effective lengths in assessing the effect of the restraints has had the same effect on this comparison as it had on the comparison with the National Building Code requirements. The recommended value of the creep factor, ψ , of $1/3$ does not give an adequate account of the effect of sustained loading on the columns of the investigation. A larger value of ψ and a consideration of non-linear concrete behavior would probably give a more realistic comparison.

9.3.2 Comparison for the Double Curvature Columns

1. ACI Building Code

FIGURE 9.2(a) shows the comparison between the analysis strengths and the strengths predicted by ACI Building Code, ACI 318-63 ⁽¹⁾ for the columns bent in double curvature. For a nominal factor of safety of greater than 1.5, the use of the long column formula of ACI 318-63 leads to predicted strengths which are on the safe side. For a nominal factor of safety of less than 1.5, the ACI reduction formula overestimates the failure strengths for the intermediate values of slenderness ratio considered.

2. National Building Code of Canada (1965)

FIGURE 9.2(b) shows the comparison between the analysis strengths and the strengths predicted by the National Building Code for the columns bent in double curvature. As was the case with the single curvature columns, the use of a linear elastic theory in predicting the column effective length factors leads to an underestimation of the strengths for

the shorter columns where non-linear behavior occurred in the columns, and an overestimation of the strengths for the more slender columns where non-linear behavior occurred in the beam. However, the effect of using the linear elastic effective length factors is not as pronounced with the double curvature columns because the fixed end restraint reduced the amount of non-linear behavior in both the beam and the column.

3. Recommendations of the European Concrete Committee

FIGURE 9.2(c) shows the comparison between the analysis strengths and the strengths predicted using the CEB Recommendations for the double curvature columns. The interpretation of the recommendations has been described in SECTION 9.3.1.

The use of linear elastic theory in predicting the effective lengths had the same effect on the double curvature column failure loads as it had in the comparison of single curvature column failure loads. The recommended value of $\psi = 1/3$ to account for creep was again insufficient in assessing the effect of sustained load.

9.3.3 Moment Magnification Design Procedure

Another method of design has been proposed by Spang ⁽⁴¹⁾. It is based on an evaluation of the magnified moment in a long column using linear elastic theory. Spang's investigation shows a good correlation between the results using this method and the strength predictions obtained using Pfrang's ⁽³⁴⁾ method of analysis. Pfrang's analysis in this case considers a non-linearly elastic concrete column with linearly elastic end restraints and short-time loading only.

Comparison curves have not been drawn using this proposed method

of design because the predicted design strengths were unconservative for the columns in this investigation, even for low levels of sustained load. In addition, the predicted column strengths were unconservative for the more slender columns under short-time loading because of the departure of the restraining beam from a linear behavior.

9.3.4 Discussion of the Design Procedures

The results of the comparisons indicate that none of the design methods give adequate results for the columns investigated. The magnified moment method has perhaps the best basis of derivation because of its simulation of actual behavior, and it may be useful in predicting the effect of sustained loading on column capacity. However, the value of the magnified moment would have to be assessed considering the level of sustained load and perhaps non-linear behavior in both the beam and the column.

9.4 Limitations of the Method of Analysis

The application of the method of analysis proposed in this thesis may be limited or affected by the following factors:

1. insufficient verification because of a lack of experimental evidence,
2. evaluation of concrete properties,
3. insufficient number of boundary conditions relating the deformations to the applied loads,
4. limitations of the computer
5. calculation of creep under variable stress,
6. errors induced in the closure of the trial and error procedures.

Each factor is discussed separately in the following sections.

9.4.1 Verification of the Method of Analysis

The results of this analysis were compared to the experimental results of other investigators in CHAPTER VI. Although the comparisons were favorable and supported the applicability of the method of analysis, the amount of experimental evidence available was limited, particularly with regard to slender columns in frames subjected to sustained load. Thus further experimental data is desirable to check the analysis over a broad range of variables. While the absence of test data should not seriously affect a qualitative study of behavior, it may affect a quantitative application of the results to design procedures.

9.4.2 Evaluation of Concrete Properties

An attempt has been made in this thesis to define the concrete properties for any set of conditions using as a basis the properties exhibited under a known set of conditions. This form of property evaluation is limited by a lack of information in the following major areas.

1. The effect of varying atmospheric conditions on creep-stress-time behavior.
2. The effect of the level of sustained load on the concrete strength at any time.
3. The correlation between the cylinder strength and the structural concrete strength (k_3 factor).

It should be noted that the method of analysis developed in this thesis can be applied using other concrete properties.

9.4.3 Relationship Between Deformations and Applied Loads

The method of analysis is limited to the cases where a sufficient number of boundary conditions and equations of statics are available for each member to allow a solution to be obtained. In other words, it must be possible to derive a conjugate beam for each member.

9.4.4 Computer Limitations

The major limitation in the computer application of the analysis was the time required by the computer for the solution of each framework. This prevented the obtaining of a large number of solutions in a short period of time and also would prevent the use of a commercial computer installation because of economic reasons.

The computer programs in their present form (APPENDIX A) were limited by available computer capacity to a consideration of only a few members and a small number of loading stages. However, the available capacity could be extended and more efficiently used through the use of such features as subroutines and tape storage.

9.4.5 Calculation of Creep Strains Under Variable Stress

The rate of creep method was used in this thesis to calculate creep strains under variable stress. One of the major assumptions of this method of calculation is that creep is a permanent inelastic effect which is not removed upon the removal of the load. An alternative method of calculation known as the superposition method is also discussed by Ross (39). According to this method, creep is completely removed upon removal of the load. Ross has shown that the errors from using either method are similar in magnitude. In a comparison with actual creep data under increasing load,

the superposition method overestimates the creep and the rate of creep method underestimates the creep. The reverse situation is true under decreasing load. In the column investigation of Holley and Mauch (18), the superposition method gave slightly lower failure loads than did the rate of creep method.

9.4.6 Errors of the Trial and Error Procedures

The allowable errors of closure for the trial and error procedures of the analysis will have a negligible effect on the predicted behavior as long as their magnitude is controlled. This was done quite efficiently in the investigation by allowing the computer to set the magnitudes at values just large enough to prevent continuous calculation loops from forming. However, in a few cases the unstable behavior of the column would result in the computer establishing the limits of convergence at magnitudes which may have affected the results. These particular cases had to be re-computed until favorable results were obtained.

9.5 Discussion of Other Methods of Analysis

Other methods of analysis which have been used for the investigation of long columns in frameworks include the following:

1. analysis based on first order theory
2. analysis of isolated columns
3. analysis of isolated columns having linearly elastic end restraints
4. analysis using non-linear elastic moment-curvature relationships for both the columns and the restraining members
5. analysis using an effective or reduced modulus for concrete.

9.5.1 Analysis Based on First Order Theory

The limitations of an analysis which does not consider secondary moments are well known. However, where secondary moments are small, this type of analysis provides reasonably good results. Where secondary moments are not small, first order results can be used as a reference point for the consideration of second order effects.

9.5.2 Analysis of Isolated Columns

Many of the investigators, whose works were reviewed in CHAPTER II, have proposed methods of analyses for isolated columns. In a number of cases the analyses were based on non-linear but elastic moment-curvature relationships. The results of this thesis indicate that this approach is not suitable for a practical investigation of the behavior of columns in frames because of the large influence of the restraining members on this behavior.

9.5.3 Analysis of Isolated Columns Having Linearly Elastic End Restraints

Columns have been analysed using linearly elastic end restraints to approximate the effect of frame action. Examples of this type of analysis include the investigations of Broms and Viest (6) and Pfrang and Siess (33,34).

Under short-time loading, the results of this thesis indicate that the beam could be replaced by a linearly elastic restraint for the shorter columns and the resultant changes in failure load would be small. For the longer columns, however, the non-linear behavior of the beam reduced the failure loads from those which would have resulted from using linearly elastic column restraints. Another problem arising from this

method appears to be the correlation between the actual beam stiffness and the stiffness assigned to the restraint.

Under sustained loading, the results of this thesis indicate that the restraining beams exhibited very little linear behavior.

9.5.4 Analysis of Frames Using Moment-Curvature Relationships

A method of analysis of frames based on the formulation of unique load-moment-curvature relationships for typical cross-sections of all frame elements has been used at the University of Texas (3,13). The correlation has been good between the analytical results and the experimental results obtained from the short-time loading of reinforced concrete, closed rectangular frames.

Under short-time loading, the results of this thesis indicate that unique load-moment-curvature relationships will give good results provided that the loads are applied in such a manner as to prevent significant unloading at any section in the frame through a redistribution of moment. If significant unloading does occur, the assumption of a non-linear elastic response to the unloading may result in an erroneous prediction of behavior.

Under sustained loading, the results of this thesis indicate that because moment will be redistributed on a large scale due to large changes in member stiffnesses and deflections, a unique relationship between load, moment, and curvature for any member cross-section will normally not exist.

9.5.5 Reduced Modulus Approach

The investigation of the effect of sustained load on the behavior

of columns using a reduced modulus approach has been recommended by many investigators including Broms and Viest (6), Pfrang (32), and Green (16). Green has been the only one of these investigators who has attempted to base the value of the reduced modulus on actual concrete creep behavior. He has reported a good correlation with actual test results under short durations of loading.

For longer durations of loading, the results of CHAPTER V indicate that the errors in predicted deformations may be as high as 50 per cent using a reduced modulus approach (one creep stage) to predict column behavior. However, the investigation in CHAPTER V also suggests that an effective or reduced modulus approach may not cause significant errors in predicting the behavior of simply supported beams. The major source of errors in a reduced modulus computation stems from the fact that a varying stress-time condition cannot be considered.

CHAPTER X

SUMMARY, CONCLUSIONS, AND RECOMMENDATIONS

10.1 Summary

This thesis presents a method of analysis which can be used in the investigation of the behavior of reinforced concrete structures under sustained load. The analysis, which is general in derivation, applies discreteness to the cross-sections, the member lengths, and the duration of sustained load, and utilizes numerical integration and trial and error procedures to obtain the equilibrium configurations of frameworks under load. The analysis considers the varying stress-time nature of the sustained load problem and also recognizes that concrete is a visco-elasto-plastic material.

The material properties and assumptions explicitly defined in this thesis may impose limitations on the results of this thesis, but they are not limitations on future applications of the method of analysis.

A good correlation was obtained between the results of experimental tests and the results obtained using the method of analysis. Because of the time element involved in experimental investigation, however, these investigations were not extensive enough to completely verify the method of analysis.

The analysis was applied to the investigation of the behavior under sustained load of a number of restrained reinforced concrete long columns. Results were presented regarding the load-moment behavior, the

deformation characteristics, and the failure loads. The discussion of the results included a discussion of the limitations of the proposed method of analysis and also of existing methods of analysis and design.

10.3 Recommendations for Further Research

The investigation of the behavior under sustained load of re-strained reinforced concrete long columns was limited to only a small range of possible cases. The following research should be conducted before making a quantitative application of the results to design.

1. More experimental investigation is needed to verify the method of analysis within the scope of the investigation.
2. The complete range of e/t values should be investigated.
3. The complete range of possible ratios of end eccentricities should be investigated.
4. A range of possible ratios of nominal column stiffness to nominal beam stiffness should be investigated including the effects of frames that are not laterally restrained.
5. The effect of varying the amount and yield point of the compression steel and tension steel in both the beam and the column should be studied.
6. The effect of other variables such as concrete strength, thickness to width ratio, steel yield point, etc. should be studied.
7. Where possible, the parameters of level of sustained load and slenderness ratio should be variables in the above investigations.

10.3 Conclusions and Recommendations

The conclusions and recommendations presented in this section

have been based on this investigation and thus are limited to restrained, tied columns with small eccentricity ratios.

Sustained loading caused substantial increases in column deflections over the corresponding values under short-time loading. The values of maximum deflection approached one per cent of the column length in this investigation. The increases in deflection under sustained load caused direct increases in the deflection moments of the columns bent in symmetrical single curvature and indirect increases in the deflection moments of the columns bent in double curvature. The substantial changes in the deflection moments caused significant changes in both the relative stiffnesses of the columns and the maximum moments in the columns.

In the lower portion of the range of slenderness ratios investigated, both the single curvature and double curvature columns exhibited stable failures. For a slenderness ratio of ten, sustained loading had little effect on the failure loads from the corresponding values under short-time loading. In fact, in the double curvature columns, these failure loads were increased over the short-time values through decreases in column stiffness and the resulting decreases in end moment in the columns. This characteristic may be exhibited by the single curvature columns if slenderness ratios of less than ten are investigated.

The more slender columns of the sustained load investigation exhibited unstable failures under loads which were substantially lower than the corresponding values under short-time loading.

The behavior of the frames studied was influenced considerably by the non-linear behavior of the concrete in the frame elements. Non-linear concrete response occurred in the shorter columns as the failure

load was approached and also in the beams which restrained the longer columns. The non-linear response was increased under sustained load.

The behavior of the columns in the frames under sustained load was greatly influenced by the decrease in column stiffness which resulted when the reinforcement on the concave side of the column yielded under sustained load. To counteract this effect, either a larger steel area or a higher yield steel or both could be used.

The use of first order theory to evaluate the design moments for beams may seriously underestimate these moments if the beams are restraining long columns. First order theory does not predict the redistribution of moment in a frame, and since this is substantial when long columns are exposed to sustained load, the actual load factor for the beam may be considerably lower than the nominal load factor assumed in the design.

The points of inflection in structural elements in a frame are subject to considerable movement because of the redistribution of moment under sustained load. This factor should be taken into account in designing reinforcing steel in frame elements.

The present methods of design and analysis do not adequately predict framework behavior if the framework is under sustained load.

LIST OF REFERENCES

LIST OF REFERENCES

1. ACI Committee 318 - "Building Code Requirements for Reinforced Concrete (ACI 318-63)", American Concrete Institute, 1963.
2. ACI-ASCE Committee 441 - "ACI Bibliography No. 5 - Reinforced Concrete Columns", American Concrete Institute, Detroit, 1965, pp 21-23.
3. Breen, J.E. - "The Restrained Long Concrete Column as a Part of a Rectangular Frame", Ph.D. Dissertation, University of Texas, Austin, Texas, June 1962.
4. Breen, J.E. and Ferguson, P.M. - "The Restrained Long Column as a Part of a Rectangular Frame", Journal ACI, Proceedings Volume 61, No. 5, May 1964.
5. Bresler, B. and Selna, L. - "Analysis of Time - Dependent Behavior of Reinforced Concrete Structures", Symposium on Creep of Concrete, ACI Publication SP-9, 1964, pp 115-128.
6. Broms, B. and Viest, I.M. - "Ultimate Strength of Hinged Columns", Transactions ASCE, Volume 126, 1961.
7. Chang, W.F. - "Critical Length of Long Hinged and Restrained Concrete Columns", International Symposium on the Flexural Mechanics of Reinforced Concrete, ASCE, 1966.
8. Dischinger, F. - "Untersuchungen über die Knicksicherheit, die elastische Verformung und das Kriechen des Betons bei Bogenbrücken", Der Bauingenieur, Volume 18, 1937, pp 487, 538, and 595.
9. Dischinger, F. - "Elastische und Plastische Verformungen der Eisenbeton-tragwerke und insbesondere der Bogenbrücken", Der Bauingenieur, Volume 20, 1939, pages 53, 286, 426, and 563.
10. Distefano, J.N. - "Creep Buckling of Slender Columns", Proceedings ASCE, Volume 91, No. ST3, Part I, June 1965, pp 127-150.
11. European Concrete Committee - "Recommendations for an International Code of Practice for Reinforced Concrete", English translation published by the American Concrete Institute and the Cement and Concrete Association, 1964.
12. Freudenthal, A.M. and Roll, F. - "Creep and Creep-Recovery of Concrete Under High Compressive Stresses", Proceedings ACI, Volume 54, No. 12, June 1958, pp 1111-1142.

13. Furlong, R.W. - "Long Columns in Single Curvature as a Part of Concrete Frames", Ph.D. Dissertation, University of Texas, Austin Texas, June 1963.
14. Furlong, R.W. and Ferguson, P.M. - "Tests of Frames with Columns in Single Curvature" accepted for publication in Symposium on Columns, ACI Publication SP-
15. Gaede, K. - "Knicken von Stahlbetonstäben unter Kurz - und Langzeitbelastung", Deutscher Ausschuss für Stahlbeton, Heft 129, Berlin, 1958.
16. Green, R. - "Behavior of Unrestrained Reinforced Concrete Columns Under Sustained Load", Ph.D. Dissertation, University of Texas, Austin Texas, January 1966.
17. Hoff, N.J. - "A Survey of the Theories of Creep Buckling", Proceedings of the Third U.S. National Congress on Applied Mechanics, Pergamon Press, New York, 1958, pp 29-49.
18. Holley, M.J. and Mauch, S.P. - "Creep Buckling of Reinforced Concrete Columns", Research Report R63-7, School of Engineering, Massachusetts Institute of Technology, Cambridge Massachusetts, January 1963.
19. Hognestad, E. - "A Study of Combined Bending and Axial Load in Reinforced Concrete Members", Bulletin No. 399, University of Illinois Engineering Experiment Station, November 1951.
20. Hognestad, E., Hanson, N.W., and McHenry, D. - "Concrete Stress Distribution in Ultimate Strength Design", Journal ACI, Volume 27, No. 4, December 1955, pp 455-479.
21. v. Karman, T. - "Untersuchungen über Knickfestigkeit", Mitteilungen über Forschungsarbeiten auf dem Gebiete des Ingenieurwesens, No. 81, Berlin, 1910.
22. Krieg, K.H. - "Einfluss des Betonkriechens auf die Knicksicherheit Krummer Stahlbetonstäbe", Beton und Stahlbetonbau, Volume 19, No. 2, February 1954, pp 45-47.
23. Martín, J. and Olivieri, E. - "Tests of Slender Reinforced Concrete Columns Bent in Double Curvature", Reinforced Concrete Column Symposium, American Concrete Institute, 1966.
24. McHenry, D. - "A New Aspect of Creep in Concrete and Its Application to Design", Proceedings ASTM, Volume 43, 1943, pp 1069.
25. Naerlović-Veljković, N. - "Der Einfluss des Kriechens auf die Tragfähigkeit von Stahlbetonsäulen", Österreichisches Ingenieur, Archiv Band XIV, Heft 2, June 1960.

26. National Building Code Committee - "National Building Code of Canada 1965", National Research Council, Ottawa, 1965.
27. Neville, A.M. - "Properties of Concrete", Sir Isaac Pitman and Sons Ltd., London, 1963, pp 239.
28. Neville, A.M. and Meyers, B.L. - "Creep of Concrete: Influencing Factors and Prediction", Symposium on Creep of Concrete, ACI Publication No. SP-9, 1964, pp 1-31.
29. Newmark, N.M. - "Numerical Procedure for Computing Deflections, Moments, and Buckling Loads", Transactions ASCE, Volume 108, 1943, pp 1161.
30. Ostlund, L. - "Stability of Concrete Structures Submitted to Long-Time Loads", Nordisk Betong, Volume 1, No. 1, 1957, pp 77-87.
31. Pauw, A. - "Static Modulus of Elasticity of Concrete as Affected by Density", Journal ACI, Volume 32, December 1960.
32. Pfrang, E.O. - "A Study of the Influence of Creep on the Behavior and Capacity of Reinforced Concrete Columns", Technical Report No. 4, Department of Civil Engineering, University of Delaware, Newark Delaware, October 1964.
33. Pfrang, E.O. and Siess, C.P. - "Analytical Study of the Behavior of Long Restrained Reinforced Concrete Columns Subjected to Eccentric Loads", Civil Engineering Studies, Structural Research Series No. 214, University of Illinois, Urbana Illinois, June 1961.
34. Pfrang, E.O. and Siess, C.P. - "Behavior of Restrained Reinforced Concrete Columns" Proceedings ASCE, Vol. 90, No. ST5, October 1964, pp 113-136.
35. Pickett, G - "Shrinkage Stresses in Concrete-Part 2", Proceedings ACI, Volume 2, 1946, pp 361-398.
36. Prentis, J.M. and Ross, A.D. - "Slender Reinforced Concrete Columns", Concrete and Constructional Engineering (London), Volume 43, No. 9, September 1948, pp 261-270.
37. Rasch, C. - "Spannungs-Dehnungs-Linien des Betons und Spannungs-Verteilung in der Biegedruckzone bei Konstanter Dehngeschwindigkeit", Deutscher Ausschuss für Stahlbeton, No. 154, Berlin, 1962.
38. Roll, F. - "Long-Time Creep Recovery of Highly Stressed Concrete Cylinders", Symposium on Creep of Concrete, ACI Publication No. SP-9, 1964, pp 95-114.
39. Ross, A.D. - "Creep of Concrete Under Variable Stress", Proceedings ACI, Volume 54, March 1958, pp 739-758.

40. Rüsçh, H. - "Researches Towards a General Flexural Theory for Structural Concrete", Journal ACI, July 1960, pp 1-28.
41. Spang, J.M. Jr. - "Design Method for Long Reinforced Concrete Columns", M.C.E. Thesis, University of Delaware, Newark Delaware, June 1966.
42. Sturman, G.M., Shah, S.P., and Winter, G. - "Micro-Cracking and Inelastic Behavior of Concrete", International Symposium on the Flexural Mechanics of Reinforced Concrete, ASCE, 1966.
43. Tremper and Spellman - "Shrinkage of Concrete - Comparison of Laboratory and Field Performance", Highway Research Record No. 3, Highway Research Board, National Research Council, 1963, pp 30-61.
44. Troxell, G.E., Raphael, J.M., and Davis, R.E. - "Long-Time Creep and Shrinkage Tests of Plain and Reinforced Concrete", Proceedings ASTM, Volume 58, 1958, pp 1101-1120.
45. Viest, I.M., Elstner, R.C., and Hognestad, E. - "Sustained Load Strength of Eccentrically Loaded Short Reinforced Concrete Columns", ACI Proceedings, Volume 52, 1956, pp 727-755.
46. Warner, R.F. and Thurlimann, B. - "Creep Failure of Reinforced Concrete Columns", IABSE Publications, Volume 22, 1962, pp 335-361.
47. Washa, G.W. - "Plastic Flow of Thin Reinforced Concrete Slabs", Proceedings ACI, Volume 44, 1947, pp 237.
48. Washa, G.W. and Fluck, P.G. - "Effect of Sustained Loading on Compressive Strength and Modulus of Elasticity of Concrete", ACI Proceedings, Volume 46, No. 11, May 1950, pp 693-700.
49. Washa, G.W. and Fluck, P.G. - "Effect of Compressive Reinforcement on the Plastic Flow of Reinforced Concrete Beams", Proceedings ACI, Volume 49, October 1952, pp 89-108.

APPENDIX A
FLOW DIAGRAMS FOR COMPUTER
APPLICATION OF THE ANALYSIS

A.1 Nomenclature Used in Computer Application

A.1.1 Subscripting Variables

K = subscript defining the loading stage

K = 1 - quick loading stage to value of sustained load

$1 < K \leq \text{NAP}$ - sustained load stages

K = NAP - last sustained load stage

$\text{NAP} < K \leq \text{NAP} + \text{MAX}$ - quick loading stages following sustained load stages

K = NAP + MAX - last loading stage considered

J = subscript defining the position of an analysed cross-section on the beam

J = 1 - cross-section at the joint

J = N - last cross-section analysed

I = subscript defining the position of an analysed cross-section on the column

I = 1 - cross-section at the joint

I = LC - last cross-section analysed

L = subscript defining the position of a point of analysis on the cross-section

L = 1 - top face of the beam or right face of the columns

L = M + 1 - bottom face of the beam or left face of the columns

A.1.2 Input Variables Common to All Loading Stages

CL = column length

PULT = approximate maximum column load. This variable is used in determining an initial strain distribution at a column cross-section

DLLL = uniform sustained load on the beam

BL = beam length

TC = thickness of column

TB = thickness of beam

BB = beam width

BC = column width

DPT = d'/t = ratio of depth to steel to total member thickness

PSB = percentage of steel in the beam (= $A_s/t_B b_B$)

PSC = percentage of either top or bottom steel in the column.

For the symmetrically reinforced section considered,

$$PSC = \frac{A_s}{2 t_c b_c}$$

FPC = concrete compressive strength at age of first loading of specimen

EU = failure strain under short-time loading

AK3 = ratio of maximum possible concrete stress to concrete strength at age of loading

AK2 = ratio of tensile strength of concrete at age of loading to compressive strength of concrete at age of loading

SMOD = modulus of elasticity of reinforcing steel

FY = yield strength of reinforcing steel

M = number of fibres in a cross-section

XC = distance between the column cross-sections being considered

XB = distance between the beam cross-sections being considered

YEND = variable used to converge the deflection at the fixed end of the column bent in double curvature

FROT = variable used to converge the rotations at a joint

A.1.3 Variables Dependent on the Loading Stage

PC(K) = axial load in column during loading stage K

ESH (K) = shrinkage strain up to the end of loading stage K

EMAX (K) = strain at maximum stress for the loading stage K.
This variable is used in the calculation of curvature and stress increments and in calculating the permissible error in strain.

DELE (K) = maximum strain increment or error during loading stage K

DELS (K) = maximum stress increment during loading stage K

DELPB (K) = permissible variation in beam axial load during loading stage K

DELPC (K) = permissible variation in column axial load during loading stage K

DELMB (K) = permissible variation in beam bending moment during loading stage K

DELMC (K) = permissible variation in column bending moment during loading stage K

DELY (K) = permissible variation in column deflection during loading stage K

DELT (K) = permissible variation in joint rotation during loading stage K

F1(K), F2(K), F3(K) = coefficients of the cubic equation for creep during loading stage K

A.1.4 Calculated Variables

FLOP, FAIL = variables used to recognize a failure occurring during any loading stage

PCHA1, PCHA2 = variables used to determine the failure load of a column

SAD1 → SAD16 = variables used to recognize continuous looping within the program

SCOR1, SCOR2 = variables used in determining the initial trials of stress and strain distribution during a loading stage

CMOD = concrete modulus of elasticity

EO = concrete strain at first reaching of the maximum stress

NIP = NAP + MAX = number of loading stages analysed

ET4 = strain at point $L = 1$ of a cross-section

ET1 = strain at point $L = M + 1$ of a cross-section

ZZ = variable used in the calculation of strain and stress increments

EINC = permissible variation in strain or strain increment

SINC = stress increment

ETB1 = total strain in a fibre of a beam

BPB = variable used in the calculation of beam axial load

BMB1 = variable used in the calculation of bending moment in a beam cross-section

RBR = variable used in the calculation of beam rotation

FUD = variable used in the calculation of the initial assumption of strain distribution in a cross-section

EEE = variable used in the calculation of the initial assumption of strain distribution in a cross-section

ETC1 = total strain in a fibre of a column

CPC = variable used in the calculation of axial load in a column

CMC = variable used in the calculation of bending moment at a column cross-section

RCR = variable used in the calculation of column rotation

Z = variable used in the calculation of deflections

NN = variable used in the calculation of deflections

RR = variable used in the calculation of bending moment to be resisted at a cross-section

JK = variable used in the calculation of beam rotation

ML = variable used to define the last calculation point in a cross-section. $ML = M + 1$

S,V,C, COM, SS = variables used to perform operations peculiar to computer calculation

TT = variable used in the calculation of the far end deflection of a double curvature column

YFE (K) = far end deflection of the column bent in double curvature after loading stage K

ROTB (K) = beam rotation at the joint at the end of loading stage K

ROTC (K) = column rotation at the joint at the end of loading stage K

RB (J) = equivalent concentrated angle change at cross-section J of the beam

YB (K,J) = deflection of beam at cross-section J after loading stage K

BMB (K,J) = bending moment to be resisted at cross-section J of the beam during loading stage K

PHIB (K,J) = curvature at cross-section J of the beam after loading stage K

FPSB (K,J) = stress in top steel at cross-section J of the beam after loading stage K (if top steel exists)

EPSB (K,J) = strain in top steel at cross-section J of the beam after loading stage K (if top steel exists)

FSB (K,J) = stress in bottom steel at cross-section J of the beam after loading stage K (if bottom steel exists)

ESB (K,J) = strain in bottom steel at cross-section J of the beam after loading stage K (if bottom steel exists)

R(L) = equivalent concentrated load at position L of a cross-section

ETB (K,J,L) = total strain at position L of beam cross-section J after loading stage K

EELB (K,J,L) = instantaneous component of strain at position L of beam cross-section J after loading stage K

ECRB (K,J,L) = creep component of strain at position L of beam cross-section J after loading stage K

SIGB (K,J,L) = stress at point L of beam cross-section J after loading stage K

RC (I) = equivalent concentrated angle change at column cross-section I

YC (K,I) = column deflection at cross-section I after loading stage K

YPC (K,I) = trial column deflection at cross-section I after loading stage K

BMC (K,I) = bending moment at column cross-section I during loading stage K

PHIC (K,I) = curvature at column cross-section I after loading stage K

FPSC (K,I) = stress in steel at right face of column cross-section I after loading stage K

EPSC (K,I) = strain in steel at right face of column cross-section I after loading stage K

FSC (K,I) = stress in steel at left face of column cross-section I after loading stage K

ESC (K,I) = strain in steel at right face of column cross-section I after loading stage K

ETC (K,I,L) = total strain at position L of column cross-section I after loading stage K

EELC (K,I,L) = instantaneous component of strain at position L of column cross-section I after loading stage K

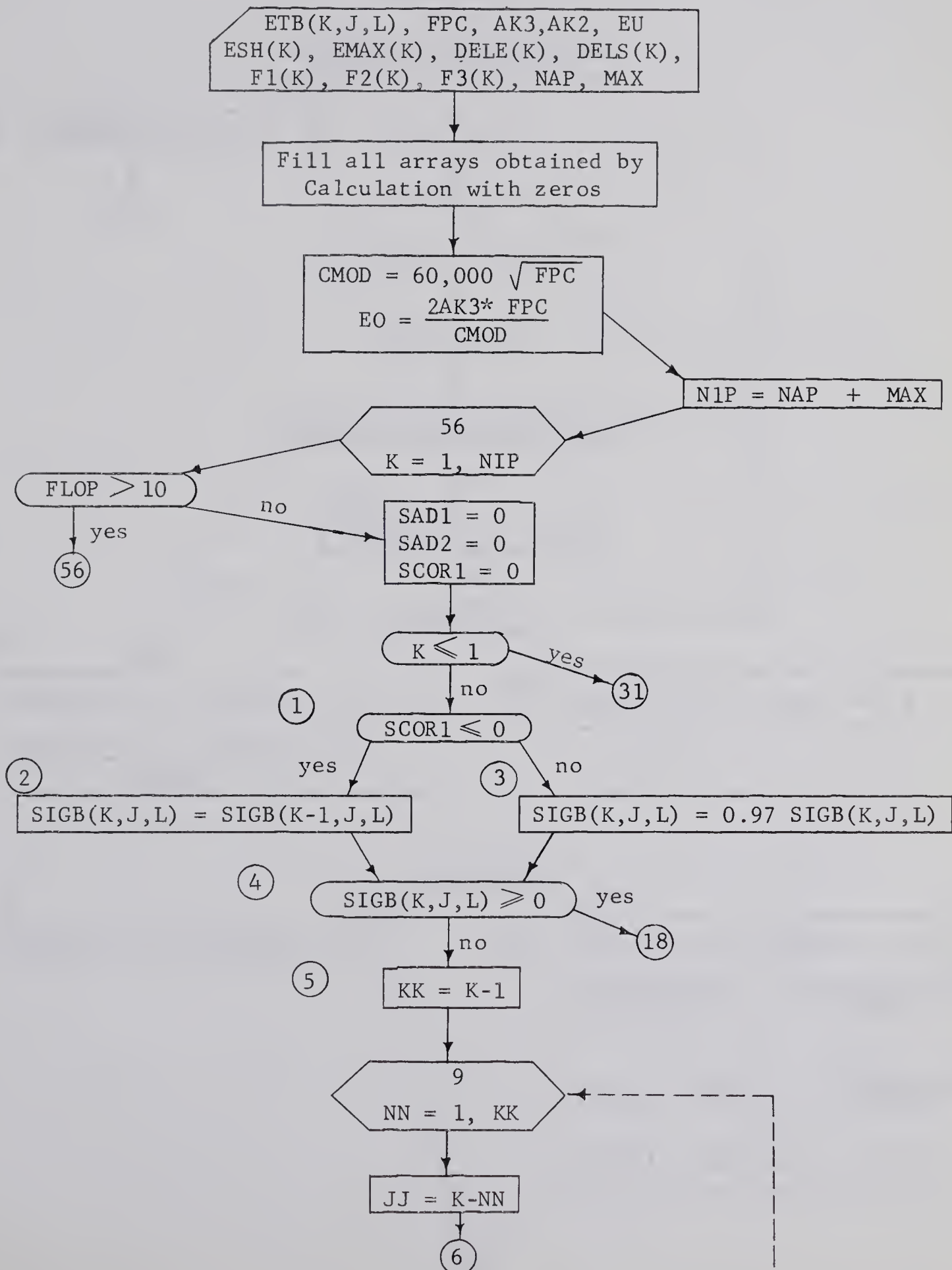
ECRC (K,I,L) = creep component of strain at position L of cross-section I after loading stage K

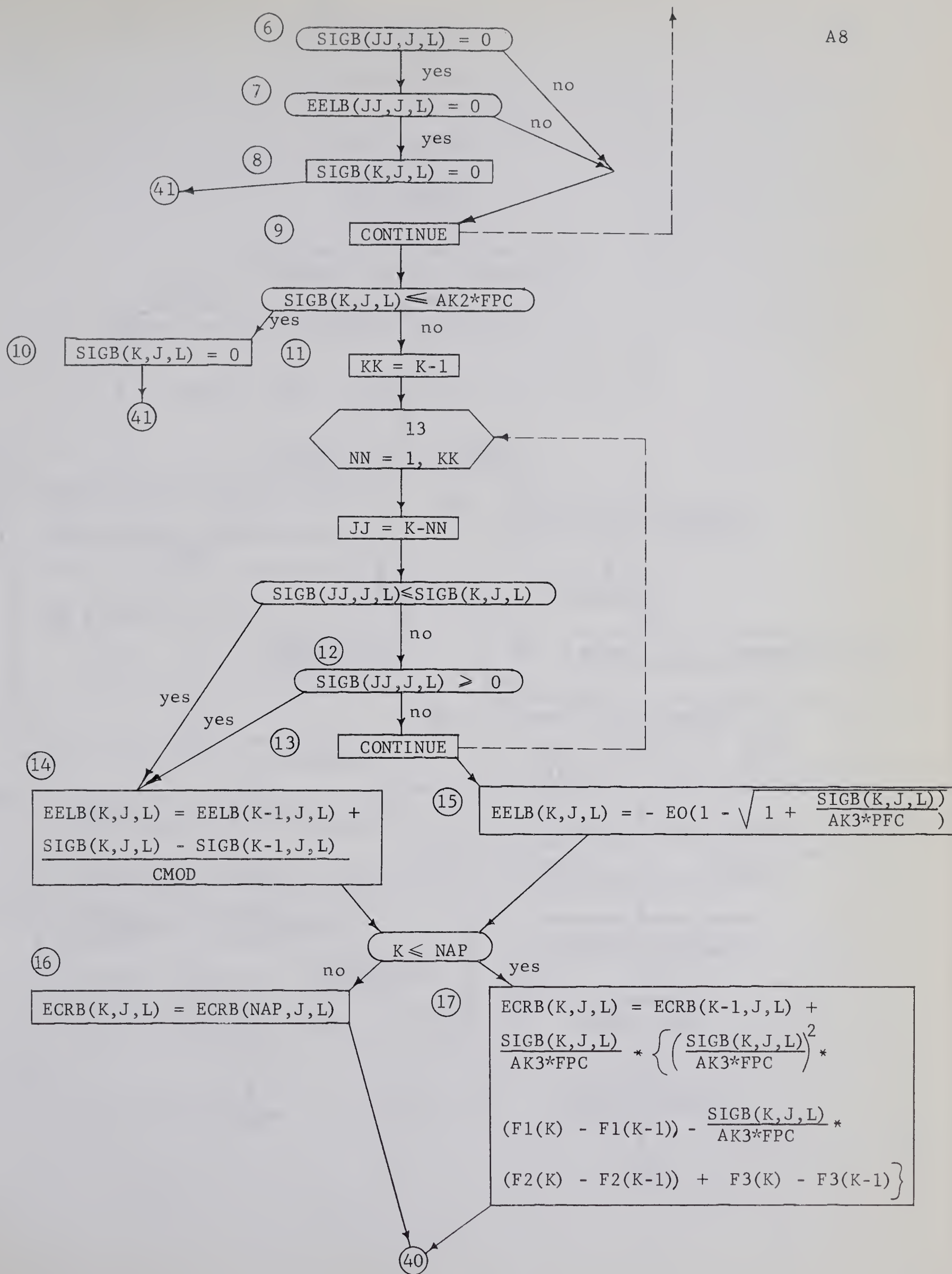
SIGC (K,I,L) = stress at position L of column cross-section I after loading stage K

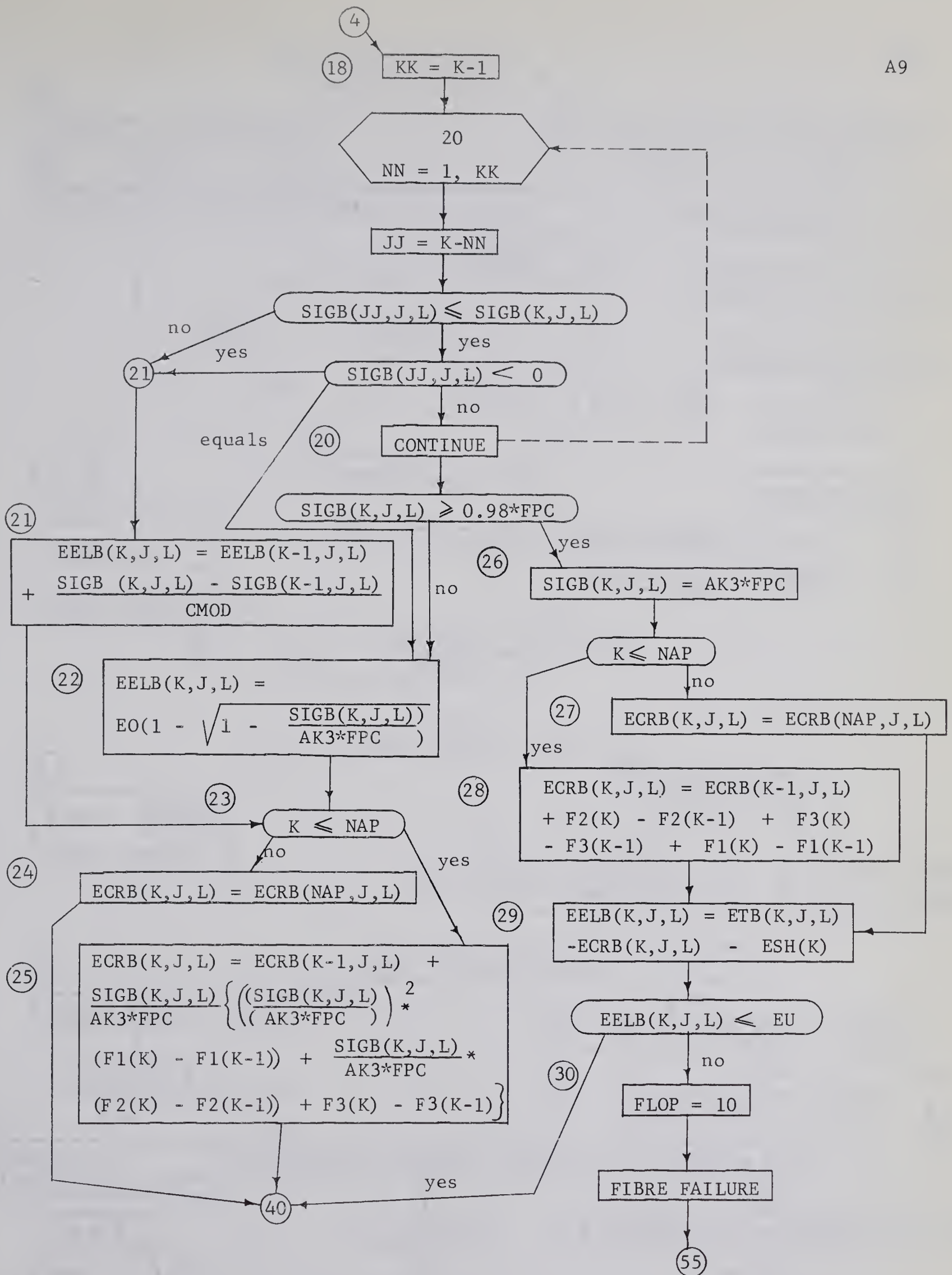
A.2 Flow Diagram for Fibre Analysis

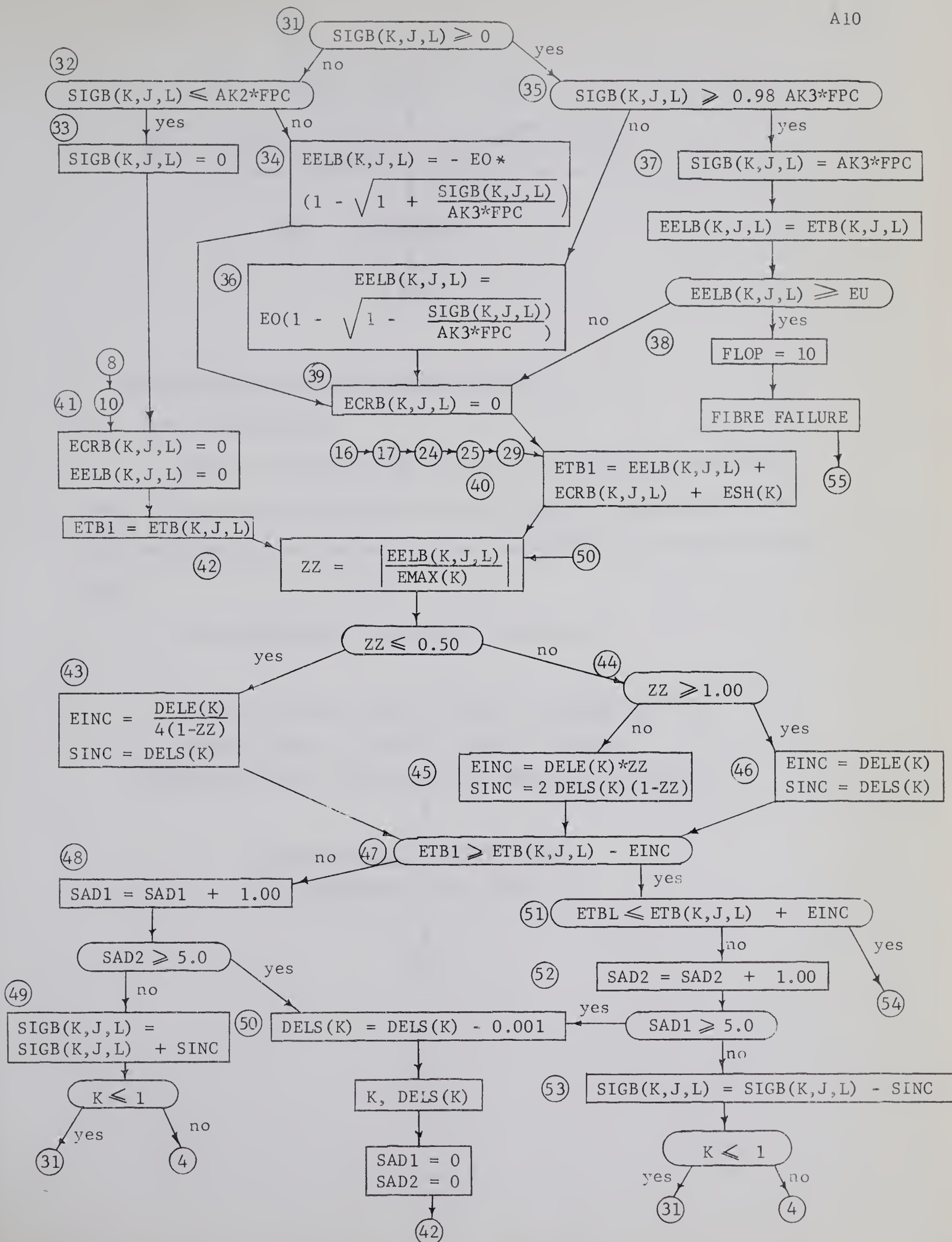
The variables used are the beam variables defined in SECTION

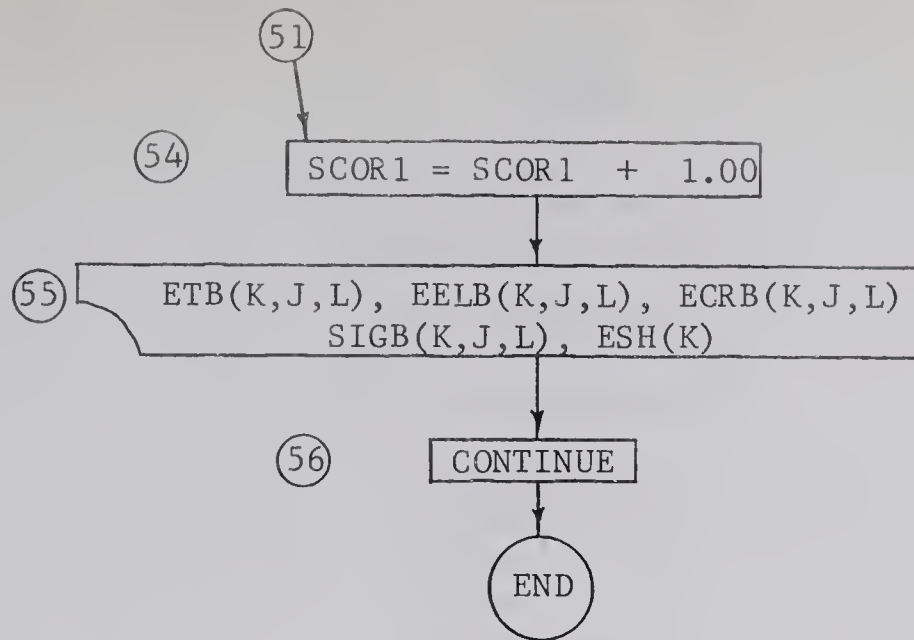
A.1. A column fibre is treated identically.









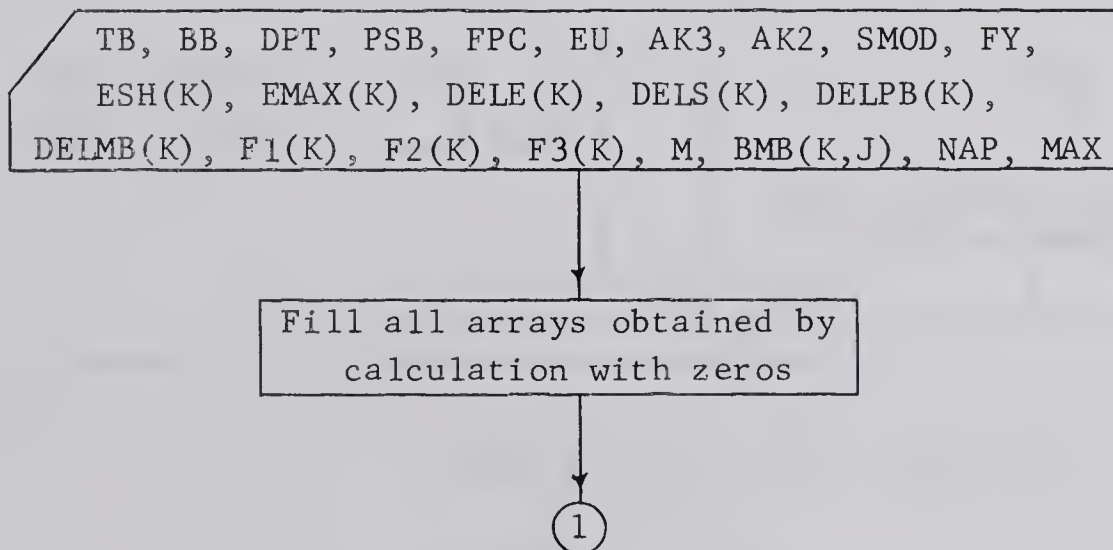


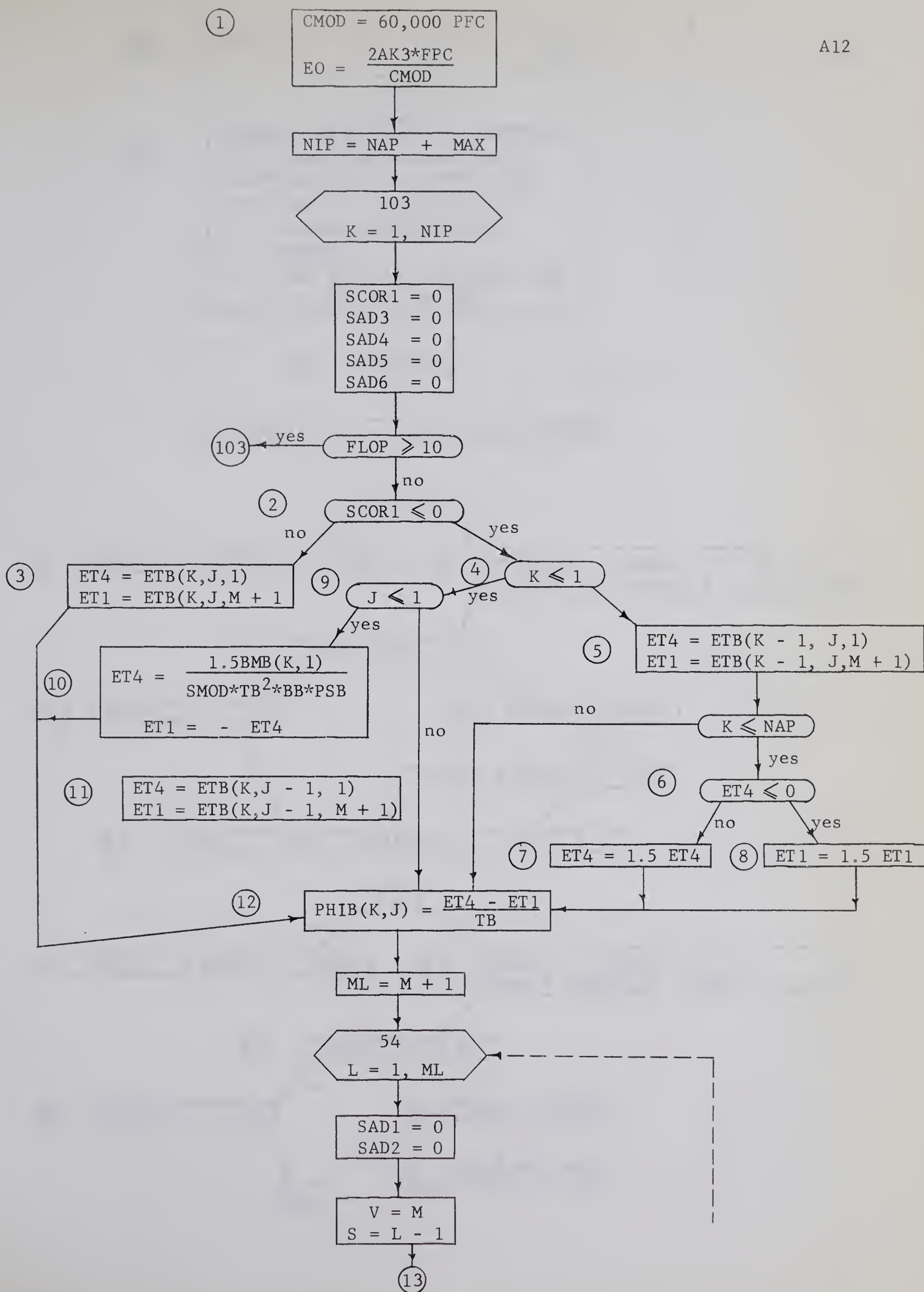
A.3 Flow Diagrams for Cross-Section Analysis

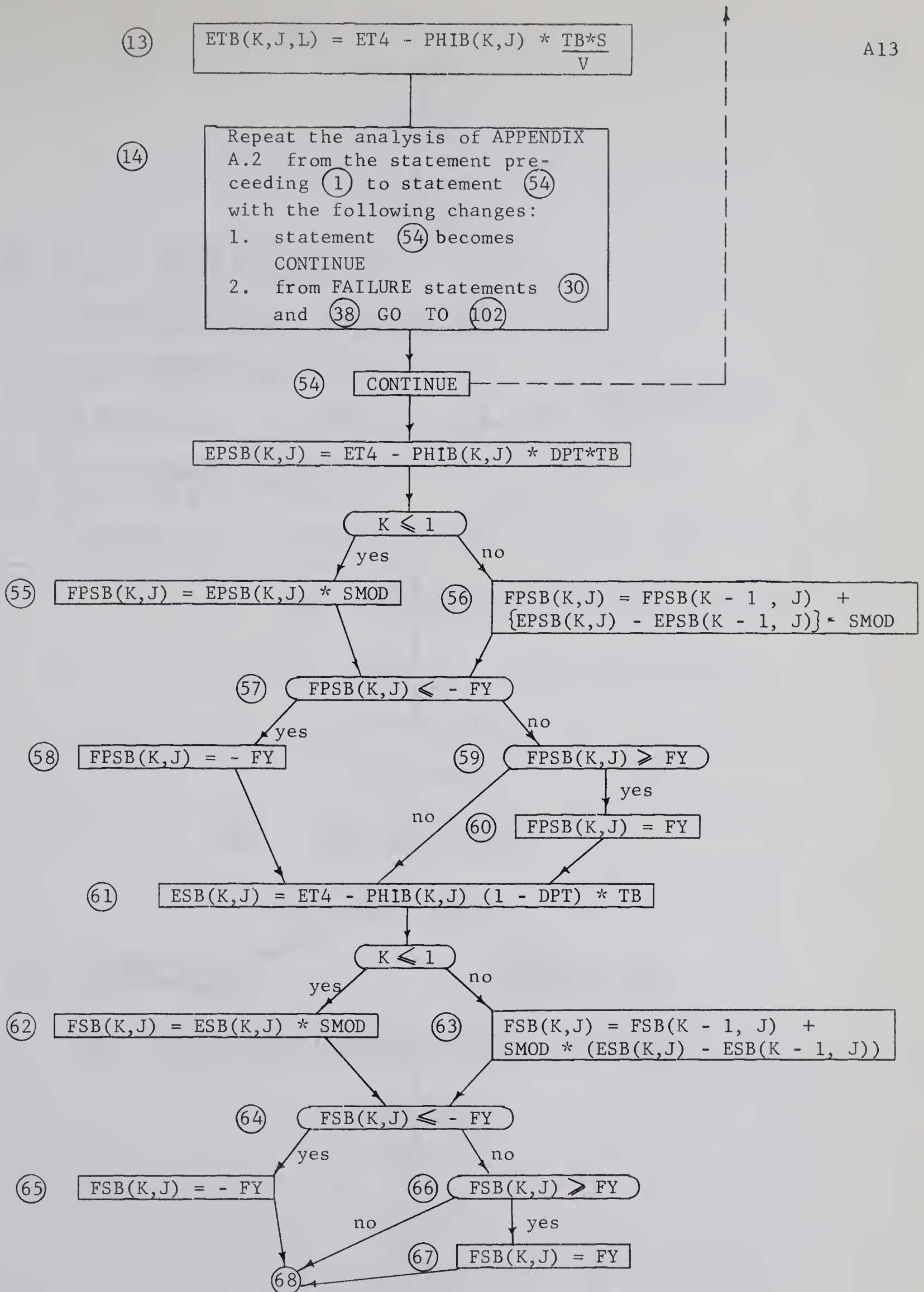
A.3.1 Beam Cross-Section

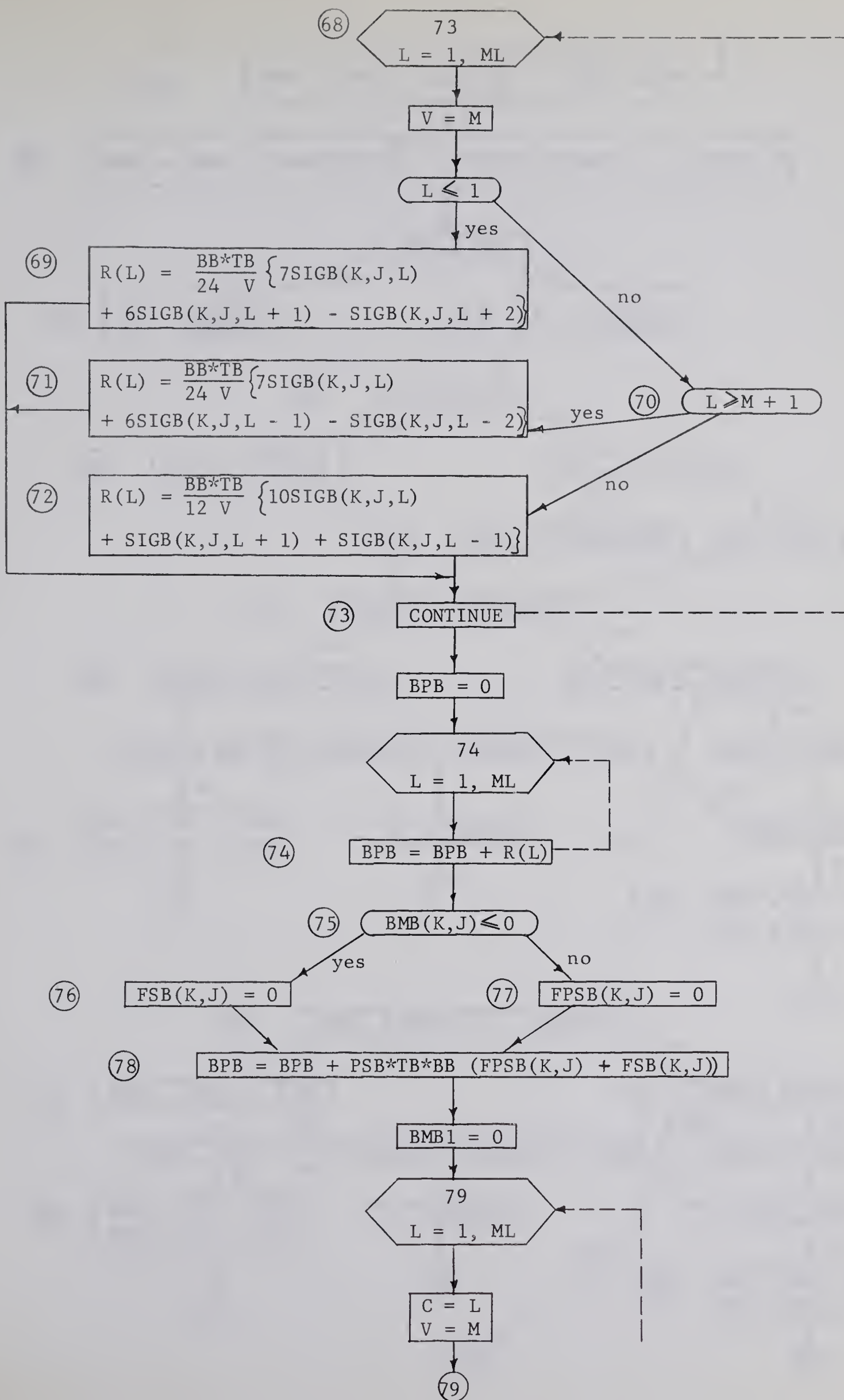
The flow diagram is for a cross-section with no compression steel. To analyse sections with various amounts of compression steel, minor modifications can be made to the statements in the range from (75) to (77).

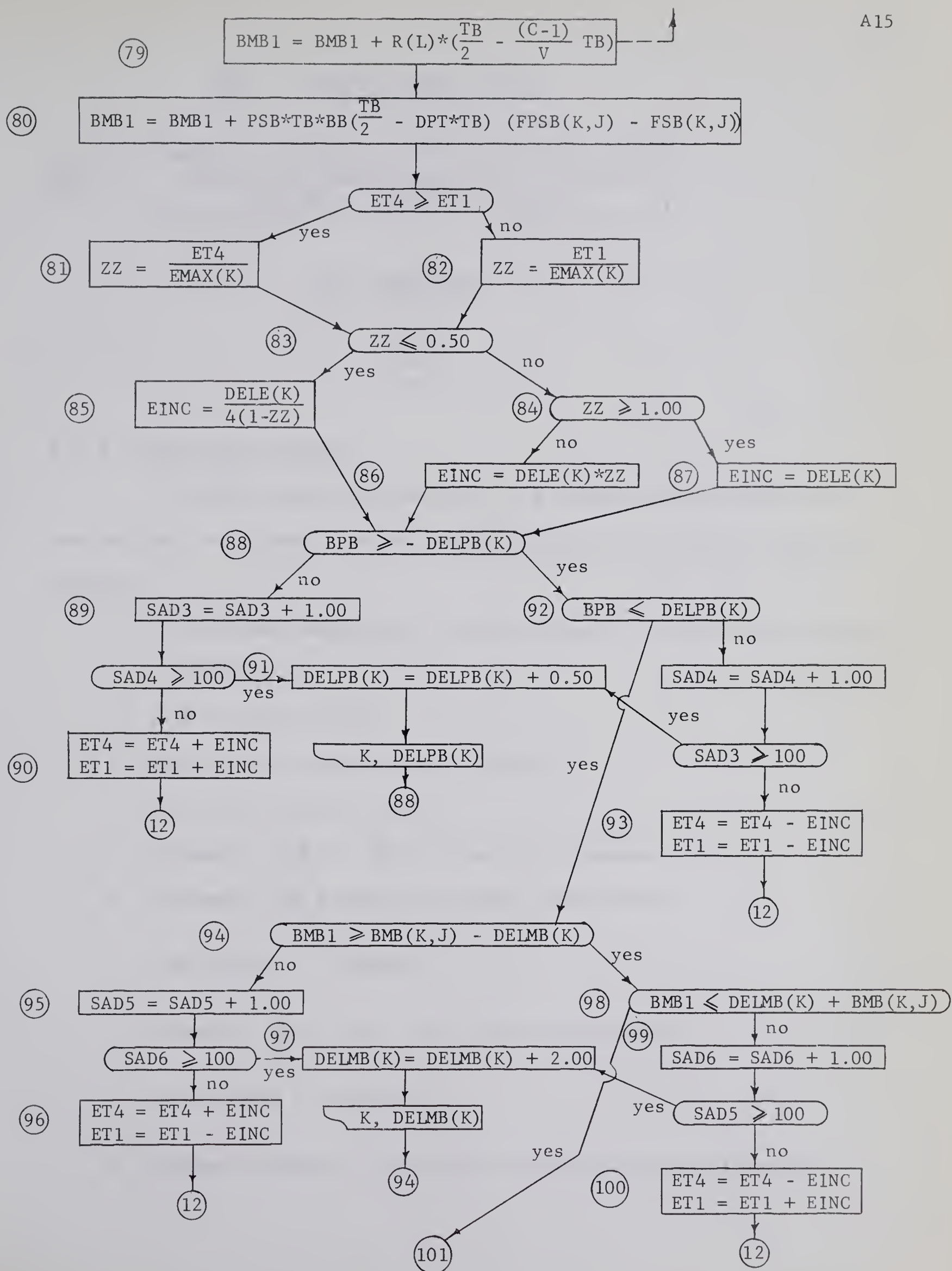
The nomenclature is defined in SECTION A.1.

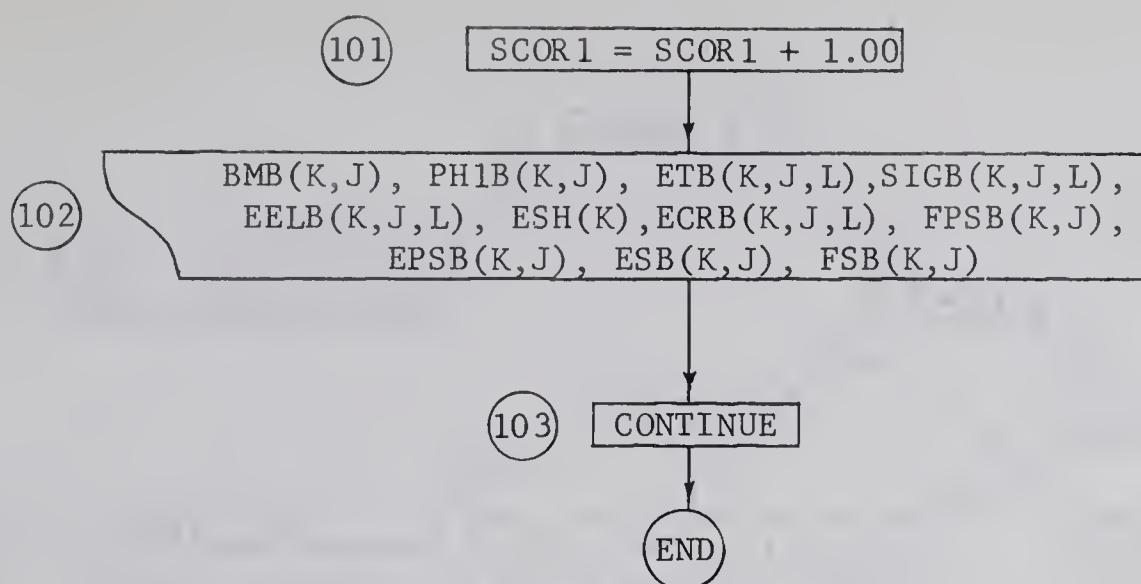












A.3.2 Column Cross-Section

The flow diagram for analysis of a column cross-section is the same as that for a beam cross-section (SECTION A.3.1) with the following changes.

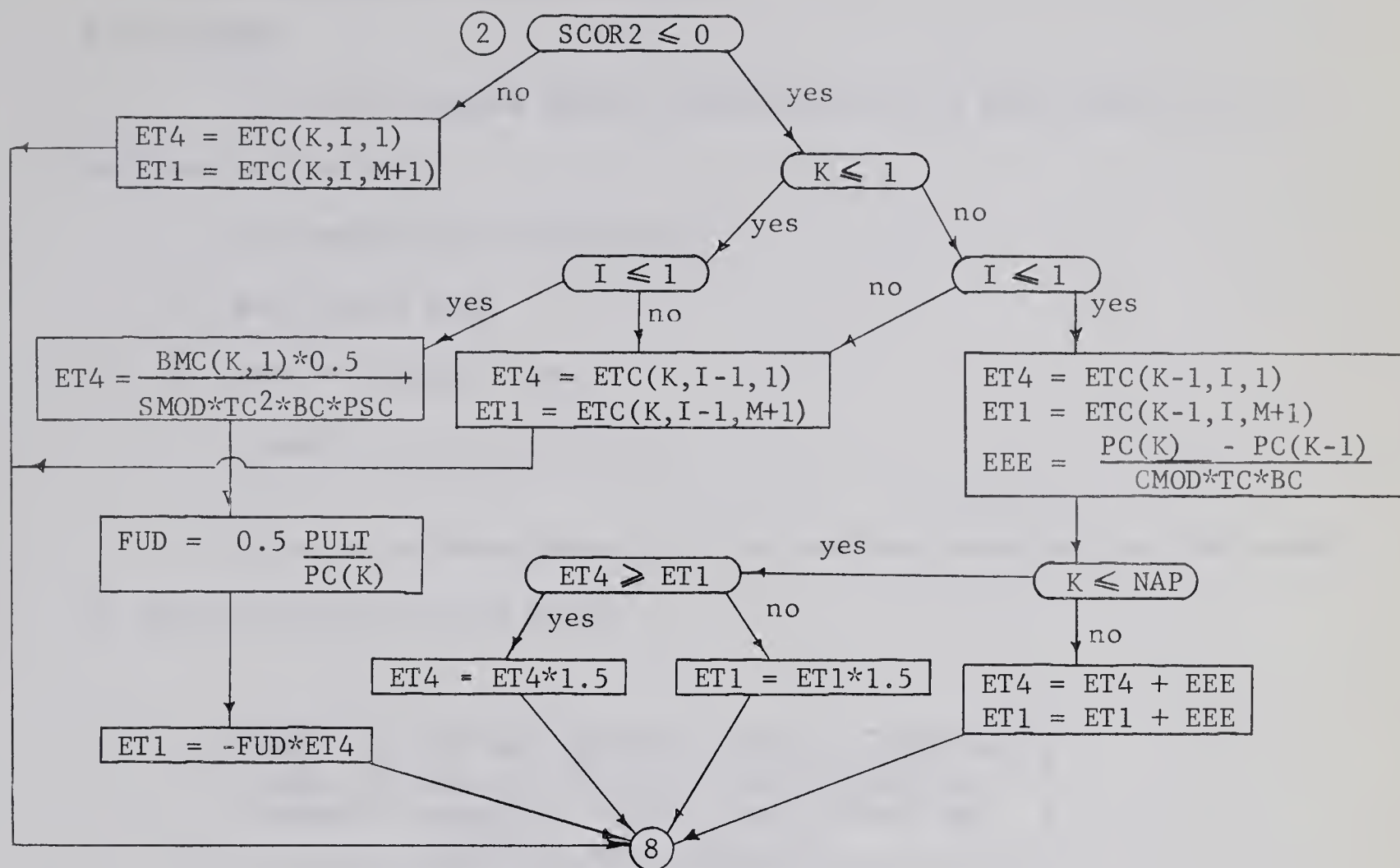
1. The column nomenclature is used instead of the beam nomenclature.
(SECTION A.1)
2. SCOR2 replaces SCOR1
3. SAD7 to SAD12 replace SAD1 to SAD6
4. PULT and PC(K) are read in
5. Statements (75) to (77) inclusive are removed
6. Statement (88) becomes (in column nomenclature)

$$CPC \geq PC(K) - DELPC(K)$$

7. Statement (92) becomes (in column nomenclature)

$$CPC \leq PC(K) + DELPC(K)$$

8. Replace statements (2) to (8) inclusive with the following:



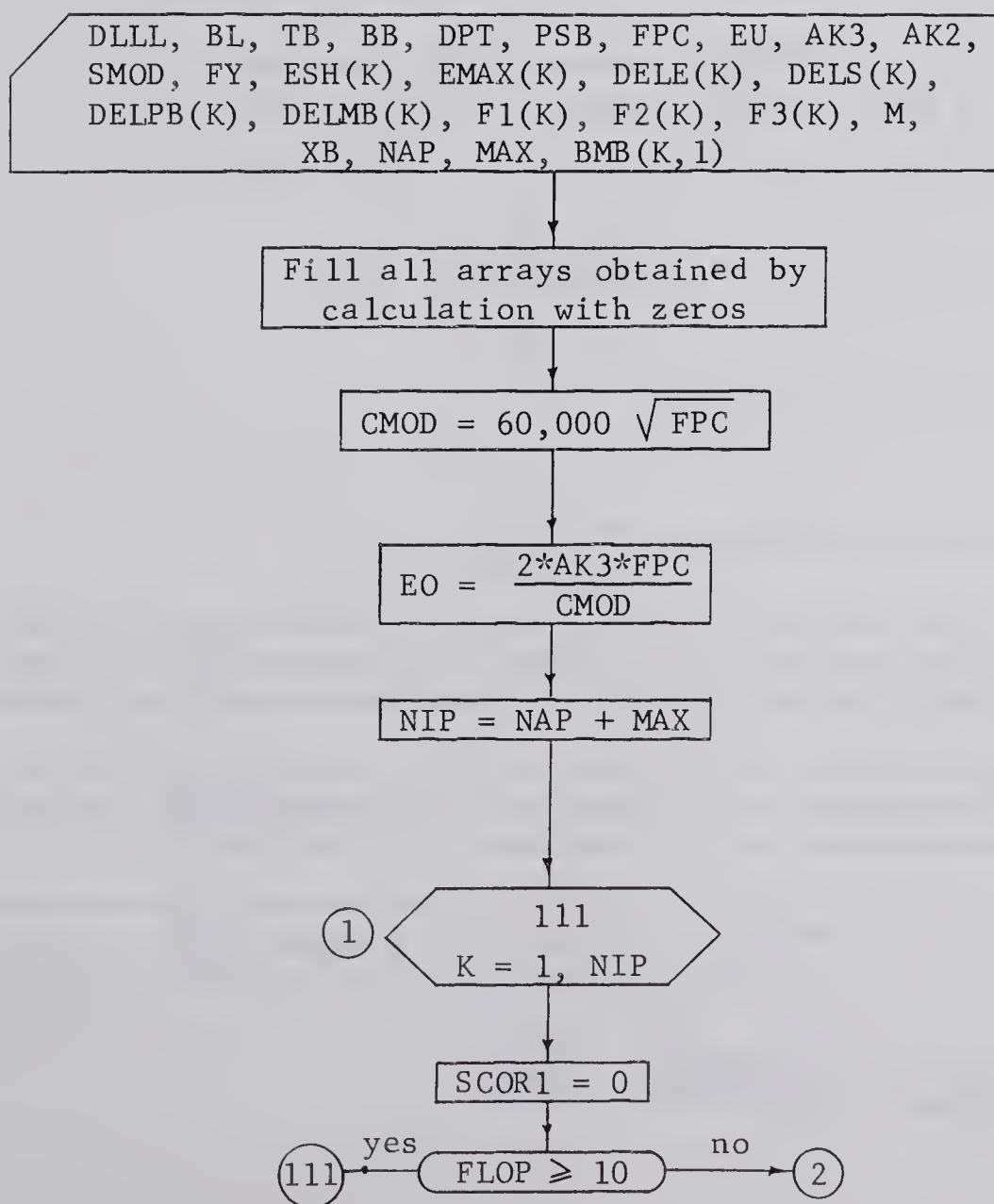
A.4 Flow Diagrams for Member Analysis

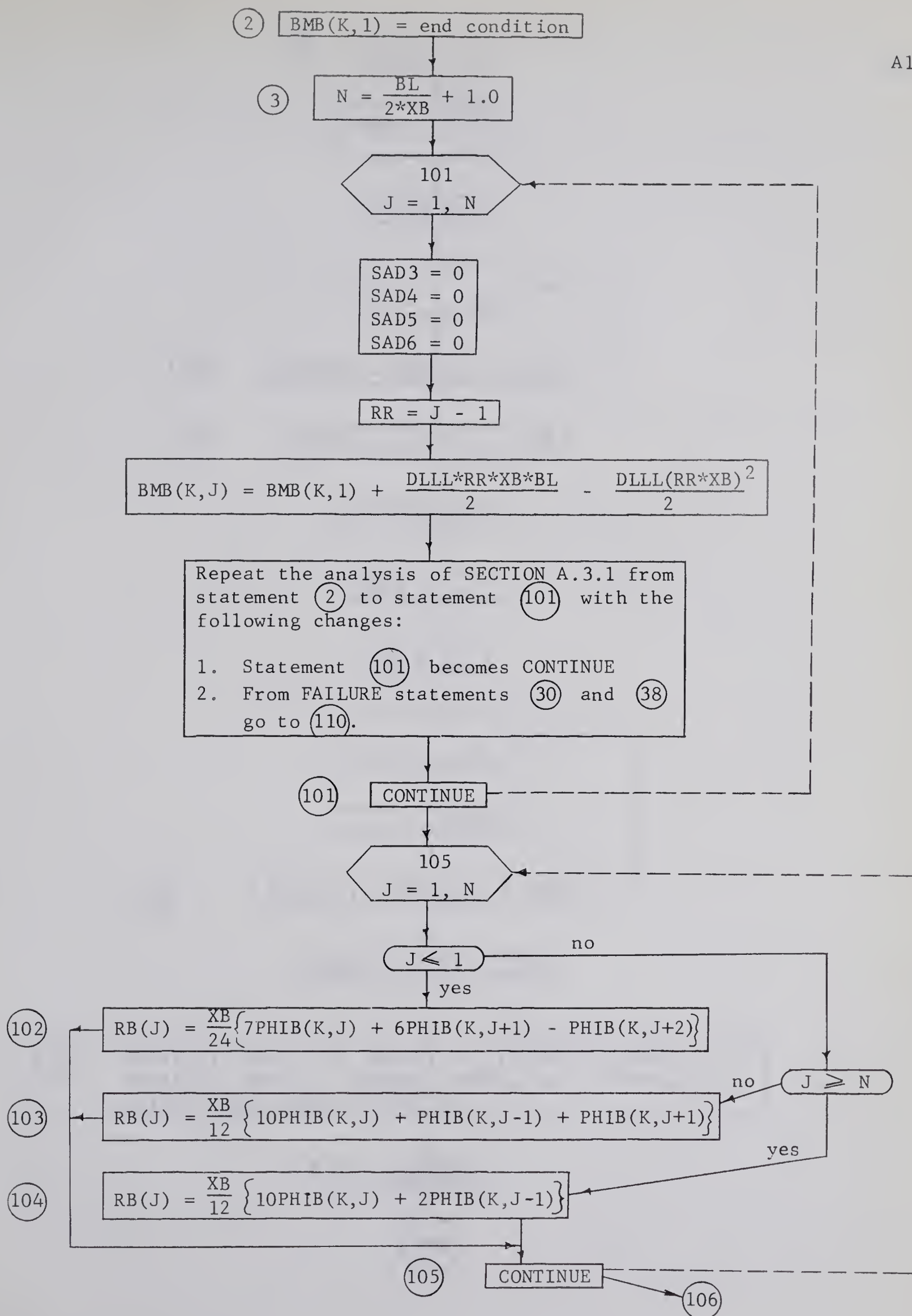
A.4.1 Beam

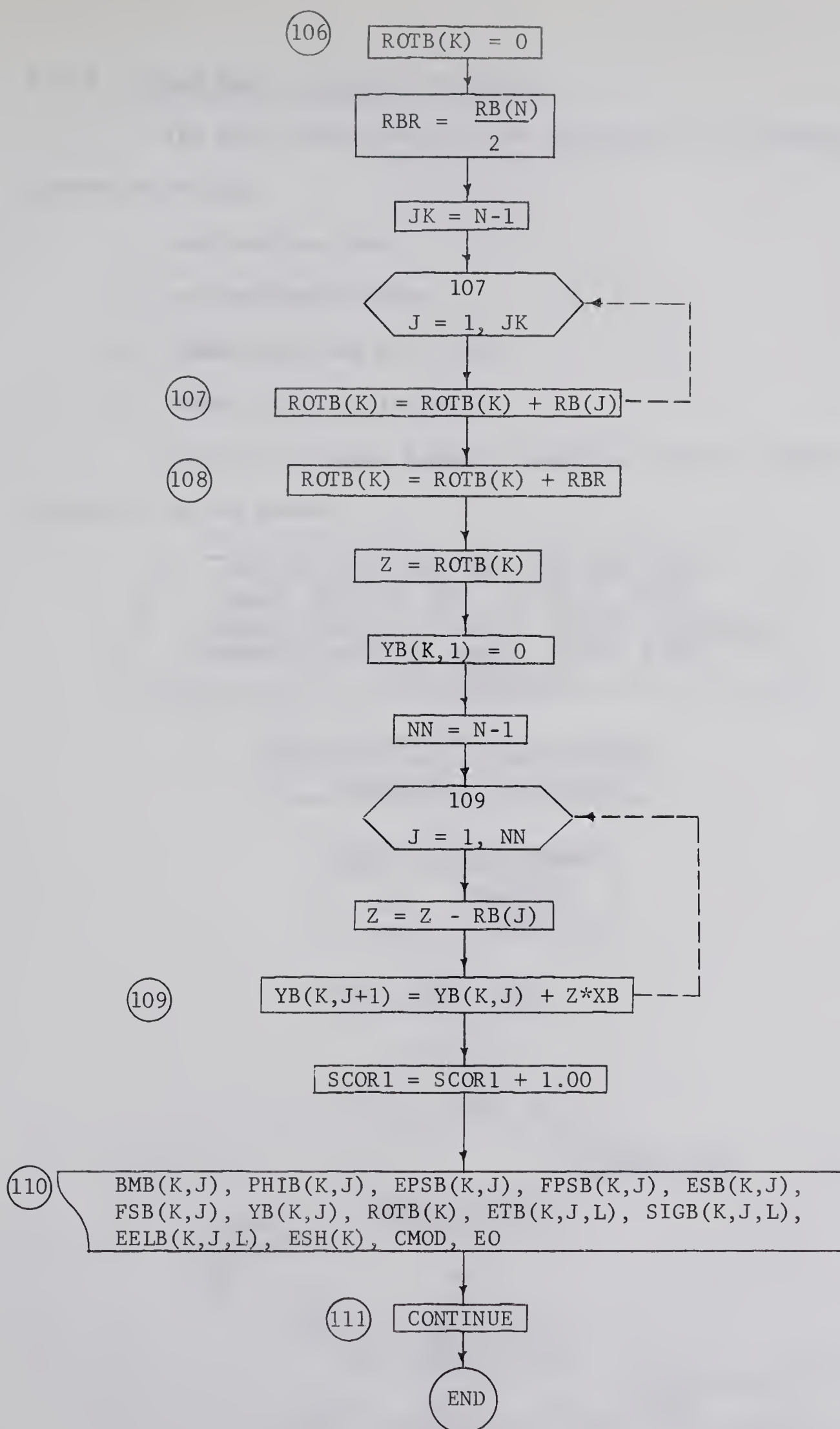
The flow diagram depicts the analysis of a beam subjected to a uniform load having:

1. no compression reinforcement
2. zero axial load
3. zero end deflections
4. symmetrical end restraints

The use of beam symmetry in the analysis requires that the number of panel points be an odd number.





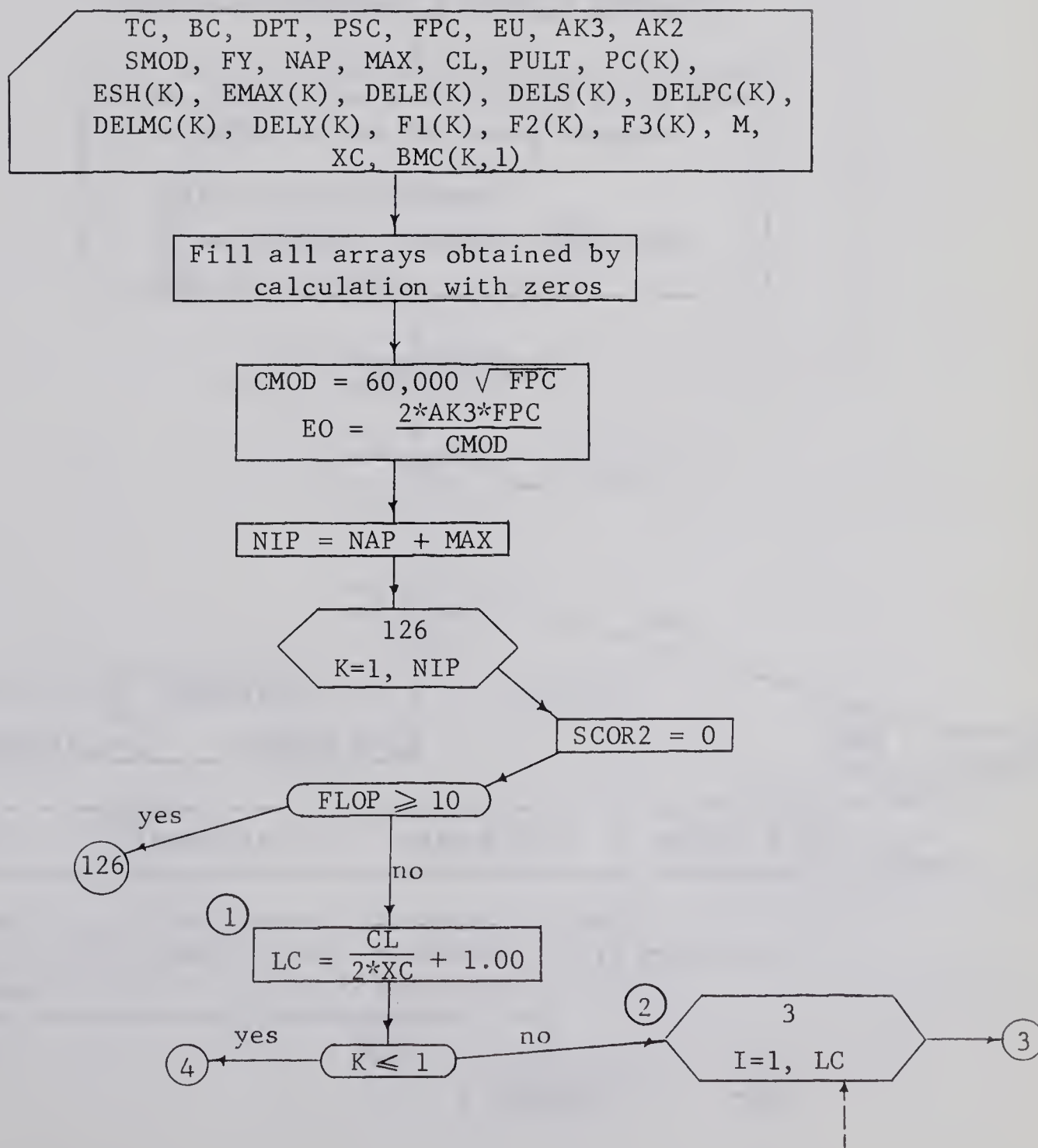


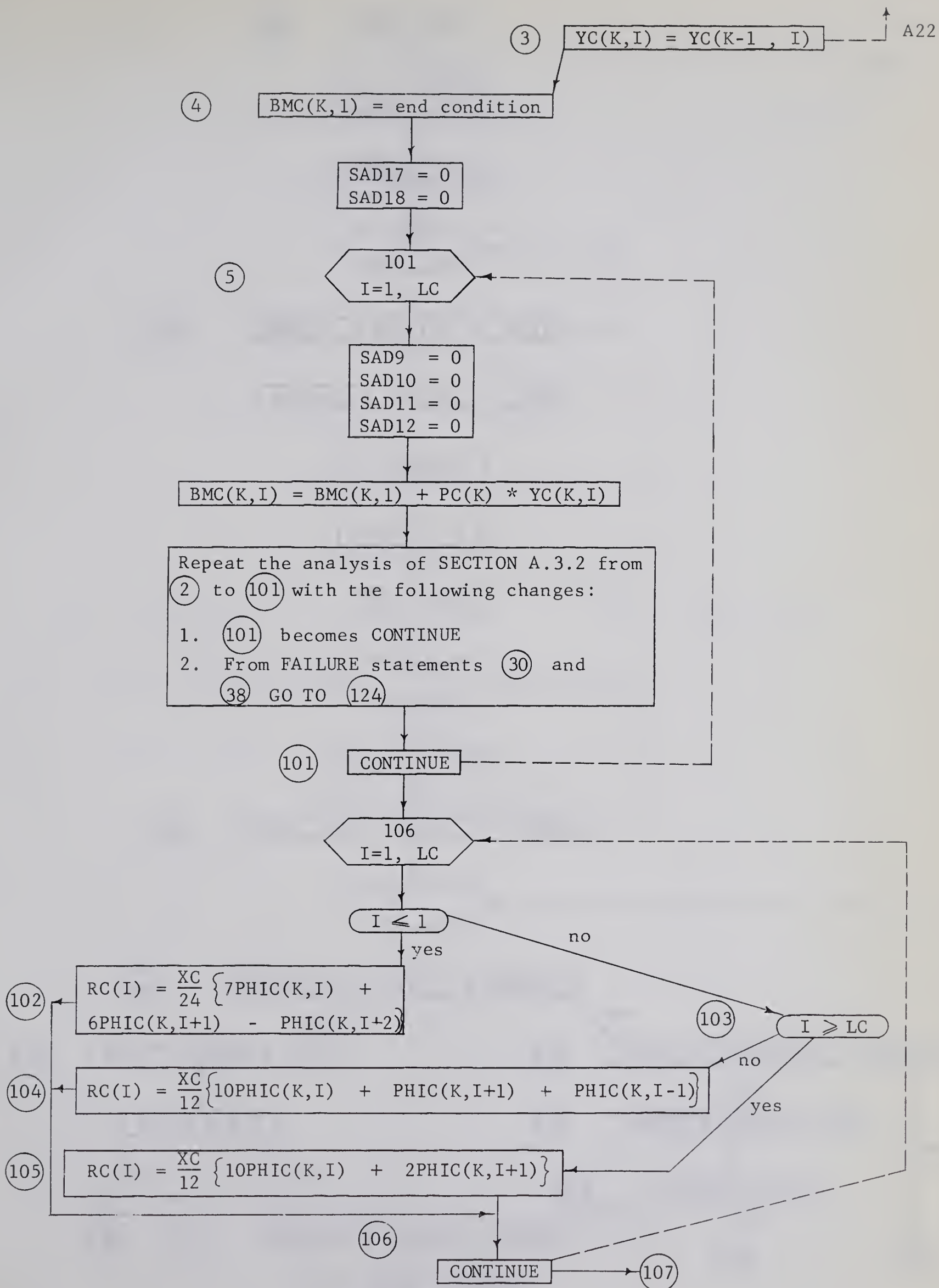
A.4.2 Column Bent in Single Curvature

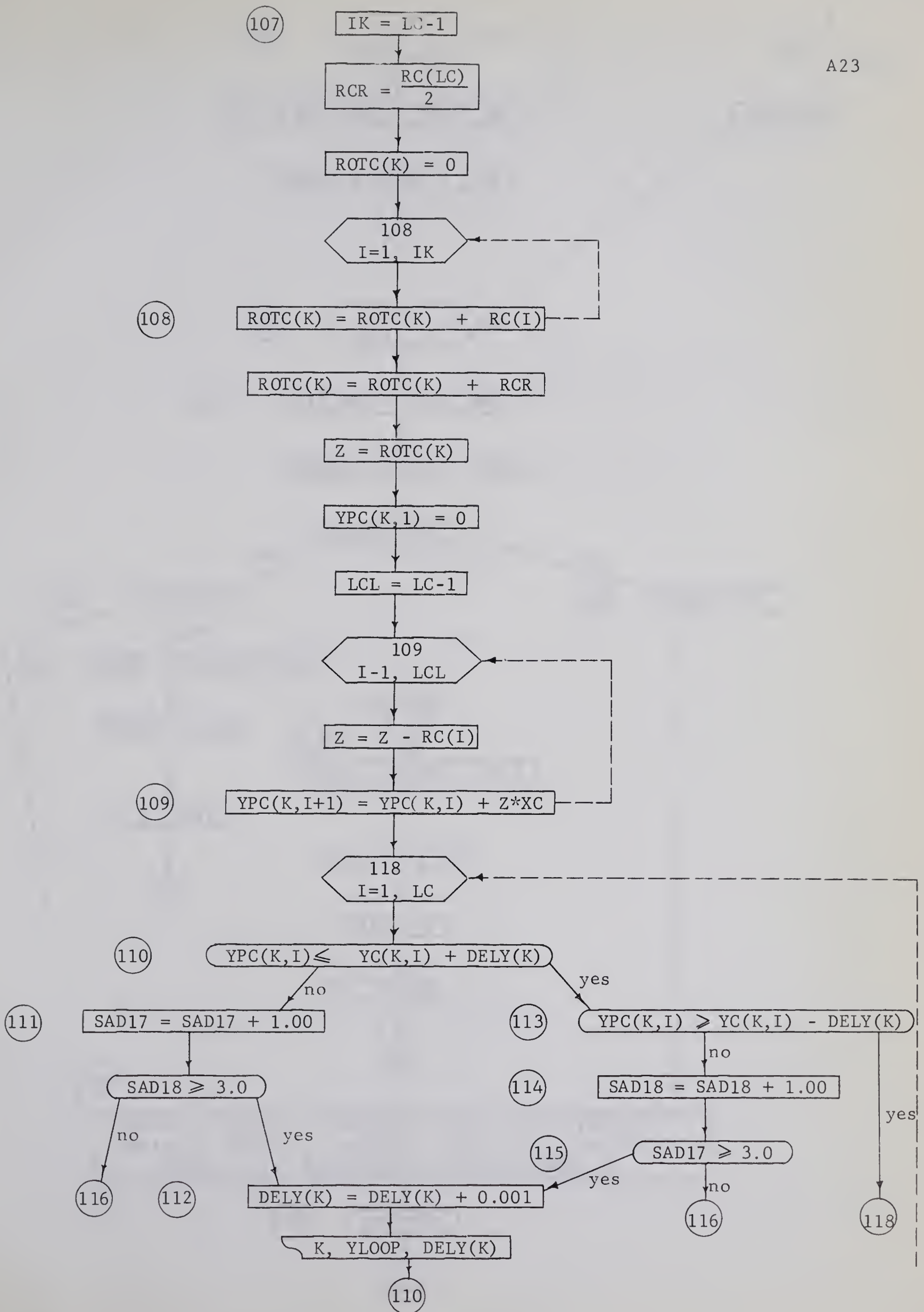
The flow diagram depicts the analysis of a column bent in single curvature having:

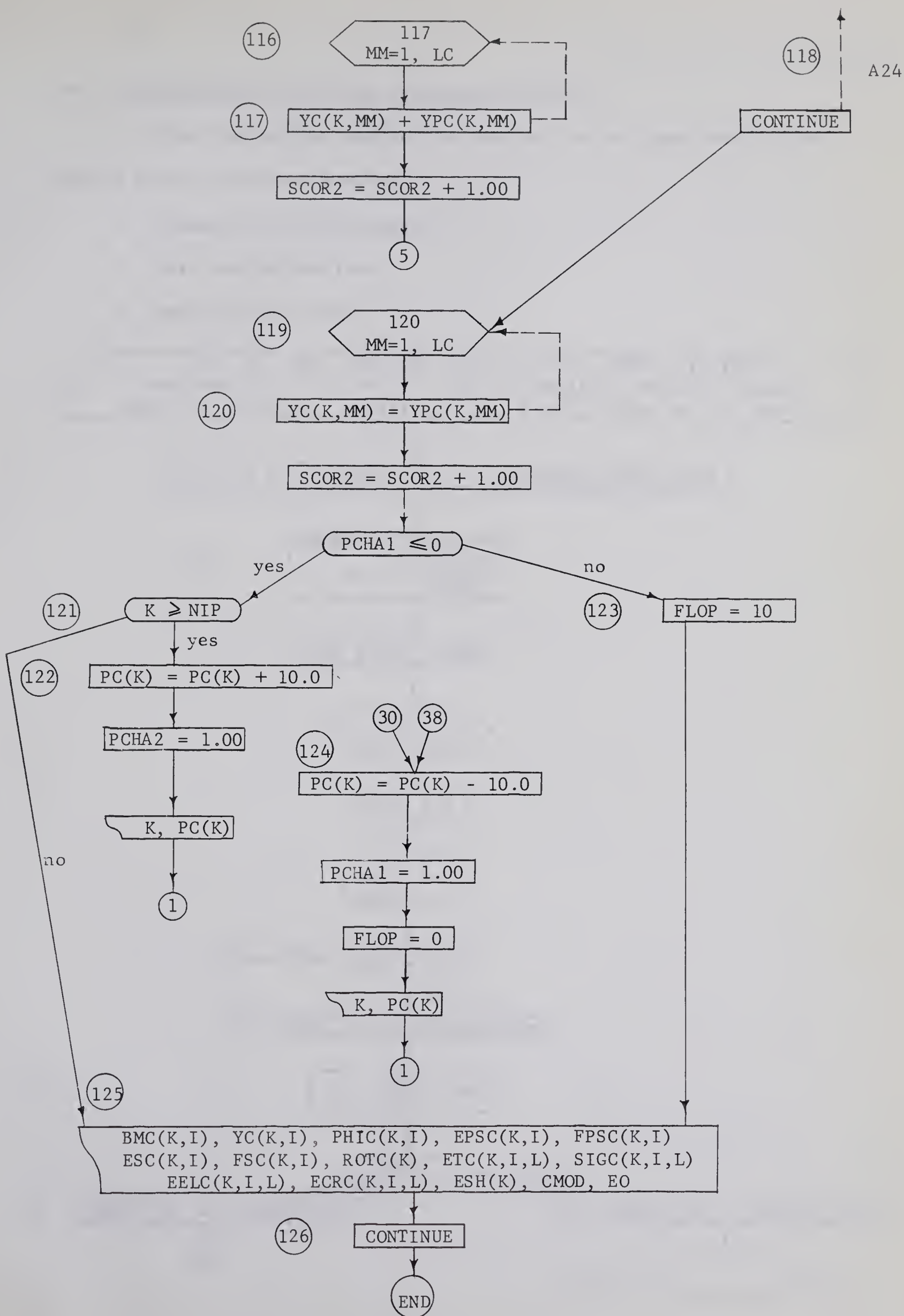
1. zero uniform load
2. zero end deflections
3. symmetrical end restraints
4. symmetrical reinforcement

The use of column symmetry requires that the number of panel points be an odd number.





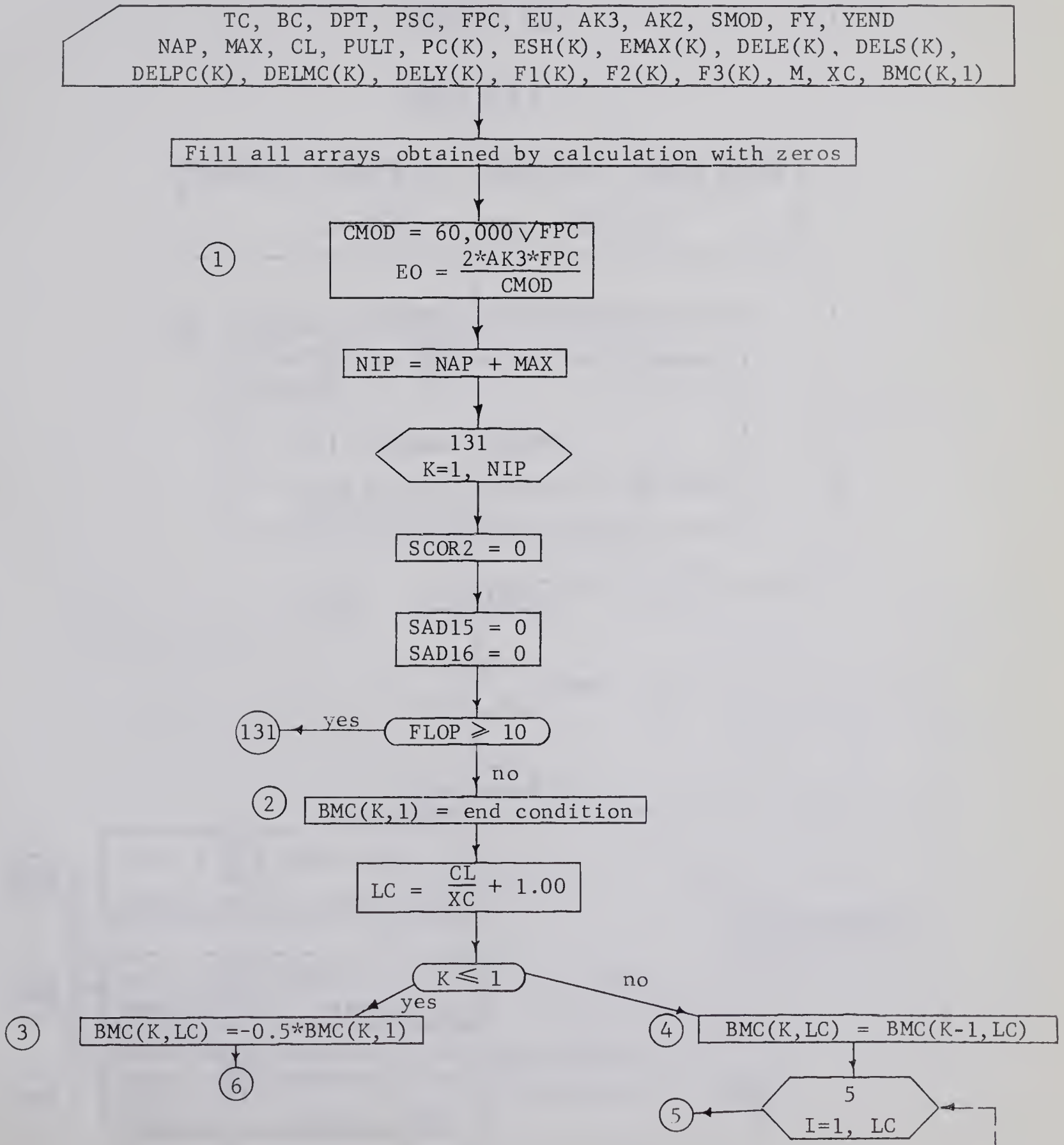


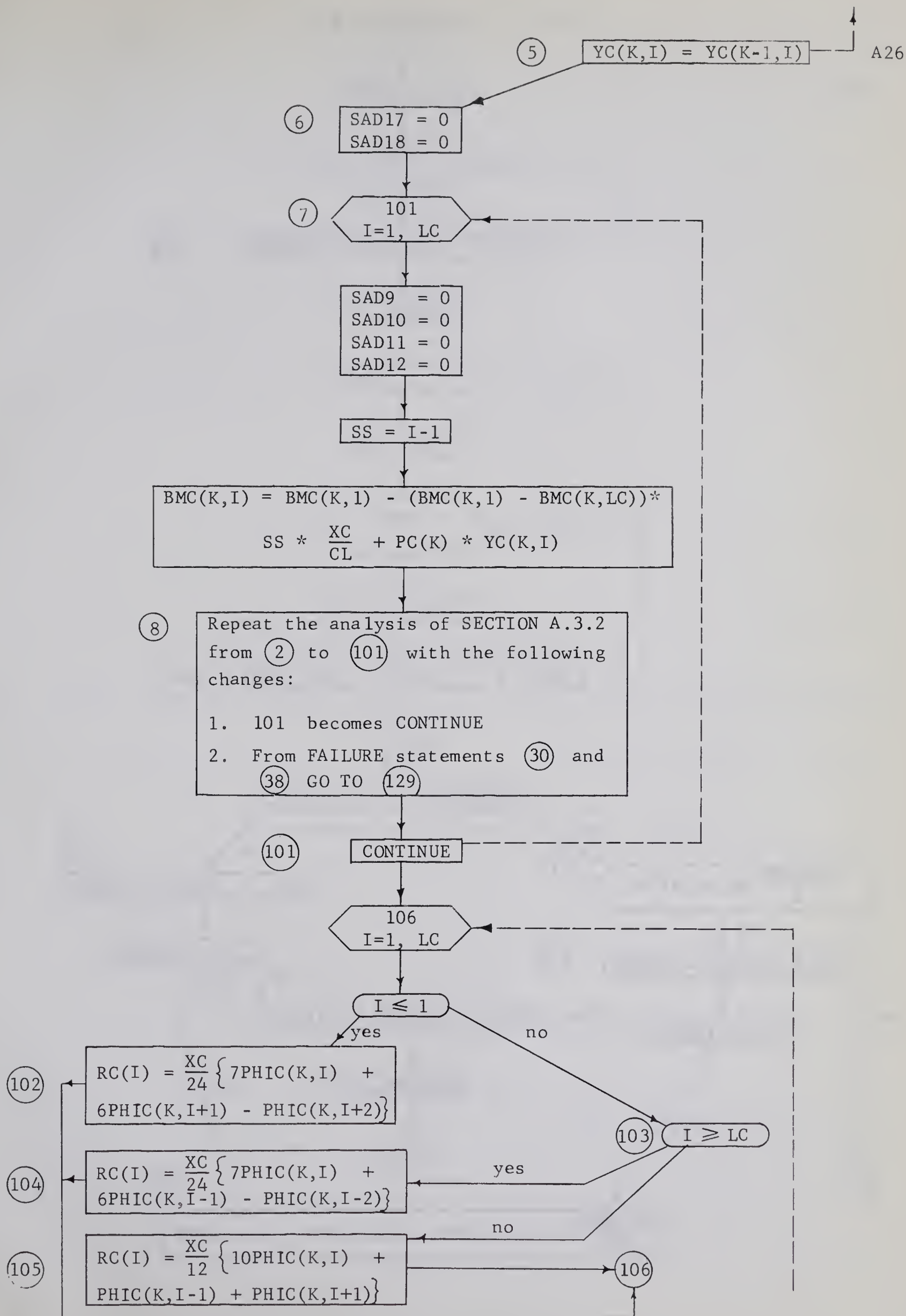


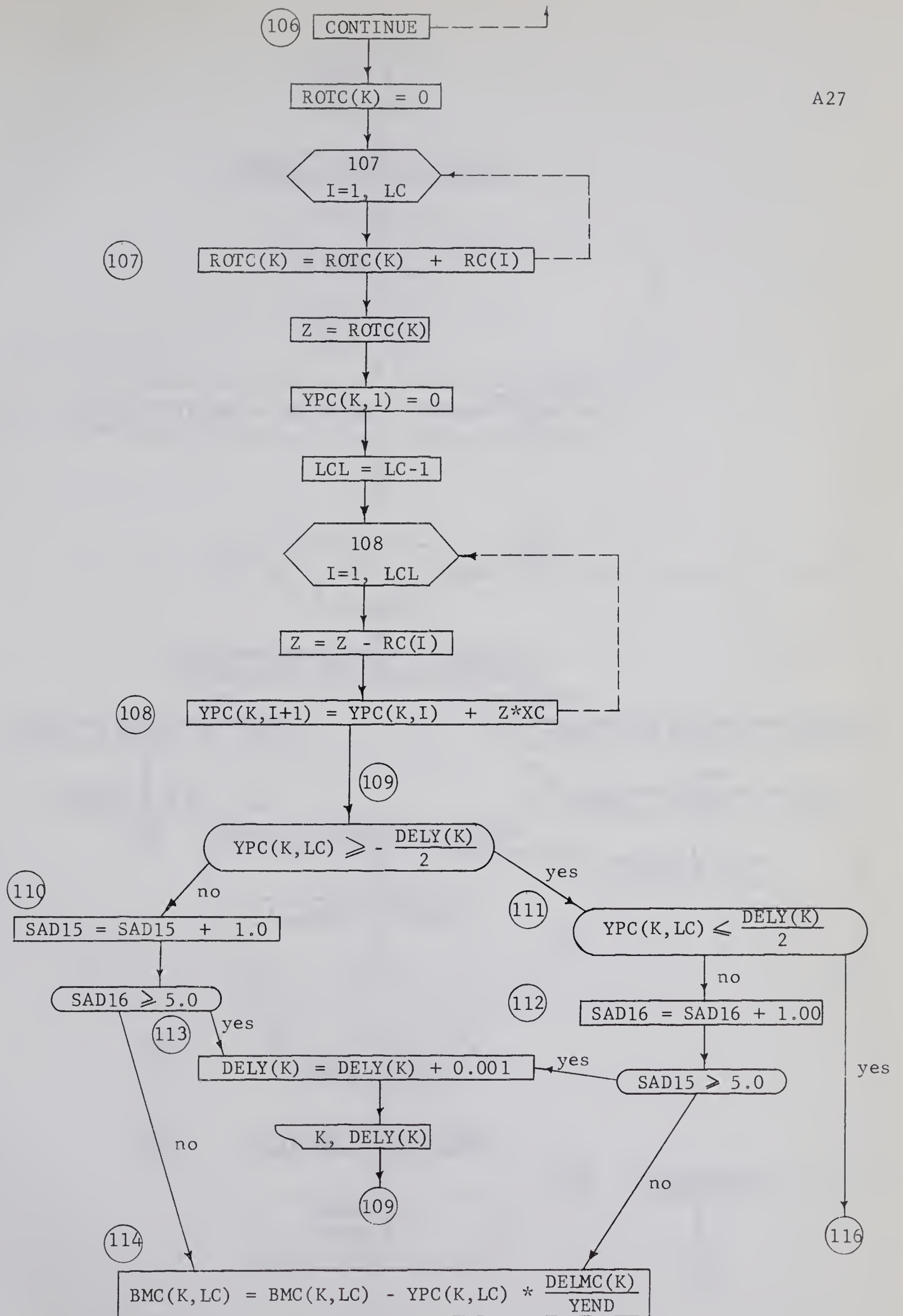
A.4.3 Fixed Ended Column Bent in Double Curvature

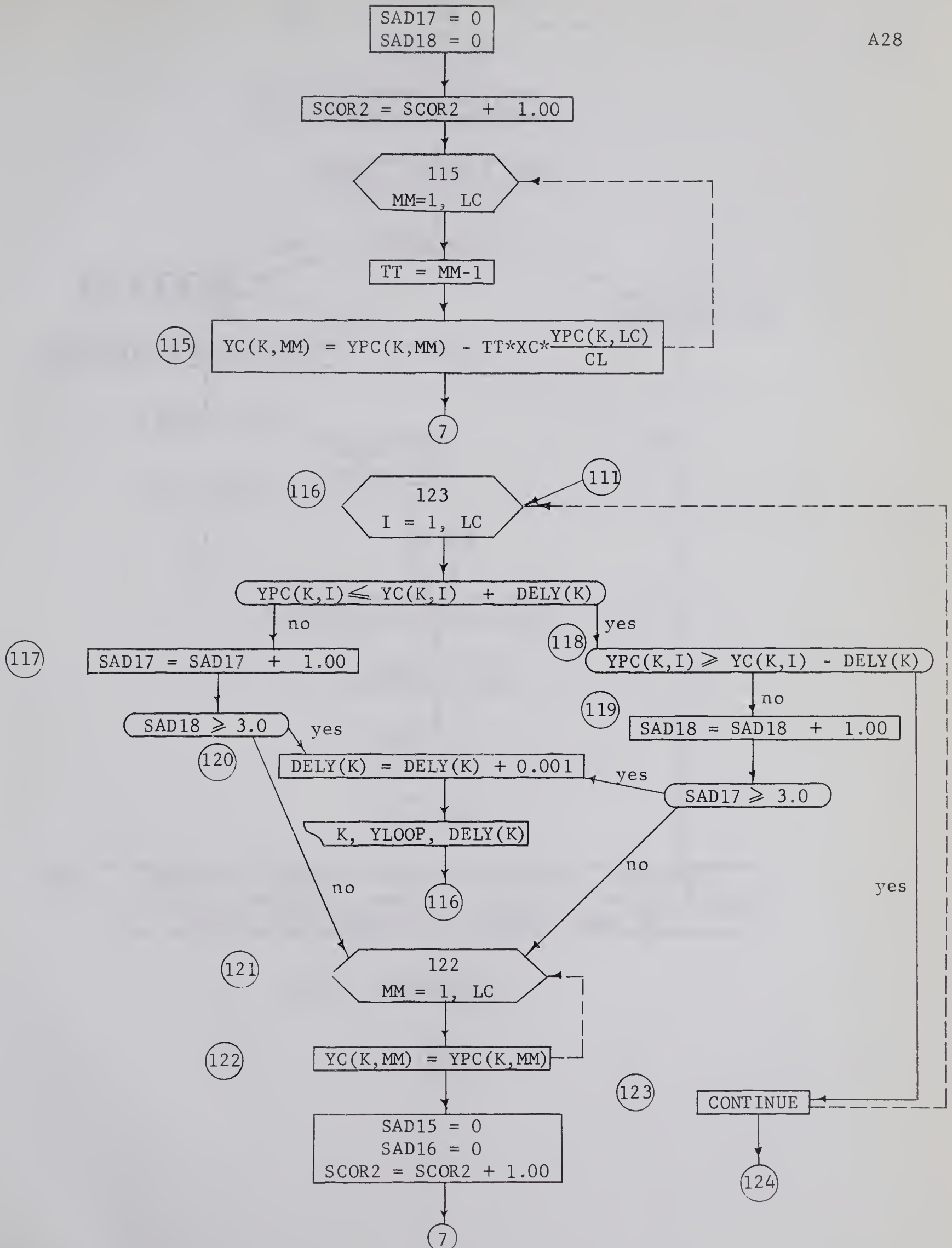
The flow diagram depicts the analysis of a fixed ended column bent in double curvature having:

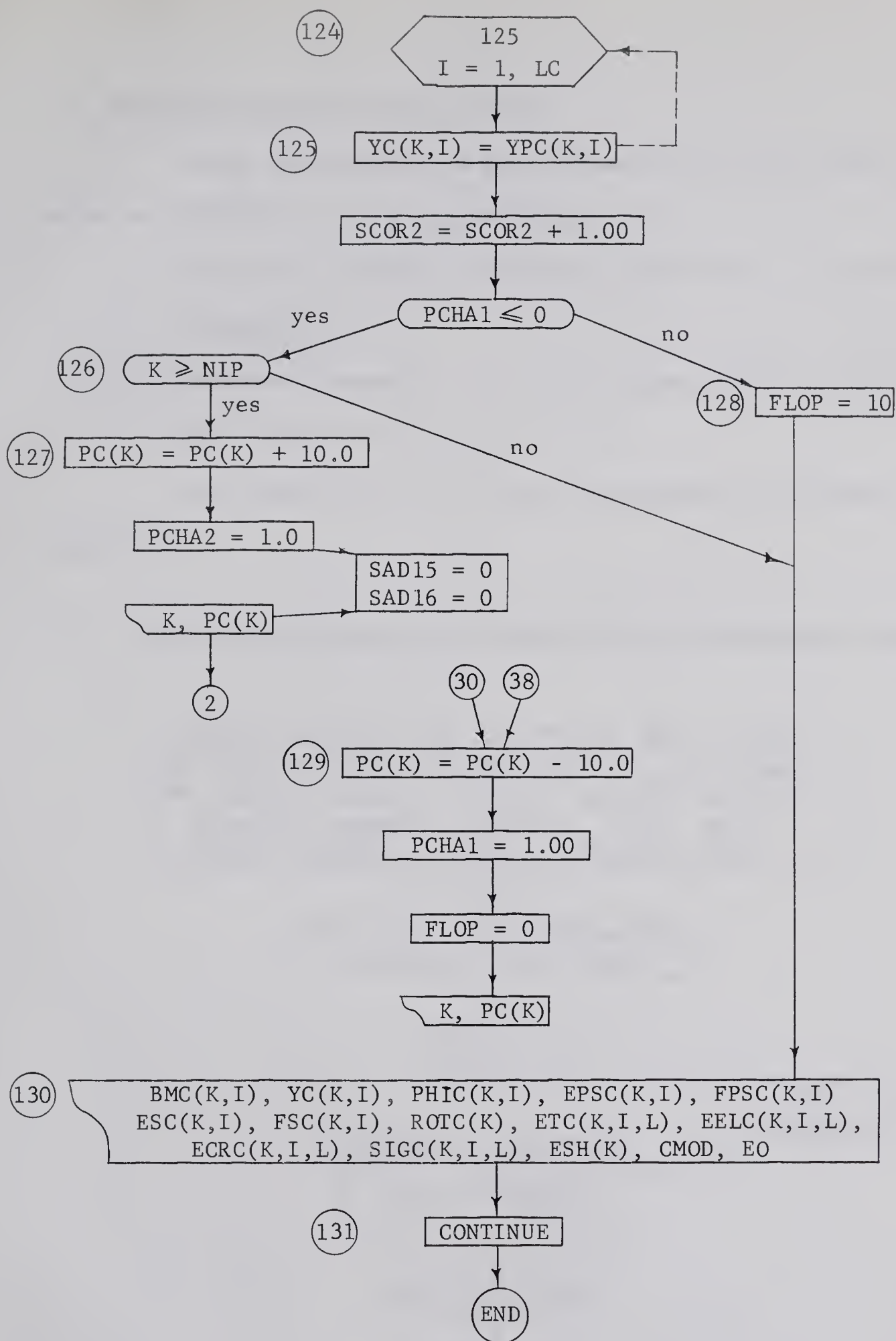
1. symmetrical reinforcement
2. zero end deflections
3. zero uniform load











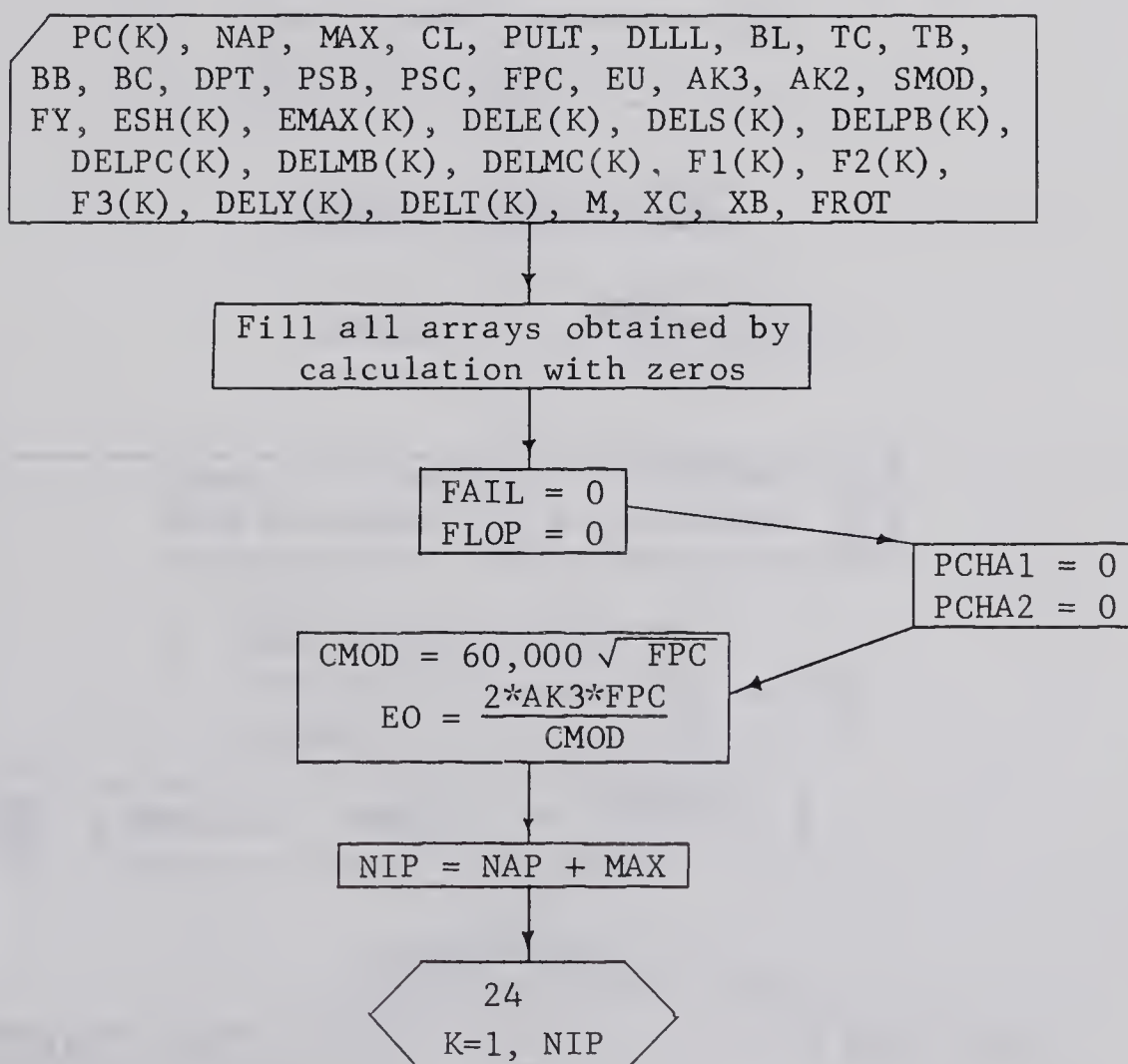
A.5 Flow Diagrams for Frame Analysis

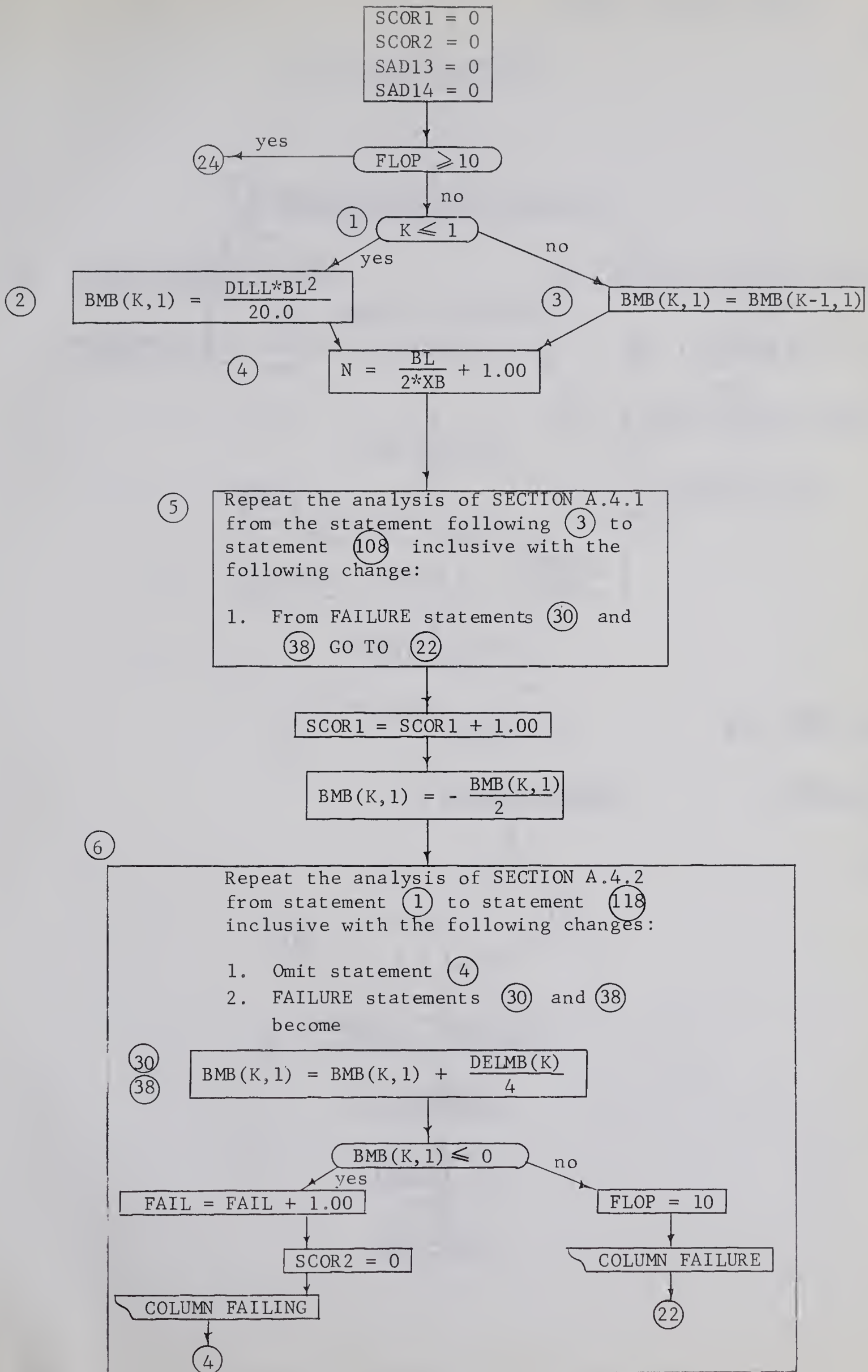
These flow diagrams depict the analysis of the model frameworks of CHAPTER VII. Two possibilities exist:

1. The model framework containing columns bent in symmetrical single curvature.
2. The model framework containing columns fixed at one end and bent in double curvature.

The assumptions of the model frameworks are included in CHAPTER VII.

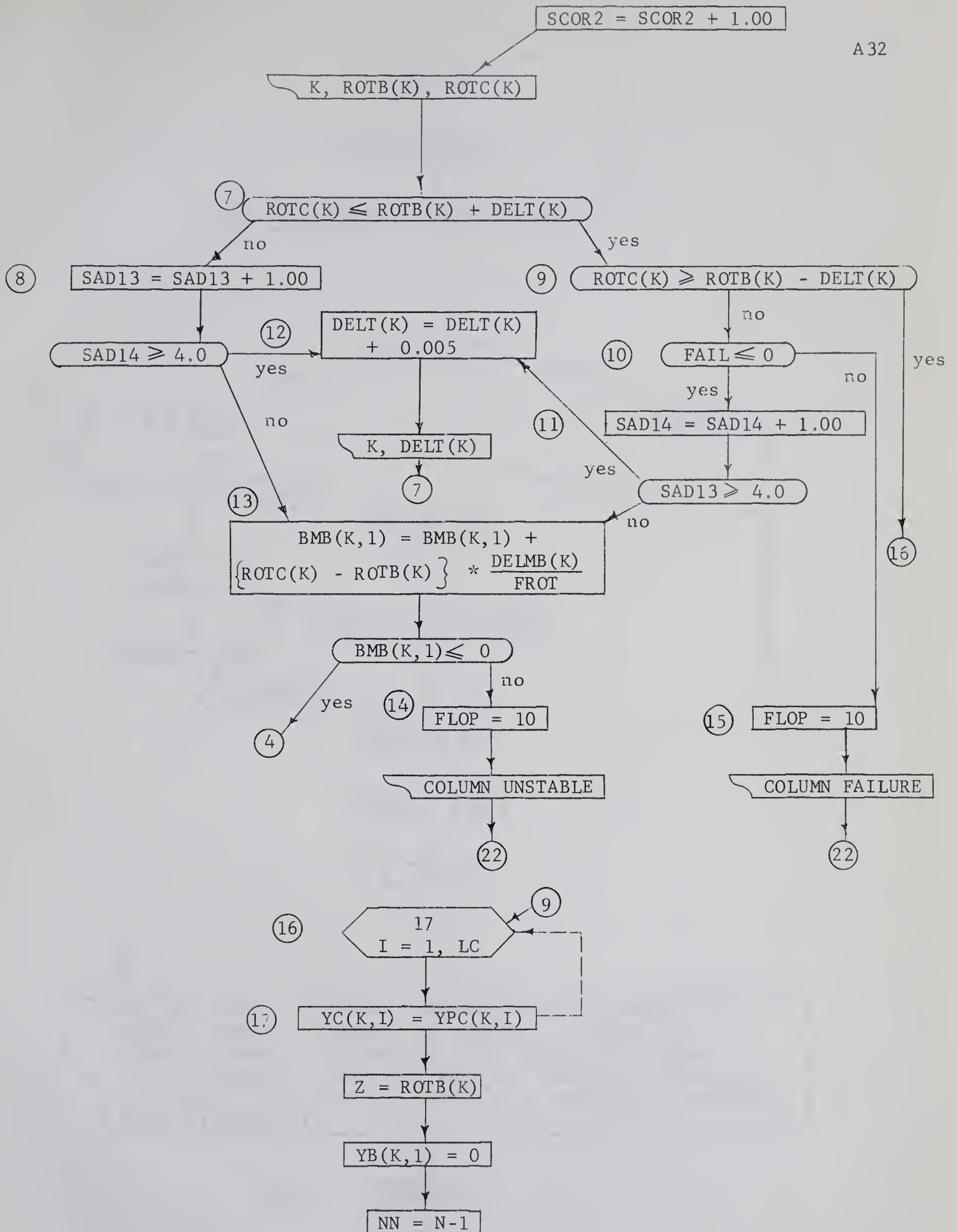
A.5.1 Framework Containing the Columns Bent in Symmetrical Single Curvature

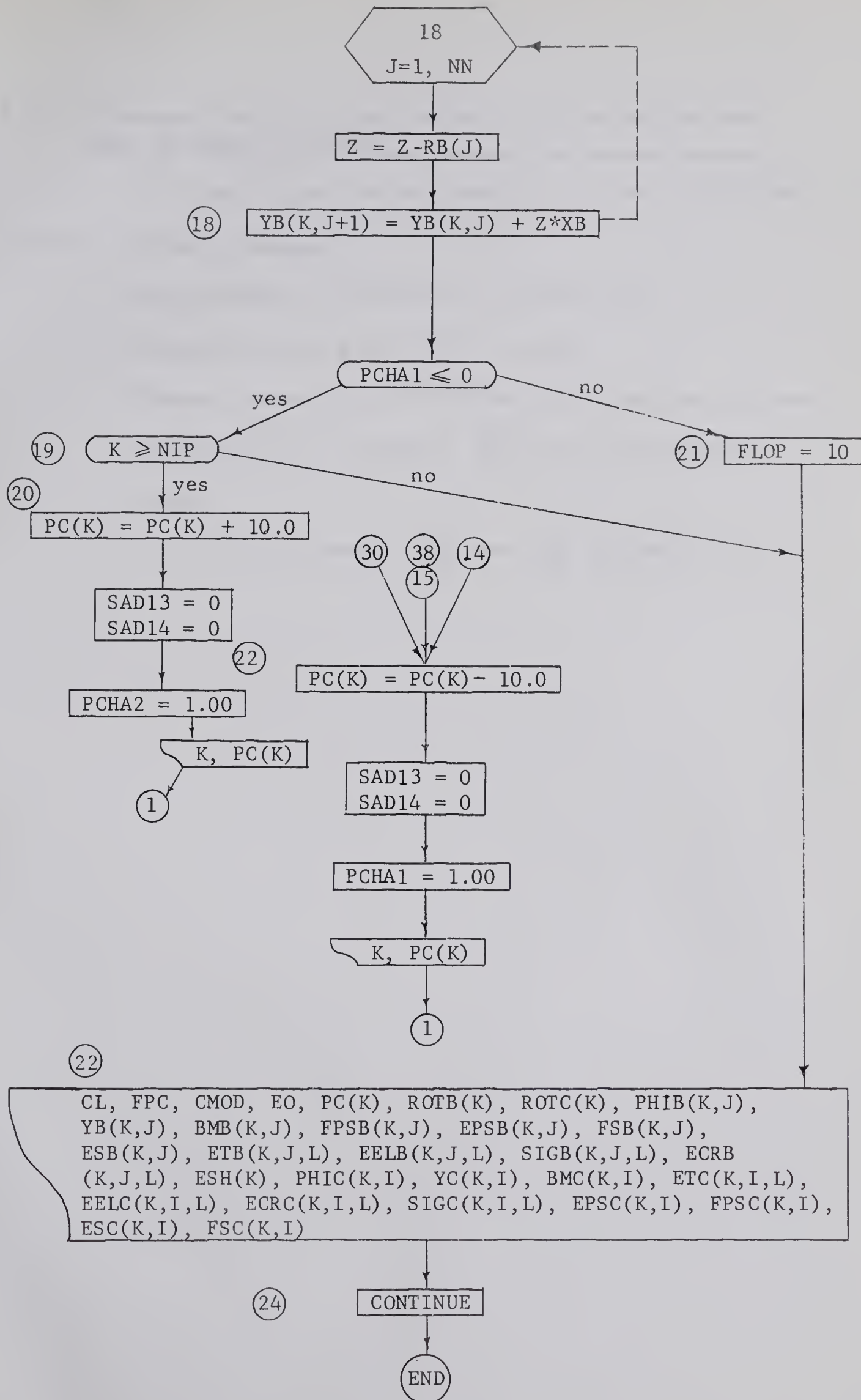




SCOR2 = SCOR2 + 1.00

A32





A.5.2 Framework Containing the Columns Fixed at One End and
Bent in Double Curvature

The flow diagram for this analysis is that of SECTION A.5.1
with the following changes:

1. Insert $SAD15 = 0$ and $SAD16 = 0$ before (6)
2. Change the first part of (6) to read:

"Repeat the analysis of SECTION A.4.3 from the statement
following (2) to statement (123) with the following
changes:

1. Failure statements (30) and (38) become:"

APPENDIX B
COMPARISON OF RESULTS OF
A BEAM AND A COLUMN CONSIDERING
VARIOUS DEGREES OF DISCRETENESS

TABLE B.1
COMPARISON OF BEAM RESULTS FOR
VARIOUS DEGREES OF DISCRETENESS

No. of creep stages	No. of panels	No. of fibres	Y t=25 yr (in)	end θ t=25 yr	f_s t=25 yr (ksi)	f_c max t=25 yr (ksi)
one creep stage	6	5	1.864	.02513	-23.79	1.944
		10	1.865	.02511	-22.99	1.956
		15	1.864	.02518	-23.53	1.926
	10	5	1.869	.02549	-23.79	1.944
		10	1.870	.02550	-22.99	1.956
		15	1.864	.02538	-23.53	1.926
	20	5	1.868	.02562	-23.79	1.944
		10	1.871	.02573	-22.99	1.956
		15	1.866	.02566	-23.53	1.926
three creep stages	6	5	1.945	.02702	-24.38	1.971
		10	1.939	.02708	-24.59	1.938
		15	1.939	.02708	-24.14	1.948
	10	5	1.953	.02717	-24.38	1.953
		10	1.944	.02715	-24.59	1.938
		15	1.937	.02699	-24.14	1.948
	20	5	1.950	.02717	-24.38	1.971
		10	1.939	.02708	-24.59	1.938
		15	1.942	.02706	-24.14	1.948
five creep stages	6	5	1.943	.02618	-24.87	1.950
		10	1.924	.02592	-24.53	1.942
		15	1.928	.02606	-24.50	2.047
	10	5	1.948	.02658	-24.87	1.950
		10	1.929	.02632	-24.53	1.942
		15	1.926	.02630	-24.50	2.047
	20	5	1.945	.02676	-24.87	1.950
		10	1.928	.02653	-24.53	1.942
		15	1.926	.02653	-24.50	2.047
seven creep stages	6	5	1.902	.02558	-24.56	1.864
		10	1.881	.02535	-24.15	1.861
		15	1.886	.02546	-24.57	1.908
	10	5	1.908	.02594	-24.56	1.908
		10	1.887	.02567	-24.15	1.861
		15	1.882	.02564	-24.57	1.908
	20	5	1.909	.02619	-24.56	1.864
		10	1.891	.02599	-24.15	1.861
		15	1.886	.02592	-24.57	1.908

TABLE B.2
COMPARISON OF COLUMN RESULTS FOR
VARIOUS DEGREES OF DISCRETENESS

No. of creep stages	No. of panels	No. of fibres	Y t=25 yr (in)	end θ t=25 yr	f'_s t=25 yr (ksi)	f_s t=25 yr (ksi)	f_c max t=25 yr (ksi)	M t=25 yr (in k)
one creep stage	6	5	1.576	.02238	50.0	20.63	1.740	522.64
		10	1.577	.02239	50.0	20.60	1.740	522.77
		15	1.577	.02239	50.0	20.59	1.740	522.82
	10	5	1.603	.02263	50.0	20.36	1.764	528.41
		10	1.586	.02238	50.0	20.69	1.752	524.89
		15	1.560	.02203	50.0	20.95	1.740	518.78
	20	5	1.598	.02250	50.0	20.36	1.764	527.31
		10	1.594	.02247	50.0	20.33	1.764	526.79
		15	1.577	.02224	50.0	20.59	1.740	522.64
two creep stages	6	5	1.132	.01682	50.0	28.89	1.576	423.43
		10	1.132	.01683	50.0	28.86	1.576	423.55
		15	1.133	.01684	50.0	28.84	1.576	423.63
	10	5	1.134	.01682	50.0	28.89	1.576	424.01
		10	1.135	.01683	50.0	28.86	1.576	424.14
		15	1.135	.01684	50.0	28.84	1.576	424.23
	20	5	1.131	.01678	50.0	28.89	1.576	422.90
		10	1.135	.01681	50.0	28.86	1.576	423.86
		15	1.135	.01682	50.0	28.84	1.576	423.48
three creep stages	6	5	1.107	.01649	50.0	29.98	1.572	417.79
		10	1.098	.01642	50.0	30.31	1.569	415.90
		15	1.095	.01633	50.0	30.28	1.569	415.02
	10	5	1.098	.01637	50.0	30.32	1.575	414.99
		10	1.098	.01632	50.0	30.33	1.569	415.02
		15	1.098	.01636	50.0	30.28	1.569	415.83
	20	5	1.097	.01633	50.0	30.31	1.575	415.58
		10	1.101	.01637	50.0	30.31	1.569	416.02
		15	1.100	.01633	50.0	30.28	1.569	415.73

TABLE B.2

(Continued)

No. of creep stages	No. of panels	No. of fibres	Y t=25 yr (in)	end θ t=25 yr	f'_s t=25 yr (ksi)	f_s t=25 yr (ksi)	f_{cmax} t=25 yr (ksi)	M t=25 yr (ksi)
five creep stages	6	5	1.076	.01620	50.0	31.70	1.570	410.89
		10	1.079	.01625	50.0	31.73	1.601	411.57
		15	1.090	.01647	50.0	31.40	1.606	414.09
	10	5	1.074	.01620	50.0	31.70	1.589	409.60
		10	1.076	.01620	50.0	31.75	1.585	410.84
		15	1.073	.01619	50.0	31.75	1.601	410.11
	20	5	1.073	.01614	50.0	31.71	1.589	409.56
		10	1.070	.01611	50.0	31.75	1.601	408.55
		15	1.070	.01612	50.0	31.75	1.601	409.23
seven creep stages	6	5	1.055	.01583	50.0	31.93	1.540	406.21
		10	1.052	.01576	50.0	31.95	1.536	405.38
		15	1.052	.01576	50.0	31.93	1.566	405.47
	10	5	1.061	.01585	50.0	32.04	1.562	407.56
		10	1.062	.01588	50.0	32.04	1.586	406.88
		15	1.051	.01574	50.0	31.95	1.566	404.40
	20	5	1.062	.01592	50.0	32.06	1.576	407.78
		10	1.059	.01587	50.0	32.05	1.580	406.42
		15	1.051	.01578	50.0	31.96	1.539	404.76

B29850